BIO- AND MULTIFUNCTIONAL POLYMER ARCHITECTURES

Preparation, Analytical Methods, and Applications

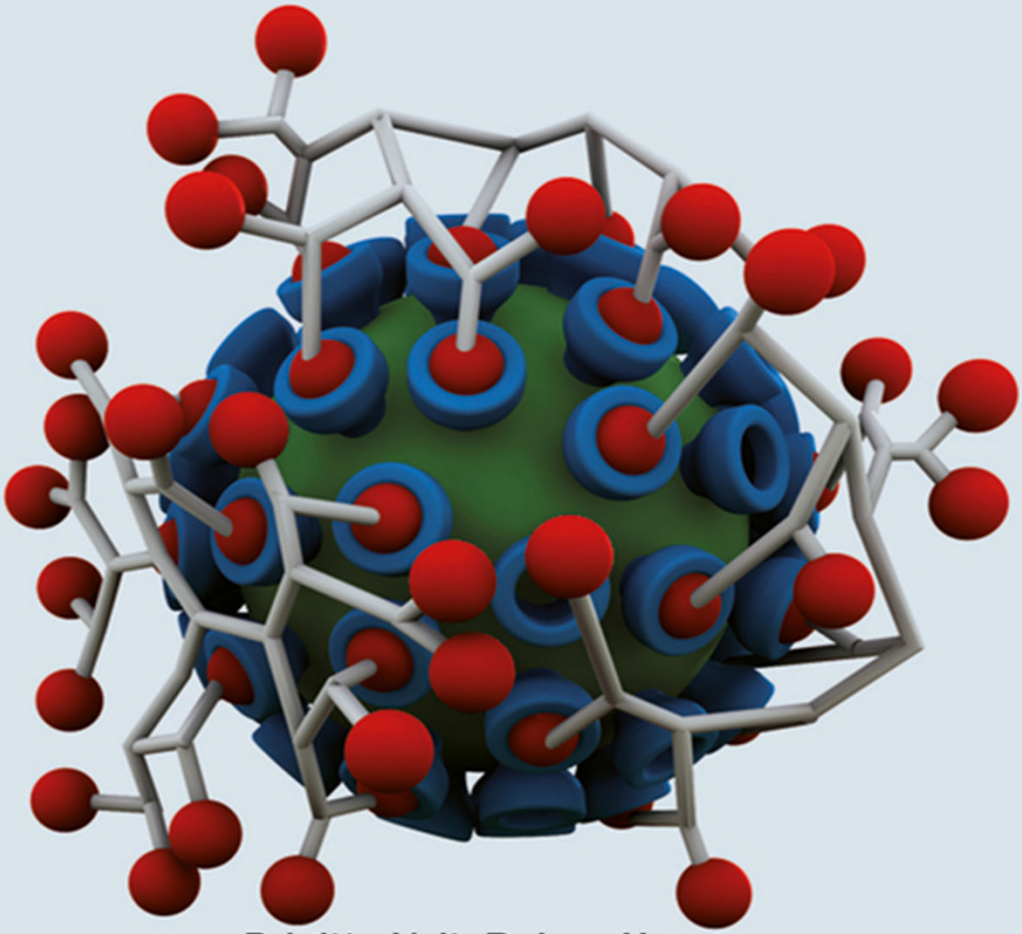

Brigitte Voit, Rainer Haag,
Dietmar Appelhans, and Petra B. Welzel

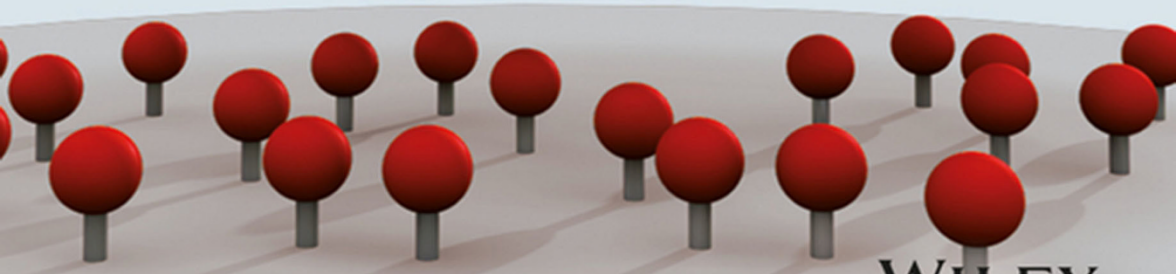

WILEY

BIO- AND MULTIFUNCTIONAL POLYMER ARCHITECTURES

BIO- AND MULTIFUNCTIONAL POLYMER ARCHITECTURES

Preparation, Analytical Methods, and Applications

BRIGITTE VOIT
RAINER HAAG
DIETMAR APPELHANS
PETRA B. WELZEL

WILEY

Published by John Wiley & Sons, Inc., Hoboken, New Jersey
Published simultaneously in Canada

Library of Congress Cataloging-in-Publication Data:

Names: Voit, Brigitte, author. | Haag, Rainer, author. | Appelhans, Dietmar, author. | Welzel, Petra B., author.
Title: Bio- and multifunctional polymer architectures : preparation, analytical methods, and applications / by Brigitte Voit, Rainer Haag, Dietmar Appelhans, Petra B. Welzel.
Description: Hoboken, New Jersey : John Wiley & Sons, 2016. | Includes bibliographical references and index.
Identifiers: LCCN 2015041264 | ISBN 9781118158913 (cloth)
Subjects: LCSH: Polymers–Biotechnology. | Polymers in medicine. | Biomedical materials.
Classification: LCC TP248.65.P62 A67 2016 | DDC 668.9–dc23
LC record available at http://lccn.loc.gov/2015041264

Set in 10.5/13.5pt Times by SPi Global, Pondicherry, India

Printed in the United States of America

10 9 8 7 6 5 4 3 2 1

CONTENTS

PREFACE

Synthetic polymers have revolutionized modern life over the last century and provide highly versatile materials for everybody's daily comfort. In contrast, bio- and multifunctional polymers are about to change our lives with innovative system solutions, especially in the biomedical area. This research field is currently subject of intense efforts and bears a large innovation potential for the future, especially at the interphase between materials and biomedical sciences. Also in the context of emerging research areas such as chemical biology, nanobiotechnology, and synthetic biology, the control of material-biointerphases is of outmost relevance.

In this textbook we highlight recent developments in designing and realizing synthetic multifunctional polymer architectures, which are of special importance for application in bionanotechnology and biomedicine. In the last 20 years, a significant progress has been made in controlling the structure and molar mass of macromolecules, implementing functional units, inducing specific self-assembly behavior, and combining synthetic structures with biological function. In addition, a much deeper understanding of the biological and physical interactions between a biosystem and a synthetic material as well as strong interdisciplinary cooperations between polymer chemists, cell biologists, and medical scientists evolved, which allow today a much more precise and rational approach toward custom-made biocompatible, bioactive synthetic macromolecular architectures and biointerfaces as well as bioconjugates for biomedical applications.

Due to this progress that has been made in the recent years and the high impact on biotechnology and biomedicine, this textbook will provide the basic synthetic tools available to tailor-make multifunctional polymers and to control their biointeractions and self-assembly, and on the other hand, it will highlight functional materials and system applications that are based on the availability of such complex and multifunctional macromolecules.

This textbook will allow an easy access into the field especially for advanced and graduate students as well as experienced researchers in natural sciences and biomedical specialists entering the field or being interested in and working at the interface between polymeric materials and biomedicine. Target study areas are bioengineering, biomaterials science, biomedical science, chemistry biophysics, polymer science, and regenerative medicine.

Brigitte Voit
Rainer Haag
Dietmar Appelhans
Petra B. Welzel

ACKNOWLEDGMENTS

The book would not have been possible without the help of numerous people for which we are deeply thankful. Firstly, we would like to acknowledge the major contributions of Prof. Carsten Werner for the concept and details of the biomaterial and biomedical application parts of the book. Various coworkers contributed to subchapters; this includes Dr. Mikhail Tsurkan, Dr. Mirko Nitschke, Dr. Ulrich Scheler, Dr. Albena Lederer, Dr. Susanne Boye, Dr. Martin Müller, and Dr. Ulrich Oertel who contributed to Chapters 3 and 4. Dr. Juliane Keilitz and Dr. Wiebke Fischer took over major parts in Chapters 3, 5, and 6 and helped significantly in editing and finalizing the full book. A number of students and postdocs have to be named who greatly helped with making schemes and figures: Tim Erdmann, David Gräfe, Jörg Kluge, Banu Iyisan, and Dr. Emanuel Fleige. Marlen Groß and Maximilian Keitel are highly acknowledged for their technical support.

1

INTRODUCTION

Materials that can be applied in bionanotechnology and biomedicine are a subject of current research. Bio- or multifunctional polymeric materials might help solving many of today's medical problems and allow, for example, a safer use of medicinal products and implants, a more targeted and specific drug administration, and finally even *in vivo* tissue engineering for effective regenerative medicine. Furthermore, specially designed functional materials provide new perspectives in diagnosis and fundamental studies of biological processes as well as significantly increase the number of controllable targets in medical treatments.

The aim of this book is to outline why and how synthetic bio- and/or multifunctional polymers are particularly promising in this context. Therefore, chemical and physical tools that are available to custom-make polymers and to control specific biointeractions will be introduced. Combining up-to-date polymer synthesis knowledge with a fundamental understanding of the biosystem and ways to control specific biological interaction has led to highly promising advances in the design of specific polymers for biomedical applications, which has been recently successfully demonstrated.

1.1 WHAT MAKES POLYMERS SO INTERESTING?

Various types of materials like metals and alloys, ceramics, different inorganic scaffolds, and low and high molar mass organic molecules are proven instrumental for the broad variety and the specific needs of bionanotechnology as

Bio- and Multifunctional Polymer Architectures: Preparation, Analytical Methods, and Applications, First Edition. Brigitte Voit, Rainer Haag, Dietmar Appelhans, and Petra B. Welzel.

well as biomedicine applications. Synthetic polymers play a very special role in this context because they are organic in nature and can be tailor-made in many forms to mimic the complexity of the natural biomacromolecules that define and control life. Thus, polymer scientists have taken up the challenge of identifying important design rules that come from nature and at least partially implemented them, essentially reduced, into synthetic polymer structures. Biomacromolecules in the form of polynucleotides and polypeptides contain a large complexity of information in a single molecule that is the base for tertiary structure formation, recognition, bioactions, and biointeractions. This is achieved in biology by a full sequence and molar mass control during the synthesis of the biomacromolecules as well as by an amazing control of the interplay of noncovalent interactions such as found in hydrophobic or electrostatic interactions and hydrogen bonding.

Synthetic macromolecules have similar basic structural features as biomacromolecules, which has given rise to many different kinds of polymers that can seamlessly interface with biosystems and provide particular advantages for new biomedical applications. The first of these features are that they are formed by a large number of repeating units (monomers). Secondly, they can be prepared in different molar masses. *Constitution* (composition) and *connectivity* (linear, branched) of the repeating units are already two important parameters that can be varied in synthetic macromolecules. In addition, the characteristics of polymers can be significantly broadened by combining several comonomers in one polymer chain. These can be randomly distributed within a linear polymer chain or added in a special sequence and in a specific topology (see polymer architectures), which results in block, star, and graft copolymers, for example.

Since the *variety of monomer structures is nearly unlimited* synthetic polymers offer many more variation possibilities with regard to introduction of specific chemical units and functions than, for example, proteins where a limited number of amino acids is found in nature. Similarly, there is theoretically also no limit to the number of different monomer units that can be combined in one polymer chain. However, so far, the exact sequence of the monomers has not been controllable by common synthetic approaches since polymerization is usually a statistical process.

A specific feature of polymers and the major difference to naturally occurring proteins and polynucleic acids is their dispersity. This can account on the one hand for the chemical composition in copolymers, whereby each individual chain may have a different sequence of the comonomers (= isomers). However, it is especially prominent when one looks at the molar mass. The statistic nature of the polymerization process always results in a mixture of macromolecules of different lengths with a specific distribution in molar mass.

In analogy to proteins, however, one can further define a "primary structure" in synthetic polymers, which describes not only the *constitution* but also the *configuration* of the monomer units within the polymer chain. Although monomer units are usually introduced *head-to-tail*, sometimes, *head-to-head* or *tail-to-tail* connections are observed that reduce the potential order in the chain. Similarly, *cis*- and *trans*-configuration within individual monomer units may have to be considered that can significantly change the material's properties as can be seen in the comparison of poly(*cis*-1,4-isoprene) (natural rubber) to poly(*trans*-1,4-isoprene) (a brittle material without commercial use). A specific feature in polymers is tacticity, which describes the arrangement of the substituent in a repeating unit and can be isotactic (always in the same direction), syndiotactic (controlled alternating), or atactic (random) (Fig. 1.1). Isotactic polypropylene is a million-ton-scale technical thermoplastic material that is used widely in packaging, whereas atactic polypropylene is a viscous oil with no practical use (see Chapter 2).

In further analogy to proteins, macromolecules can also have a *secondary structure*, which is the arrangement of the chain in a coil, wormlike, or rigid structure, which is mainly defined by the rigidity of the repeating units and specific physical interactions with the solvent or nearby polymer chains. Finally, a *tertiary structure* can also be assigned, which describes the arrangement of the polymer chains toward each other in the bulk state. Today, one

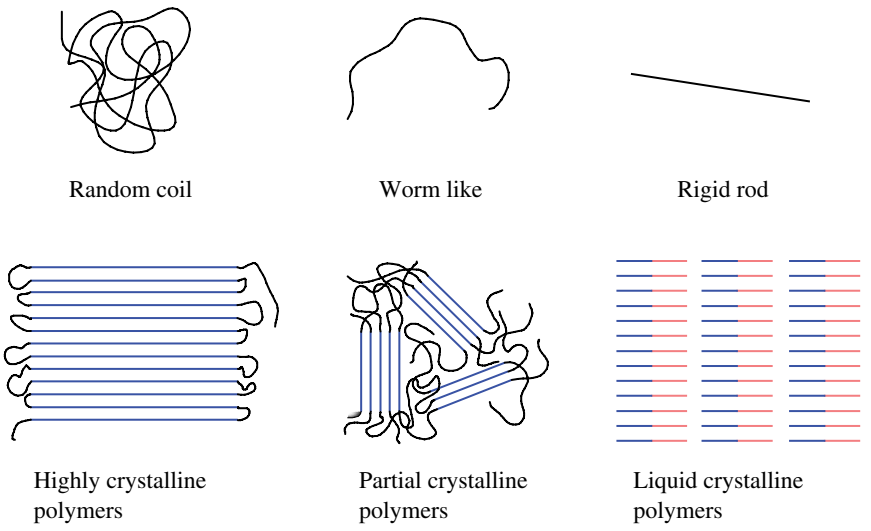

FIGURE 1.1 Structure and form of polymer chains in solution and melt (top) and possible ordered bulk structures (bottom).

could stretch the term "tertiary structure" in polymers even further to include their self-assembly and aggregation status in solution, which can lead to very complex and rather well-defined nanostructures.

The statistical synthesis process and the many parameters determining a polymer product tend to make it a complex and often rather ill-defined material. However, new methods in polymer synthesis have recently evolved and existing methods have been further developed that allow much higher control of a polymer's constitution, connectivity, molar mass, configuration, and even its "tertiary structure" formation and self-assembly. So, the ultimate goal to prepare synthetic macromolecules with the same precision found in nature but with precisely adjusted combinations of functionality—even beyond nature—may come within reach.

1.2 MACROMOLECULAR ENGINEERING AND NANOSTRUCTURE FORMATION

For many years, synthetic processes for polymers have been optimized with regard to reducing costs, increasing production output, and allowing high reproducibility. In addition, methods have been developed to control the configuration of polymers so that the thermal and mechanical properties of structural polymers and their order in bulk can be defined.

However, with the focus in research shifting from large-scale structural polymers to tailor-made functional polymers, polymerization methods have evolved, which allow *macromolecular engineering* of synthetic macromolecules mainly involving controlled polymerization techniques (see Section 3.2) and efficient polymer analogous reactions (see Section 3.3). For biomedical applications, bioconjugation and self-assembly processes have obtained an even more prominent role. Polymer chemists are presently taking lessons from nature by attempting to essentially simplify and generalize in order to use this knowledge to produce something that is even better for a very specific target.

As a result, polymers with narrow dispersity can be now prepared that have well-defined block structures and in some cases even star and dendritic topologies. Control of the end functionality and effective organic polymer analogous reactions allow highly efficient bioconjugation. In addition, due to a much higher understanding of the behavior of macromolecules in solution, self-assembly strategies can be used to prepare complex multifunctional nanostructures in solution as ideal carrier structures for targeted and controlled drug delivery such as core–multishell nanocarriers (Fig. 1.2; see also Chapter 6).

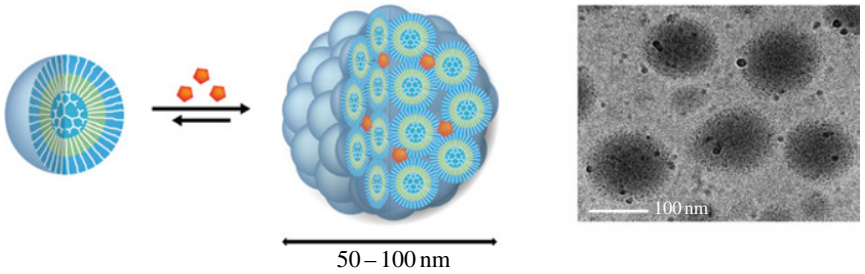

FIGURE 1.2 Supramolecular aggregate formation and drug encapsulation of dendritic core–multishell architectures (left) and cryo-TEM structure elucidation of the formed drug complexes (right). Source: Radowski et al. [1], figure 4. Reproduced with permission from John Wiley & Sons.

1.3 SPECIFIC NEEDS IN BIONANOTECHNOLOGY AND BIOMEDICINE

For any material that is meant to eventually be applied in contact with a biosystem, specific needs arise that increase with the complexity of the application. This is certainly also true for polymers. Besides a high level of control over and knowledge of the chemical structure, architecture, and molar mass, which are essential prerequisites for admission in biomedical applications, one also has to be able to control the biointeractions. Polymers can be fully bioinert or may have various aspects of biocompatibility like low cell toxicity and low unspecific protein adsorption, or may exhibit specific bioactivity. Furthermore, they can be biostable, which is a major prerequisite for most conventional implants. But stable materials have to be excreted completely from a human body when used as a carrier system, or they may degrade in a biological system, which leads to the need to consider the fate of the degradation products. Some polymers are already very well established in biomedical applications. For example, poly(ethylene glycol) (PEG) is used in particular to introduce water solubility into drugs and carrier systems and to reduce any unspecific biointeractions due to its property to cause negligible protein adsorption, but the biointeractions have to be elucidated with extreme care for any new polymer.

Applications of polymers can vary broadly from short-term peripheral like a simple coating that lubricates a surface of a catheter to enhance comfort and biocompatibility up to permanent implants and finally active and responsive systems that actively interfere with biological processes. In their role as carriers for diagnostics and treatment, polymers can either just be a “neutral” material acting as a reservoir or they can carry targeting functions or actively respond to stimuli for inducing delivery. Increasing complexity of the macromolecular

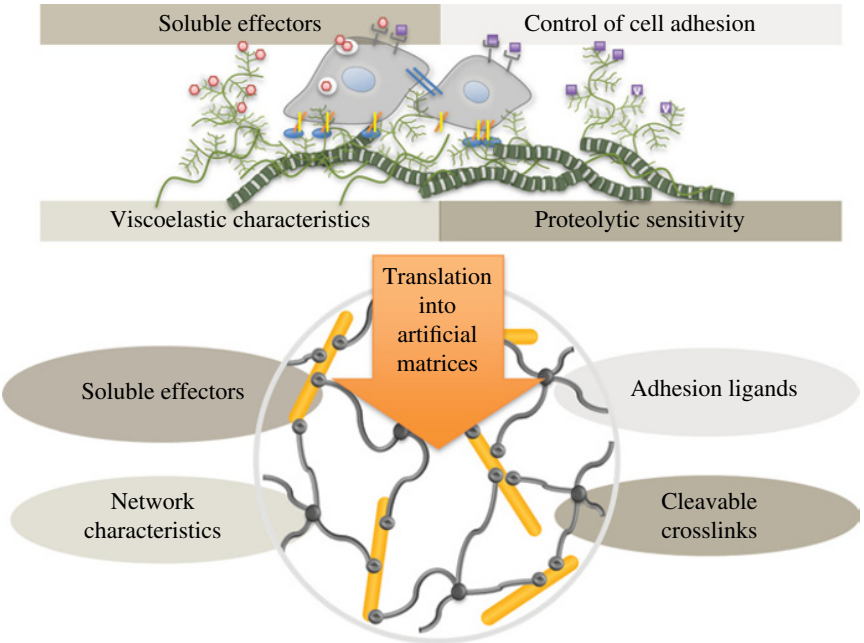

FIGURE 1.3 Scheme of biohybrid starPEG–glycosaminoglycan networks for recapitulating and modulating cell-instructive ECM signals.

architectures and use of bioactive conjugates results in similar regulatory requirements as necessary for pharmaceuticals and complicates market introduction in many cases.

Therefore, more interdisciplinary research work is needed between polymer chemistry, biology, and medicine, and specific characterization tools have to be developed, to meet these new challenges.

Still, huge progress is being made due to synthetic tools and specific characterization methods now available and the first promising structures have already evolved. Even *in vivo* tissue engineering is no longer a vision of the future, because there are now bioconjugate scaffolds that not only act as simple base for cell adhesion but also recapitulate and modulate functional features of biological microenvironments to direct cellular fate decision and tissue regeneration (Fig. 1.3).

REFERENCE

[1] Radowski, M. R.; Shukla, A.; von Berlepsch, H.; Böttcher, C.; Pickaert, G.; Rehage, H.; Haag, R. *Angewandte Chemie, International Edition* 2007, *46*, 1265–1269.

2

TERMINOLOGY

2.1 POLYMER ARCHITECTURES

Macromolecules are large organic molecules that consist of a number of individual, repeating units (monomers). Molecules having only a small number of repeating units (degree of polymerization DP < 20) are called oligomers, and those having a larger DP are commonly called polymers. In the simplest case, the repeating units are all just of one kind of monomer forming so-called homopolymers, which are linearly connected and create, for example, a *coil structure* in solution and in bulk (Fig. 2.1).

In a chain growth polymerization, monomers can be introduced in various ways, most commonly head-to-tail but also head-to-head. In addition, for monomers that remain unsaturated, *cis*- and *trans*-configurations have to be considered like for *cis*- and *trans*-poly(isoprene).

Furthermore, stereoisomerism or the "tacticity" of polymers plays a prominent role in controlling the self-assembly and crystallinity in the bulk material. This has its origin in the different spatial arrangements of substituents X (Fig. 2.2). If the substituents X of the vinyl polymer are either all above or all below a plane, the polymers are called *isotactic*. Their chains consist of a regular sequence of constitutional repeating units containing carbon atoms with the same configuration. If the substituted carbon atoms have alternating configurations, the polymer is called *syndiotactic*. If there is a random spatial orientation (configuration) of the substituents X, the polymers are called *atactic*.

Bio- and Multifunctional Polymer Architectures: Preparation, Analytical Methods, and Applications, First Edition. Brigitte Voit, Rainer Haag, Dietmar Appelhans, and Petra B. Welzel.

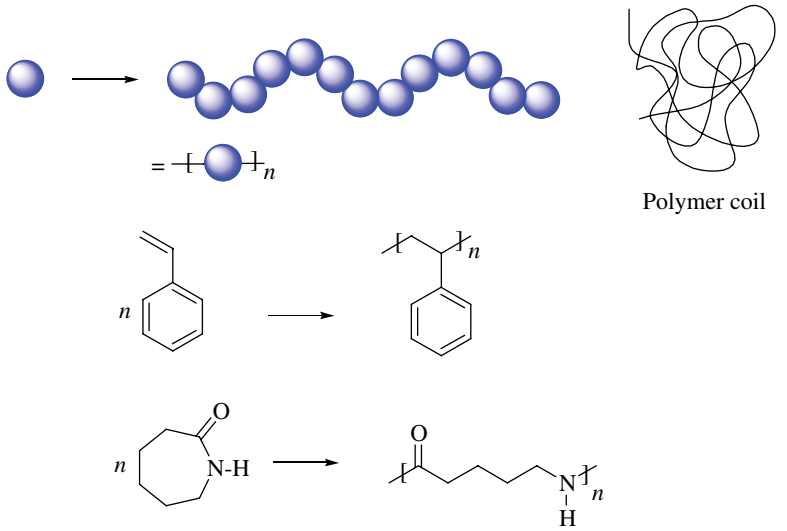

FIGURE 2.1 Schematic representation of linear homopolymer formation from one type of monomer unit and the possibly resulting coil structure; supplemented by the examples of polystyrene and poly(ε-caprolactam) (or nylon 6).

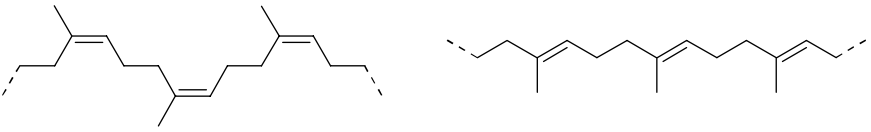

Poly(*cis*-1,4-isoprene)
natural rubber

Poly(*trans*-1,4-isoprene)
gutta-percha, balata

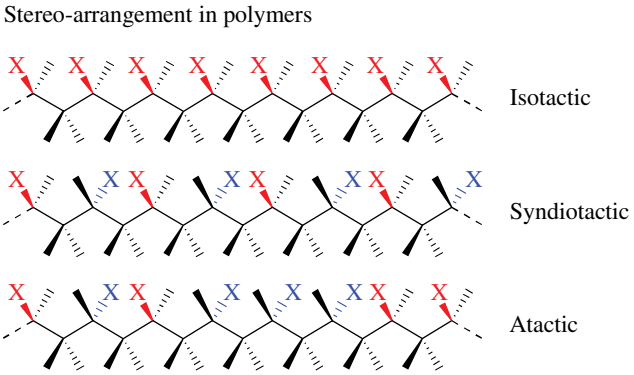

FIGURE 2.2 Monomer arrangements in linear homopolymer chains. (*See insert for color representation of the figure*.)

Short- and long-chain branching can be introduced into polymers. Extreme forms are cross-linked structures, networks, and gels or even perfect dendrimers (Fig. 2.3). These macromolecules have then a *branched architecture*.

Although many of the technically important polymers like polyethylene, polystyrene, and poly(methylmethacrylate) are homopolymers, copolymers, which are made of two or even a larger number of different repeating units, are also very common. The latter can be randomly distributed within a linear polymer chain or added in a special sequence and in a specific topology to create homo- and copolymer architectures (Fig. 2.4).

A specific feature of polymers is the dispersity, which can account for the chemical composition in copolymers, whereby each individual chain may have a different sequence of comonomers (isomers), but this is especially prominent when one looks at the molar mass. Due to the statistic nature of the polymerization process, a mixture of macromolecules of different lengths with a specific distribution in molar mass is always obtained. Thus, values given for the number of repeating units (degree of polymerization DP or P) are always averaged numbers following a certain mathematical description of the distribution curve. These molar mass values can go from a few hundreds g/mol ($DP < 20$) for oligomers to millions g/mol ($DP > 1000$) for ultrahigh molar mass products. Depending on the polymerization process and the amount of control that can be exerted, these distribution curves can be monomodal, broad (Schulz–Flory distribution), or narrow (Poisson distribution), or they can be bi- or multimodal, as is often observed when side reactions or branching occurred (Fig. 2.5).

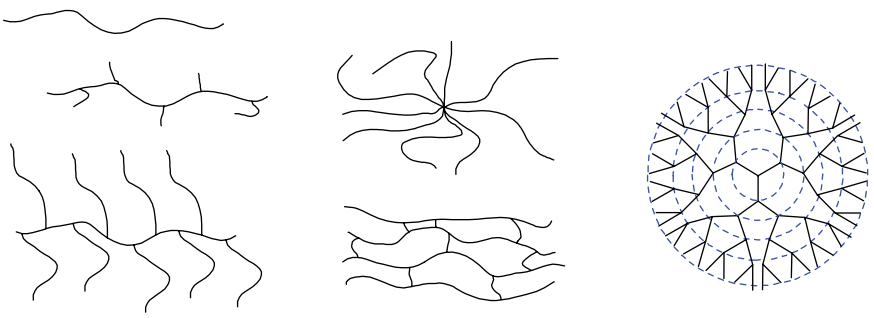

FIGURE 2.3 Schematic representation of linear polymers, short- and long-chain branching (brush) polymers, star-type polymers, and cross-linked polymer chains. The dendrimer structure on the right is an extreme form of highly short-chain branched macromolecules.

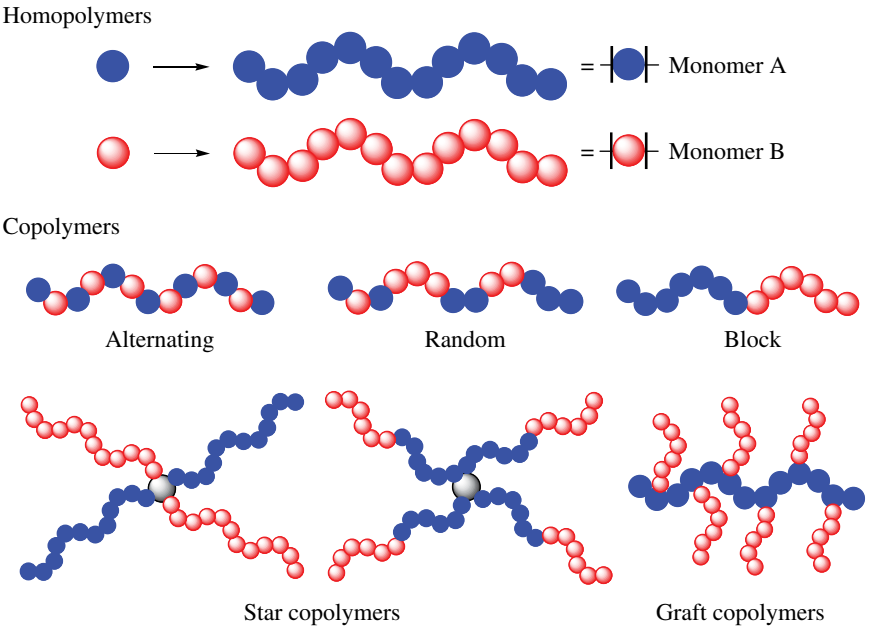

FIGURE 2.4 Examples of homo- and copolymer architectures.

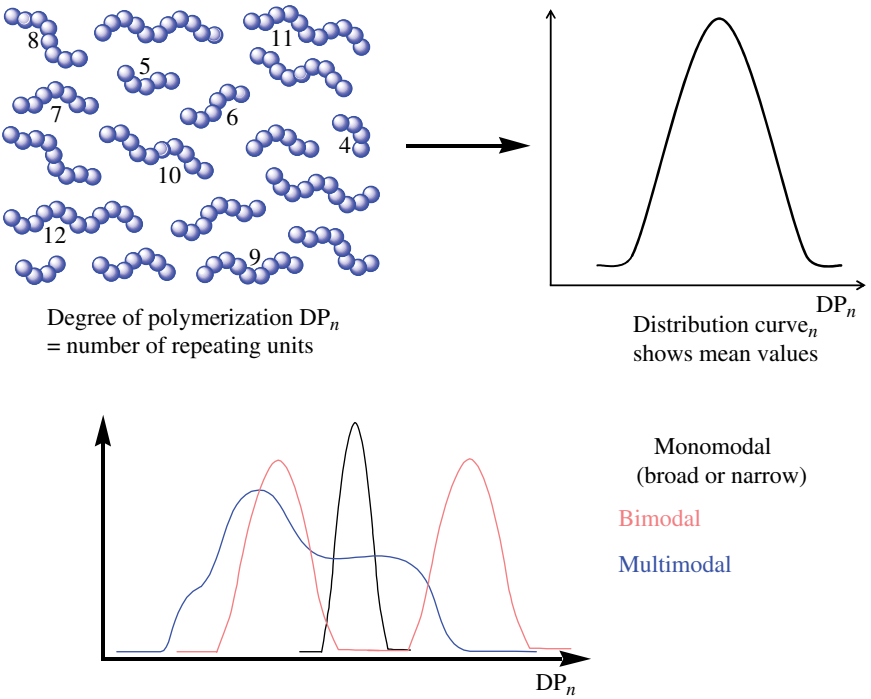

FIGURE 2.5 The mixture of macromolecules of chains with different degrees of polymerization results in a distribution curve. These can be monomodal (broad or narrow), multimodal, or bimodal.

Polymers, especially amphiphilic block and graft copolymer architectures, can further assemble in more complex structures like micelles, polymersomes, defined aggregates, core–shell structures, etc. These structures will be discussed in more detail in Chapter 5.

2.2 MULTIFUNCTIONALITY

Multifunctionality is a highly fashionable term that, although it is still missing a clear definition, is currently being applied to describe various features for macromolecules. First and foremost, it is used to point out that a single macromolecule can have more than one or two functional groups of different natures with various chemical functionalities like an acid or amino group, a charged unit, a hydrogen-bonding unit, a metal complexing unit, a pH-responsive unit, a photoactive unit, etc., which have been introduced into a single polymer chain by using various comonomers or by polymer analogous reactions. This definition has to be clearly differentiated from the term *multivalency* (see Section 2.7), which describes a single macromolecule with several functionalities of the same nature that lead to a cooperative action and enhanced activity or binding capacity. Nevertheless, one has to keep in mind that multifunctionality can also lead to multivalency!

The second, much broader definition of multifunctionality describes any single macromolecule, polymer assembly, or complex material mix that exerts more than one function. Of course, a single macromolecule, which contains, for example, biotin units as well as metal binding units can fulfill two functions: It can bind to streptavidin as well as metal ions. A block copolymer, which consists of a hydrophilic poly(ethylene glycol) chain and a hydrophobic chain, can self-assemble into a polymersome and take up the function of a nanocarrier. In addition, the PEG chain will induce low, unspecific biointeractions that can supply the needed biocompatibility function. A catheter made from a polymer that is coated with a responsive hydrogel that is loaded with an anticoagulant drug fulfills the function of the catheter as technical tool with the needed mechanical properties. Second, it has a low unspecific protein and bacteria adhesion due to the soft hydrogel coating. Furthermore, due to less tissue damage, easy entering into the blood vessels, and less risk for any bleeding, the patient's comfort level is increased. The drug loaded in the hydrogel can be released when reaching the targeted area, for example, in heart surgery, to avoid thrombus formation. This list of examples can be extended indefinitely, which also illustrates the complexity of the term *multifunctionality*.

Thus we would like to reduce the definition of *multifunctional polymer* within this book to its basic meaning of macromolecules and macromolecular

assemblies, which can either undergo different specific interactions and binding actions with various substances or react to diverse stimuli from a number of chemical and biological functional groups that have been structurally introduced.

2.3 BIOCONJUGATES

Bioconjugates comprise a large and multifaceted group of biomolecules, including proteins, nucleic acids, lipids, and carbohydrates, which are customized by a covalent attachment of different molecular entities to provide additional or altered functional features. The conjugated units are often small molecules involving drugs, radionuclides, toxins, and fluorophores but can also consist of larger, polymeric structures such as inhibitors, enzymes, or extended polymer chains. Likewise, the utilized conjugation reactions are very diverse, and common variants include the formation of thioethers, amide bonds, carbon–nitrogen double bonds, and several others.

The most common examples of bioconjugates still consist of proteins carrying fluorophores, biotin, or poly(ethylene glycol). However, many additional types of bioconjugates have been explored in the recent past (Fig. 2.6).

The term "bioconjugate" covers combinations of biomolecules, for example, antibody–enzyme conjugates, and biomolecules linked to synthetic molecules like PEGylated proteins.

Analogs of biomolecules carrying an attached second component have sometimes been referred to as bioconjugates as well. Furthermore, the term bioconjugation has been used in numerous cases when noncovalent molecular interactions were considered, for example, in the complexation of glycosaminoglycans and proteins such as heparin sulfate and growth factors.

2.4 BIOCOMPATIBILITY

The term biocompatibility receives particular attention in the development of materials for medical applications, including polymeric structures. This is especially true in efforts to maximize the intended functionality of the utilized materials while minimizing undesired side effects, which often result from the response of the organism to foreign material through the activation of the blood coagulation and the immune system. Obviously, the related response phenomena are primarily triggered by interfacial processes and the question whether or not a given set of material characteristics fulfills the resulting

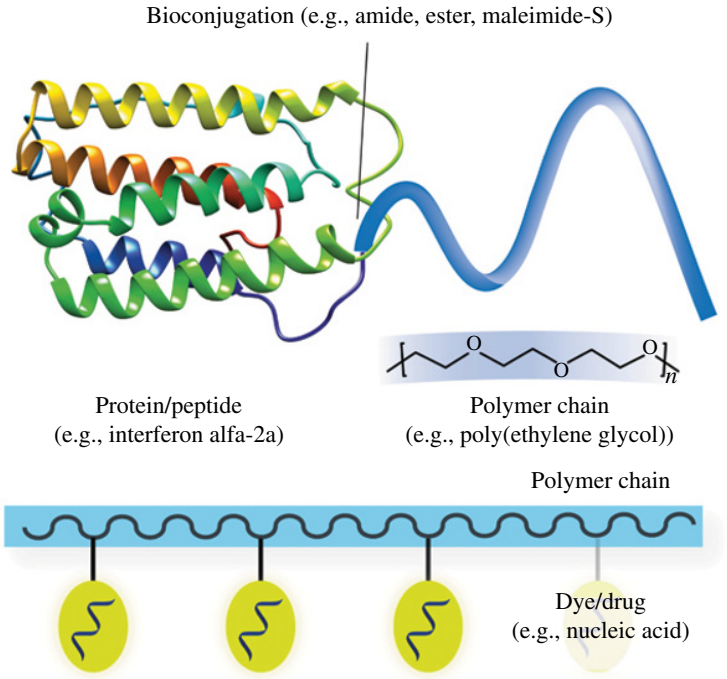

FIGURE 2.6 Schematic representation of possible bioconjugate structures; top: protein—linear synthetic polymer chain conjugate, bottom: synthetic polymer chain conjugated in the side chain with dye or drug molecules, for example, oligonucleotides. Source: Gibbs et al. [1]. Reproduced with permission from American Chemical Society.

requirements has to be answered in view of the particular circumstances of the application: "The ability of a material to perform with an appropriate host response in a specific application" is commonly cited as Williams' definition [2], largely in accordance with a number of similar definitions [3]. Ratner more recently pointed out that new definitions are required for the term "biocompatibility" and made respective proposals [4]. A variety of test procedures have been proposed to assess the biocompatibility of materials experimentally, that is, prior to the intended application, and correlations of intrinsic material's characteristics and the resulting responses of biological tissues have been reported [5]. However, the current understanding of the compositional and structural causes of bioincompatibility reactions is still incomplete and provokes more dedicated research to allow for the rational design of safe and effective materials.

Biocompatibility is also a keystone of regulatory aspects for the application of biomaterials and is reflected in related standards such as the ISO Standard 10993.

2.5 BIODEGRADATION

A biomaterial is a material that interacts with biological systems and can either be of natural or synthetic origin. The degradation of biomaterials can be divided into two main areas, which are called degradation and biodegradation. Degradation takes place via unknown cleavage mechanisms or simple chemistry like hydrolysis or oxidation. Biodegradation describes an environment-mediated cleavage and is also defined as the "breakdown of a substance by external triggers *in vitro* or *in vivo*," which can be further specified according to the level of degradation [6]. Typical external triggers are enzymes, pH, and oxidative/reductive conditions. Primary biodegradation only leads to an alteration of the chemical structure, which results in the loss of a specific property of the substance. An environmentally acceptable biodegradation is achieved when all undesirable properties of the compound are lost. This correlates to primary biodegradation but takes into account that it depends on the environment when a substance can be considered as fully degraded. Ultimate biodegradation refers to the complete breakdown of a compound to either fully oxidized or reduced simple molecules (such as carbon dioxide/methane, nitrate/ammonium, and water).

However, the *in vitro* degradability of a material by an isolated enzyme does not necessarily mean that it is also biodegradable *in vivo*, because the biodegradability of a substance strongly depends on the site and mode of action, for example, if it is used as a drug delivery agent, suture, or implant. Therefore, the biocompatibility and degradability not only of the initially introduced material but also of its degradation by-products are of particular importance.

2.6 BIOACTIVITY

In general, bioactivity defines the effect of any substance upon a living organism or on living tissue and is, as such, not restricted to polymeric structures or materials. However, the common use of the term refers to specific molecular recognition events, which result from the capability of biomolecules to undergo highly effective noncovalent interactions. Examples include the binding of cellular receptors to their molecular ligands, antibodies recognizing antigens, molecular inhibitors that associate with a target molecule, and enzymes interacting with their substrates (Fig. 2.7).

In the context of this book, the term "bioactivity" is mainly applied to polymers that incorporate elements capable of molecular biological recognition, such as peptide sequences serving as cell adhesion ligands and polyanionic sites that utilize electrostatic interactions for the biomimetic presentation of

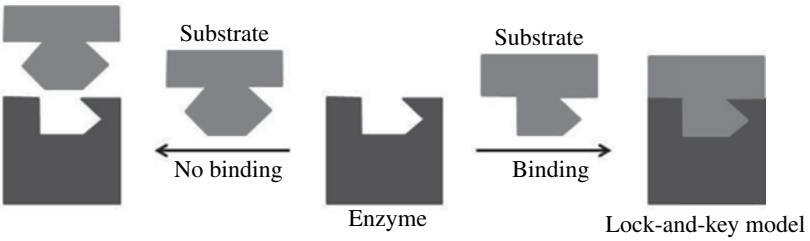

FIGURE 2.7 Schematic representation of the concept of biomolecular recognition exemplified for enzyme–substrate interactions. Note that the interaction involves a combination of geometrically matching intermolecular forces that are additionally modulated by thermodynamic and kinetic effects.

signaling molecules. Bioactivity can result in the fragmentation or formation of polymeric architectures, for example, through enzymatic cleavage or linkage of peptide-functionalized polymers, including matrix metalloprotease-sensitive polymer networks or transglutaminase (FXIIIa)-catalyzed cross-linking.

Bioactivity is generally dosage dependent, which often requires careful consideration to achieve the desired effect.

2.7 MULTIVALENCY

Multivalency is a key principle in nature for achieving strong yet reversible interactions between multifunctional molecules and biological surfaces (Figure 2.8). Interactions between an m-valent receptor and an n-valent ligand ($m, n > 1$; and $m \neq n$) are considered multivalent. Interactions between a number of monovalent ligands ($m = 1$) with a multiple receptor or vice versa are not multivalent. The n number of equivalent binding pockets of the multivalent receptor already gives monovalent ligands favorable interaction conditions, because an m-valent receptor binds first m times more often to the monomer ligand than to the corresponding monovalent receptor. If the receptor and ligand have identical binding sites, they are homomultivalent. If they have multiple binding sites, which are different from each other, they are considered to be heteromultivalent.

In addition to multivalent interactions, the term polyvalency is used, especially if polyfunctional ligands bind to receptors on interfaces like cell membranes, which offer a large number ($n >> 10$) of two-dimensionally distributed binding sites, such as extended biological surfaces (e.g., bacteria, cells, viruses) [7, 8].

To characterize multi- or polyvalent binding effects, Whitesides et al. [7] proposed an amplification factor β (Eq. 2.1) that is composed of taking the ratio

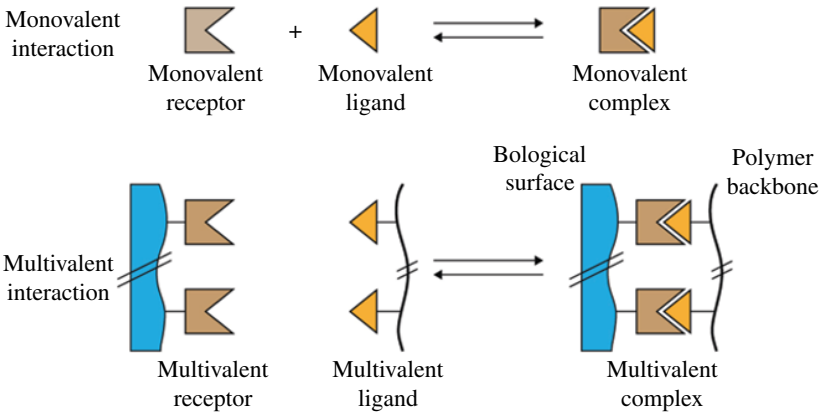

FIGURE 2.8 Comparison between monovalent and multivalent interactions of multifunctional polymers with biological receptors, for example, proteins.

of the binding constants for the multivalent binding [K_{multi}] of a multivalent ligand and a multivalent receptor with the binding constants for the monovalent binding [K_{mono}] of a monovalent ligand and a multivalent receptor:

$$\beta = \frac{K_{multi}}{K_{mono}} \tag{2.1}$$

An advantage of this amplification factor is that it can be used even if the multiplicity of effective bonds is unknown. A disadvantage is that it simultaneously also includes the influence of the cooperativity and the symmetry effect.

Despite repeated clarification in the literature, there is still a widespread misconception that multivalent interactions are inherently associated with positive cooperativity [8]. A multivalently enhanced binding may also be useful when the binding is not additive or positively cooperative. As a result, multivalent drugs can be conceivably administered in much smaller doses at the target receptor because of the stronger binding and higher specificity without losing any more efficacy than corresponding monovalent analogs.

In all multivalent systems, the structures connecting the different ligands as part of a rigid skeleton or even as a flexible polymer chain play a crucial role. The term "spacer" is used regardless of the chemical nature and structure of this connecting polymeric link. Its flexibility has significant influence on the thermodynamic description, as noticeably different symmetry factors for very flexible and very rigid ligands have to be taken into consideration here.

2.8 BIONANOTECHNOLOGY

Nanotechnology deals with the design, synthesis, study, and application of materials at the nanometer scale, that is, sizes of about 1–100 nm. When it is used in connection with biology or medicine, it is referred to as bionanotechnology or nanobiotechnology. Both terms are often used synonymous to describe the interdisciplinary technology that sits at the interphase between nanotechnology and biological systems. However, one can distinguish between two different approaches, one of which is the use of nanotechnology to study and understand biological systems while the other aims at the use of biomaterials to generate new nanomaterials.

One example are magnetic nanoparticles [9], which have to be coated with a polymer layer (e.g., poly(ethylene glycol) (PEG), dextran, poly(vinyl pyrrolidone) (PVP), fatty acids, polypeptides, chitosan, gelatin, etc.) in order to protect them and adjust their solubility as well as retention time in the body. The polymer layer also serves as a platform for the attachment of targeting molecules, therapeutics, or other imaging tags (Fig. 2.9).

A prominent example for the generation of new nanomaterials from biopolymers is the so-called DNA origami. This method allows the synthesis of complex DNA structures of about 100 nm size from a single strand of the natural

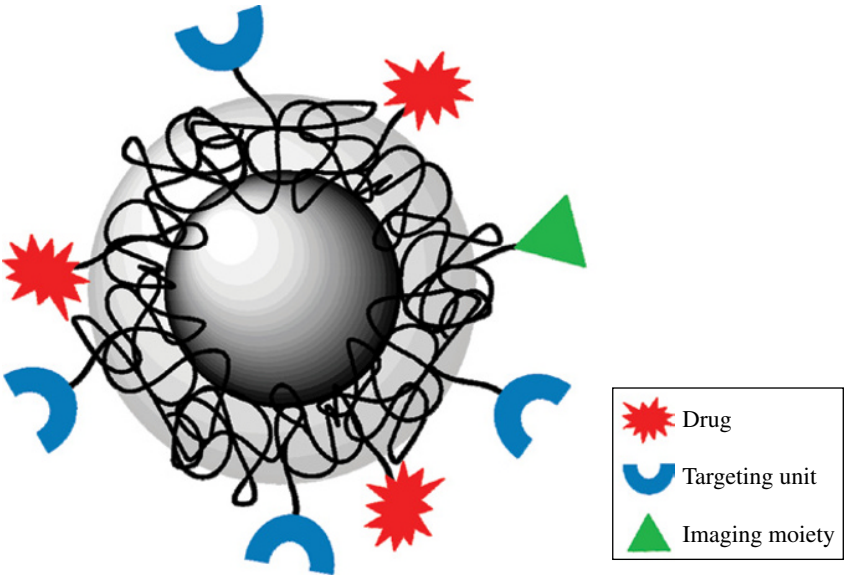

FIGURE 2.9 Schematic representation of a magnetic nanoparticle with the protective polymer layer and attached targeting, therapeutic, or imaging moieties.

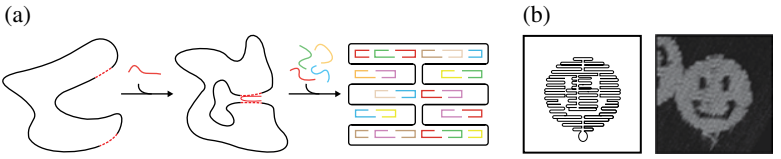

FIGURE 2.10 (a) The concept of DNA origami for the fabrication of 2D and 3D nanostructures; (b) Examples of realized structures through DNA assembly. Source: Adapted from Rothemund [10], figure 2. Reproduced with permission from Nature Publishing Group.

polymer DNA. Using hundreds of short DNA strands called staples, this DNA strand can be folded into two- and three-dimensional structures in a single step (Fig. 2.10). This method has already been used to construct transmembrane channels as well as nanostructures for the transport of molecular loads into cells.

Another example is the use of natural motor proteins—so-called ATPases—as nanomotors for the delivery of drugs, genes, or peptides. ATPases use chemical energy provided by the hydrolysis of adenosine-5′-triphosphate (ATP) and transform it to mechanical work with nearly 100% efficiency. This enables them to move objects thousands of times their weight at high speed.

REFERENCES

[1] Gibbs, R. M.; Park, S.-J.; Anderson, D. R.; Watson, K. J.; Mirkin, C. A.; Nguyen, S. T. *Journal of the American Chemical Society* 2005, 127, 1170–1178.

[2] Williams, D. F. *The Williams Dictionary of Biomaterials*; Liverpool University Press, Liverpool: 1999.

[3] Black, J. *Biological Performance of Materials*; CRC Press, Boca Raton: 2006.

[4] Ratner, B. D. *Journal of Cardiovascular Translational Research* 2011, 4, 523–527.

[5] Williams, D. F. *Biomaterials* 2008, 29, 2941–2953.

[6] McNaught, A. D.; Wilkinson, A. *IUPAC Compendium of Chemical Terminology (Gold Book)*; Blackwell Scientific Publications, Oxford: 1997.

[7] Mammen, M.; Choi, S.-K.; Whitesides, G. M. *Angewandte Chemie International Edition* 1998, 37, 2754–2794.

[8] Fasting, C.; Schalley, C. A.; Weber, M.; Seitz, O.; Hecht, S.; Koksch, B.; Dernedde, J.; Graf, C.; Knapp, E. W.; Haag, R. *Angewandte Chemie International Edition* 2012, 124, 10622–10650.

[9] Yigit, M. V.; Moore, A.; Medarova, Z. *Pharmaceutical Research* 2012, 29, 1180–1188.

[10] Rothemund, P. W. K. *Nature* 2006, 440, 297–302.

3

PREPARATION METHODS AND TOOLS

In this chapter, some basic fundamentals and the most common methods and techniques for the synthesis and modification of functional and well-defined macromolecules and bioconjugates are described. Please note that it is not the aim to give all details and aspects of polymerization methods used widely today. For that, the reader is referred to textbooks in polymer chemistry [1, 2].

3.1 GENERAL ASPECTS OF POLYMER SYNTHESIS

The formation of synthetic polymers is a process that occurs via chemical connection of many hundreds up to many thousands of monomer molecules. As a result, macromolecular chains are formed. They are, in general, linear but can be branched, hyperbranched, or cross-linked as well. However, depending on the number of different monomers and how they are connected, homopolymers or one of the various kinds of copolymers can result. The chemical process of chain formation may be subdivided roughly into two classes, depending on whether it proceeds as a chain growth or as a step growth reaction (Fig. 3.1).

The buildup of the polymer chain with monomer conversion differs significantly depending on the class of polyreaction used. In a chain growth process, the molar mass increases rapidly and reaches a plateau value already at low monomer conversion; if chain growth is well controlled or "living," then a linear dependency of degree of polymerization versus monomer conversion

Bio- and Multifunctional Polymer Architectures: Preparation, Analytical Methods, and Applications, First Edition. Brigitte Voit, Rainer Haag, Dietmar Appelhans, and Petra B. Welzel.

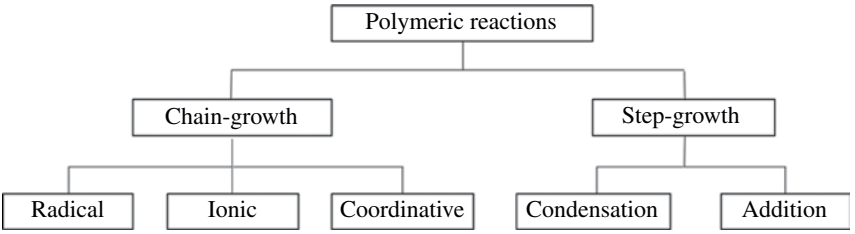

FIGURE 3.1 Classification of reaction mechanisms used to build up polymers.

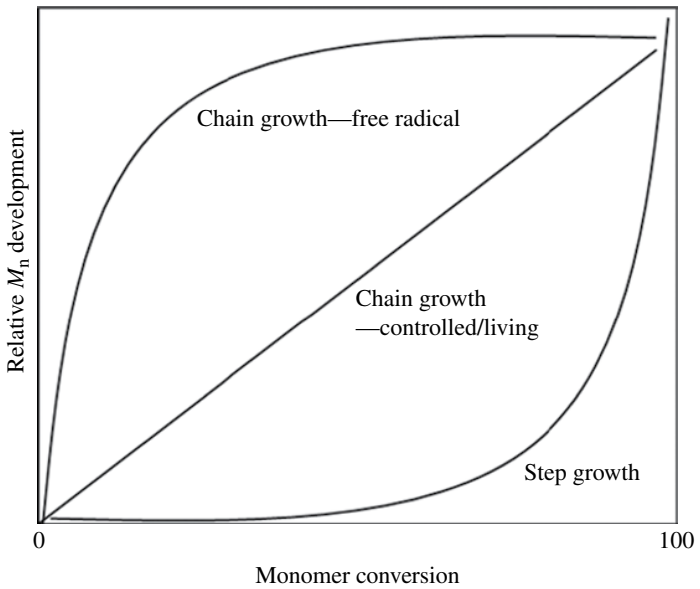

FIGURE 3.2 Schematic representation of the development of molar mass, for example, M_n, with monomer conversion for chain growth (free radical), chain growth (living) and step growth mechanisms for the polymer buildup reaction.

can be achieved. In contrast, in a step growth process only at very high functional group conversion (>90%) high molar mass products can be achieved (Fig. 3.2).

3.1.1 Chain Growth Polymerizations

Chain growth polymerizations (also called addition polymerizations in the English terminology, which should not be mistaken as polyaddition that belongs to the step growth processes) are characterized by the occurrence of activated species, so-called initiators and active centers. The initiator adds one monomer molecule after the other in a way that at the terminus of each new

species formed by a monomer addition step, an activated center is created, which again is able to add the next monomer molecule. Active initiators are formed from compounds that create radicals via homolytic bond scission, from metal complexes, or from ionic (or at least highly polarized) molecules in the initiating steps. From there the chain growth can start as a cascade reaction upon manifold repetition of the monomer addition and reestablishment of the active center at the end of the respective new product. Finally, growth of an individual macromolecule is arrested in either a termination or a transfer step. While termination leads to the irreversible disappearance of an active center, chain transfer results in the growth of a second chain while the first one is terminated. Here, the active center is transferred to another molecule (solvent, initiator, monomer, etc.) where it is able to initiate further chain growth. The resulting "dead" polymer, on the other hand, can continue its growth only when activated in a subsequent transfer step. Because in general this reactivation does not occur at the terminal monomer unit but somewhere in the chain, branched or cross-linked products will result. In conclusion, chain growth polymerizations are typical chain reactions involving a start-up step (initiation) followed by many identical chain reaction steps (propagation)—stimulated by the product of the first start-up reactions. Transfer processes may continue until, finally, the active center disappears in a termination step.

Monomers appropriate for chain growth polymerizations either contain double or triple bonds or are cyclic, having a sufficiently high ring strain. Depending on the nature of the active center, chain growth reactions are subdivided into radical, ionic (anionic, cationic), or transition metal-mediated (coordinative, insertion) polymerizations. Accordingly, they can be induced by different initiators or catalysts. Whether a monomer polymerizes via any of these chain growth reactions—radical, ionic, and coordinative—depends on its constitution and substitution pattern. Also, external parameters like solvent, temperature, and pressure may also have an effect. The two main processes for the synthesis of ton-scale commercial polymers (Fig. 3.3) are free radical polymerization (done in bulk or heterogeneous systems like in emulsion and dispersion polymerization) and insertion polymerization for polyolefins.

Due to the high importance of chain growth polymerization for polymer production, huge efforts have been undertaken to understand and elucidate the kinetics involved in the chain growth process and the parameters influencing molar mass, dispersity $Đ$, and the nature of the resulting macromolecules. In Figure 3.4, the kinetic steps, exemplified for a free radical process, are outlined.

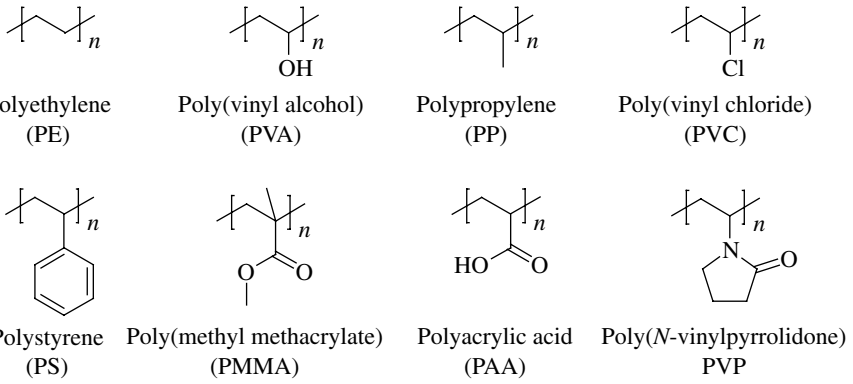

FIGURE 3.3 Examples of commercially important polymers prepared by chain growth processes (Note: PVA is formed from poly(vinyl acetate) after an additional polymer analogous reaction).

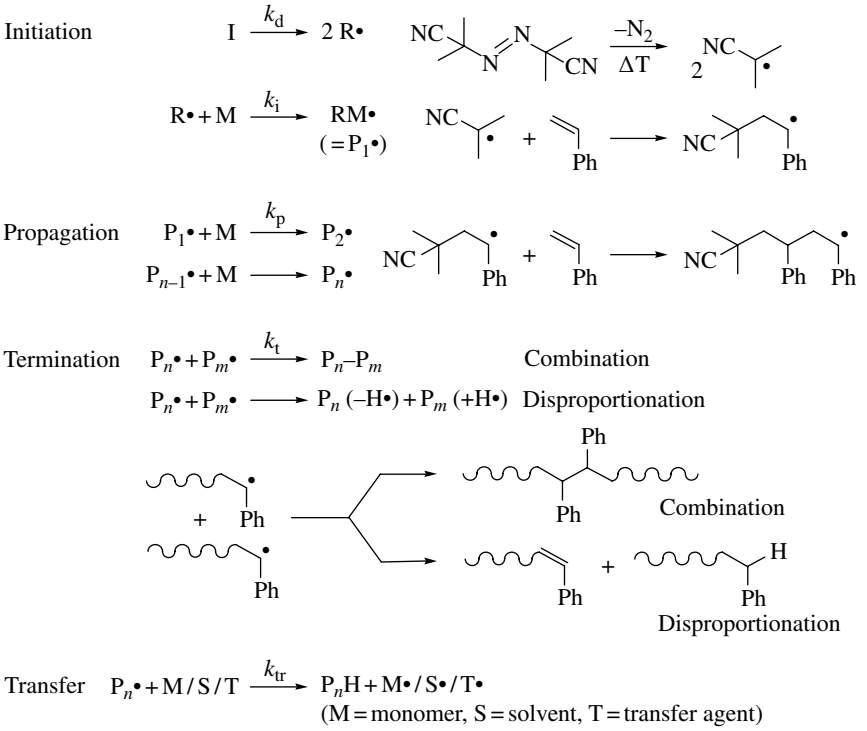

FIGURE 3.4 Polymerization steps and kinetic equations relevant in the chain growth polymerization exemplified for the free radical polymerization of styrene initiated with azobisisobutyronitrile (AIBN) (k_{index} denote the kinetic constants for decomposition (d), initiation (i), propagation (p), termination (t), and transfer (tr)).

The high versatility in the possible monomer structure with the chance to introduce polar, charged, or specifically interacting units as pendent groups onto a mostly all-carbon backbone prepared by the chain growth process made this type of polymer building reaction from the beginning highly attractive to produce "functional" polymers as in contrast to "structural" materials. Thus, poly(acrylic acid), a very common polyelectrolyte, is prepared by free radical polymerization as well as many other functional homo- and copolymers. In recent years, the strong advances in controlling chain end activity and thus allowing to much better control molar mass, dispersity, and architecture of the polymers made the chain growth process the ideal method to prepare tailor-made, multifunctional polymers.

3.1.2 Step Growth Polymerizations

In step growth reactions, no specific activated centers are present to force the connection of the monomers. Instead, the monomers are tied together in discreet, independent steps via conventional organic reactions such as ester, ether, amide, or urethane formation. Depending on whether small molecules are set free in the connection step, one distinguishes between polycondensations and polyadditions.

Evidently, monofunctional molecules cannot result in polymer chains via step growth polymerizations. Instead, each monomer molecule as well as all intermediates must possess two functional groups. When more than two reactive groups are present in a monomer, branched or cross-linked products will result. Moreover, step growth polymerizations are categorized according to how the functional groups are assigned to the monomers. When each monomer bears two identical functional units, the process is called AABB-type polycondensation/polyaddition. Here, mixtures of at least two different types of monomers are required, bearing the complementary functional groups. If, on the other hand, each monomer molecule bears the two complementary functional groups required for step growth polymerization, the process is called AB-type polycondensation/polyaddition.

As a consequence of the lack of special active centers, the chain formation in step growth polymerizations occurs via a sequence of accidental and independent reaction events. It proceeds via dimers, short and longer oligomers until, finally, at conversions higher than 99% long chains are formed, which are called condensation polymers (polycondensates) or addition polymers, respectively. Apart from high degrees of conversion, also a very precise 1:1 equivalence of the complementary functional groups is essential to achieve very high molar masses. Polycondensation and polyaddition reactions have

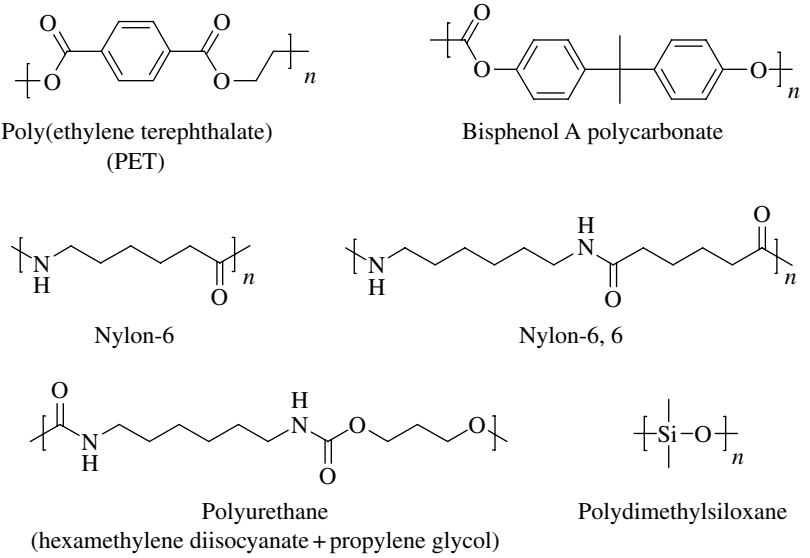

FIGURE 3.5 Examples of commercially important polymers prepared by step growth polymerization.

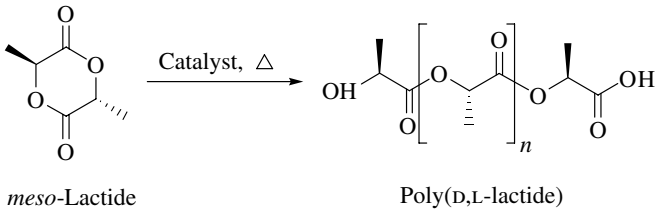

FIGURE 3.6 Cationic ring-opening polymerization (CROP) of *meso*-lactic acid dimer toward poly(D,L-lactide).

high technical importance for a variety of structural polymer materials like polyesters, polyamides, and polyurethanes (Fig. 3.5) and are often prepared in bulk at high temperatures.

Many naturally occurring biomacromolecules like polypeptides and polyesters look like they are polycondensates due to the amide and ester bonds in the main chain, but nature uses processes that are closer to a chain growth than a step growth kinetic scheme even though each monomer unit is selectively added in an individual step. Also, a number of interesting biodegradable polyesters, for example, poly(lactic acid), are prepared by ring-opening cationic polymerization or enzymatically from the cyclic dimeric monomer structure (see Fig. 3.6 and Section 3.6). Other polyesters, like poly(hydroxyl butyrate), can be prepared by a microbial synthesis in a biotechnological process.

3.1.3 Modification of Polymers

The third possibility for synthesizing polymeric substances is the modification of existent natural or synthetic macromolecules. Chemical modifications are reactions on macromolecules without degradation of the main chain (macromolecular substitution routes, "polymer analogous reactions") like hydrolysis, esterification, and etherification of side groups. These reactions have very high technical importance, for example, poly(vinyl alcohol), a very widespread polymer used in many polymerization processes as stabilizers as well as in many hygiene and cosmetic products, is only prepared after a chain growth polymerization of vinyl acetate and subsequent ester hydrolysis of the resulting poly(vinyl acetate) to poly(vinyl alcohol) (see Fig. 3.7). Partial hydrolysis leads to PVA–PVAc copolymers, which are technically important stabilizers. Other examples of technically important products prepared by polymer analogous reactions are ion exchange resins based on cross-linked polystyrene beads. Those polymer beads can be sulfonated or quaternary amino groups are introduced in order to achieve the charged units in the final resin product.

However, for many years, polymer analogous reactions were neglected in the "macromolecular engineering" of well-defined polymers since often the reactions had been random and nonquantitative and side products could not be removed from the products. However, in the recent years with the development of highly efficient organic reactions and their transfer into polymer chemistry approaches, polymer analogous reactions had a major revival not only for introducing functional side groups but also for efficiently modifying polymer chain ends and even coupling those to polymers and biomacromolecules.

3.2 CONTROLLED POLYMER SYNTHESIS

The past decade has witnessed the explosive development of controlled/living polymerization processes that allow synthesis of macromolecules with *precisely controlled* architecture, molar mass, and functionality from a wide range of

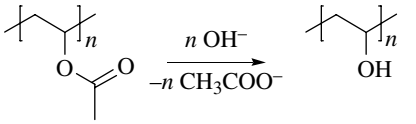

Poly(vinyl acetate) (PVAc) Poly(vinyl alcohol) (PVA)

FIGURE 3.7 Synthesis of poly(vinyl alcohol) by hydrolysis of poly(vinyl acetate).

monomers [3]. It was recognized that properly designed polymer-based materials (block copolymers, polymer brushes, stars, "hairy" nanoparticles, etc.) are able to self-assemble into well-defined ensembles that exhibit new and frequently predictable properties. As a result, a plethora of new functional materials have been designed and prepared, including molecular composites, hybrids, and bioconjugates that already found numerous applications in various branches of science and technology. Development of efficient, diverse, and, at the same time, technically simple synthetic tools (such as polymerization for "everyone") [4] allows designing and synthesis of new polymer-based materials even in *nonspecialized laboratories* (e.g., physical or biological)—in the places where these materials can be further tested. This significantly extends a number of researchers dealing with polymers. This can considerably shorten the distance between designing of new polymers and their application that is extremely valuable for multidisciplinary branches of science (nanoscience, biology, materials science, medicine, electronics, etc.).

The term "controlled polymer synthesis" similar as the term "macromolecular engineering" developed roughly within the last 30 years and describes polymerization processes that allow a higher control over the molar mass, dispersity, chain end activity, architecture, copolymer composition, and finally property design as it can be achieved in, for example, a free radical polymerization showing irreversible chain termination and transfer. This term comprises various forms of control from a full "living polymerization" exhibiting no chain termination at all throughout the polymerization (and is accounted only for anionic polymerization of specific monomers under very stringent and specific conditions) to "living-type" polymerizations where part of the characteristic features of the a living polymerization is retained and to processes where at least block copolymer structures can be obtained but low control of the chain end, molar mass, and dispersity is given. Actually, the term is not very precise and clear definitions are still missing even though recently more groups elaborate in kinetic and mechanistic studies after in the beginning the design of new polymer structures dominated. In Table 3.1, the major characteristics of living and controlled polymer synthesis are summarized. Most importantly, any control is only achieved when irreversible termination of the growing chain end is avoided or at least significantly suppressed.

3.2.1 Anionic Polymerization

Anionic polymerization, due to the charged nature of the chain end, is much more prone for exerting control than any radical polymerization since typical termination reactions like radical–radical combination and disproportionation

TABLE 3.1 Differences and Common Features of Living Anionic and Controlled Radical Polymerization Processes (Kinetic Constants According to Fig. 3.4)

Living Anionic Polymerization	Controlled Radical Polymerization
No termination	Irreversible termination suppressed
Initiation spontaneous, $k_i >>> k_p$	Initiation as fast or faster than growth, $k_i \geq k_p$
Growing species is active throughout the full polymerization	Growing species only active for a very short time
	$M_w/M_n << 2$, mostly 1.1–1.3
Poisson distribution $M_w/M_n < 1.01$	Large variety also of functional monomers can be used
Limited freedom in monomer structure due to high sensitivity to protonic impurities	Robust with regard to polymerization conditions and impurities
Very stringent polymerization conditions and often low temperatures are necessary	
Common Features	
First-order kinetics with regard to monomer conversion	
M_n increases linearly with monomer conversion	
DP defined by $[M]/[I] \times$ monomer conversion	
No or only controlled transfer	
Thus, active chain end controls:	
• New monomer addition: M_n increases further	
• Block copolymer formation possible through second monomer addition	
• End group functionalization possible	
• Access to complex polymer architectures	

cannot take place. However, the anionic chain end is extremely reactive and can react easily with oxygen or any protic impurity, which can result from traces of water, air, any protic solvent, or from monomer functional units. This reactivity is enhanced with increasing temperature. Thus, very stringent polymerization conditions have to be applied like very low reaction temperature (typically below 0°C), and solvents and monomers have to be purified rigidly from water traces. Thus, the monomers and solvents used in this polymerization process are limited avoiding any proton donors. Still, the term "living polymerization" was first defined for the anionic polymerization of styrene (in THF at −100°C) by Szwarc [1] proofing that no chain termination occurred, that each chain started at the same time as soon as initiator was added, and that the amount of growing chain ends stayed constant over the whole polymerization process. Chain ends have to be actively stopped by adding a terminating agent

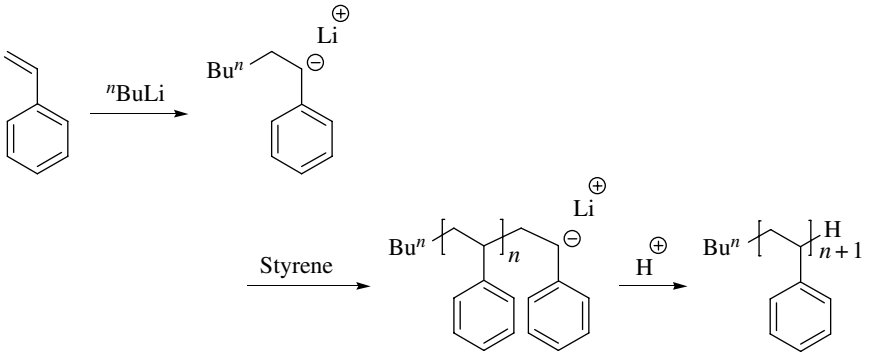

FIGURE 3.8 Living anionic polymerization of styrene initiated by *n*-butyllithium (^{n}BuLi).

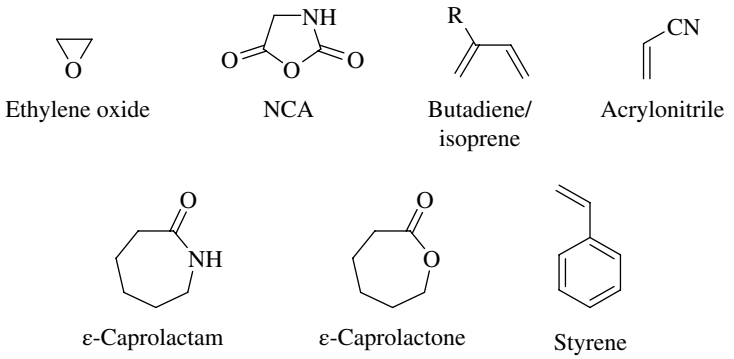

FIGURE 3.9 Important monomers for anionic polymerizations.

like water, alcohol, or amines. Thus, molar mass develops linearly with monomer conversion and a narrow Poisson distribution is found for the molar mass distribution with M_w/M_n as low as 1.01. Figure 3.8 shows the anionic polymerization of styrene using *n*-butyllithium as the initiator, which adds in a nucleophilic addition to the double bond of styrene.

A variety of important monomers are polymerized via anionic polymerization including cyclic ones like ethylene oxide as base for poly(ethylene oxide) (PEO) or poly(ethylene glycol) (PEG) and *N*-carboxyanhydrides (NCAs) used for making polypeptides and caprolactam, the monomer of nylon 6 (Fig. 3.9). Whereas in all cases rather stringent conditions have to be used to allow at least an efficient polymerization, for technical products often not fully "living" conditions are achieved, which leads to broader molar mass distributions.

As initiators nucleophilic substances are used like amines, phosphanes, alkoxides, carbanions, and Grignard reagents. Strong electron acceptor monomers like cyanoacrylate can be already initiated by water (used in

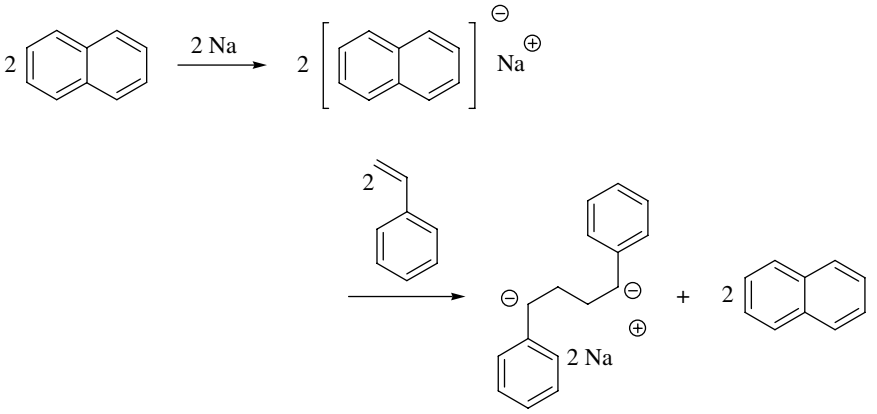

FIGURE 3.10 Formation of the distyryl dianion as bifunctional initiator for the anionic polymerization.

superglue), whereas less electron-accepting monomers need stronger nucleophilic initiators. Important are also the solvents used; whereas in THF an initiator like ^{n}BuLi dissociates quickly in free anions, in toluene ionic associates are formed, which have first to dissociate before a defined initiations takes place. Initiators can also be generated by electron transfer as commonly done by using naphthaline sodium and styrene in THF (Fig. 3.10). Here, naphthaline is reduced by sodium metal and an electron is transferred to styrene which resonance stabilizes to a distyryl dianion, which then acts as a bifunctional initiator. In this case, the resulting polymer chain has two identical end groups and a molecular weight that is doubled compared to a monofunctional initiator.

Since any well-working anionic polymerization needs a terminating agent to be stopped, early on this reaction step has also been used to introduce functional units into the chain end. Thus, a living anionic chain end stopped with CO_2 and water leads to carboxylic end groups. Very prominent is end group functionality control in PEO by initiation as well as terminating agents (Fig. 3.11). Ethylene oxide initiated with sodium hydroxide and stopped with HCl leads to PEG with two OH end groups. Initiation with methanolate and stopping with HCl leads to a monomethyl ether PEG; stopping with chloroethyl amine leads to an amino-functionalized PEG (Fig. 3.11), and by this a large variety of end-functionalized PEGs are today available from a number of suppliers. This includes PEG oligomers and low molar mass polymers (typical molar masses between 200 and 2000 g/mol) with azide and active ester end groups well suited for bioconjugation. Please note that PEG is also available through ring-opening cationic polymerization.

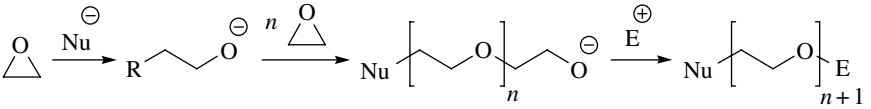

FIGURE 3.11 Poly(ethylene glycol) synthesis having active functional end groups (Nu^-, nucleophile or OH^-; E^+, electrophile or proton).

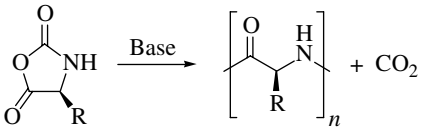

FIGURE 3.12 Anionic *N*-carboxyanhydride (NCA) polymerization toward polypeptides.

Interesting is also the ring-opening polymerization (ROP) of so-called NCAs, which leads to polypeptides (Fig. 3.12) [5].

Anionic polymerization dominated in the beginning the preparation of block copolymers and is still the method of choice if very low dispersities are aimed for the individual block since no other methods allow so well to avoid chain termination and other side reactions. But this is only achieved under the prerequisite of very stringent control of the polymerization conditions and posing extremely high demands on the purity and dryness of solvent and monomer. Still, it offers the highest end group control and thus allows easily to introduce specific end functions, for example, for bioconjugation or polymer–polymer coupling. It is also the ideal method for block copolymer formation through the chain extension with a second or even a third monomer or for the preparation of star- and comb-shaped polymers. Exiting and very complex polymer architectures are formed up to now by anionic polymerization, which further allow well-controlled self-assembly. But an increasing amount of controlled radical polymerization (CRP)-derived block copolymers is being today reported (see Section 3.2.3).

3.2.2 Cationic Polymerization

Cationic polymerizations are initiated by electrophilic initiators. During the reaction of the electrophile with the electron-rich monomer, a carbenium ion is formed, which by itself can again react with a monomer. Figure 3.13 shows common monomers suitable for cationic polymerization. There are many that are polymerized through *cationic ring-opening polymerization* (CROP). Typical initiators are Brønsted acids (H_2SO_4), Lewis acids ($AlCl_3$, BF_3), or carbenium ions (tritylium cation, acylium ion), as solvents dry

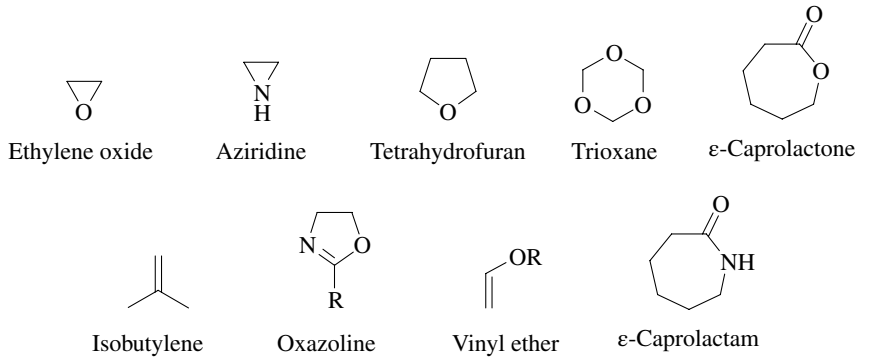

FIGURE 3.13 Typical monomers for the cationic polymerizations.

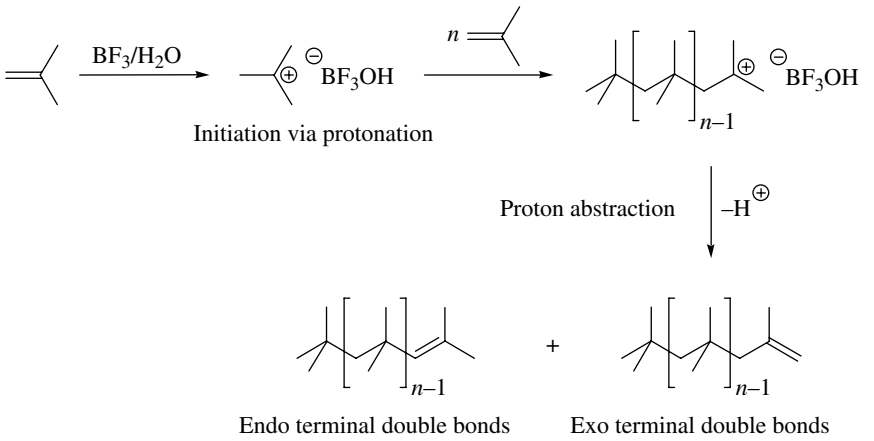

FIGURE 3.14 Typical initiation reaction of isobutylene via protonation and the two main types of products with unsaturated end groups formed.

dichloromethane, acetonitrile, or chlorobenzene work well and reaction temperatures vary from −70 to −150°C.

Even though termination in cationic polymerization cannot occur via chain coupling, most of the cationic polymerizations do not show features of a controlled polymerization due to a high tendency for chain transfer and other termination reactions. Figure 3.14 shows the technically highly important cationic polymerization of isobutylene with the typical unsaturated end groups as a result of proton transfer. In that case, only at temperatures below 0°C reasonable high molar masses can be achieved when chain transfer is suppressed. Furthermore, living-type cationic polymerization has been developed for isobutylene, which allows end group and molar mass control for the preparation of, for example, amphiphilic gels and thermoplastic elastomers (based on polyisobutylene and polystyrene blocks) used in biomedical applications [6, 7].

CROP is widely used also for a number of technical important polymers. Thus, the biodegradable polyester polylactic acid (PLA) is a result of CROP of the cyclic dimer (formed by D or L-lactic acid), initiated usually with Lewis acids like Sn(II) octanoate (Fig. 3.6). PLA is used widely in medicine, for example, for surgery as sewing yarn, as bone replacing parts, or for wound covering since its degradation can be well controlled and the degradation products are nontoxic although an acidification of the surrounding tissue occurs. The degradation behavior is highly dependent on the crystallinity achieved, which itself depends on the D- and L-lactic acid content (crystalline, 1–2 years; amorphous, several weeks).

Similarly, the biodegradable polyesters polyglycolic acid and poly(ε-caprolactone), also used for implantable devices (degradation even slower than that of PLA), drug delivery, and suture materials, are prepared by CROP using stannous octanoate and other catalysts as cationic initiators [8].

A further technically important polymer produced via cationic polymerization is poly(ethylene imine) (PEI). PEI is polymerized from aziridine via protons (Fig. 3.15). It is a highly branched product due to chain growth also through the secondary amines, and it is used, for example, for paper treatment and coatings. More recently, it has also drawn interest for biomedical applications despite its relatively high cytotoxicity [9].

Another very interesting class of materials that are polymerized via cationic polymerization is polyoxazolines [10]. Their properties like solubility, hydrophilicity, or special functionality can be controlled by the monomer substituent in 2-position. Methyl- and ethyloxazolines are hydrophilic and nontoxic and lead to water-soluble polymers with high potential in biomedical use [11], whereas oxazolines with propyl, butyl, octyl, dodecyl, and phenyl in 2-position lead to hydrophobic polymers. The monomers are readily prepared by the reaction of ethanolamine with various R-substituted methyl esters (Fig. 3.16).

Polyoxazolines are known since the 1960s. They can be produced in a living-type manner at rather high temperatures (40–120°C) using mineral acids, Lewis acids, carbocations, benzylpyridinium/benzylanilinium ions, acid halogenides, and rather often benzyl halogenides and methyltrifluoromethanesulfonate. Molar masses can be controlled by the initiator concentration and it is possible to reach dispersities below 1.1. Depending on the nucleophilicity of the counterion, one proposes either a stable, fast initiating oxazolinium ion or a ring-opening covalent species. For iodide and tosylate as counterion, the ionic mechanism dominates, for chlorides, the covalent one. The living nature of that type of polymerization allows, for example, controlled chain end functionalization via termination with functional amines as well as

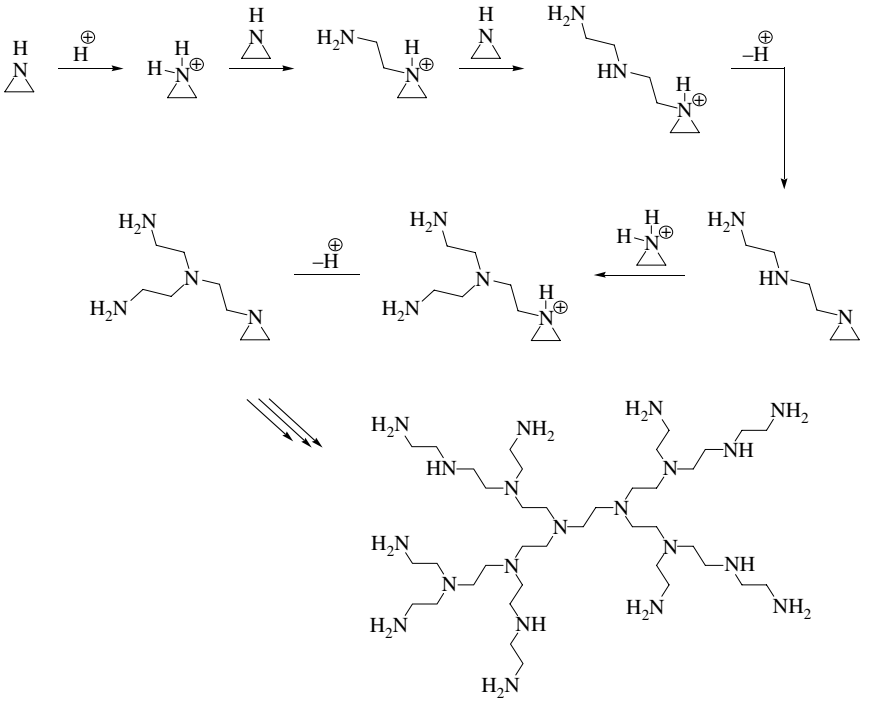

FIGURE 3.15 Cationic polymerization of aziridine toward highly branched poly-(ethylene imine).

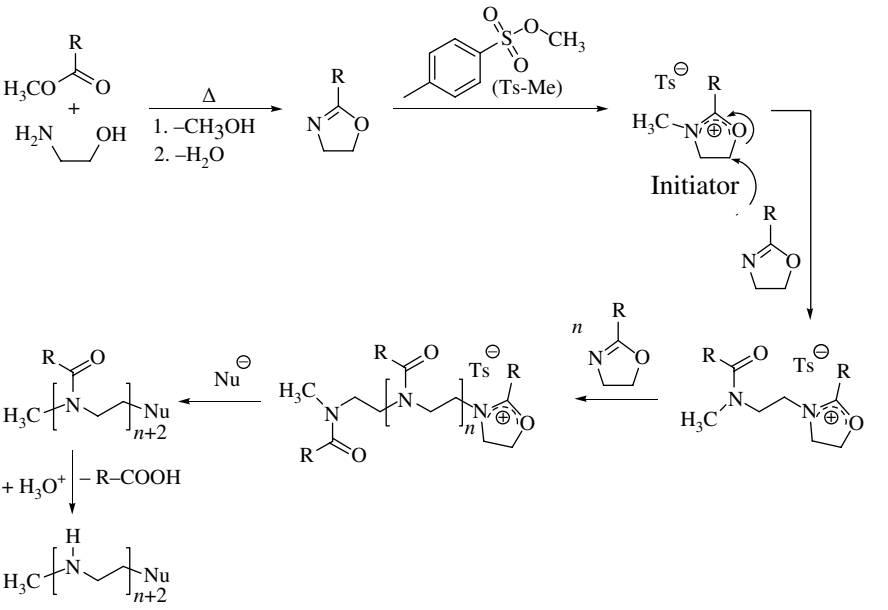

FIGURE 3.16 Monomer synthesis and cationic polymerization of oxazolines (Nu^- = nucleophile, e.g., amine) followed by acid hydrolysis toward linear poly-(ethylene imine) for R = Me, Et.

the possibility to build block copolymers and graft copolymers. Furthermore, poly(2-methyloxazoline) and poly(2-ethyloxazoline) can be hydrolyzed leading to linear PEI.

3.2.3 Controlled Radical Polymerization

Recently, there has been tremendous progress in achieving higher control in free radical chain addition polymerization by suppressing chain termination reactions and reducing the content of free radicals in the system [12]. All basic concepts involve a reversible chain termination reaction leading to a "dormant" chain that "sleeps" most of the time and is active only for a very short time to allow monomer "insertion" into the labile bond (Fig. 3.17). These systems are called "quasi-living" or controlled radical polymerization (CRP) and show features of the "living" ionic chain addition reaction.

In a well-controlled radical system, the monomer conversion is first order, molar mass increases linearly with monomer conversion, and the molar mass distribution M_w/M_n is below 1.5. In addition, chain end functionalization and subsequent monomer addition allow the preparation of well-controlled polymer architectures, for example, block copolymers and star polymers by a radical mechanism, which had been up to now reserved for ionic chain growth polymerization techniques.

Three major systems, and various subsystems, are distinguished so far:

1. Atom transfer radical polymerization (ATRP)
2. Stable free radical polymerization (SFRP) or nitroxide-mediated radical polymerization (NMRP or NMP)
3. Reversible addition–fragmentation chain transfer (RAFT).

Reversible activation/deactivation:

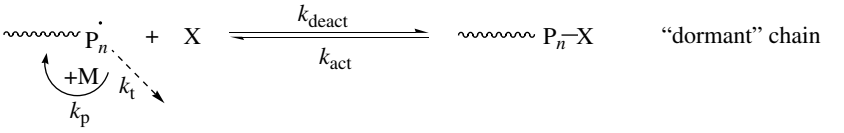

Degenerative exchange

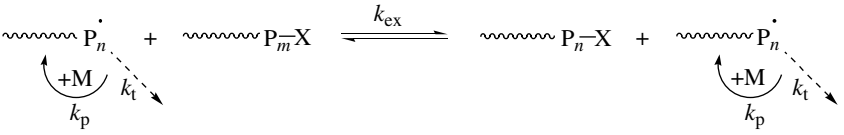

FIGURE 3.17 General principles of controlled radical polymerization reducing the concentration of active radicals.

3.2.3.1 Atom Transfer Radical Polymerization

The mechanism (Fig. 3.18) of the ATRP is based on the reversible activation of alkyl halides by redox reaction of a complexed metal with the halogen terminal group of the initiator or the growing chain end [13]. Thus, the initiating step is the homolytic cleavage of the carbon–halogen bond in the organic halide R—X by oxidation of the metal M_t in the metal complex M_t^n–Y/ligand. Consequently, the initiating radical species $R^{\cdot}$ and the oxidized metal complex are formed. At this point, $R^{\cdot}$ can add monomer units to enable chain propagation, or else it can react with the halogen on the oxidized metal to regenerate the dormant species R—X. The activation constant K_{act} leading to a free radical at the growing chain end is low compared to the deactivation constant K_{deact}, and therefore, the equilibrium is strongly on the side of the dormant species reducing the amount of free radicals. Secondary or tertiary chloride or bromide compounds can be used as initiator in combination with copper(I)chloride, and, for example, (substituted) bipyridine or tetradendates (e.g., tris(*N*, *N*-dimethyl-2-aminoethyl) amine MeTREN) are applied as ligands. The initiator/copper/ligand ratio and the reaction temperature have to be optimized for each monomer system; however, a broad variety of monomers including styrenics as well as acrylics and methacrylics were polymerized under controlled ATRP conditions so far.

ATRP is a very potent method for preparing block copolymers by sequential monomer addition as well as star polymers using multifunctional initiators. Furthermore, it can be applied also in water and in heterogeneous polymerization systems, for example, emulsion or dispersion polymerization.

3.2.3.2 Nitroxide-Mediated Radical Polymerization

The SFRP or NMRP has been studied in the beginning using the stable free radical TEMPO (2,2,6,6-tetramethyl-1-piperidinyloxy) or its adducts with,

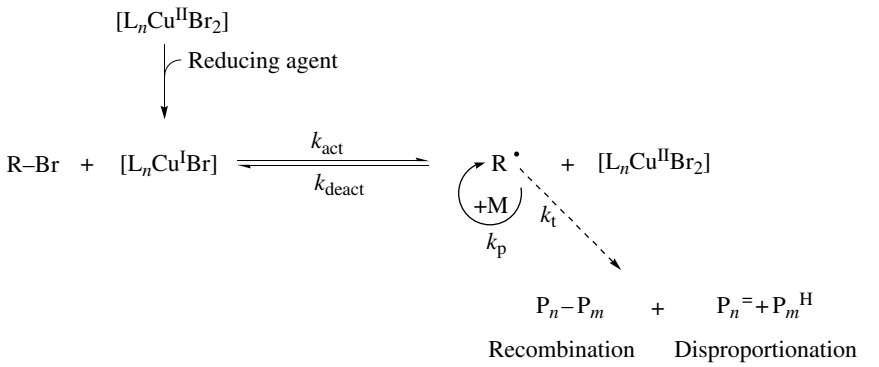

FIGURE 3.18 Simplified mechanism of ATRP.

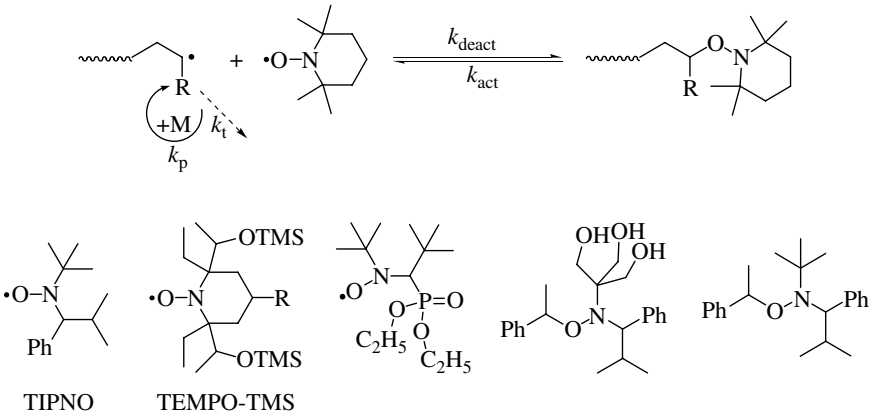

FIGURE 3.19 General concept of NMRP highlighted using TEMPO as stable radical and some examples for advanced stable nitroxide radicals and Hawker adducts.

for example, styrene derivatives. It is based on the formation of a labile bond between the growing radical chain end or monomeric radical and the nitroxide radical (Fig. 3.19). Monomer is inserted into this bond when it opens thermally. The free radical necessary to start the reaction can be created by adding a conventional radical initiator in combination with, for example, TEMPO or by starting the reaction with a preformed adduct of the monomer with the nitroxy nitroxide radical using the so-called unimolecular initiators (Hawker adducts).

The thermal lability of the R—C—O—N bond system controls the reversibility of the chain termination and limits also the use of NMRP. SFRP of styrene at about 130°C is studied intensively. In this case, high control and high molar mass products could be achieved. It was found that the thermal autopolymerization of the styrene monomer plays an important role in the mechanism of the reaction. Therefore, first experiments using different monomers in the presence of TEMPO and a radical initiator failed with regard to the control. However, new nitroxide adducts with a different R—O—N bond stability have been developed, for example, by Hawker [14], which work also for styrene derivatives as well as for acrylates. End group functionalization in NMRP can be achieved by using a functional radical initiator in combination with a stable radical or functionalized nitroxide adducts.

3.2.3.3 Reversible Addition-Fragmentation Chain-Transfer Polymerization

In the RAFT mechanism, the chain equilibrium process is based on a transfer reaction; thus, no radicals are formed or destroyed [15, 16]. When the RAFT agents behave ideally, the kinetics can be compared to the one of a conventional free radical polymerization. The release of initiating radicals through

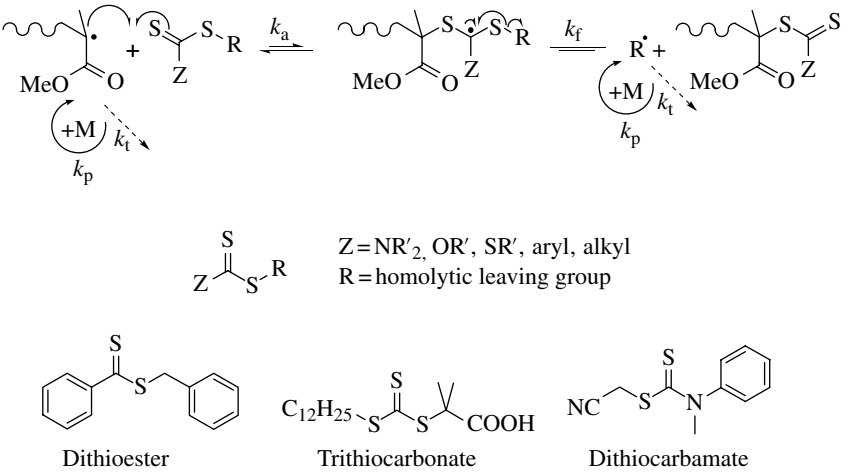

FIGURE 3.20 RAFT polymerization process based on a dithioester RAFT agent and some examples of RAFT agents (Z = modifies addition and fragmentation rates; R is free radical leaving group and defines initiating ability).

chain transfer at the beginning and the addition–fragmentation step, necessary to minimize the irreversible termination events, are the basis on which the RAFT mechanism relies (Fig. 3.20). During the reaction, chains are alternatively converted from propagating radicals to polymeric transfer agents and vice versa, generating an equilibrium. This enables the incremental growths of the chains with conversion, giving living character to the process. The choice of RAFT agents is very important for the achievement of well-defined products: They should have a high transfer constant regarding the monomers being polymerized, which means a high rate of addition, and suitable leaving groups for the propagating radical. As a result, dithioesters, trithiocarbonates, and certain dithiocarbamates can be successfully employed to obtain narrow dispersity for styrenes and (meth)acrylates in batch polymerization. RAFT can be performed at a broad temperature range and has a high tolerance to a large variety of functionalities (e.g., OH, COOH, NR_2). Very similar is the MADIX (macromolecular design via interchange of xanthates) approach, which employs xanthates.

3.2.4 Metal-Catalyzed Polymerization

The initiation of polymerizations by metal-containing catalysts broadens the synthetic possibilities significantly. In many cases, it is the only useful method to polymerize certain kinds of monomers or to polymerize them in a stereospecific way. Examples for metal-containing catalysts are chromium oxide-containing catalysts (Phillips catalysts) for ethylene polymerization;

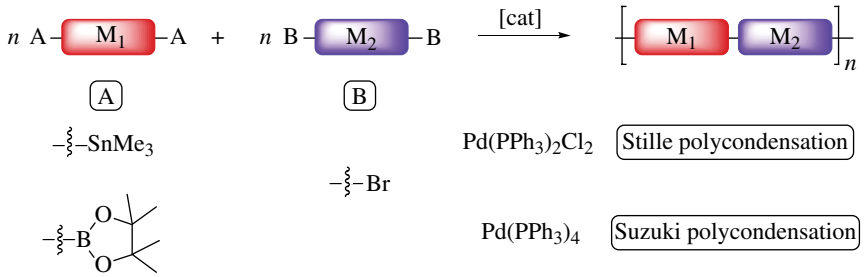

FIGURE 3.21 Synthesis of polyarylenes via C—C coupling by A_2+B_2 Stille and Suzuki polycondensation (M_1, M_2 = arene like phenyl).

metal organic coordination catalysts (Ziegler–Natta catalysts) for the polymerization of ethylene, α-olefins, and dienes; palladium catalysts; and the metallocene catalysts that initiate not only the polymerization of (cyclo)olefins and dienes but also of some polar monomers. More recently, progress in catalytic developments led to a number of new materials by ring-opening metathesis polymerization (ROMP).

Furthermore, a number step growth metal-catalyzed C—C combining reactions like Stille, Kumada, or Suzuki coupling, Heck and Sonogashira–Hagihara reactions, a.o., are employed especially for the preparation of highly aromatic and conjugated polymers (see Fig. 3.21).

An example of C—C coupling that shows characteristics of chain growth for the preparation of conjugated polymers will be given in Section 3.2.5 (Fig. 3.26).

Only few of the metal-catalyzed reactions allow the synthesis of well-controlled polymer structures. Thus, in the following, only two recent developments leading to rather defined polymer architectures will be addressed: functional and branched polyolefins by late transition metal catalysis and ROMP.

3.2.4.1 Functional and Branched Polyolefins by Late Transition Metal Catalysis

Incorporating functional units and controlled branching into polyolefins is of high interest [17]. Even small amounts of polar moieties can increase adhesion properties and compatibility of polyolefins with other materials. Another attractive feature is the fine-tuning of the polyolefin property profile by short- or long-chain branching, which controls crystallinity, solubility, and rheology. In regard to the desirable incorporation of polar monomers, early transition metal-based Ziegler catalysts and metallocenes are, unfortunately, highly sensitive to polar reagents. By comparison, late transition metal complexes are generally much more functional group tolerant in a polyinsertion as a

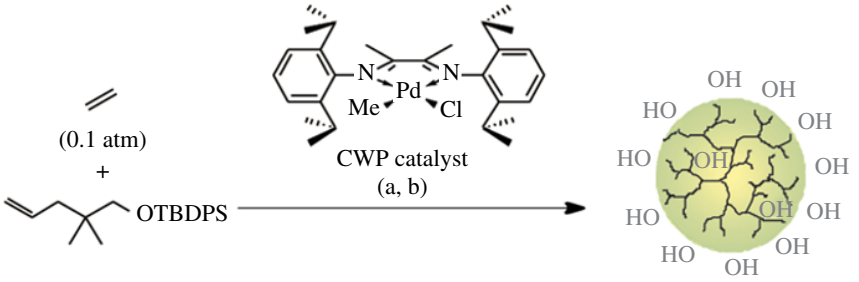

FIGURE 3.22 Synthesis of functional and branched polyethylene core by chain walking polymerization (CWP) (a: $NaBAr_4$; b: deprotection of alcohol). Source: Popeney et al. [21]. Reproduced with permission from American Chemical Society.

result of their less oxophilic nature. In addition, they can provide access to unique polyolefin branching structures.

Most known effective late transition metal-catalyzed polymerization systems are based either on neutral nickel(II) complexes of formally monoanionic bidentate ligands or on cationic iron cobalt, nickel, or palladium complexes of neutral multidentate ligands with nitrogen donor atoms substituted with bulky groups. N,O-substituted neutral nickel catalysts are very functional group tolerant. Grubbs and coworkers have copolymerized with those catalysts ethylene with five-functionalized norbornenes and high molecular weight polymer was obtained in ethylene homopolymerization in the presence of added polar reagents, such as ethers, ethyl acetate, acetone, and also water [18].

In 1995, a report by Brookhart and coworkers [19] on the discovery of a new class of catalysts for the polymerization of ethylene and α-olefins was received with strong interest in academia and industry. These catalysts, based on known nickel(II) and palladium(II) complexes of bulky substituted diimine ligands, are unique in polymerizing ethylene to highly branched, high molecular weight homopolymers at remarkable reaction rates. This work was further developed by Guan and coworkers leading to the term "chain walking polymerization" (CWP) [20]. Ethylene pressure has been used to control the competition between isomerization (chain walking) and monomer insertion processes for ethylene coordination polymerization catalyzed by a palladium–diimine catalyst. The topology of the polyethylene varies from linear with moderate branching to "hyperbranched" structures. Recently, a water-soluble molecular transporter with a dendritic core–shell nanostructure has been prepared by combining the late transition metal-catalyzed CWP for generating a highly nonpolar dendritic polyethylene core (Fig. 3.22), followed by anionic ROP of glycidol to graft a hydrophilic hyperbranched polyglycerol shell [21].

3.2.4.2 Ring-Opening Metathesis Polymerization

ROMP is a transition metal alkylidene-triggered process in which cyclic olefins, whether mono-, bi-, or multicyclic, undergo ring opening and are concomitantly joined together to form a polymer chain [22]. ROMP is thus a chain growth polymerization and belongs, together with Ziegler–Natta-type polymerizations and group transfer polymerizations, to the family of poly-insertions. The mechanism is based on olefin metathesis.

Historically, complex mixtures, usually based on a metal halide or oxo-halide, a tin alkyl, an alcohol, and an additive, have been used to generate the metal alkylidene *in situ*. However, with these initiators, usually no control is achieved and thus the polymers produced by such ill-defined systems display broad dispersities. With organometallic coordination catalyst systems containing molybdenum or tungsten, it is possible to bring about ROP of cycloolefins to linear unsaturated polymers, for example, of cyclopentene to poly(1-pentenylene).

Tremendous efforts have been put into the development of well-defined "single-site" transition metal alkylidenes. Mainly the work of R.H. Grubbs and R.R. Schrock (awarded with the Chemistry Nobel Prize 2005, shared with Y. Chauvin) led to the development of well-defined transition metal alkylidenes that rapidly outrivaled the traditional initiator systems. These initiators have the advantage of being well-defined compounds and in particular of possessing preformed metal alkylidenes (Fig. 3.23).

"Schrock catalysts" are high oxidation state molybdenum (or tungsten) alkylidenes and are highly active in the ROMP of a vast variety of cyclic alkenes such as substituted norborn-2-enes, norbornadienes, 7-oxanorborn-enes, cyclooctatetraenes (COTs), and 1,4-cyclooctadienes (CODs). The "living" polymerizations triggered by Mo-bis(*t*-butoxide)-derived initiators usually lead to the formation of all-*trans*, highly tactic polymers. Living, Schrock initiator-triggered polymerizations are best terminated by aldehydes in a Wittig-type reaction.

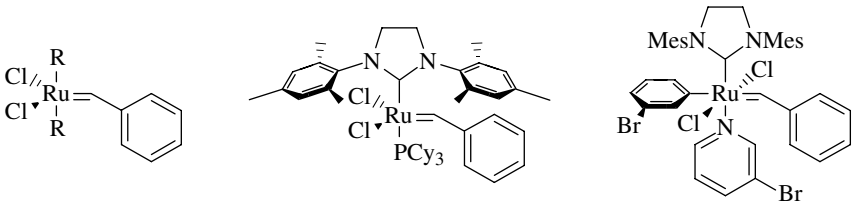

First-generation
R = PPh_3 or PCy_3

Second-generation

Third-generation

FIGURE 3.23 Selection of Grubbs-type initiators of first to third generation.

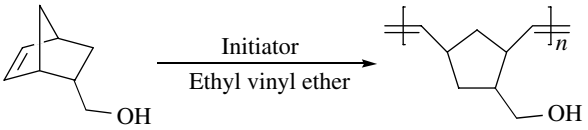

FIGURE 3.24 ROMP of norborn-5-ene-2-methanol with a Grubbs-type initiator in solution.

Grubbs-type initiators are well-defined ruthenium alkylidenes. Compared to molybdenum- or tungsten-based Schrock catalysts, the reactivity of ruthenium-based Grubbs catalysts is somewhat different. In terms of polymer structure, ROMP of norborn-2-enes and norbornadienes using ruthenium-based systems generally results in the formation of polymers that, in most cases, predominantly contain *trans*-vinylene units. Polymerizations initiated by Grubbs-type initiators are best terminated by the use of ethyl vinyl ether, yielding methylidene-terminated polymers.

The main advantage of the use of "single-site" transition metal alkylidenes in ROMP is the "living" character, which allows high control over molar mass, leads to narrow dispersity, and offers the chance for block copolymer formation of olefinic, even functional monomers (Fig. 3.24) otherwise not polymerizable by other methods.

3.2.5 Chain Growth Condensation Polymerization

As outlined previously, exciting progress with regard to control of structure and molar mass was achieved for polymers, which can be prepared by *chain growth* polymerizations, like ionic polymerization, NMRP, ATRP, RAFT, and ROMP techniques, applicable for olefins or some other monomers. In that case, the polymerization starts from an initiator and propagates via addition of monomers to a growing chain end on a one-by-one manner. However, synthesis of a number of industrially important polymers, such as polyamides, polyesters, and also *conjugated polymers*, involves *polycondensation* that proceeds through a *step growth* mechanism. In this case, the synthesis involves a statistical coupling of monomers and/or earlier formed oligomers. Because of this peculiarity of the mechanism, a molecular engineering with conjugated polymers and preparation of complex polymer architectures from such polymers remained for a long time illusive. Even homopolymerizations, if they proceed through the step growth mechanism, usually result into materials with a high molecular weight distribution that is undesired for achieving of high-quality materials with predictable properties.

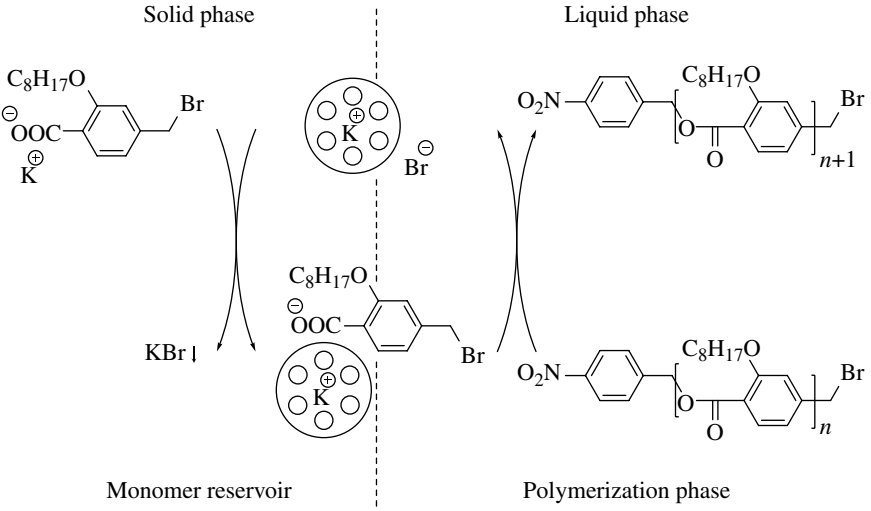

FIGURE 3.25 Mechanism of the controlled polycondensation in a biphasic system. Source: Yokozawa and Suzuki [24]. Reproduced with permission from American Chemical Society.

However, in recent years, polycondensation reactions have been developed, which proceed according to a chain growth mechanism and allow control over molar mass and chain end providing the chance for the preparation of block copolymers and complex architectures [23]. The change of the step growth into a chain growth mechanism can be achieved by different approaches: (i) activation of the polymer end group by differing substituent effects between monomer and polymer; (ii) phase transfer polymerization in a biphase system comprising a monomer storage and a polymerization phase, employing phase transfer catalysts (Fig. 3.25); (iii) transfer of the reactive species, derived from the initiator, to the polymer chain end; or (iv) activation of the polymer chain end by transferring the catalyst to it.

This concept has been further transferred even to the synthesis of conjugated polymers where high control of the structure is essential for high performance in optoelectronic applications. This development is governed by the discovery of the Yokozawa [25] and McCullough [26] groups. They found that the Kumada polycondensation into regioregular poly(3-alkylthiophenes) follows the chain growth but not the step growth mechanism, as it was believed for years. It is now generally accepted that the polymerization proceeds by an extension of tail-to-tail dimers formed in the first step from the Ni(dppp)Cl_2 (dppp = propane-1,3-diylbis(diphenyl-phosphane)) or similar catalyst precursors and two Grignard-type monomer molecules (Fig. 3.26) [27].

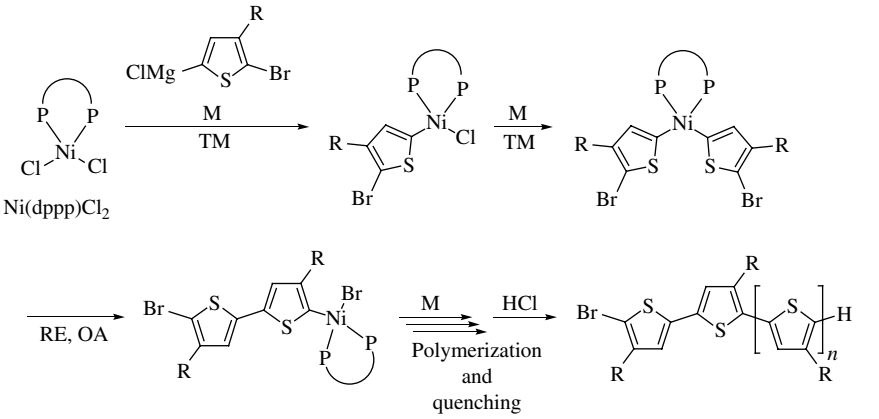

FIGURE 3.26 Concept of the Kumada catalyst transfer polycondensation. dppp, propane-1,3-diylbis(diphenylphosphane); TM, transmetallation; RE, reductive elimination; OA, oxidative addition.

In the key step, responsible for the unusual chain growth character of the polycondensation, a Ni(0) species formed at the reductive elimination step, associates with the nearest thiophene ring forming an associated pair, then "moves" toward a growing polymer chain end, and finally inserts *intra*molecularly into the terminal C—Br bond. It was found that in optimized conditions the polycondensation has a "near living" performance. Although generally it allows worse control over the reaction course than truly living anionic polymerizations, dispersities less than 1.2 were reported for polythiophenes and even all-conjugated block copolymers were already prepared via sequential addition of monomers. It has been further demonstrated that the chain growth mechanism is also achievable for Kumada polycondensation using phenylene-based monomers and for fluorenes via Suzuki chain growth polycondensation.

3.3 EFFECTIVE POLYMER ANALOGOUS REACTIONS

As already indicated in Section 3.1.3, besides chain and step growth polymerizations, new polymer structures can also be achieved by modifying a precursor polymer structure with new functionalities. Even though this is the base for a number of technically important polymers including polyvinyl alcohol and, for example, ion exchange resins, for many years, this method was not considered to be suitable for the reliable large-scale synthesis of well-controlled polymer architectures, mostly because it is very difficult to achieve very high

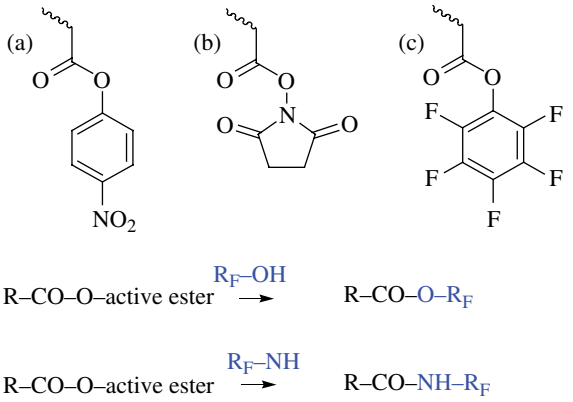

FIGURE 3.27 Examples of active esters used for efficient polymer analogous reaction toward functional esters or amides; (a) 4-nitrophenylester, (b) *N*-hydroxysuccinimide (NHS) ester, and (c) pentafluorophenylester.

conversion in polymer analogous reactions, side products cannot be removed, and thus heterogeneous material results.

Still, especially esterification and amidation reactions have been widely explored early on for specific polymer modification and bioconjugation (Section 3.5) with preference on using effective coupling agents like carbodiimides and active ester as known from biochemistry. Active esters introduced as side groups through polymerization of suited monomers or as end groups onto polymer chains, using living-type polymerizations or polycondensations with chain end control, allow introducing a variety of further functionalized ester units by transesterification, and they can react efficiently with amines toward amides. From the wide variety of active esters, mainly 4-nitrophenyl, pentafluorophenyl, and succinimido esters are the most prominently used examples (Fig. 3.27). Further details can be found in Section 3.5.

In the last decade, the combination of CRP techniques and newly found or reinvented highly effective and selective organic reactions termed as the "click chemistry" has been demonstrated to be a versatile tool for the specific construction of novel functional macromolecules [28]. In 2001, Sharpless et al. [29] introduced the term "click chemistry" with its famous representative, the cycloaddition of azides with alkynes under copper catalysis. He defined a "click reaction" with a set of criteria: "The reaction must be modular, wide in scope, give very high yields, generate only inoffensive byproducts that can be removed by nonchromatographic methods, and be stereospecific (but not

necessarily enantioselective)" with further specifications for easy-to-realize reaction conditions and easy product isolation. The most well-known reactions satisfying the philosophy of "click" chemistry are, besides the most popular 1,3-cycloaddition between azides and alkynes, thiol–ene, oxime, Diels–Alder and pyridyl disulfide reactions, as well as the Michael addition and activated ester coupling. Although Sharpless has seen the application of the click chemistry mainly in the pharmaceutical area, quickly click reactions were established also in the field of polymer chemistry, since these suddenly offer a feasible pathway especially where other polymer synthesis techniques come to their limits. The end group functionalization of polymers by click chemistry enables a wide diversity of functional soft materials comprising also the linking of incompatible polymer chains and preparation of biohybrids through bioconjugation (see Sections 3.5 and 5.5). It is particularly important that these reactions are highly effective because of the small quantity of functional end groups in polymer chains. Furthermore, the click reaction is used in numerous examples for the introduction of functional side chains and functionalities in linear and dendritic polymers, whereby such reactions again need a high effectiveness and selectivity in order to lead to homogeneous materials, especially since functionalities attached onto polymer chains are usually characterized by lower reactivity. Another field of research is the direct construction of so far inaccessible linear and dendritic polymers with the help of click reactions.

Due to the rather easy accessibility of novel functional polymer materials by click reactions, their potential scope of applications has significantly broadened in the last years. Through the preparation of functional thin polymer films, biohybrids, or self-assembly structures from end group or side chain functionalized polymers and functional block copolymers, applications, for example, as adhesives or additives, but especially also in optoelectronics, biomedicine, drug delivery, biochips, and micro- and nanoelectronics become accessible.

The fast development of click chemistry leads of course also to the search for new reactions expanding the scope. Barner-Kowollik and colleagues [30] have extended the definition of "click chemistry" especially for the field of polymer synthesis, and they refined the original criteria in the following way: "Single reaction trajectory, chemoselective, wide in scope, modular, stable compounds, high yields, fast timescale, large-scale purification possible, equimolarity." The first four requirements are taken without alteration from Sharpless' original definition, whereas the remaining criteria are adapted to requirements from synthetic polymer chemistry.

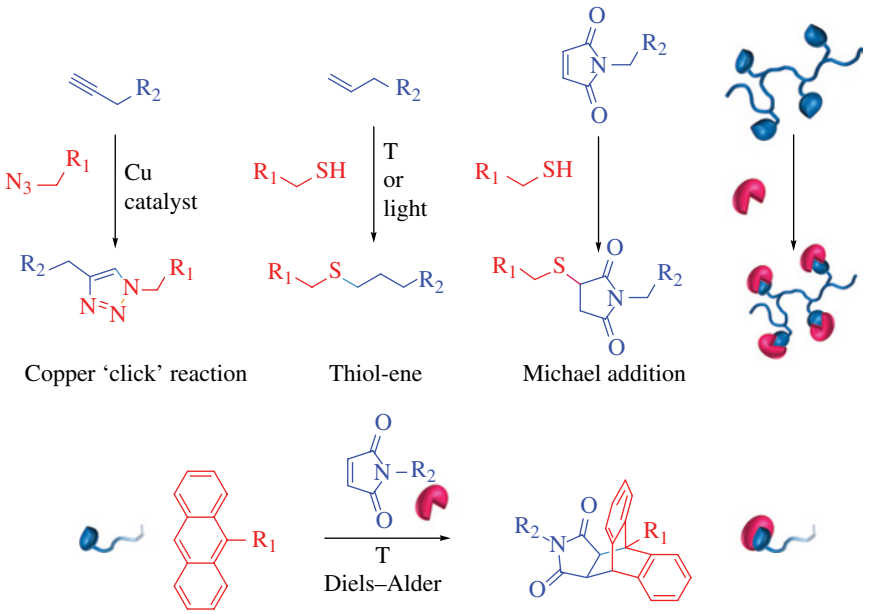

FIGURE 3.28 Some examples of efficient reactions used for polymer modification that allow also orthogonal coupling (REO chemistry). (*See insert for color representation of the figure.*)

In Figure 3.28, a number of well-established reactions fitting the aforementioned criteria and being extensively employed recently in polymer chemistry are outlined. It is of special interest that many of these reactions are orthogonally specific to certain functionalities, which means they can be selectively carried out in the presence of various functionalities and allow one-pot modifications of polymers with more than one functionality and without employing any protective groups. This classifies them as robust, efficient, and orthogonal (REO) approaches.

Especially, the copper-mediated reaction of alkynes with of azides, which are readily available and introduced into polymers, gained high interest but shows limitations in biomedical applications where even traces of copper should be avoided. Thus, recently, copper-free click reactions have been developed [31], relying on the original thermal Huisgen 3+2 cycloaddition reaction but employing highly activated alkynes like the strained cyclooctyne that allow effective cycloaddition reaction at rather low temperatures that are tolerated by biological systems. In that case, the regioselectivity of the reaction is lost, but this is for many bioconjugate applications not relevant. A number of cyclooctyne derivates for bioconjugation and biofunctionalization are commercially available (Fig. 3.29).

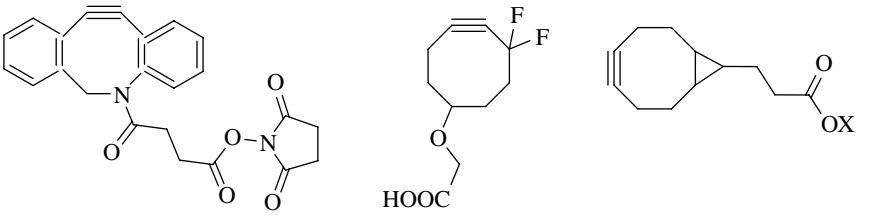

FIGURE 3.29 Commercial strained cyclooctynes (dibenzylcyclooctyne (DBCO)-NHS, difluorinated cyclooctyne (DIFO) acid, bicyclenonyne (BCN) carbonate) for introduction into (bio)macromolecules.

3.4 PEGYLATION

Many biomolecules, such as peptides, proteins, and DNA/RNA, are rapidly degraded by enzymes within hours. Therefore, these molecules have not been considered as drug candidates for a long time. Only after Davis and Abuchowski introduced PEGylation in the 1970s [32] a series of protein–PEG conjugates have been investigated as macromolecular drugs and some of them received market approval over the last decade. PEGylation changes the physicochemical properties of a protein drug, like its conformation, electrostatic interactions, or hydrophilicity, and therefore has many advantages [33]. On the one hand, PEGylation improves the solubility of the protein in aqueous media and, on the other hand, enhances biomolecule stability by shielding it from proteases. Another benefit of the shielding is the reduction of the immunogenic response to the administered protein drug. These effects lead to a longer half-life in blood circulation and therefore improve the drugs bioavailability significantly, which in turn decreases the frequency of administration that is necessary to achieve a constant blood level (see Fig. 3.30).

One example for PEGylated proteins is PEGASYS® [34], which is a protein-based drug (Fig. 3.31) that contains a PEG chain with a molecular weight of 40 kDa. The advantage of PEGylation is the half-life extension that is expressed by a far better pharmacokinetic profile. In contrast to the native protein that is degraded in less than 8 h, PEGASYS lasts over one week and requires only a weekly dosing. This is especially relevant because an intravenous (i.v.) injection is needed.

In the first generation of PEGylated drugs, the attachment of PEG was usually achieved with a functional group that is reactive toward the hydroxyl end groups of PEG, which were typically anhydrides, acid chlorides, chloroformates, or carbonates [38]. In the second generation, more efficient groups like aldehydes, esters, and amides are reacted with the biomolecule to achieve

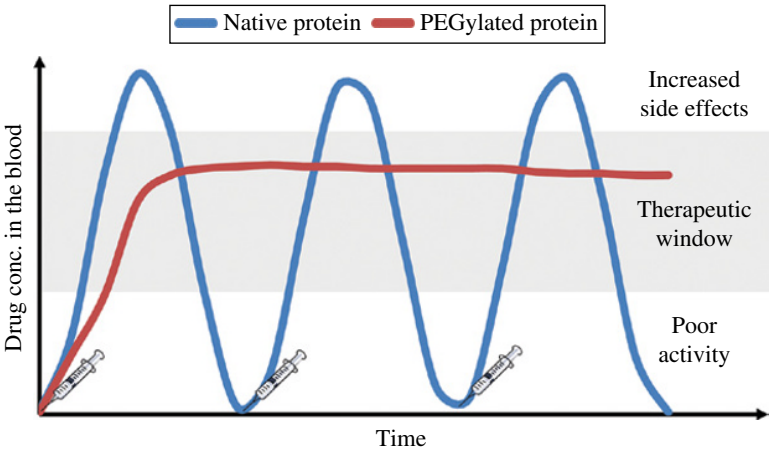

FIGURE 3.30 Blood level of native versus PEGylated protein.

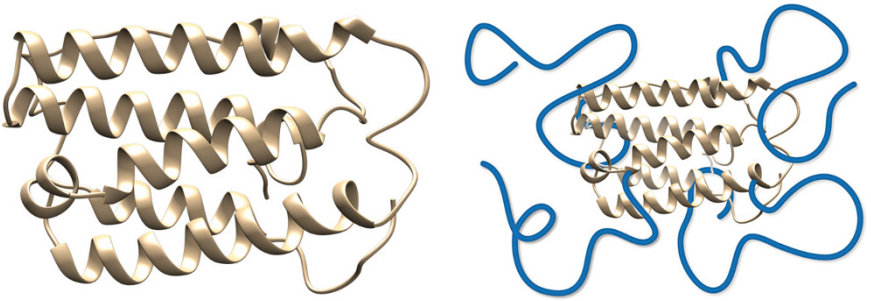

FIGURE 3.31 Molecular structure of pure interferon α-2a (left) and a schematic representation of its PEGylated analog [35, 36]. Source: Klaus et al. [37]. Reproduced with permission from Elsevier.

conjugation. Additionally, heterobifunctional PEGs were made available bearing maleimide, vinyl sulfone, pyridyl disulfide, amine, carboxylic acids, or NHS esters. The third generation of PEGylated drugs has branched, Y-shaped, or comb-shaped PEG chains attached and shows lower viscosity and no organ accumulation, for example, pegaptanib (see Table 3.2). While traditionally rather one long PEG chain (e.g., 40 kDa, about 910 repeat units) was conjugated, more recently introduced PEGylated proteins of the third generation carry several shorter ones (e.g., pegaptanib, 9× 10 kDa, see Table 3.2) or branched, Y-shaped, or comb-shaped PEG chains to avoid increased viscosities and clogging of small capillaries (Table 3.2).

Multiple-protein functionalization has some drawbacks such as blocking of active sites and incomplete coupling reactions that lead to complex mixtures.

TABLE 3.2 PEGylated Proteins Currently on the Market

Drug (Brand Name)	Company	Protein	Polymer	Indication
Pegademase bovine (Adagen)	Enzon (1990)	Adenosine deaminase	5 kDa PEG	Severe combined immunodeficiency disease (SCID)
Peginterferon α-2b (PegIntron)	Schering-Plough/ Enzon (2000)	Interferon α	12 kDa PEG	Hepatitis C
Peginterferon α 2a (PEGASYS)	Hoffmann-La Roche (2001)	Interferon α	40 kDa PEG	Hepatitis C
Peg-asparaginase (Oncaspar)	Enzon (1994)	L-asparaginase	5 kDa PEG	Leukemia
Pegfilgrastim (Neulasta)	Amgen (2002)	G-CFS	20 kDa PEG	Neutropenia
Pegaptanib (Macugen)	Pfizer (2004)	VEGF inhibitor	40 kDa PEG	Wet age-related macular degeneration
Pegloticase (Krystexxa)	Savient (2010)	Uricase	90 kDa PEG bzw. approx. 9 PEG chains with 10 kDa each	Chronic gout
Certolizumab pegol (Cimzia)	Nektar/UCB Pharma (2008)	Monoclonal antibody	40 kDa PEG	Rheumatoid arthritis and Crohn's disease
Methoxy-PEG-epoetin α (Mircera)	Roche (2007)	Erythropoietin	30 kDa PEG	Anemia associated with chronic kidney disease
Pegvisomant (Somavert)	Pfizer (2002)	Human growth hormone antagonist	4–5 PEG of5 kDa	Acromegaly

Therefore, also genetically modified proteins are used that either introduce unnatural amino acids for bi-orthogonal coupling (e.g., azides for click reactions) or passive protein sequences are attached to act in a similar fashion as the PEG chain. Here, the so-called PASylation (proline, alanine, serine; see Fig. 3.32) has shown to form random coils and no additional linker chemistry is required. PASylation is the only technique that results in a single mass pure biopolymer, although protein expression becomes more tedious, which leads to lower yields. Other alternatives to PEGylation are HESylation (hydroxyethyl starch conjugation) or PGylation (polyglycerol conjugation) (see Fig. 3.32).

PEGylation is also the most widely used bioinert polymeric surface coating currently used [39]. Although it is considered as a gold standard for protein-resistant surfaces, recent observations indicate that PEGylation is far from being the optimal candidate for biomedical applications. Even though PEG is

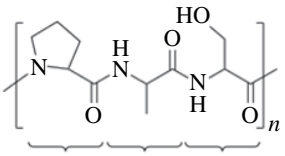

Proline Alanine Serine

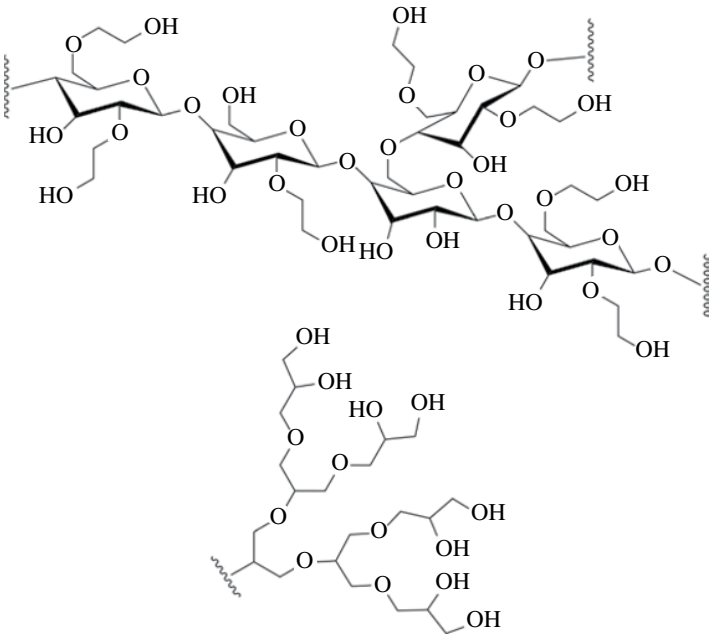

FIGURE 3.32 Structures of polymers that have been used for PASylation (top), HESylation (middle), and PGylation (bottom).

a polyether and thus relatively stable under physiological conditions, it has been reported that degradation can occur, especially at elevated temperatures, in the presence of oxygen and transition metal ions, or *in vivo* in the presence of enzymes [40].

Finally, it should be noted that the term PEGylation is today used very widely and unspecifically. Originally only used for the introduction of PEG chains to proteins and various biobased drugs, now many researchers use the term "PEGylation" for all kinds of synthetic approaches, which involve the introduction of PEG chains to organic low molar mass or polymeric substances—synthetic or biological—or to material surfaces. In all these cases, the modification with PEG chains is applied to increase solubility in polar solvents, mainly in water, and to enhance biocompatibility.

3.5 BIOCONJUGATION

The main goal in the formation of bioconjugates is to expand the physical–chemical properties of biologically active molecules by including synthetic components or addition of bioactivities to artificial structures [41]. Incorporation of biologically or physically active molecules into biological compounds is proposed to extend their *in vitro* and *in vivo* applications, which could also reveal their structure–property relations. Advanced synthetic strategies, such as solid phase synthesis, allow for the creation of all types of natural biopolymers as well as their conjugation during synthesis. Nevertheless, the length restrictions of synthetic biopolymers limit such conjugation schemes to relatively small molecule applications, and many conjugation approaches still demand the use of biopolymers purified from natural sources. Creation of similar natural bioconjugates requires delicate synthetic schemes that allow for covalent or noncovalent linkage of biological and artificial molecules without interfering with their original properties. For example, polynucleotide conjugations cannot be achieved via its backbone, which contains gene information, and most proteins can be conjugated only through the reactive groups on the surface of their globular structure in order to prevent denaturation. Despite the great variety of the chemical and physical properties of bioconjugates, general approaches for bioconjugation can be easily grouped. First, one distinguishes pure physical conjugation, where a synthetic and a biological moiety are linked by noncovalent conjugation as there are ionic, H-bonding, or hydrophobic interactions. In this strategy, well-defined conjugates and less defined aggregates can result. On the other hand, bioconjugation through covalent linkage usually results in well-defined, isolated

conjugate molecules. In that case, there are two main approaches: The conjugation can be created by direct chemical linkage of an unmodified biological synthetic component or by an indirect approach, which is a multistep synthesis for the formation of bioconjugates involving first the modification of the biological part with more reactive and selective functions when their synthetic or biological counterparts cannot be directly linked with a high efficiency (Fig. 3.33). For the formation of bioconjugates in polymer chemistry, "grafting to" or "grafting from" procedures are defined. In "grafting to," a preformed synthetic oligomer or polymer chain is linked directly to the biomacromolecule; in "grafting from," an initiator or first monomer unit is linked to the biomacromolecules and from that the synthetic polymer chain is build up, usually by a controlled chain growth polymerization (see Section 3.2).

The direct conjugation is a fast and simple approach that is utilized for the formation of bioconjugates often without additional purification. This method can be very efficient in the attachment of low molecular weight molecules to

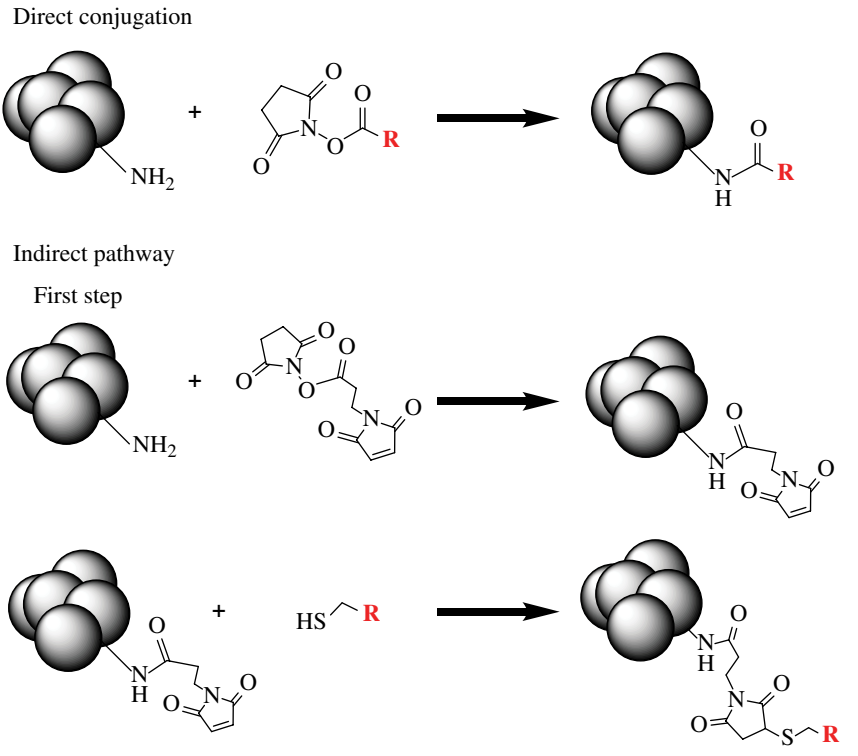

FIGURE 3.33 Conjugation strategies.

highly diluted biopolymers. For example, this method is routinely used for fluorescent labeling in order to visualize the biological components with a fluorescent microscope. Both the biomolecule and its synthetic counterpart should possess functional groups that are available to be coupled with a high efficiency, which is especially important for the conjugation of macromolecules where reactivity is slowed by diffusion. The direct synthetic strategy is commonly limited to the conjugation of molecules that can be effectively performed in aqueous solutions. This seems to be an obvious requirement, but in the case of bioconjugation chemistry, it is a synthetic challenge because the majority of biopolymer chemistry is confined by aqueous solutions while many polymers and fluorescent molecules require dissolution in organic solvents for effective reactivity. Additionally, the absence of suitable chemical groups or possible low concentration of both conjugated components and difficulties in the conjugate purification from the starting components often require alternative synthetic routes.

An alternative approach in the formation of bioconjugates is the indirect pathway. It is a multistep synthesis where in the first step a typically low molecular weight reactive unit with a well-defined reactive site is introduced into the biomacromolecule of interest in order to allow its further conjugation through more efficient chemical reactions such as click chemistry (Fig. 3.34; see also Section 3.3). This expands the possible synthetic pathways for efficient molecular conjugation. The low molecular weight component can be used in a large excess making primary conjugation more efficient while the second conjugation is performed through click chemistry, which commonly reach complete conjugation within few minutes. Although it often requires advanced synthetic skills, this approach allows for high efficiency conjugations of relatively inert molecules with limited amount of the reactive groups, which, otherwise, could not be effectively coupled.

3.5.1 Polynucleotide Conjugates

Polynucleotides in mammalians are strictly located in intercellular compartment. Their presence in the intracellular environment usually is indicative of pathological processes such as virus infection. As a result, the extracellular environment contains a variety of DNA and RNA nucleases, which are one of the protective mechanisms against viral infections. DNA and RNA conjugations are often used to prevent unnecessary enzymatic cleavage. Polynucleotides contain genetic information that is encoded in the alternating sequences of their monomers. Hence, polynucleotide conjugation is limited to the terminal

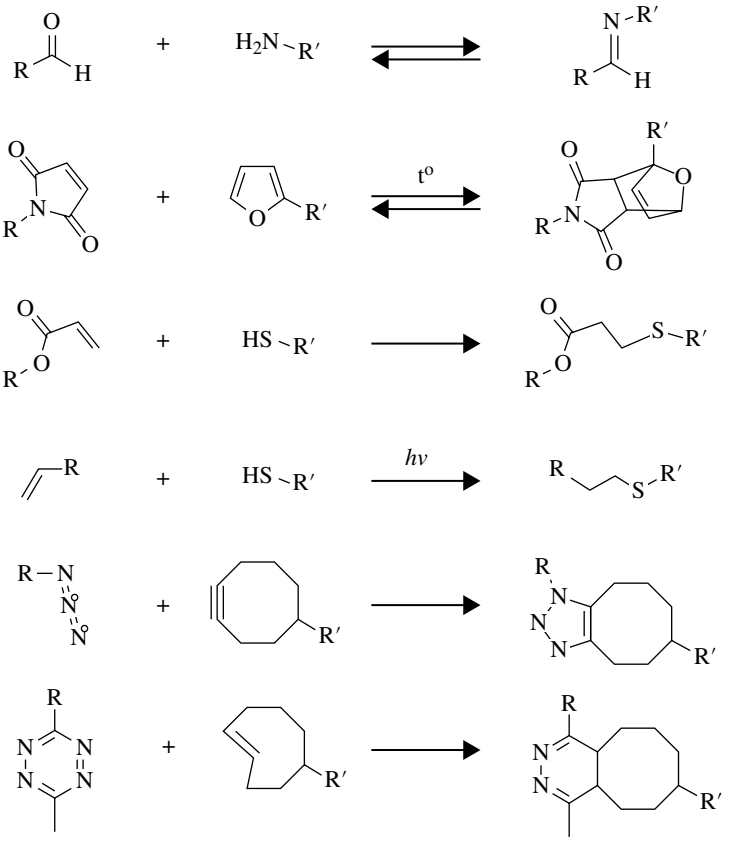

FIGURE 3.34 Examples of reactions of click chemistry used in bioconjugation (cf. also Section 3.3).

or noncovalent coupling in order to sustain their biological activity. The terminal conjugation is performed to synthetic polynucleotide (Section 3.7.1.2) in which the terminal nucleotide is functionalized during the solid-state synthesis with a reactive group able to participate in click chemistry (Fig. 3.34). Such artificial polynucleotide motive can be utilized for the formation of a variety of conjugates by mixing with various synthetic components having suitable complementary units for the click reactions.

The anionic nature of polynucleotides is utilized in the formation of their noncovalent conjugates. Their simple mixing with natural macromolecules, such as chitosan [42] or various cationic artificial polymers [43], leads to the spontaneous noncovalent complex formation that under special conditions can exist as nanoparticles capable for i.v. injections (Fig. 3.35). The lifetime for blood circulation of extracellular DNA molecules in mammalians is in

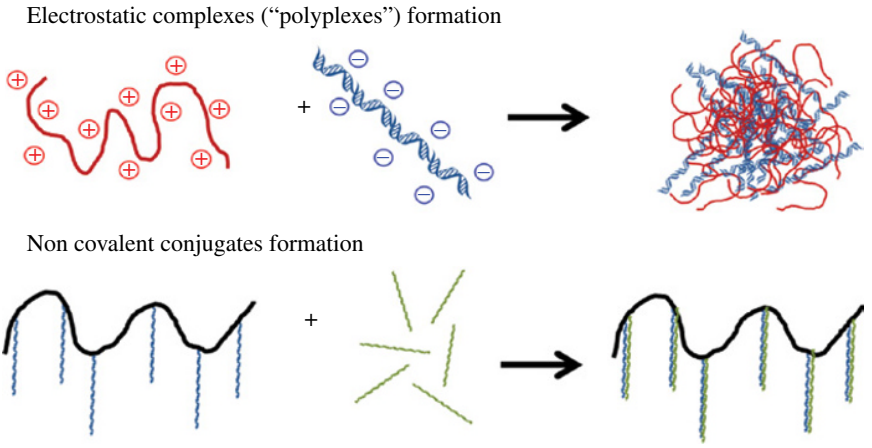

FIGURE 3.35 Schematic representation of DNA or RNA nanoparticles (polyplexes) by cationic polymers through electrostatic interactions and noncovalent conjugate formation.

hour scale and only some minutes are required for RNA hydrolysis, while their cationic polyplexes are nearly completely insensitive to the nuclease cleavage.

3.5.2 Protein Conjugates

Conformation of proteins defines their biological activity that requires to sustaining the tertiary structure of proteins after the conjugation. Thus, the protein conjugation majorly is focused on the coupling of the reactive groups on the protein surface. Proteins are used the most for a very broad variety of bioconjugates when compared to other biopolymers, and with only few exceptions, their conjugation is focused on the coupling of free amino and thiol groups. The thiol group of cysteine residue is the most attractive target for protein conjugation because it allows orthogonal, highly effective, and selective coupling with a variety of reactive groups (Fig. 3.36). Nevertheless, cysteine is the second least abundant amino acid residue after tryptophan, which often exists in its nonreactive disulfide form. Protein engineering allows for protein excretion with additional cysteine residues, but such technique is time-consuming and expensive; thus, it is not commonly applied for the formation of the protein conjugates.

Lysine residues are commonly present on the surface of the majority of proteins and, therefore, are an easy target for conjugations. There are several

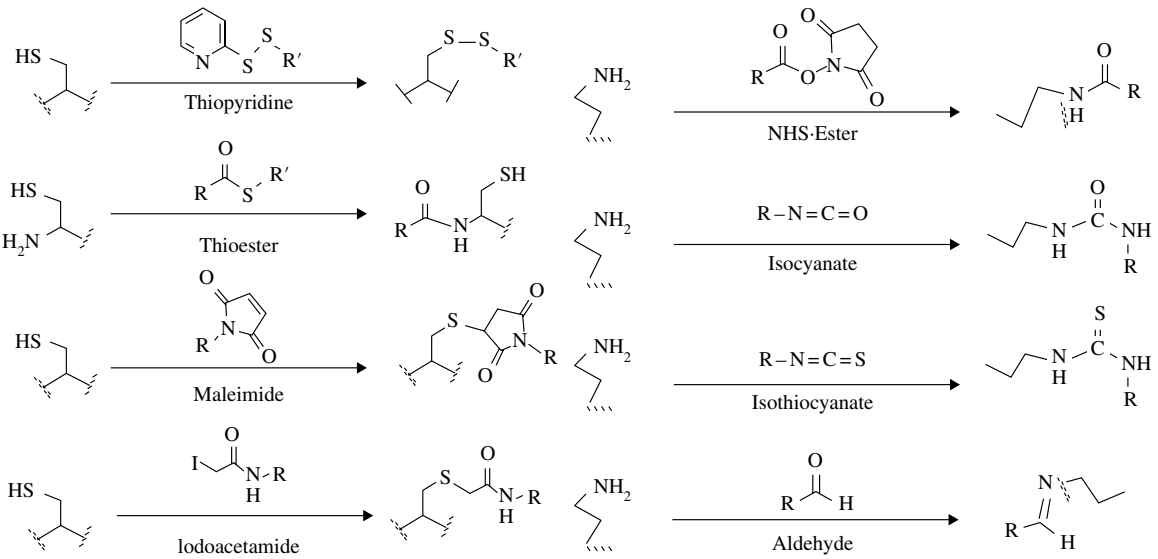

FIGURE 3.36 Bioconjugation strategies for cysteine (left) and lysine (right) residues.

synthetic strategies for lysine conjugations. The most utilized is through NHS ester, which reacts fast with free amino groups but can lead to urea side product formation after the conjugation. Isocyanates and isothiocyanates are also very reactive toward amino groups, and such reactions do not lead to any side products upon conjugation (Fig. 3.36). Nevertheless, these reactive groups undergo relatively fast hydrolysis in aqueous solutions especially at physiological pH. Together, they provide several synthetic pathways for any conjugation strategy. Similar to polynucleotides, the low molecular weight polypeptides do not have a defined conformational structure and, therefore, can be directly conjugated during the synthesis.

3.5.3 Polysaccharide Conjugates

Among natural biopolymers, polysaccharide conjugates are the least studied in terms of both their formation and functions. Similar to protein and polynucleotides, the creation of synthetic polysaccharide conjugates has the aim to extend our understanding of the carbohydrate biological function in nature. Incorporation of biologically or physically active molecules into carbohydrate structures aims at broadening both *in vitro* and *in vivo* applications in order to reveal their structure–property relations. While proteins and polynucleotides mainly exist as linear polymers, nearly all carbohydrates in mammalian systems are present in the form of a conjugate with other complex structures such as proteins (glycolipids, glycoproteins, etc.) and lipids (GPI anchors). Therefore, appropriate conjugation strategies should be always considered in the design and synthesis of carbohydrates projects. While solid phase synthesis is considered to be a routine for polypeptides and polynucleotides allowing for their straightforward conjugation, polysaccharide synthesis is a privilege of a few research groups worldwide, which limits current conjugation approaches to the modification of carbohydrates purified from natural sources.

About 10 different monosaccharides, which are present in mammalian systems, can be divided into two distinguished groups in respect to the presence or absence of carboxyl and amine functionalities in their structure. Correspondingly, the chemistry strategies utilized for the conjugation of such carbohydrates are different [44, 45]. The carboxyl and amine functional groups upon which conjugation can be performed without a strong disruption of the polysaccharide structure are the main target for the conjugation. The conjugation of carbohydrates that do not possess these functional groups is more complex and usually requires a strong interference of the native carbohydrate structure. Conjugation of such carbohydrates with other biopolymers

such as peptides, proteins, or polynucleotides is a synthetic challenge because it requires the use of incompatible chemicals or solvents.

3.5.3.1 Conjugation of Carbohydrates Containing Carboxyl and/or Amine Functional Groups

The most available method for the modification of carbohydrates is the selective bonding of a targeting molecule to bare amine groups. This conjugation approach is similar to the conjugation of amino groups in proteins and commonly is performed via NHS esters. Nevertheless, this highly selective technique has several superior limits in the case of natural carbohydrate modifications, the main of which is that it can be applied only to the polysaccharides containing free amino groups, which is usually acetylated or sulfated in natural carbohydrates. Another restriction is that the molecule that is to be attached to a polysaccharide should have a carboxylic group available for the conjugation and cannot have any free amino group itself. The examples of functional molecules utilized in this technique are usually limited to synthetic molecules, which further can be utilized in multistep conjugation via click chemistry.

Application of carbodiimide chemistry for the formation of a covalent bond between carboxylic groups of polysaccharides and any amino group of a labeling molecule is a common method for the conjugation of glycosaminoglucans but also can be used for any other saccharide that possesses a carboxylic acid functionality. In this technique, the labeling is achieved through the formation of NHS esters of carboxylic groups within polysaccharides and followed by reaction with the amino group of a desired molecule. NHS esters of carboxylic acids are relatively stable and, therefore, can be purified and stored under appropriate conditions that simplify their applications. The unique of this method is any molecule containing a free amino group can be covalently attached to the polysaccharides including natural proteins and polynucleotides that are soluble only in aqueous solution. This approach also is utilized in the multistep conjugation via click chemistry.

3.5.3.2 Conjugation of Bare Carbohydrates

Conjugation of carbohydrate hydroxyl groups that are present in a large amount at their backbone is commonly restricted to organic solvents under very “nonnatural” conditions because of hydroxyl’s low reactivity in aqueous media. Therefore, this technique cannot be utilized for the conjugation of many naturally occurring polysaccharides without their appropriate modification due to low solubility of such carbohydrates in organic solvents. Application of such approach for the formation of the conjugates with other biopolymers

is also very restricted. Hydroxyl functionalities in aqueous solutions can to some extent react with isothiocyanate derivatives such as commercially available rhodamine and fluorescein isothiocyanates. The reaction of isothiocyanates with alcohols in organic chemistry is commonly carried out in nonaqueous solutions because of their pure solubility and fast hydrolysis that is comparable to the rate of the reaction with the hydroxyl groups. Nevertheless, the limited solubility of rhodamine and fluorescein isothiocyanate in aqueous solutions allows for their reaction with hydroxyl groups of carbohydrates. The yield of reaction can be also significantly increased by use of low temperature and mixture of DMF/H_2O as the solvent where most of polysaccharides are still soluble, but the hydrolysis reaction is slow.

Reductive amination is another approach for labeling of carbohydrates in aqueous solutions. It limited to the functionalization of only the terminal saccharide unit in polysaccharides. Reductive amination as a labeling technique is also applied to the product of carbohydrate nitrous acid cleavage followed by reaction with a primary amine containing label and next reduction with sodium cyanoborohydride or similar reducing agent [46, 47]. Low yield in case of high molecular weight polysaccharides and synthetic difficulty of this procedure has restricted its wide use.

3.6 ENZYMATIC POLYMER SYNTHESIS

Enzymes are natural catalysts that exhibit a number of advantages like (i) high catalytic activity, (ii) high reaction selectivity, and (iii) render harsh reaction conditions unnecessary. During the last decades, enzymes were engineered in order to render them applicable to nonnatural substrates and nonaqueous solvents and nowadays are used in a wide range of organic transformations [48]. In enzymatic polymerization reactions, one has to differentiate isolated enzyme catalysis from bacterial polymer synthesis that uses the complex enzyme mixtures of whole cells, for example, for the technical production of poly-3-hydroxybutyrate. The focus in this chapter is on enzymatic synthesis by isolated enzymes via nonbiosynthetic (nonmetabolic) pathways [49]. The use of enzymes for polymer synthesis offers the advantages of controlling the polymer structure by exploiting the enzyme's enantio- and regioselectivity, substituting heavy metal catalysts with environmentally benign enzymes, applying mild reaction conditions, and enabling syntheses that could not be achieved otherwise. One example is the high activity of enzymes in macrolactone polymerizations. Disadvantages of *in vitro* enzyme-catalyzed polymerizations are the low activity in nonaqueous media that requires the use of

higher amounts of enzyme. This issue can be addressed by increasing the enzyme's stability, for example, by immobilization (e.g., Novozyme 435), which then allows recycling and reuse [50].

In the area of enzymatic polymer synthesis, one can distinguish between enzymatic polymerization and enzymatic polymer modification. Of the six main enzyme groups (see Table 3.3), three have been used as catalysts for enzymatic polymerization and four have been used in enzymatic polymer modification reactions.

Enzymatic polymerization can be divided with regard to the polymerization mechanism into polycondensation and ROP reactions. A prominent example of polycondensation reactions is the esterification reaction (Fig. 3.8a). An activation of the carboxylic acid-containing monomer can be achieved by esterification with an alcohol. The resulting polymerization reaction is then called a transesterification (Fig. 3.37b). Since these are reversible reactions, the equilibrium needs to be shifted to the product side that requires the removal of the formed water (esterification) or alcohol (transesterification). In polycondensation reactions, the product molecular weight and the end group

TABLE 3.3 Classification and Examples of Enzymes as Well as Typical Polymers Synthesized by *In Vitro* Enzymatic Catalysis [49]

Enzymes	Example Enzymes	Polymers Synthesized
Oxidoreductases	Peroxidase, laccase, tyrosinase, glucose oxidase	Polyphenols, polyanilines, vinyl polymers; including polymer modifications
Transferases	Glycosyltransferase, acyltransferase	Polysaccharides, cyclic oligosaccharides, polyesters; including polymer modifications
Hydrolases	Glycosidase (cellulase, amylase, chitinase, hyaluronidase), lipase, peptidase, protease	Polysaccharides, polyesters, polycarbonates, polyamides, polyphosphates, polythioesters; including polymer modifications
Lyases	Decarboxylase, aldolase, dehydratase	
Isomerases	Racemase, epimerase, isomerase	
Ligases	Ligase, synthase, acyl-CoA synthetase	Used for polymer modifications

Source: Kobayashi and Makino [49]. Reproduced with permission from American Chemical Society.

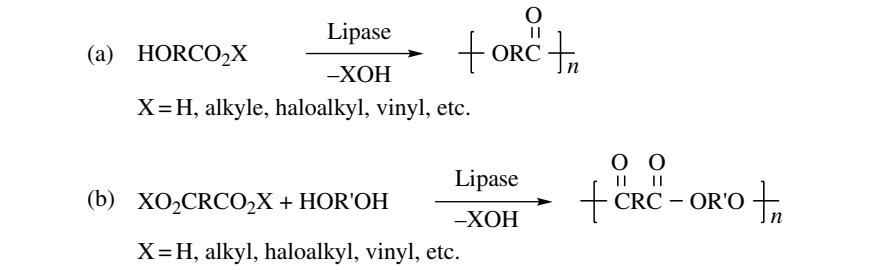

FIGURE 3.37 Polycondensation reaction via (a) esterification and (b) transesterification reactions.

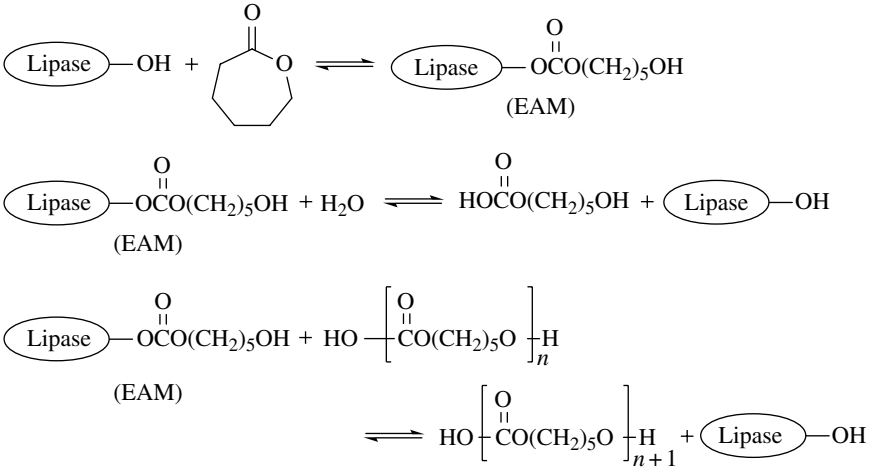

FIGURE 3.38 Mechanism of enzyme-catalyzed ring-opening polymerization (ROP).

structure depend on the enzyme water content, the enzyme/substrate ratio, the monomer/substrate ratio, and the reaction temperature.

ROPs (Fig. 3.38) are very atom economic processes since no leaving groups are required. The polymerization of lactones by chemical means is usually slow and can be significantly enhanced by using enzyme catalysts. The mechanism of ROP is shown in Figure 3.38 [51] and is supposed to start by nucleophilic attack of the lipase serine residue at the carbonyl group of the lactone forming a so-called enzyme-activated monomer (EAM). The initiation proceeds via reaction of a nucleophile, such as H_2O, alcohol, or amine, with the EAM complex to form the monoadduct. Chain growth takes place when the hydroxyl end group of a chain acts as the nucleophile that reacts with the EAM complex leading to an elongation of the chain by one repeat unit. ROP can be performed in bulk as well as in organic solvents and water, and examples of monomers for enzyme-catalyzed ROP are shown in Figure 3.39.

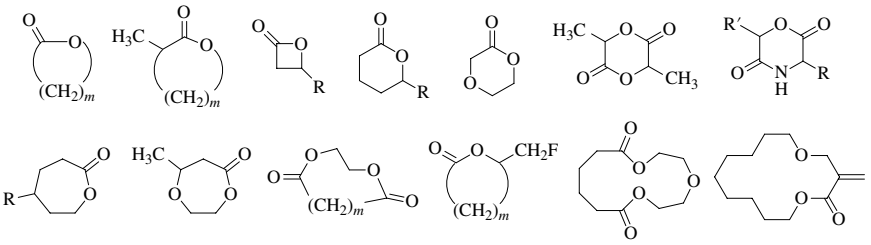

FIGURE 3.39 Examples of cyclic monomers for enzyme-catalyzed ring-opening polymerization reactions.

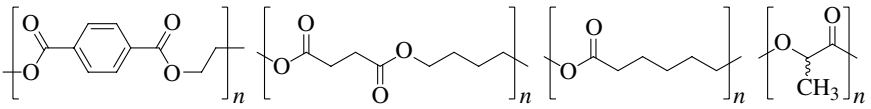

FIGURE 3.40 Examples of polyesters.

An important group of enzymatically derived polymers is polyesters. In nature, they hold the fourth place after the three major biomacromolecules (nucleic acids, proteins, and polysaccharides). Important polyesters are poly(ethylene terephthalate) (PET), poly(butylene succinate) (PBS), poly(ε-caprolactone) (poly(ε-CL)), and poly(lactic acid) (PLA) (see Fig. 3.40). The former two are industrially produced via polycondensation and the latter two via ROP. Additionally, enzymes can be used to hydrolyze ester bonds, which offers the possibility to recycle commercially used materials, for example, PET [52].

Natural polysaccharides like cellulose or amylose can be obtained via polycondensation reactions, while chitin and glycosaminoglycans (GAGs) are synthesized by ROP [49]. One group of unnatural polysaccharides is hybrid polysaccharides obtained from two different polysaccharide components and is very difficult to synthesize via conventional chemical synthesis.

Other examples of enzymatically derived types of polymers are polycarbonates, polyamides, polyphosphates, polythioesters, polyaromatics, or vinyl polymers (see Fig. 3.41).

Another field of enzymatic polymer synthesis is the enzyme-catalyzed modification of preformed polymers by esterification or transesterification. Thereby, it is possible to either introduce functional side groups into an existing polymer with a stable backbone (no polyester) to synthesize functional homopolymers as well as random copolymers or to generate multiblock copolymers by enzymatic transesterification between two different homopolymers.

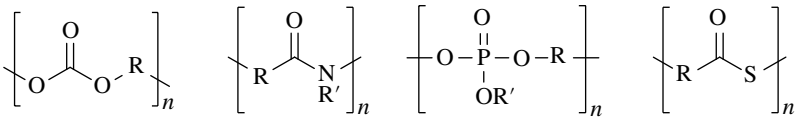

FIGURE 3.41 Examples of enzymatically derived types of polymers.

3.7 SOLID PHASE SYNTHESIS AND BIOTECHNOLOGICAL APPROACHES

3.7.1 Solid Phase Synthesis

Solid phase synthesis refers to a heterogeneous synthesis that is carried out on the surface of a solid phase in a gas or a solvent. The compound of interest that undergoes chemical modification is always attached to the solid phase, while the reagents and side products of its modifications are in solution or gas phases. This is the main difference of solid phase synthesis from, for example, heterogeneous catalysis or a variety of other chemical modifications that can be performed on a surface of a solid material. Solid phase synthesis is advantageous because of the quick phase separation that can be performed by a simple filtration in the case of reaction in a liquid phase. The synthesized compound always remains on the solid resin, while the side products are simply washed away. This benefit of solid phase synthesis is especially important for synthesis of complex alternating polymers such as peptides, DNA, RNA and oligosaccharides where the stepwise growth of the polymer chains can be automated. Today, solid phase synthesis is mostly associated with the synthesis of such biological polymers.

Considering the limitation in the biotechnological approaches of oligonucleotide replication as well as peptides and oligosaccharide expression, the synthesis time and the cost efficiency of solid phase synthesis make it the method of choice for short biopolymer production. The diversity of orthogonal protection strategies developed for solid phase synthesis allows the site-specific modification of biopolymer chains, which is critical for drug conjugation or biomaterial formation. Solid phase synthesis is also the only method for the synthesis of biopolymers containing unnatural functional units, which can expand their applications beyond the biological systems.

3.7.1.1 Solid Phase Peptide Synthesis

Proteins, as a biopolymer class, are one of the main structural and regulatory units in living organisms. Proteins consist of linear chains of alpha amino acid

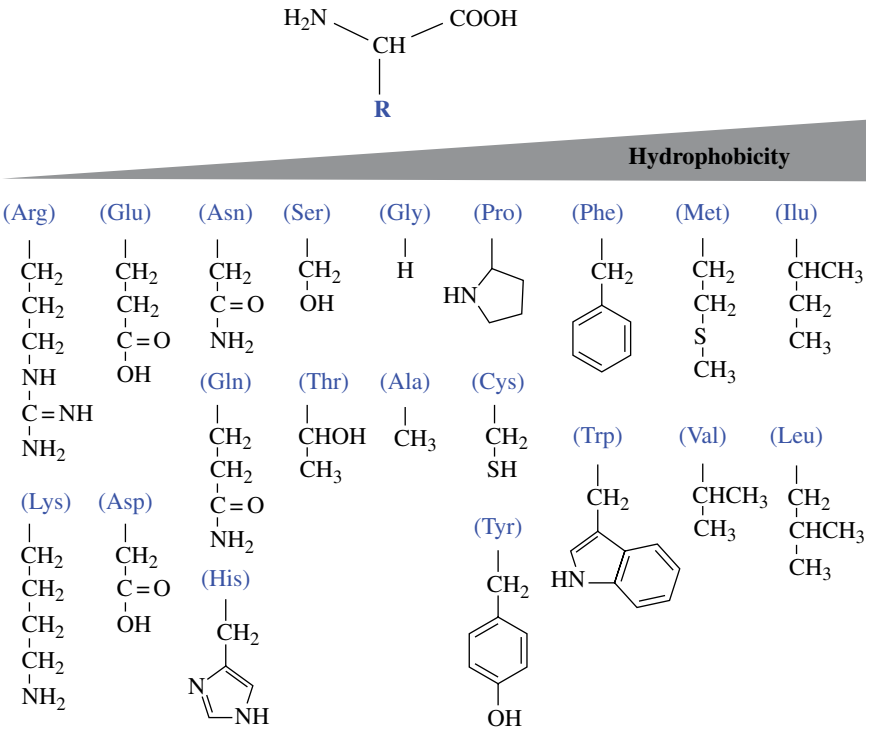

FIGURE 3.42 Structure and the three-letter code of the main mammalian amino acids. The amino acids are aligned toward the increasing relative hydrophobicity under physiological conditions.

residues that determine their structural and corresponding biological characteristics. There are 20 natural amino acids that make up the sequences of mammalian proteins (Fig. 3.42). Amino acids vary in their side chains, which represent nearly all main functional groups in organic chemistry (amine, amide, carboxylic acid, aromatic rings, etc.). The diversity of the amino acid side groups highly complicates the development of protein synthesis because each side group requires a special protection strategy. Solid phase peptide synthesis (SPPS) is usually limited to the synthesis of peptides of up to 50 amino acids, as its application for the synthesis of longer polypeptides is limited due to strong steric effects. Other methods such as chemical ligation [53] or protein expression [54] are used for syntheses of such polypeptides.

SPPS was originally developed by Robert Bruce Merrifield in 1963 and involves stepwise additions of protected amino acids to a growing peptide chain, which is covalently bound to a solid resin particle. The solid support for peptide synthesis must maintain a stable physical form that allows filtration in all of the

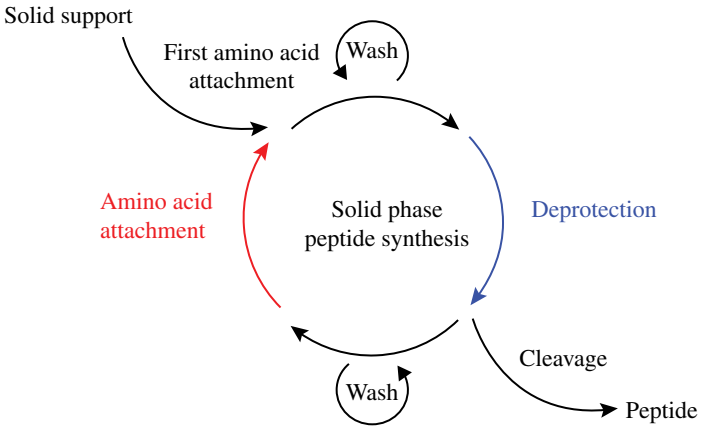

FIGURE 3.43 Synthetic scheme for solid phase peptide synthesis.

solutions that are used during the synthesis process. It also has to contain a functional group that allows its modification and the attachment of the first amino acid through a linker that would later allow removal of the synthesized peptide. In modern SPPS, the derivatives of polystyrene are commonly used as a solid support for SPPS, besides rare syntheses of highly hydrophobic peptides that are typically performed on polymeric polystyrene (PS) beads or PEGylated resins. The C-terminus of the peptide could be synthesized in a form of carboxylic acid or amide depending on the resin used for the synthesis. The general scheme for peptide synthesis is shown in Figure 3.43 and consists of several main steps. This first step of SPPS is the first amino acid attachment to a solid support. This initial step is followed by stepwise deprotection—amino acid attachment cycle that is repeated until the peptide sequence is completed. The cleavage of the synthesized peptide from the solid support is the last step of the synthesis.

Peptide sequences are always written from N-terminus to C-terminus, which represents the direction of their biosynthesis. In SPPS, the growth of the peptide chain goes from C-terminus toward N-terminus; therefore, the first amino acid in SPPS is the last amino acid in synthesized peptide sequence.

Protection Strategies

The essential part of SPPS is the protection of amino acid functional groups, which should not participate in peptide bond formation. To prevent undesired reactions with those functionalities, the so-called protection groups are required. There are two types of protection groups used in SPPS. The first protects the functional groups of amino acid side chains and should remain stable during the peptide synthesis process but be easily removed after the synthesis is complete. The second is a protection group of the alpha amino group in amino acids. This

protection group should be stable during the amino acid coupling but needs to be deprotected after the coupling is finished in order to allow the following amino acid to be attached. Importantly, the deprotection of the alpha amino group must be performed without interfering with the protections of amino acid functionalities. In other words, the deprotection of alpha amino group and the side chain functionalities must be orthogonal and is critical for successful SPPS. The combination of protection groups that can be removed independently from one another is known as protection strategies. There are two main protection strategies that refer to the names of the protection of alpha amino groups: *t*-butoxycarbonyl (*t*-Boc) and 9-fluoroenylmethyloxycarbonyl (Fmoc).

The first is *tert*-butyloxycarbonyl or, for short, Boc-based protection strategy (Fig. 3.44). The Boc group is stable in the presence of bases but labile

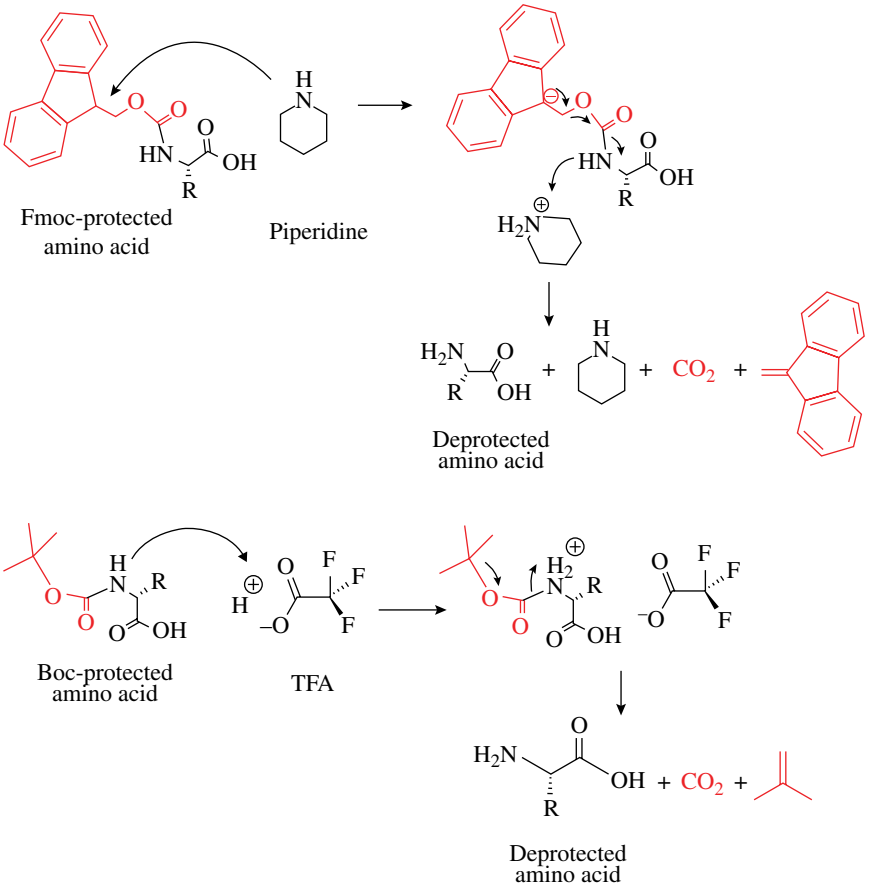

FIGURE 3.44 Deprotection mechanism of alpha amino groups in Fmoc and Boc protection strategies.

to acid hydrolysis and, therefore, can be removed quickly by exposure to a strong acid like trifluoroacetic acid (TFA). The side chain groups in this case are mostly protected by benzyl groups. While the TFA treatment is relatively safe, the deprotection of benzyl groups is performed by hydrolytic cleavage by anhydrous HF. This requires plastic glassware and special care due to the high toxicity of HF. 9-Fluoroenylmethyloxycarbonyl or Fmoc-based strategy is based on the properties of Fmoc to be removed by strong nucleophiles (usually piperidine) while remaining stable in the presence of strong bases. The side protection groups in this case could be any acid labile moieties that are stable to nucleophilic substitution such as the Boc group. The variety of protection groups and the simplicity of their deprotection in Fmoc-based strategy have resulted in its domination in common peptide synthesis.

Peptide Bond Formation

In order to create a peptide bond, a carboxylic group of one amino acid is activated and attached to the amino group of another. The activation of the carboxylic group can be archived through, for example, the creation of chloro anhydride or a semistable *n*-hydroxysuccinimide (NHS) ester, which would react with any unprotected amino group forming a corresponding amide. Currently, carbodiimide chemistry is found to be the most suitable for the peptide bond formation due to both the high reactivity and low side product formations. While classical carbodiimides like dicyclohexane carbodiimide (DCC) are still in the use, highly reactive species such as *O*-(benzotriazol-1-yl)-*N*,*N*,*N*′,*N*′-tetramethyluronium tetrafluoroborate (TBTU) are reagents of choice in the modern peptide synthesis labs. Because the carbodiimide adduct of a carboxylic group is unstable, the reaction is carried out through the formation of the so-called active esters with 1-hydroxybenzotriazole (HOBT). The formed active ester is a very reactive species; nevertheless, its stability is enough to perform long-term couplings (>1 h) in order to achieve high yields. In some cases, double coupling with capping is used to achieve higher purity of the final products. The double coupling refers to the repeated step of the same amino acid attachment, when the resin is washed and the same reagents are added for the second time in order to increase the conversion of the introduced amino acid. The double coupling is found to be effective for synthesis of hydrophobic peptides where the efficiency of the coupling reaction is low. It is also commonly used for the synthesis of long peptides and becomes indispensable for peptides longer than 30 amino acids. The capping is an additional step of acetic anhydride reaction with unprotected amino groups of the synthesized peptide, which prevents sequence mistakes and simplifies the purification.

Cleavage from Support

The final step in peptide synthesis is the cleavage of the synthesized peptide from the resign and removing all of the side chain protection groups. The resin linker and the side protection groups are designed to be labile by acid hydrolysis and usually are removed by reactions with strong acids such as TFA in the presence of water. In the Fmoc protection strategy, all of the side protection groups are also removed by acetic hydrolysis. The cleavage reactions of side protection groups create a large amount of positively charged ions, which can react with the deprotected peptide. Such side reactions are especially efficient if the peptides contain nucleophiles in their sequences such as sulfur-containing residues (Cys, Met) or any aromatic amino acid residues (Phe, Tyr, Trp). Strong nucleophiles, phenol or triisopropylsilane (TIPS), also known as scavengers of cations, are typically added to the cleavage solution in order to prevent these unnecessary side reactions. Another reagent dithiothreitol (DTT) is added to the cleavage solutions in the case of cysteine-containing peptides. DTT prevents disulfide bond formation between cysteine residues of the peptides and is necessary if the cleavage is not performed in an inert atmosphere. The cleavage usually takes several hours and the deprotected peptide can be separated from the resin by simple filtration. Peptide precipitation in diethyl ether removes the components of the cleavage mixture that are soluble in diethyl ether, while the final peptide purification is commonly achieved by high-performance liquid chromatography resulting in high peptide purity.

Orthogonal Protection Strategies for Cysteine

Disulfide bridges dictate the conformational stability of proteins, and their precise formation is important for successful peptide synthesis. Simple oxidation with air or some stronger reagents such as iodine solution in acetic acid are typically used for the creation of disulfide bonds between two cysteines. For peptides that contain more than two cysteine residues, it is required to develop orthogonal protection strategies in order to control the specificity of the oxidation. The application of different deprotection conditions allows to expose one cysteine for oxidation while keeping the other inert. There are many orthogonal protection strategies for site-specific disulfide bond formation; the most common ones are shown in Figure 3.45.

3.7.1.2 Solid Phase Synthesis of Polynucleotides

Polynucleotides consist of alternating chains of nucleotides that are nucleoside molecules connected by a phosphate ester bond at 3′ and 5′ positions as shown in Figure 3.46. Nucleosides consist of a pentose and nucleobases that

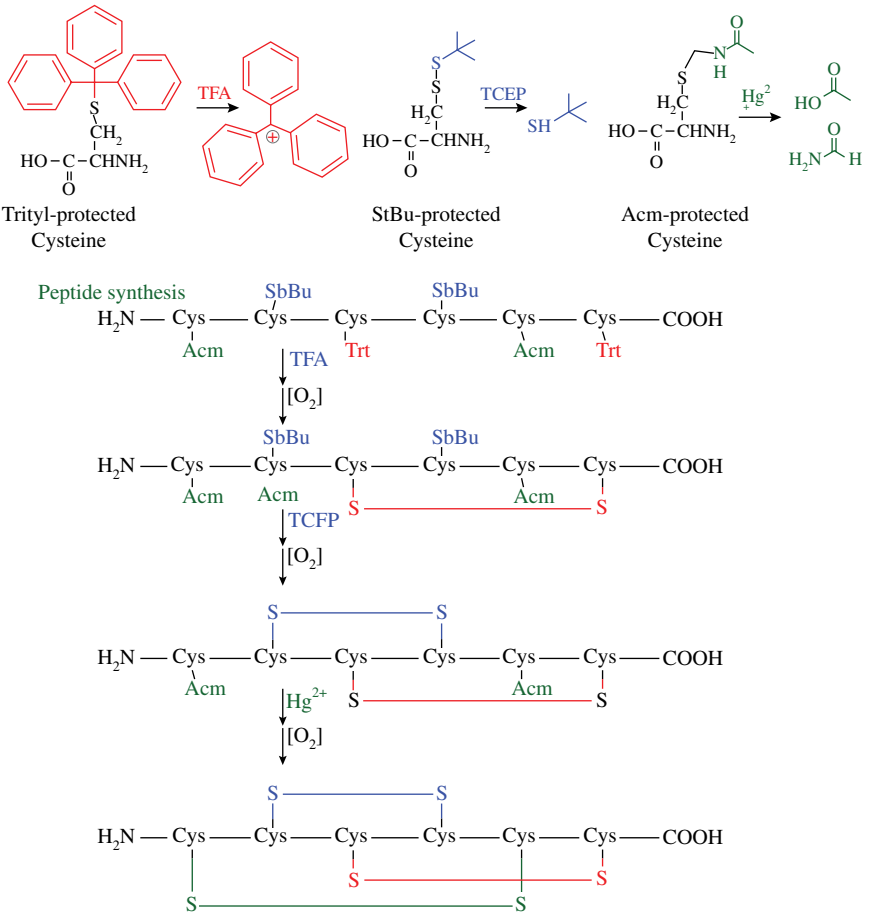

FIGURE 3.45 Orthogonal side chain protection strategies for cysteine and their application for site-directed disulfide bond formation.

are linked via beta-glycosidic bond. The saccharide part of nucleosides could be ribose (ribonucleic acid RNA) or deoxyribose (deoxyribonucleic acid DNA), which define the difference in the biochemical properties of polynucleotides. Nucleobases are the letters of the polynucleotide code that stores all the genetic information in organisms. The defined binding position of the phosphate bond between nucleosides allows differentiation between the beginning (5′) and the end (3′) of polynucleotides.

Whereas enzymes synthesize DNA and RNA in a 5′ to 3′ direction, chemical oligonucleotide synthesis is carried out in the opposite, 3′ to 5′ direction using a solid phase approach. Solid phase polynucleotide synthesis requires stepwise creation of a phosphate ester internucleotide linkage. Currently, phosphoramidite

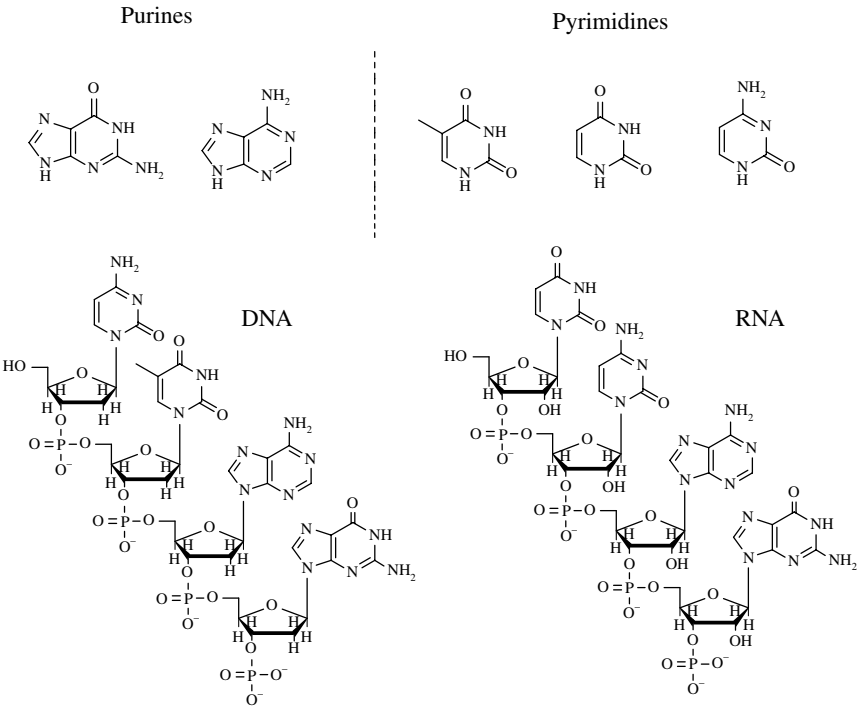

FIGURE 3.46 Bottom: chemical structure of a polynucleotides (DNA, RNA). Top: chemical structure of nucleoside bases.

chemistry is applied in automated solid phase synthesizers for the creation of up to 150 base pair polynucleotide with acceptable yield (Fig. 3.47). The synthesis consists of several repeating steps, which are coupling, capping, oxidation, and deprotection.

The similarity of nucleobases resulted in a relatively simple protection strategy when compared to peptide solid phase synthesis. Nucleobases containing an exocyclic amino group (cytosine, adenine, and guanine) required a protection group, while others can be used in the synthesis without any protection groups. The protection of the amino group is achieved via creation of amide bond, which could be cleaned by an acid catalysis when the synthesis is complete and the formed polynucleotide is removed from the resin. In DNA synthesis, only the 5′ position of the pentose needs temporary protection. The extra 2′ hydroxyl group in ribose requires protection during RNA synthesis, which commonly is achieved by *tert*-butyldimethylsilyl ether (TBS). This extra protection group is the only difference in the synthesis of DNA and RNA. Any solid phase synthesis of polynucleotides starts with the attachment

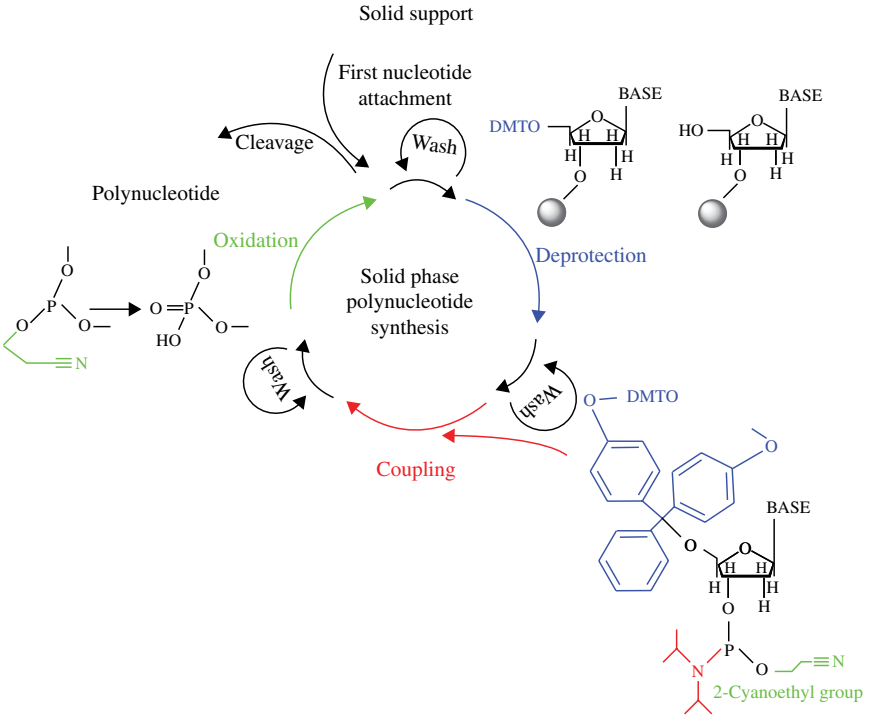

FIGURE 3.47 Left: schematic view of the solid phase polynucleotide synthesis. Right: the structure of DNA building block with the protection (red) and activation groups (blue). (*See insert for color representation of the figure*.)

of the first phosphoramidite to the solid support and finishes with an acidic cleavage of the formed DNA from the resin. Anhydrous acetonitrile is the main solvent of the synthesis because some of the steps (coupling) are extremely sensitive to the presence of water.

The synthesis itself is repeating steps that can be easily automated and is schematically shown in Figure 3.43. The first step is the deprotection of DMT group that is removed by a very diluted solution (1–2%) of organic acids such as TFA. The acidic cleavage of DTM (detritylation) is very fast and does not interfere with the solid face resin, which also cleaved by an acidic catalysis, but requires higher greater than 90% acid concentration and an extensive reaction time. The resin with the attached phosphoramidite is extensively washed to remove the products of the reaction. Next, nucleoside phosphoramidite (or their mixture if combinatory method is applied) is coupled to the freed 5′ position of the attached phosphoramidite. This step is catalyzed by an acidic azole

catalyst such as 2-ethylthiotetrazole or similar. The activation is very fast and requires less than a minute for its completion in the case of DNA synthesis. This step requires extra time (>5 min) for the formation of RNA because of steric hindrance of the 2′-O-protectection group in ribonucleoside phosphoramidites. In the coupling step, 5–20-fold excess of the attaching phosphoramidite is used. Generally, the excess of phosphoramidites decreases with increasing the scale of the synthesis. The side products and unreacted phosphoramidites are removed by washing after the coupling is finished. The following capping step is necessary to terminate any unreacted 5′-OH groups (0.1–1%), which can result in accumulation of the DNA molecules with a missing nucleotide. The capping is performed by acetic anhydride with 1-methylimidazole, which forms a relatively stable ester bond with unreacted 5′-OH groups. The amount of capped 5′-OH groups increases with the prolongation of synthesized polynucleotide chain, which is the main limit in the synthesis of long polynucleotides. The final step in the polynucleotide synthesis is oxidation of the formed phosphite triester linkage in order to stabilize it by transferring into the phosphate triester form. The oxidation is usually performed by treatment with iodine in the presence of a weak base. In some cases, the oxidation could be substituted with sulfurization in order to obtain phosphorothioate, which is more stable toward enzymatic cleavage compared to the natural phosphate nucleotide linkage.

Currently, oligonucleotide synthesis is efficient for the creation of up to 150 nucleotide long DNA or RNA molecules. This technology can be easily upscaled to industrial amounts of polynucleotide synthesis if necessary. Nevertheless, the main market of DNA synthesis is primers for polymerase chain reaction (PCR). It typically requires only micromolar concentration of short (18–24 bp) DNA molecules, which defined the modern instrument and resin requirements for polynucleotide synthesis. The synthesis is usually performed with micromole scale on functionalized glass bits, which are nonswelling but can be quickly washed. Such resin has a lower loading amount compared to peptide synthesis but allows very fest washing and does not require time-consuming preliminary swelling. Similar to peptide synthesis, polynucleotide solid phase synthesis allows inclusion of nonnatural nucleotides or various functional molecules in order to introduce new physicochemical properties or for their following conjugation.

3.7.1.3 Solid Phase Polysaccharide Synthesis

The late understanding of oligosaccharide importance in many physiological and regulatory mechanisms of living matter resulted in glycomics being underappreciated when compared to proteomic and genomic fields. Peptide

and oligonucleotide syntheses are currently considered to be routine methods in many research and industrial labs. A great variety of synthetic precursors for peptide and oligosaccharide syntheses are commercially available, while the reagents and precursors for carbohydrate synthesis still require synthesis in the lab. Moreover, in contrast to peptides and polynucleotides, carbohydrates are often branched, which requires the use of nonlinear protection strategy for their synthesis. About 10 various monosaccharides are found in the chains of mammalian polysaccharides (Fig. 3.48); a much greater diversity is present in other organisms and plants. The small physicochemical difference between the monomers in carbohydrate polymer chains complicates the purification of the synthesized polysaccharide from its side products. As a result, polysaccharide or carbohydrate polymer solid phase synthetic approaches are still in the early stage of development.

The comprehensive automated solid phase synthesis of polysaccharides becomes possible only in the late 1990s, after the work introduced by the lab of Seeberger [55]. In the modern version, the solid phase synthesis of oligosaccharides involves two main steps: the deprotection and coupling (Fig. 3.49). Coupling is achieved by glycosylation of a free carboxylic group with glycosyl phosphates or glycosyl trichloroacetimidates. The reaction has to be carried out at −15°C and double coupling is necessary to be performed for the completion of the reaction. The low temperature is critical for the efficient couplings that require a cooled reaction vessel. 9-Fluorenylmethoxy carbonyl (Fmoc) and levulinoate ester could be used as the temporary protection groups. The deprotection step is achieved by a nucleophilic base for 9-Fmoc group or hydrazine hydrolysis for acetate or levulinoate ester. The groups could be removed selectively (orthogonally) in the presence of each other; thus, the building block containing these two protective groups could be used for the creation of branched oligosaccharides [56, 57].

The solid phase polysaccharide synthesis is performed on Merrifield's polystyrene resin functionalized with 4-octenediol linker. This linker is stable during the synthesis cycles but can be cleaved by Grubbs' catalyst (cross-metathesis reaction) resulting in fully protected polysaccharide, which can be used for further functionalization or deprotected in its native state. The final purification is achieved by high-performance liquid chromatography, which in some cases also can be used to separate the different stereoisomers of the final products [58].

A complex synthesis of the precursors and the sophisticated coupling–deprotection steps restricted the common use of the proposed solid phase synthesis approach, while the liquid phase synthesis is still a reasonable alternative for most carbohydrate chemists. Nevertheless, the perspectives of solid phase synthesis are not questioned with increased commercial

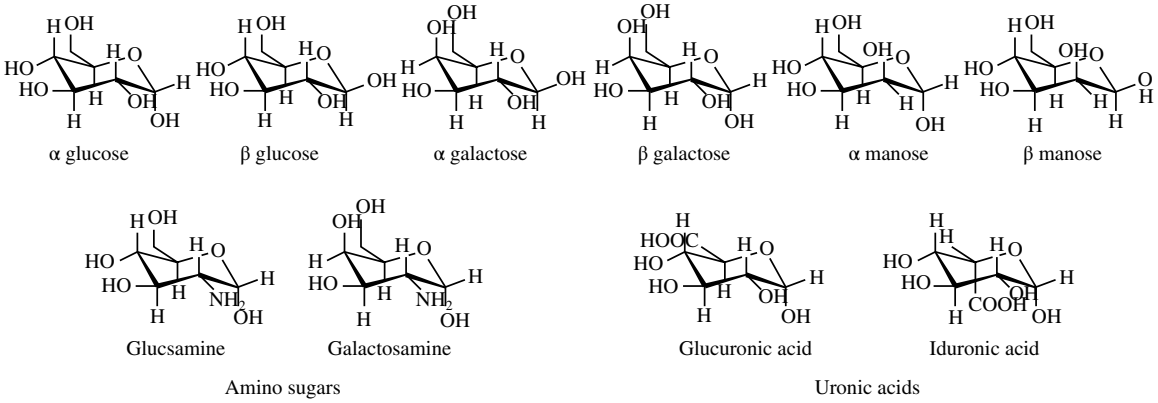

FIGURE 3.48 The chemical structure of monosaccharides currently applied in the solid phase synthesis.

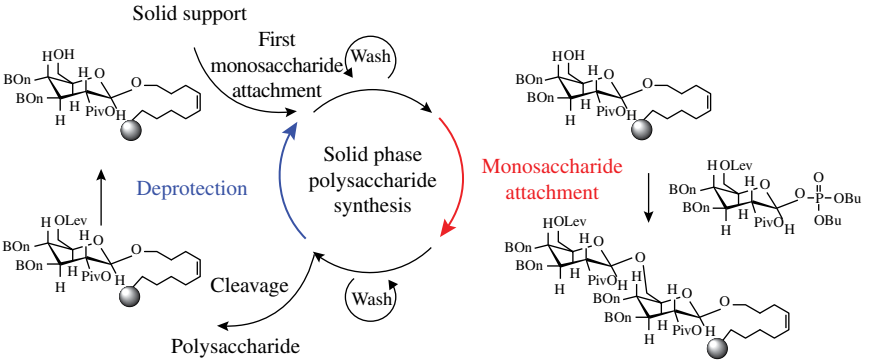

FIGURE 3.49 Schematic view of the solid phase polysaccharide synthesis.

availability of the building blocks and the new engineering solutions for the automated synthesizers where inbuilt temperature control could promote the use of such synthetic approach in glycomics.

3.7.2 Biotechnology Approaches in the Synthesis of Biopolymers

Biosynthesis (the formation of chemical compounds by a living organism) of biopolymers developed concurrently with the success of solid phase synthetic approaches. Currently, proteins and polynucleotides can be produced industrially via biosynthesis, while polysaccharide development is mainly unexplored. Such biotechnology approaches often can produce proteins and polynucleotides in their natural conformations and also allow for their modifications through genetic engineering. Biosynthesis is the only available method for the production of high molecular weight biopolymers, which cannot be produced by any other synthetic approaches. Nevertheless, biosynthesis has several limitations defined by the variety of enzymatic reaction that can take place in the cells during or after the synthesis. Both polynucleotides and proteins can acquire undesired mutations, cleavage, or misfolding and, therefore, should be properly checked after expression in bacterial or cell culture. Purification of the synthesized biopolymers from cell cultures, which typically contain a large amount of various compounds, can be a challenge. Additionally, production of low molecular weight proteins (<20 amino acids) and polynucleotides (<100 base pairs) by biosynthetic methods is usually not attractive as these can be more easily produced by solid phase synthesis methods. With a few exceptions, biosynthetic approaches are limited by the naturally occurring amino acids or nucleotides of the cells they are translated in. Thus, biosynthesis and solid phase synthetic approaches do not compete but rather complement each other. Biosynthetic schemes are used for high molecular

weight natural polynucleotides and proteins, while solid phase synthesis is applied to peptide and oligonucleotides formation, which allows implementation of a variety of unnatural functionalities.

3.7.2.1 Polynucleotide Biosynthesis

There are two techniques for polynucleotide synthesis that are applied for the production of medium- to large-sized DNA. PCR is commonly utilized for amplification or modification of medium-sized DNA motifs (150–10,000 base pairs). For larger DNA sequences (>10,000 base pairs), genetic engineering is preferred. Both require solid phase synthesis of DNA sequences: primers for PCR or short DNA pieces for gene assembly in genetic engineering methods.

Polymerase Chain Reaction

PCR reactions utilize certain thermostable DNA polymerases, which can synthesize DNA at 70–80°C and do not denaturate at higher temperature (>98°C). These polymerases allow for the stepwise heating/cooling cyclic steps that are required for DNA denaturation, primer annealing, and DNA elongation when appropriate primers are present (Fig. 3.50). Briefly, the first step of the cycle is DNA denaturation (94–98°C), which is followed by an

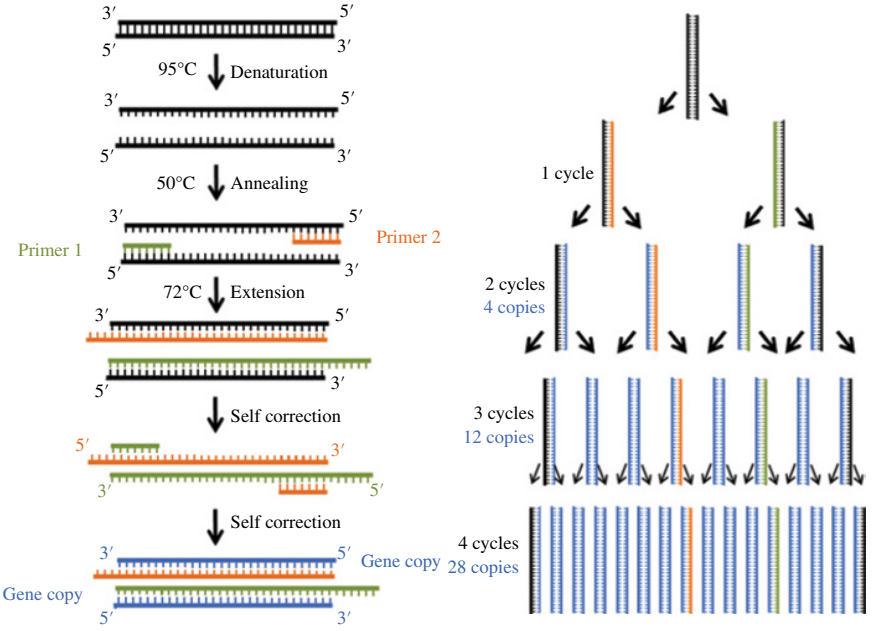

FIGURE 3.50 Schematic view of PCR cycle (left) and propagation (right). (*See insert for color representation of the figure*.)

annealing step (50–65°C) allowing the primer attachment and finally DNA elongation (70–75°C) where deoxyribonucleotide triphosphates are incorporated into the new DNA strand by the polymerase. Common PCR techniques involve 20–40 repeating cycles, depending on the amount of the required DNA and the amount of the initial DNA samples. The relatively high efficiency of PCR allows the production of nearly unlimited amount of copies from a single DNA molecule.

Affinity chromatography methods are often applied for the purification of DNA samples after PCR amplification. The chromatography columns are designed to bind a defined molecular weight range of DNA while primers and enzymes can pass through. Next, the DNA is eluted under denaturizing condition resulting in a pure product.

DNA polymerases utilized in PCR have different synthetic specificity, which is defined by the mutation frequency (about 10^{-4} errors per bp). Therefore, sequence verification is commonly needed for PCR because of high mutation probability. Some applications that are not related to the gene or protein expression have a high tolerance for mutations and therefore do not require the expensive sequencing step.

Genetic Engineering

Genetic engineering is used to synthesize large or complex DNA sequences or to produce new DNA sequence (e.g., in codon optimization) and in general can be described as two distinguished steps, which are gene design and cloning (Fig. 3.51). Gene design occurs *in silico* and is used to virtually assemble DNA molecules. First, small DNA molecules that can be synthesized by solid phase synthesis and assembled into one large DNA piece for further replication are designed. This methodology has a wide application in nanoscaled science (DNA origami) and DNA-based materials. The second part is gene cloning and combines several steps of DNA manipulation, which results in identical copies of the gene (Fig. 3.51). Bacterial plasmids are extrachromosomal cyclic DNA sequences that in nature are found exclusively in bacteria but still can be transcribed and translated in eukaryotic and yeast cells. Plasmids are beneficial tools in gene cloning because they are selectable and can occur in multiple copies per bacteria (thus increasing DNA yield) and are faithfully replicated by bacteria allowing for fast and easy DNA amplification. Using DNA computation methods, almost any DNA sequence can be designed to be included into a plasmid. Classical cloning or recombination can be used to modify plasmids in order to introduce a new gene or modify the existing nucleotide sequence. Cell membranes are rendered permeable through electroporation or through chemical means to transport the plasmid across the

cell membrane. Thus, plasmid reaches the cell cytoplasm where it can be replicated. Plasmids can be rapidly multi-implanted in bacterial or eukaryote cell cultures with approximately 10^{-8} to 10^{-11} error occurrence per base pair, a low error value that is comparable for both bacteria and eukaryotes. Nevertheless, the formed DNA can undergo undesired postsynthetic modification such as DNA cleavage, insertions/deletions, or mutations or methylation, and therefore, a quality control should be performed. Because DNA cleavage results in a significant molecular weight difference between the original sequence and modified sequence, a simple gel electrophoresis can reveal such errors. DNA sequencing can evaluate the sequence, and thus mutation and methylation can be tested for.

Plasmid DNA can be separated from bacterial genomic DNA by a protocol, which includes precipitation in a denaturizing alkaline solution with following reconstitution in an acetate buffer, also known as Alkaline Lysis Miniprep. However, for applications that require only the purest plasmid DNA, chromatographic methods of purification should be applied. Commonly, the chromatographic cartridges are applied, which allow a defined range of DNA to pass through but trap the larger genomic DNA.

RNA Replication

RNA biosynthesis is similar to DNA synthesis but includes one extra step, which is transcription of DNA into RNA molecule by RNA polymerase enzyme. For replication of natural RNA of interest, a reverse transcription is

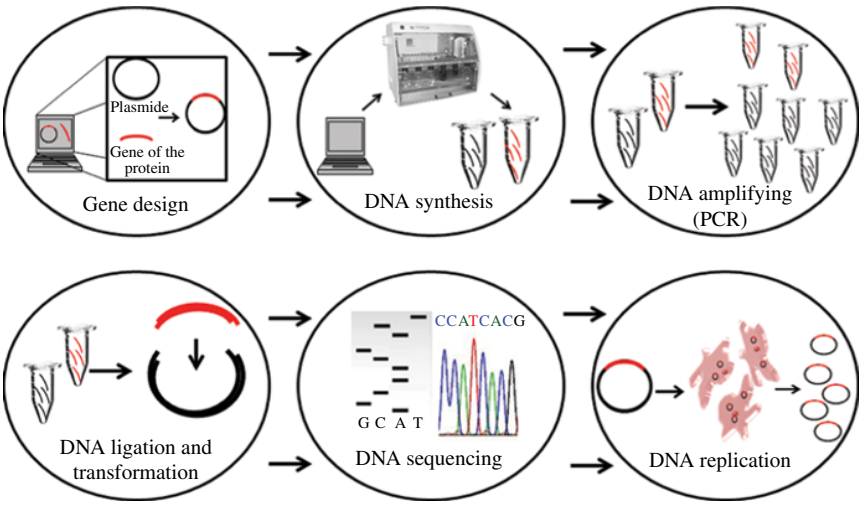

FIGURE 3.51 Schematic view of DNA replication. (*See insert for color representation of the figure.*)

applied, which allows the formation of the complementary DNA code for the RNA and its following mutation and sequencing. The main difference of the RNA production from DNA replication is the special caution during RNA purification.

3.7.2.2 Protein Biosynthesis

Protein expression became possible only after the success of DNA engineering as it allowed the production of recombinant proteins, as shown in Figure 3.52. The DNA sequence of the gene of interest can be synthesized and assembled into one complementary piece also called vector, which upon expression in the cell is translated and transcribed to the desired protein. The gene of interest and additional DNA sequences are cloned into a DNA vector using common DNA engineering methods, and the formed plasmid is then replicated in cell culture. Depending on the nature of the protein and its expression vector, gene expression can be completed in a bacterium, which is the simplest and efficient, or in eukaryotic cell cultures, which are more sophisticated and difficult, but are required for some applications.

The mechanism of the protein synthesis occurs along with normal cell processes. First, the DNA is transcribed into mRNA; then translation into protein sequence occurs. The protein's characteristics define if it will be secreted by the synthesizing cell into the surrounding medium (common for extracellular proteins) or accumulated inside the cell in cytoplasm, nucleus, or membrane. The purification strategies correspond to the protein localization. For extracellular proteins, the media can be filtered off the cells and

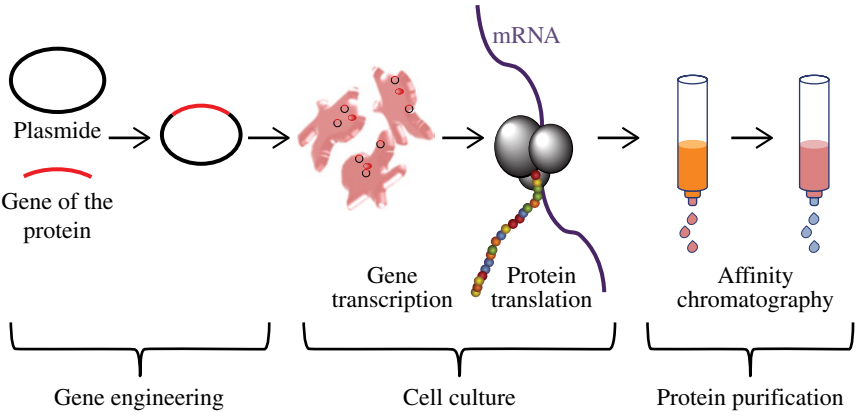

FIGURE 3.52 Schematic view of recombinant protein expression.

then the protein is purified. This method does not require cell death and therefore could be used for continuous protein productions with a cell medium flow like that commonly used in bioreactors. The cells must be destroyed, however, in order to extract the synthesized protein when the protein is accumulated within the cytoplasm, nucleus, or membrane. For both approaches, the protein is purified by affinity chromatography. A specific binding site (tag) is introduced into the peptide sequence during gene engineering for proteins that do not have specific binding sites for affinity chromatography.

3.7.2.3 Polysaccharide Bioengineering

While synthesis and modification of polysaccharides has advanced in the last years, relevant biosynthetic methods for mammalian polysaccharide production are currently unavailable with one exemption. Among the variety of extracellular polysaccharides, only hyaluronic acid (HA) has been shown to be produced by a biotechnological process. Originally, HA was produced in pathogen microbial cultures such as *Streptococcus zooepidemicus*, which provide high dispersity and poor control over the average molecular weight. Additionally, this method requires a precise discipline over the synthesis and purification to avoid possible toxin contaminations. Recombinant HA from both Gram-positive and Gram-negative bacteria allowed avoiding most of these issues by providing better control over the molecular weight and the dispersity of the product. HA expression could be achieved only by introducing the whole biosynthesis pathway with all major enzymes as it is shown in Figure 3.53.

The expression of HA includes insertion of several key gens as vectors in DNA plasmid, which allows the expression of all crucial enzymes in HA

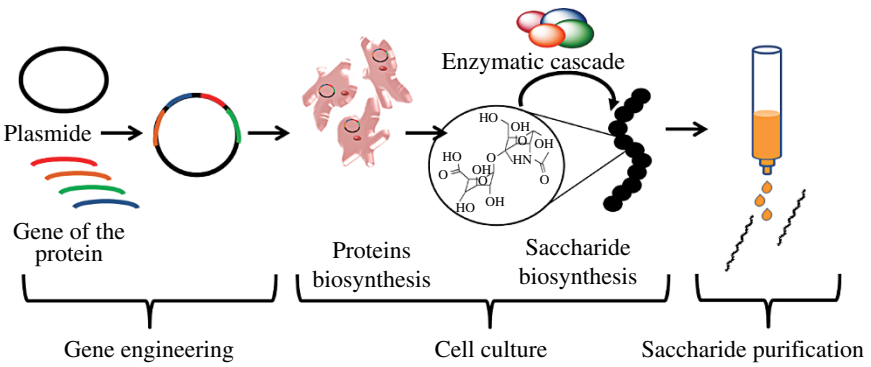

FIGURE 3.53 Schematic view of recombinant hyaluronic acid biosynthesis.

biosynthesis pathway. Precise control over the temperature and the biosynthesis time allowed the alternation of HA molecular weight through the manipulation of the enzyme activity. Nevertheless, the creation of uniform HA with defined molecular weight cannot yet be achieved by this approach because the regulatory mechanisms of initiation, elongation, and termination of HA in molecular synthesis are mostly undefined.

3.8 HYDROGELS AND HYDROGEL SCAFFOLDS

Hydrogels are a class of polymeric materials with a three-dimensional (3D) structure. Due to their high water content and their good biocompatibility, they have many biomedical applications. As one example, their use in tissue engineering as porous scaffolds for repairing and regenerating a wide variety of tissues and organs will be highlighted here.

3.8.1 Hydrogels

Hydrogels are composed of hydrophilic polymer networks (synthetic, natural, or mixed), which can swell in water [59, 60]. The molecular construction of a hydrogel network (Fig. 3.54) is held together by physical interactions like hydrophobic forces, hydrogen bonds, chain entanglement, crystallinity, electrostatic interactions, or specific interactions, that is, antibody–antigen, avidin–biotin, or carbohydrates–lectins. Physical gels can undergo disintegration in the proper conditions. The so-called chemical gels are composed of polymer molecules that have been cross-linked by covalent bonds.

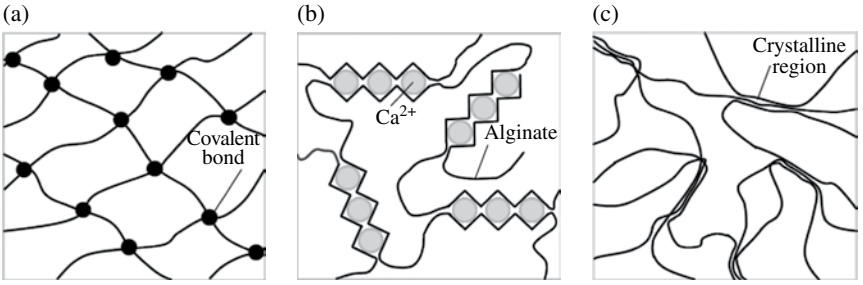

FIGURE 3.54 Schematic diagram of (a) a chemical hydrogel with covalent point cross-links (e.g., poly(ethylene glycol) (PEG) hydrogel), (b) a physical hydrogel cross-linked by ion–polymer complexation (e.g., calcium alginate hydrogel), and (c) a physical hydrogel with crystalline regions (e.g., poly(vinyl alcohol) (PVA) hydrogel).

Alternatively, hydrogels can be classified based on their composition, their preparation method, their ionic charge (neutral, anionic, cationic, ampholytic hydrogels), or their structure (amorphous, semicrystalline hydrogels).

Some methods to characterize bulk hydrogel networks and immobilized hydrogel layers will be presented in Sections 4.3 and 4.4.

3.8.1.1 Gel-Forming Materials

A variety of synthetic and naturally derived materials may be used to form hydrogels [60–63]. *Synthetic* materials include poly(hydroxyethyl methacrylate) (PHEMA), poly(ethylene oxide) (PEO), poly(ethylene glycol) (PEG), poly(vinyl alcohol) (PVA), poly(acrylic acid) (PAA), poly(methyl methacrylate) (PMMA), poly(acrylamide) (PAAm), poly(poly(propylene furmarate-co-ethylene glycol)) (P(PF-co-EG)), poly(vinylpyrrolidone) (PVP), and poly(*N*-isopropylacrylamide) (PNIPAAm) and its derivatives. Dendrimers and star polymers are exiting new materials because of their large number of functional groups available in a very small volume.

Representative *natural* materials used for hydrogel fabrication are fibrin, gelatin, collagen, cellulose, agarose, alginate, dextran, chitosan, and HA as well as other GAGs.

Moreover, by combining naturally derived polymers with synthetic building blocks, *hybrid materials* can be created offering both a defined functionality and biocompatibility as well as a high adaptability in terms of composition and structure. In the production of such hybrid systems, PEG is one of the most commonly used synthetic components since it provides excellent biocompatibility, a hydrophilic and uncharged character, and the possibility to easily modify its terminal end groups. Some biohybrid hydrogel materials will be presented in Section 5.5.

Stimuli-responsive hydrogels are polymer networks that sense and respond to changes in their external environment [64]. They can undergo dramatic changes in swelling, network structure, permeability, and mechanical strength due to external stimuli, such as changes in pH, ionic strength, electrical or magnetic fields, temperature, and changes in the concentration of biologically active molecules, like glucose or enzymes. Bioresponsive networks will be discussed in Section 6.4 in more detail.

Temperature-responsive hydrogels, mostly based on PNIPAAm and its derivatives, are widely studied and used for a variety of applications, including drug delivery and tissue engineering. If the temperature of the environment is raised to a critical value known as lower critical solution temperature (LCST), these networks tend to shrink or collapse and the systems undergo a reversible

polymer phase separation. Upon lowering the temperature below the LCST, the gels swell again. For instance, PNIPAAm coatings can be used for cell sheet engineering (cf. Section 6.5).

3.8.1.2 Synthesis of Hydrogels

Depending on the nature of the hydrogel precursor molecules (monomer/polymer, functional groups, etc.) and the desired application, different methods to synthesize hydrogel materials have been described, for example:

Formation by ionic interaction:

- Ionotropic hydrogels (e.g., calcium alginate) by mixing a polyelectrolyte with a multivalent ion
- Polyionic hydrogel ("complex coacervate" or polyion complex hydrogel) by mixing polyelectrolytes with opposite charge, for example, alginic acid and polylysine

Formation by chemical modification of hydrophobic polymers and subsequent physical or chemical *cross-linking*, for example, PVAc to PVA.

Formation by free radical reactions, including a variety of polymerizations and cross-linking of water-soluble polymers, for example, cross-linked PHEMA and PEG hydrogels, for example, photopolymerization.

Formation by condensation or addition reactions of multifunctional reactants:

- Urea or urethane bonds by reaction of isocyanates and amines or alcohols
- Amines or sulfides by Michael addition of amines or thiols to vinyl groups
- Amide bonds by reaction of amines and active esters (e.g., carbodiimide chemistry)
- Ester bonds by reaction of acids or acid chlorides and alcohols
- Schiff bases by reaction of aldehydes and amines

As building blocks polysaccharides, collagen, PAAc, PVA, PEG, and others can be used.

For *embedding of cells and for injectable hydrogels*, gel precursors that cure under mild conditions have to be selected. Gel formation processes that are due to physical changes like temperature, pH, or ionic strength and chemical reactions like Michael addition, Schiff base, or disulfide bond formation are appropriate (cf. Section 3.8.2.5).

Approaches using genetic engineering and biosynthetic methods to create unique hydrogel materials have been recently reported. Protein-based hydrogels and hybrid hydrogels containing protein domains may *self-assemble* from block and graft copolymers containing biorecognition domains driven by hydrophobic interaction (see also Section 5.5).

3.8.1.3 Application of Hydrogels

Hydrogel bulk materials and coatings are used for the fabrication of medical devices already through several decades. Early examples include the pioneering studies of Wichterle and Lim to produce contact lenses from poly(hydroxyethyl methacrylate) [65] and the work of Kolff [66] to treat patients suffering from kidney failure by means of cellulose-based membranes. Catheters used in cardiology for balloon dilatation or implantation of vascular stents are very often coated nowadays with polymer hydrogels to reduce the friction at the vessel surface. Many diagnostic assays utilize surface-bound hydrophilic polymer coatings (for preparation compare Section 3.9) to limit the nonspecific adsorption from biofluids (cf. Section 6.5). These applications, as well as several others, draw benefit from the high affinity of hydrogels toward water, resulting in advantageous mechanical properties as well as weak interactions with the molecular and cellular components of biofluids, tissues, and organs. In addition, hydrogels are used as functional coatings, for example, for cell culture carriers (cf. Section 6.5) and to prevent blood coagulation (cf. Section 6.4.2). Pharmaceutical applications are, for example, controlled drug delivery systems (DDS) (e.g., based on a change of properties under environmental stimuli). Bionanotechnology utilizes hydrogels as microdevice components, pumps and valves, medical and biological sensors, microarrays, and diagnostic imaging. In the following, we will concentrate on the use of hydrogels as cell carrier and scaffold materials in tissue engineering. A summary of selected hydrogel applications in tissue engineering can be found in Ref. 60. For the other applications, please refer to the relevant literature.

3.8.2 Hydrogels as Scaffold Materials

3.8.2.1 Tissue Engineering and Scaffolds

Tissue engineering aims to replace, repair, or regenerate tissue or organ function and to create artificial tissues and organs for transplantation [67]. As previously mentioned, hydrogels are an attractive scaffolding material (3D matrix) for cells as they are structurally similar to the natural extracellular matrix (ECM) of many tissues.

One approach is to process the hydrogel material and create a porous scaffold prior to incorporating bioactive molecules and cells by conventional or microengineering methods (Section 3.8.2.3). However, an exciting feature of many hydrogels is their ability to be mixed with cells and bioactive molecules before curing. These cell- and/or biomolecule-laden hydrogel precursor solutions can be used for injection and *in vivo* gel formation (one example will be given in Section 3.8.2.5) or for the fabrication of cell-laden scaffolds by selected microengineering techniques (Section 3.10). Finally, cell- and/or biomolecule-laden microgels can be prepared and assembled to complex 3D structures (cf. Section 3.8.2.4).

Hydrogel scaffolds have many different functions in the field of tissue engineering. They are applied as space filling agents. In addition, bioactive molecules are delivered from hydrogel scaffolds in a variety of applications including promotion of angiogenesis and encapsulation of secretory cells. Finally, hydrogel scaffolds act as 3D support structures for cell growth and function. Depending on the tissue of interest and the specific application, the required scaffold material and its properties will be quite different. Addressing these challenges, various synthetic, natural, and biohybrid polymer materials have been developed and evaluated in the recent past. For instance, alginate mixed with chondrocytes [63] and scaffolds made from PVA have been used for cartilage replacement [68]. Dextran/laminin and gelatin/laminin scaffolds were tested for neural tissue regeneration [69]. Due to their elastic properties, PVA hydrogels were also investigated for the reconstitution of vocal cords [70].

3.8.2.2 Scaffold Design Variables

Hydrogels in tissue engineering must meet a number of design criteria to function appropriately and promote new tissue formation. To create an optimized cellular microenvironment, hydrogel scaffolds should mimic the natural ECM, which provides cells with a variety of physical, chemical, and biological cues that determine cell growth and function. Thus, man-made hydrogels for regenerative therapies need to be not only biocompatible but also adaptive with respect to biological, structural, and mechanical features. Cellular adhesion, proliferation, and differentiation can be modified using specific signaling molecules, such as specific cellular binding sites and growth or differentiation factors. These signaling molecules may be incorporated into the tissue engineering matrix. A wealth of novel design concepts is currently explored to implement peptides, DNA, and modified GAGs enabling even more advanced, biomimetic, as well as bioresponsive materials. Advances in polymer synthesis and processing have led to a new generation of dynamic systems that are capable of responding to artificial triggers and biological signals with spatial precision [71, 72].

One of the continuing, persistent problems with tissue engineering is mass transport limitations. Engineered tissues generally lack an initial blood supply, thus making it difficult for any implanted cells to obtain sufficient oxygen and nutrients to survive and/or function properly. To overcome these shortcomings, prefabricated hydrogel scaffolds with interconnected macropores are applied extensively in tissue engineering (Section 3.8.2.3). Introduction of pores increases surface area-to-volume ratios for cell seeding, creates more space for cell migration and tissue invasion, and facilitates nutrient and waste transport. Additionally, macropores have been shown to enhance scaffold vascularization and wound healing. When using injectable *in vivo* gelling bulk hydrogel matrices without macropores, the degradation rates of the matrices have to be adjusted to the desired migratory activity of particular (encapsulated) cell types. The degradation of polymer hydrogels can be engineered through linkages between the building blocks that undergo cleavage upon action of specific stimuli such as light, pH changes, or enzymatic activity (Sections 3.8.2.5 and 6.4.5).

3.8.2.3 Prefabricated Hydrogel Scaffolds

A number of different methods have been described in the literature for preparing porous structures to be employed as prefabricated tissue engineering scaffolds. Each of these techniques presents its own advantages, but none are free of drawbacks [73–75].

In the following, some conventional but also microengineering fabrication techniques for hydrogel scaffolds will be presented.

Solvent Casting/Particulate Leaching

The hydrogel precursor solution is mixed with a solid porogen of controlled particle size, and the dispersion obtained is poured into a mold. Alternatively, the mold can be loaded with the porogen particles first, before it is filled with the hydrogel precursor solution. Upon cross-linking of the polymer hydrogel, producing a hydrogel–porogen network, the porogen is leached or dissolved in a selected solvent, resulting in a macroporous hydrogel scaffold. Depending on the hydrogel and the application, various porogen materials have been used for this technique, for example, inorganic salts, sugars, gelatin, PMMA, or paraffin.

Instead of single porogen particles, bulk polymer scaffold templates (e.g., made from PLGA) can be utilized for the production of macroporous hydrogels. Therefore, the hydrogel precursor solution is cast and cured around the scaffold. After degradation of the polymer scaffold with a suitable chemical, a porous hydrogel matrix is left behind.

This approach allows for tuning the pore size and porosity by changing the size of the porogen particles and their concentration in the hydrogel precursor solution. However, porogen leaching often leads to closed pores and mechanically weak materials and has the added difficulty of ensuring the complete removal of the embedded particles. If organic solvents are used, they must be fully removed to avoid any possible damage to the cells seeded on the scaffold. Owing to these drawbacks, porous structures obtained with this technique usually have a limited thickness (typically <500 μm) and often rather long scaffold preparation times (leaching step, especially water-soluble porogens).

Gas Foaming

This technique was introduced by Mooney et al. [76] and uses gas as a porogen. The porous structure is generated by nucleation and growth of gas bubbles dispersed throughout the hydrogel precursor solution. On the one hand, gas bubbles can be formed by a blowing agent that is mixed into the hydrogel precursor solution and generates a gas when it chemically decomposes. For example, sodium bicarbonate or ammonium bicarbonate has been used as a gas blowing agent owing to their ability to generate CO_2 or CO_2 and NH_3, respectively. Major advantages of this method are the rather low processing costs due to the wide availability of the most common blowing agents. Furthermore, the gas blowing agents are usually not cell toxic and no organic solvents are needed.

In another variation, dense gas CO_2 can be used to induce porosity in polymeric biomaterials. As dense gas CO_2 generally has a low solubility in hydrophilic polymers, various attempts have been made to improve the ability of dense gas to diffuse into hydrogel precursor solutions and produce porosity in hydrogel matrices, such as CO_2–water emulsion templating or the use of cosolvent systems [69]. With this technique, it is difficult to control pore size and ensure pore interconnectivity.

Phase Separation Techniques

There are several ways to prepare porous polymer scaffolds by controlled phase separation of polymer solutions in a polymer-rich phase and a polymer-poor phase.

Phase separation is induced by temperature changes, addition of another immiscible solvent, or polymerization of one of the compounds. The solvent (or nonpolymerizable polymer phase) is removed by sublimation, extraction, or evaporation.

Phase separation techniques include emulsion freeze-drying or temperature-induced phase separation, where an immiscible solvent is mixed with the polymer solution in order to form an emulsion or where temperature is lowered

in order to produce a liquid–liquid phase separation, respectively. After quenching to form a two-phase solid, the solvent is removed by sublimation to give a porous scaffold.

Cryoprocessing

Phase separation in the hydrogel precursor solution (dispersion) can be also induced by rapid freezing. After removing the solvent (often water, "ice templating") by freeze-drying (lyophilization), leaving behind voids in the regions it previously occupied, interconnected porous structures can be obtained. The pore size and morphology can be controlled by the freezing regime. By using uniaxial temperature gradients, this method allows for the fabrication of oriented pores. The scaffolds can be cross-linked afterward to increase their stability. Especially collagen but also other natural polymers like chitin and alginate are fabricated into scaffolds using freeze-drying.

Cryotropic gelation (cryogelation) is a specific type of gelation that takes place during the cryogenic treatment of the gel-forming system. By cooling the hydrogel precursor solution below the freezing temperature of water, two phases are formed in the macroscopically frozen sample: a polycrystalline phase of ice and an unfrozen liquid microphase containing highly concentrated precursor molecules. The cross-linking reaction proceeds in the nonfrozen liquid microphase. Ice crystals act as a porogen (pore-forming agent). They can be removed by thawing (melting) or by lyophilization (sublimation) of the frozen gels, which permits the creation of matrices with large interconnected pores, high total porosity, and superior mechanical strength.

Recently, the well-established network formation via chemical cross-linking (EDC/sulfo-NHS chemistry) of amino-terminated starPEG and heparin [77] was combined with the cryogelation technology (Fig. 3.55) [78]. Subzero temperature treatment (−20°C) of the gel-forming reaction mixtures and subsequent lyophilization of the incompletely frozen gels resulted in spongelike materials with a system of interconnected macropores (cryogels).

The applicability of the starPEG–heparin cryogels as 3D cell carriers for tissue engineering was exemplarily shown by seeding human umbilical vein endothelial cells (HUVECs) onto scaffolds functionalized with adhesion ligands (RGD motif). The cells migrated into the macropores and attached to the hydrogel matrix, as shown by representative fluorescence images taken after seven days in culture (Fig. 3.56).

Electrospinning

Fibrous prefabricated scaffolds can be prepared by electrospinning, which is explained in Section 3.10.

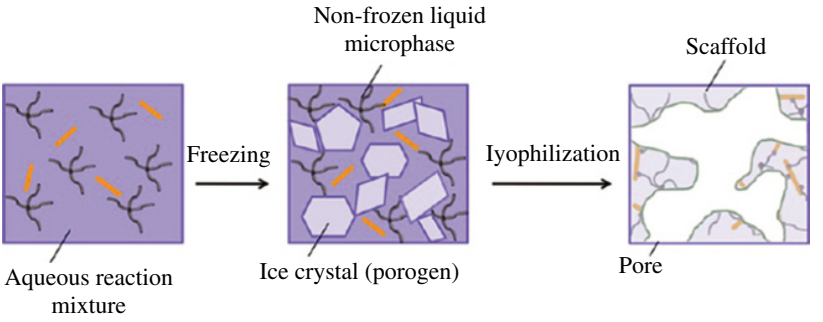

FIGURE 3.55 Formation of macroporous starPEG–heparin cryogels by combined cryotreatment of the aqueous gel-forming reaction mixture and lyophilization of the incompletely frozen gel. Yellow rods, heparin; grey crosses, starPEG. Source: Welzel et al. [78]. Reproduced with permission from American Chemical Society. (*See insert for color representation of the figure*.)

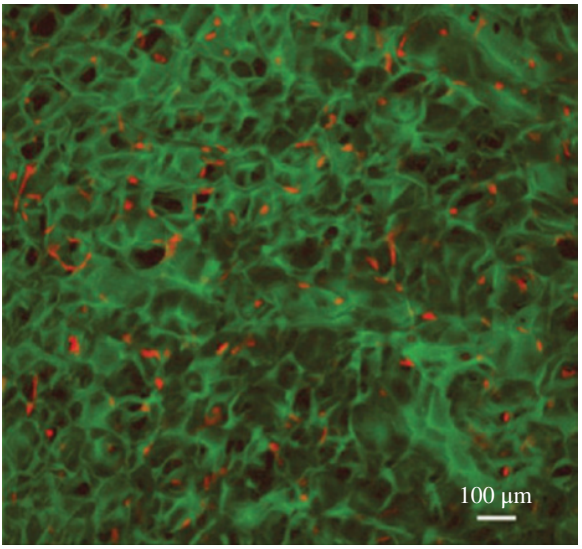

FIGURE 3.56 Representative confocal microscopy image of human umbilical vein endothelial cell colonization on RGD-modified cryogels after seven days in culture in *xy* direction (3D projection) indicating three-dimensional cell growth. Green: cryogel dyed by Alexafluor488. Red: actin of endothelial cells dyed by Alexafluor633-labeled phalloidin. (*See insert for color representation of the figure*.)

Formation of Hydrogel Scaffolds with Controlled Architecture (Microfabrication Techniques)

Most of the aforementioned techniques are limited when scaffolds with customized external shape and predefined and reproducible internal morphology (pore size, porosity, pore size distribution, and structures to increase the mass

transport of oxygen and nutrients throughout the scaffold) are required. To meet this challenge, computer-aided design (CAD) and manufacturing techniques have been introduced to tissue [73, 75].

First, a 3D structure is designed using CAD software. Data obtained from computerized tomography (CT) or magnetic resonance imaging (MRI) medical scans can be used to create a customized CAD model. This CAD model is then expressed in a series of cross-sectional layers. The complex scaffold architecture must be built using layer-by-layer (LBL) manufacturing processes known collectively as solid free-form fabrication (SFF).

For example, stereolithography can be used. It is a liquid-based technique that utilizes LBL curing of a photosensitive hydrogel precursor solution by means of a laser. Alternatively, nozzle-based systems are applied. They process the material chemically as it passes through the nozzle (ink-jet printing, 3D printing; cf. Section 3.10). Cells and biomolecules can be simultaneously printed with the scaffold material [79].

Other approaches to fabricate microstructured hydrogel scaffolds utilize soft lithography micromolding (cf. Section 3.10).

3.8.2.4 Modular Microgel-Based Assemblies

Microgel-based tissue engineering scaffold designs have attracted significant attention in recent years. Microgels are hydrogels with dimensions of several tens or hundreds of micrometers (Section 6.1.2), and due to their size and controllable biological, chemical, and mechanical properties, they are powerful tools for tissue engineering and other biomedical applications. Microgels can be manufactured by various techniques, including microfluidic drop formation, emulsification, and micromolding [80] (cf. Sections 3.10 and 6.1.2).

By using microgels with well-defined properties as building blocks, macroscale hydrogels with unique spatial properties, such as gradients in mechanical and/or biomolecular characteristics, may be built from the bottom up. Microsphere-based scaffolds additionally offer 3D pore interconnectivity and desirable pore size. For instance, chitosan microsphere scaffolds have been produced for cartilage and osteochondral tissue engineering [81].

Cell-laden microgels with controlled shapes (spheres, cubes, rods, etc.) or sizes can be combined like Lego® blocks to complex 3D scaffolds and cell constructs with customized biological and physical properties for a variety of tissue engineering applications. The microassembly concept (micromasonry) and the modular design allow for controlling the distribution of growth factors and living cells within the scaffold in 3D [82, 83] (Fig. 3.57).

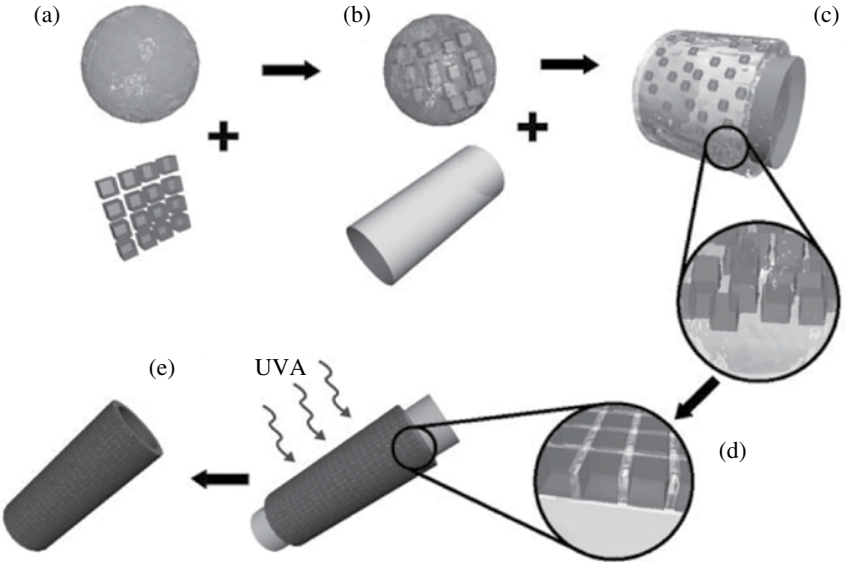

FIGURE 3.57 Schematic diagram of a micromasonry assembly process. Microgels of desired shapes were produced by photolithography and mixed with a solution containing the prepolymer (a). The solution was poured on the surface of a high-affinity PDMS mold (b) where it spread on the PDMS surface (c). The removal of the excess prepolymer solution induced a further packing of the microgels (d). The system was exposed to light to cross-link the prepolymer remaining by the units, and the structure was subsequently separated from the PDMS template (e). Source: Fernandez and Khademhosseini [83], figure 1. Reproduced with permission from John Wiley & Sons.

3.8.2.5 In Situ-Gelled Hydrogel Matrices

For many applications, the formation of the hydrogel scaffold directly inside the body offers advantages compared to the use of preformed scaffolds. In this case, an aqueous mixture of gel precursors, cell, and bioactive agents is administered using a syringe and cures *in vivo*. Such systems must offer mild gelation conditions (cf. Section 3.8.1.2) and proper gelation rates after injection in order to avoid toxicity, overheating caused by severe reactions, and rapid extravasation in the surrounding tissues. The advantages of using injectable hydrogels rely on their high adaptability to the defect shape, possibility of delivery in a minimal invasive way, and easy and effective encapsulation of cells and bioactive molecules. Injectable, *in situ*-gelled hydrogel matrices for biomedical applications have been the subject of several reviews (e.g., [84, 85]).

As an example of recent progress in this field, an injectable modular star-PEG–heparin hydrogel system is highlighted here [86]. PEG–peptide and GAG–peptide conjugates obtained by a regioselective amino acid protection strategy

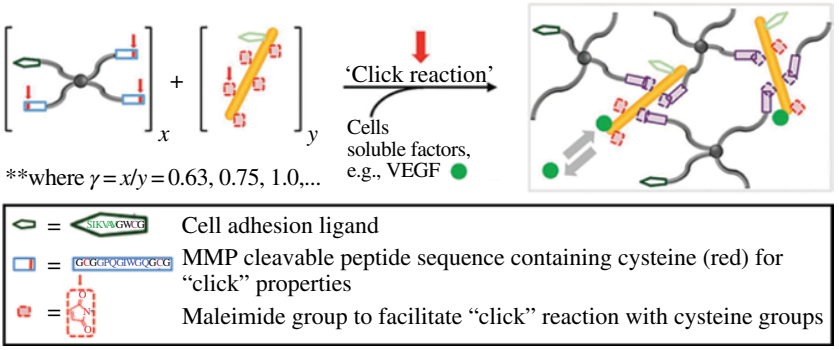

FIGURE 3.58 Schematic representation of the *in situ* gelling of poly(ethylene glycol)–peptide and glycosaminoglycan–peptide conjugates by Michael-type addition. Source: Tsurkan et al. [86]. Reproduced with permission from John Wiley & Sons. (*See insert for color representation of the figure*.)

were converted into cell-instructive hydrogel matrices capable of inducing morphogenesis in embedded human vascular endothelial cells and dorsal root ganglia. A schematic representation of the underlying *in situ* gel formation is shown in Figure 3.58. Four-arm starPEG (x) functionalized with cell adhesion ligands (green) and enzymatically degradable peptide linkers (blue), is cross-linked via "click" reaction of cysteine groups (red) with maleimide (red)-functionalized heparin (y). This noncytotoxic Michael-type addition reaction can be performed in the presence of cells and bioactive molecules.

3.9 SURFACE MODIFICATION AND FILM PREPARATION

The surface of any material governs its interactions with the environment. Knowledge over and control of these interaction is especially important when a material is in contact with the biosystem, for example, when applied as transplant, in tissue engineering, in cell cultures, and in blood contact, as well as in biosensors in medicinal diagnosis, fluids analysis, environmental monitoring, and many other areas. Whereas, on the one hand, the bulk properties of the material are essential for its successful application, for example, as a catheter or a heart valve, special attention has to be paid to render to the surface suitable biocompatible or bioactive properties, no matter of the chemical composition of the bulk material. This is usually achieved by any surface modification process by low molar mass or polymeric compounds. An essential feature of such a modification procedure is the need for a permanent and bioresistant surface finish [87].

Polymer films on the surface of a substrate, which may be polymeric or inorganic (Si-wafers or glass slides, metal, i.e., gold-cover Si-wafers), are usually prepared via spin or dip coating or by using a doctor blading or wire-wound applicator depending on the film thickness required. Self-assembled monolayers (SAMs) and the Langmuir–Blodgett (LB) or LBL techniques are used for very thin films or if a special arrangement is required.

For a better immobilization of thin films on the substrate, it is necessary to treat or precoat the substrate in order to create groups capable of establishing a strong physical interaction or a covalent connection between the substrate and polymer. Another efficient way for stabilization is to cross-link the prepared polymer films best involving also suitable substrate surface groups. This can be achieved thermally or by UV irradiation if the right active groups are implemented in the polymer structure or film formulations or by treatment with high energy like plasma or electron beam. Polymer films can also be directly prepared on surfaces by plasma polymerization (Table 3.4).

3.9.1 Self-Assembled Monolayers

Special kinds of very thin films used to change surface properties or to allow introduction of functional surface groups are SAMs [88]. They are formed by spontaneous immobilization through chemisorption of suitable end-functionalized long-chain organic molecules on the certain metal substrates. Van der Waals interactions between the organic chains, which are the driving force for the self-organization of the molecules, also play a special role here. In general, SAMs are prepared by immersing a substrate in the solution containing the molecules with the functional groups able to react with the surface or by exposing the substrate to the vapor of the reactive species. The molecules that can form SAMs are composed of the head groups that have specific affinity for a substrate and of the terminal groups. The terminal groups of the anchoring chain can be modified with other molecules either before immobilization to the substrate or after. *In situ* polymerization may also be carried out on proper SAM surfaces. The most commonly used SAM layers are alkane thiolates on gold due to the high affinity of sulfur to gold and the high chance to achieve well-defined monolayers. On metal oxide substrates, often functional trichlorosilanes are used as anchor groups, which tend to cross-link laterally after hydrolysis allowing the formation of very stable layers. However, the formation of well-organized monolayers might be hampered in this case. Figure 3.59 presents typical SAMs on Si- and Au-wafers.

TABLE 3.4 Summary of Surface Modification and Film Preparation Techniques

Method	Advantages	Disadvantages	Coating Method
SAM	• Thin layers controlled by molecule size • Monolayers possible • Easy preparation, no special equipment • Well-defined molecular orientation • Many commercially available suitable anchoring molecules with different functionalities	• Steric problems during deposition leading to film defects • Problems with stability (e.g., oxidation)	• Immersion • Incubation
LB	• Thin layers of controlled thickness • Mono- and multilayers possible • High film homogeneity • Well-defined molecular orientation	• Requires special equipment • Unstable/fragile films • Only for special molecules having amphiphilic properties	• Langmuir–Blodgett trough
LBL	• Controlled thickness and wide range in film thickness • Monolayer or multilayers • Easy preparation, no special equipment • Suitable for different preferably charged polymers and biomolecules	• Limited stability • Best only for oppositely charged molecule combinations	• Dip coating • Immersion
Immobilization of polymer films	• Stable films • Controlled thickness • Easy preparation technique • Suitable for a wide variety of polymers • Very versatile	• Requires often high-temperature annealing or UV treatment • Precoating or suitable cross-linking groups necessary • Quality of the film limited	• Solvent casting • Spin coating • Dip coating
Plasma and electron beam	• Clean technique • Solvent-free • Surface polymerization possible (initiator-free) • Versatile with regard to chemistry • *In situ* cross-linking • Surface or bulk modification depending on the technique and parameters used	• No control of polymer structure • Polymer aging due to reactive species in the film • Special equipment needed • Degradation of organic material possible • Bulk material modification possible (e-beam)	• In-glow discharge for reactive species • Any coating techniques for plasma or electron beam polymer film immobilization

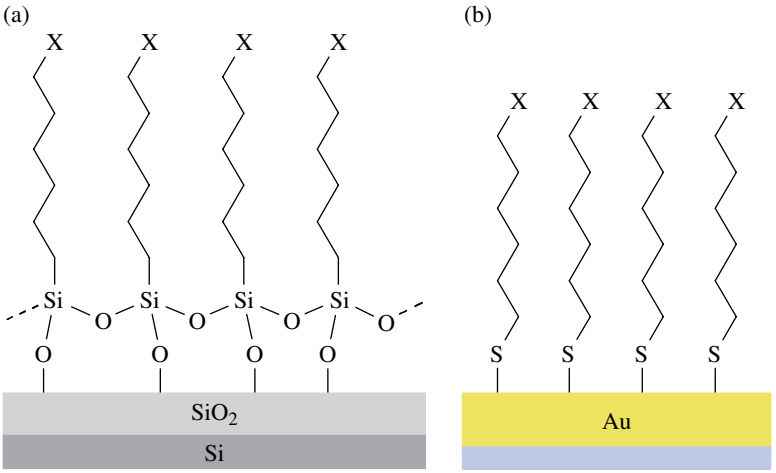

FIGURE 3.59 Schematic representations of alkane SAMs immobilized: (a) on Si-wafers by trialkoxysilane groups and (b) gold wafer by thiol groups, where X—functional (terminal) group like amino or carboxylic acid groups.

3.9.2 Langmuir–Blodgett Films

The LB technique is an alternative for the SAM systems. LB allows obtaining ultrathin films with controlled thickness and a well-defined molecular orientation. In this method, amphiphilic molecules, which are spread on a liquid surface (so-called Langmuir film), are deposited on a solid surface by dipping it in the solution. The molecules are transferred from the air–water interface to the solid substrate.

The preparation of LB films is carried out by the device called LB trough. First, the amphiphilic molecules are dissolved in a water-insoluble solvent, which is then spread by a syringe in the trough top. When the solvent evaporates, the molecules create a Langmuir film on the water surface. Next, the trough barriers press the solution at the liquid–air interface together, which increases the packing density of the molecules at the liquid–air and creates a well-organized layer. If the solid substrate, which is going to be immersed in the trough, is hydrophilic, then the first layer is deposited by withdrawing and the surface of the outcoming film will be hydrophobic and vice versa (Fig. 3.60). At each immersion step and thus film deposition step, the film surface on the substrate switches its hydrophobic/hydrophilic nature.

3.9.3 Layer-by-Layer Deposition

The LBL technique is a simple and versatile method for preparing polymeric thin films of controlled thickness on solid substrate. The most widely used method is based on the alternate deposition of oppositely charged polymers [89]. A schematic presentation of multilayer fabrication by LBL can be seen in Figure 3.61. Another method relays on the specific interactions between molecules, for example, avidin–biotin, lectin–sugar, and antibody–antigen. It is also possible to establish H-bonding multilayer assemblies.

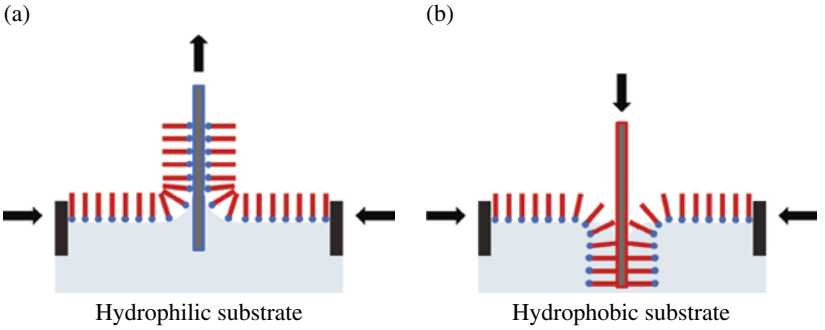

FIGURE 3.60 Langmuir–Blodgett monolayer formation on the (a) hydrophilic substrate by withdrawing from the trough and (b) hydrophobic substrate by immersion in the trough.

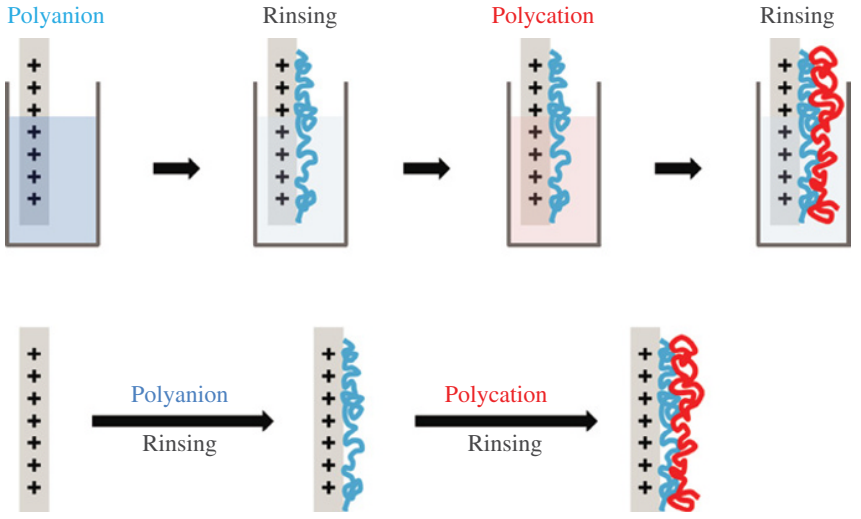

FIGURE 3.61 Layer-by-layer deposition of polyions.

3.9.4 Immobilization by Chemical Binding to Substrates

In order to immobilize polymers on the surface of a substrate (e.g., SiO_2 surface like Si-wafers or glass slides but also various other metal oxide or polymeric substrates), very often it is necessary to precoat the substrate with a substance possessing groups able to establish covalent connections between the substrate and the polymer. One of the most widely used anchoring substances for silica surfaces is organic derivatives of silicon with a silyl ether group on one end of the alkyl chain and another functional group on the other. In this method, the silyl ether groups are hydrolyzed to silanol groups (Si─OH), which covalently bind to the silanol groups present on the substrate surface (Fig. 3.62).

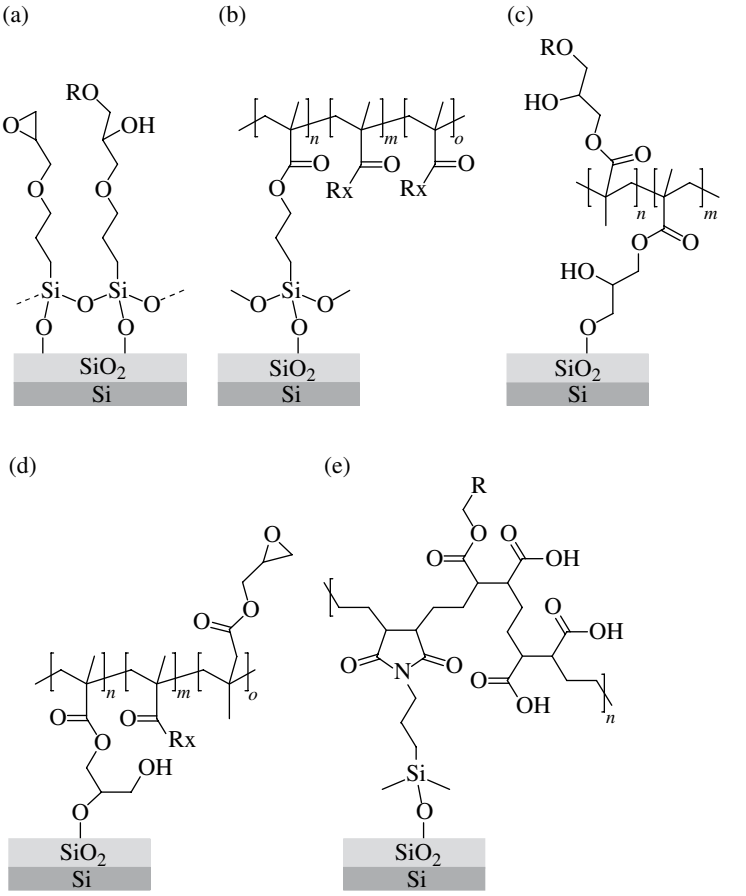

FIGURE 3.62 Schematic representation of the immobilized molecules by (a) (3-glycidyloxypropyl) trimethoxysilane, (b) 3-(trimethoxysilyl)propyl methacrylate incorporated in the poly(methyl methacrylate) (PMMA), (c) poly(glycidyl methacrylate), (d) glycidyl methacrylate incorporated in the PMMA, and (e) PEMA on 3-aminopropyl-dimethylethoxy-silane. Where Rx—pendant molecules, R—polymer.

Another example of substances used for anchoring to the Si-wafers is molecules or macromolecules containing highly reactive epoxy groups like poly(glycidyl methacrylate) or maleic anhydride copolymers. The latter can be well attached to any surface with amino functions like aminosilanized Si-wafers but also OH or amino-functionalized polymer films (Fig. 3.63). Anchoring of polymers to the gold substrates is mostly done with alkanethiols or polymers containing thiol or disulfide bonds like those found in liponic acid copolymers.

Stable polymeric films can also be formed in some cases without any additional anchoring substances or cross-linkers through physical interactions. Such polymeric layers are mostly stabilized by inter- and intramolecular hydrogen bonds that form a network between the polymer and substrate and

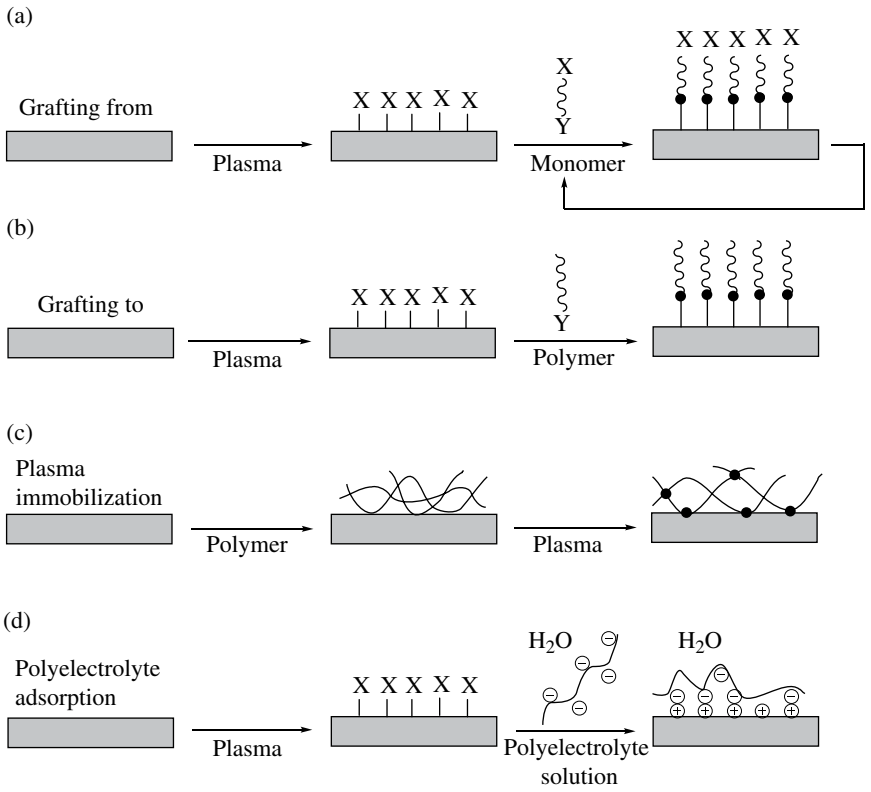

FIGURE 3.63 Schematic representation of multistep surface modification procedures for polymeric materials that comprise a low-pressure plasma treatment either for activation/functionalization (a, b, and d) or cross-linking (c). Source: Nitschke et al. [90]. Reproduced with permission from John Wiley & Sons.

between polymer macromolecules. Moreover, when high temperature is applied during the annealing of the polymer film, controlled or uncontrolled chemical reactions leading to cross-linking of the film or bonding to the substrate are possible.

3.9.4.1 Surface-Independent Grafting Methods

A surface-independent universal grafting method by dip coating from solution was recently described by Wei et al. Based on mussel-inspired dendritic polymers, several universal multifunctional coatings have been achieved, ranging from bioinert to biofunctional surfaces. In these cases, the large number of catechol and amine groups set the basis for heteromultivalent anchoring and cross-linking [91, 92].

3.9.5 Low-Pressure Plasma

An ionized medium that consists of electrons, ions, and possibly of energetic neutrals and photons, which meets some additional criteria, is called a plasma. According to this definition, the term plasma covers a wide range of phenomena. Here, the low-pressure plasma (mostly a nonequilibrium system) is highlighted as a universal tool for a wide range of surface modification strategies. These strategies can be assigned to three major cases: Depending on the choice of process gas and process parameters, material loss (plasma etching) or material deposition (plasma polymerization) can predominate. In the intermediate case, a shallow surface layer of the material is modified with respect to its chemical and/or physical properties without a pronounced material removal or deposition (surface modification) [93].

With a particular focus on polymers, two important properties of a low-pressure plasma treatment should be emphasized: (i) A low-pressure plasma provides high activation energies of several electron volts without elevated temperatures of ions and neutrals (cold plasma). For that reason, there is no thermal load to sensitive polymer materials, while most chemical bonds can be broken and surface radical sites can be formed. (ii) When a polymer is exposed to a low-pressure plasma, the surface modification effect is limited to the uppermost few nanometers (i.e., the range of impinging ions and vacuum ultraviolet photons). Hence, favorable bulk properties of the material remain unchanged.

All three cases mentioned earlier (plasma etching, plasma polymerization, surface modification) have a number of important applications related to organic materials in general and polymers in particular.

Plasma etching. Beyond simple processes for the efficient removal of organic impurities, for example, from metal surfaces (plasma cleaning), a low-pressure plasma can be employed to etch microstructures into polymer surfaces or polymer coatings. This includes well-defined 3D patterns like wells or channels using masking techniques but also random structures like a desired roughness as a prerequisite for an ultrahydrophobic surface.

Plasma polymerization. In a plasma polymerization process, a low-pressure plasma is usually generated in a carrier gas (e.g., Ar or He), which is loaded with an organic precursor (e.g., acrylic acid or allylamine). Elemental reactions like radical formation and fragmentation of the precursor molecule occur. Subsequently, the recombination of activated fragments in the gas phase as well as at an exposed surface leads to the formation of thin, highly cross-linked polymer coatings. It is important to note that plasma polymerization is not limited to unsaturated monomers as used in conventional polymerization. It also works with saturated precursors like hexamethyldisiloxane. This makes plasma polymerization a highly versatile tool for the deposition of polymeric coatings that strongly adhere to most surfaces. Under appropriate process conditions, functional groups of the precursor molecule can be largely transferred into the plasma polymer film (structure retention). The mechanical properties of the obtained coating can be adjusted by the cross-linking degree. Even vertical structure gradients can be obtained when the plasma parameters are changed during the deposition process.

Surface modification. Plasma-based surface modification of polymers frequently aims at durable changes of wettability or at a selective introduction of functional groups for subsequent chemical reactions or improved adhesion. For some applications, a simple plasma treatment, that is, a short exposure of the polymer surface to a low-pressure plasma, is adequate to reach these goals. However, a crucial point of simple plasma treatments is the lack of long-term stability. Reorientation and migration of surface moieties into the polymer bulk and/or post-plasma reactions of the activated surface lead to a gradual decay of hydrophilicity (hydrophobic recovery) or reactivity on the timescale of days or weeks. Another disadvantage of simple plasma treatments is the variety of functional groups that is simultaneously formed on the exposed polymer surface. Both problems can be solved only to some extent by the choice of process gas and process parameters. At this point, a more promising way to an appropriate surface modification is to use plasma treatments only for activation/functionalization as a part of a multistep procedure. Such strategies (Fig. 3.63) aim at a covalent or noncovalent anchorage of functional (macro)molecules at the polymer surfaces to inhibit hydrophobic recovery and to provide a more defined, chemically homogeneous surface functionalization.

3.9.6 Electron Beam Treatment

It was found early on that ionized radiation can cross-link polymer molecules due to radicals that are formed [94]. Ionized radiation can be created through electromagnetic waves via UV/Vis, gamma, or X-ray radiation or through corpuscular radiation of electrons, protons, or neutrons. For the modification of polymers, grafting, cross-linking, or selective degradation, mainly electron beam irradiation (e-beam) is used [95]. Electron beams are created by an electron accelerator. For polymer substrates, electrons with an energy of 0.5 to 2.0 MeV and final doses up to 1000 kGy m/min are suitable. Sterilization processes (gamma sterilization) and polymer modifications are usually carried out in the medium radiation regime of 100 kGy. In general, the reactions outlined in Figure 3.64 can occur upon e-beam treatment and the involved radical creation. Double bonds can form through disproportionation reactions and chains can be combined leading to cross-linking. Chain breaking reactions lead to degradation of the polymer backbone. Therefore, electron energy and dose applied to a specific polymer have to be carefully controlled in order to minimize degradation and to optimize modification since the reactions

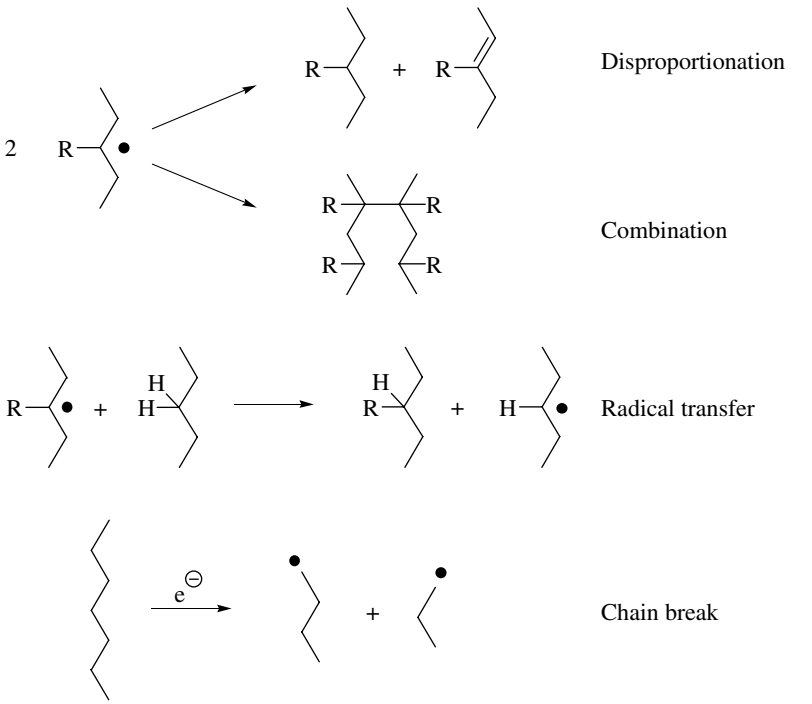

FIGURE 3.64 Reactions on hydrocarbon polymer chains induced by e-beam radiation.

induced by the e-beam are highly dependent on the chemical groups within the polymer chain, for example, long alkyl chains like in polyethylene tend to cross-link, whereas polymers with methacrylate groups like in PMMA degrade rather quickly. The depth penetration of electrons depends on the density of the material and is under doses of 1000 kGy m/min about 6000 g/m^2. Thus, significant bulk modification up to several centimeters of polymers is possible.

Through e-beam also low molar mass and polymeric molecules can be grafted onto the material without any pretreatment, initiators, or additives similar as through plasma processes. Thus, it is possible to immobilize a polymer film that has been coated on a different polymer substrate through gamma irradiation. In that way, it was, for example, possible to immobilize polyacrylic acid and poly(ethylene-*alt*-maleic acid) on PSU hollow fiber membranes directly as module with 12,000 fibers. For that the module was flashed with the reactive polymer solution and then irradiated with 25 kGy, a dose generally used for sterilization. Afterward, the nonattached polymer was removed by flashing and the carboxylic acid groups of the reactive polymer attached to the inner hollow fiber membrane could be further used for attaching antithrombogenic molecules [96].

3.10 MICROENGINEERING OF POLYMERS AND POLYMERIC SURFACES

For many applications in biomedicine, not only the multifunctionality but also the macroscopic structure or architecture of polymers is relevant. For example, cells can align to patterns on polymeric surfaces and are influenced by the macroscopic surface pattern of the underlying substrate. In this chapter, a short overview is presented on selected methods to structure polymers or polymer surfaces by microengineering techniques (Table 3.5) [97].

The most prominent technique among these is based on *soft lithography* [97]. This set of methods allows the generation of micropatterned polymer surfaces or microparticles of different shapes. Each method has certain limits such as scale and aspect ratio (cf. Table 3.5) that will be discussed in detail. Initially, two methods from soft lithography micropatterning and micromolding will be described, originally developed by Whitesides and coworkers. The technique relies on an elastomeric "soft" material that is either used as a stamp or as a mold in order to pattern surfaces 2D with a monolayer or 3D with a microstructure (Fig. 3.65). In the first case, one can obtain a fine monolayer pattern (~100 nm) but no aspect ratio can be obtained. Nevertheless, by

TABLE 3.5 Methods to Structure Polymers or Polymer Surfaces by Microengineering Techniques

Method	Resolution/Aspect Ratio	References
Soft lithography	~50 nm/small	[97, 98]
Micromolding and PRINT (particle replication in nonwetting template)	~100 nm/medium	[99, 100]
Electrospinning	~1 μm/high (fiber)	[101, 102]
Droplet-based microfluidics	~100 μm/small (spherical)	[103, 104]
Ink-jet printing	~100 μm/small to medium	[105]
3D printing	~100 μm/medium to high	[106]

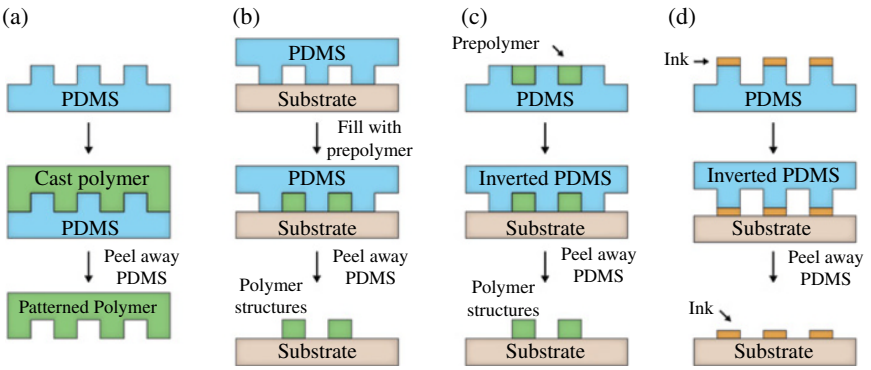

FIGURE 3.65 Schematic illustration of the major steps involved in soft lithography and three major soft lithographic techniques: (a) replica molding, (b) micromolding, (c) microtransfer printing, and (d) microcontact printing. Source: Qin et al. [97]. Reproduced with permission from Nature Publishing Group.

grafting polymer film onto reactive SAMs, also here high aspect ratios with good resolution can be obtained (Figs. 3.66).

In *micromolding techniques*, the aspect ratio and the lateral resolution are controlled by the poly(dimethylsiloxane) (PDMS) stamp, which is typically limited to an open channel structure (Fig. 3.57). Moreover, soft lithography techniques require cross-linking reactions that are initiated by external triggers, which leads to the introduction of potentially toxic substances in the products.

A variant is the so-called *PRINT* technique that allows for the construction of complete microstructures by a roll-to-roll process [100]. Particle replication

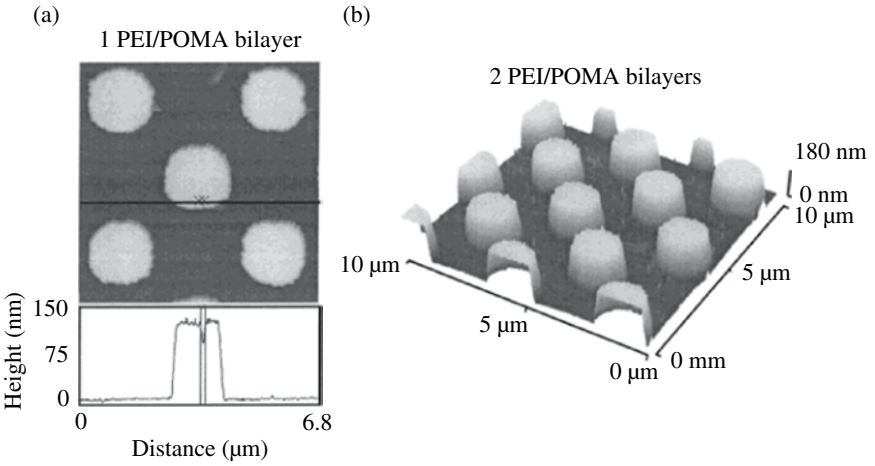

FIGURE 3.66 AFM and SEM images of a 100-nm gold film, patterned with polymer multilayers and etched. (a) AFM image, one PEI/POMA bilayer (the line scan shows a 100-nm-wide hole); (b) SEM image, one PEI/POMA bilayer. Source: Huck et al. [107]. Reproduced with permission from American Chemical Society.

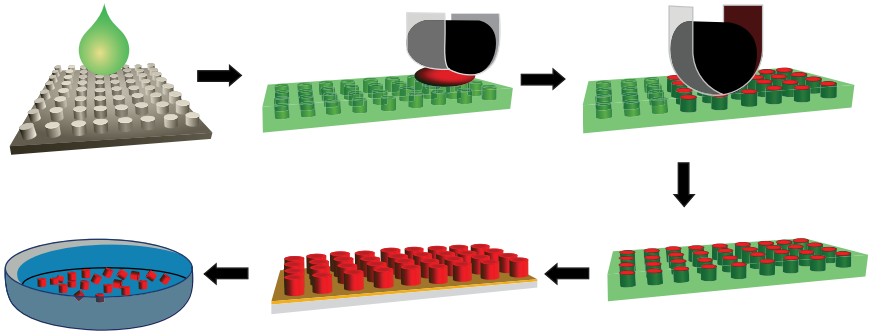

FIGURE 3.67 Schematic representation of the PRINT process. Source: Xu et al. [100], figure 1. Reproduced with permission from John Wiley & Sons.

in nonwetting templates (PRINT) is a powerful approach for micro- and nanoparticle fabrication, and the process is schematically shown in Figure 3.67. The technique is based on the preparation of a master template by soft lithography. Then a liquid fluoropolymer is poured on the surface of the master template and photochemically cross-linked; then it is peeled away, thereby generating a precise mold with micro- or nanoscale cavities that are filled with liquid substance. Then the liquid is converted to a solid, for example, by UV-triggered cross-linking, and the array of particles can be removed from the

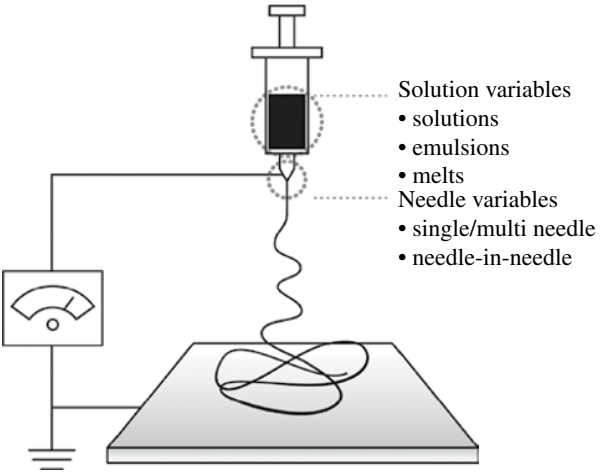

FIGURE 3.68 Schematic representation of an electrospinning setup.

mold. This is achieved by bringing the mold in contact with a harvesting film, which enables the particles to be easily handled, chemically modified, and analyzed. Free-flowing particles with controlled shapes can be obtained by separating the harvesting film from the particles.

In *electrospinning*, an electrical charge is used to draw very fine fibers from a liquid [101]. These fibers typically have sizes in the micro- or nanometer scale, and the setup for their fabrication is schematically shown in Figure 3.68. A high voltage is applied to the end of a capillary containing the polymer solution or melt. When the voltage is sufficiently high, the liquid becomes charged and forms a so-called Taylor cone. Upon further increase of the electric field, the repulsive electrostatic force overcomes the surface tension and the charged strand erupts from the surface. The strand of polymer solution then dries and the fibers are deposited on the collector forming a nonwoven fibrous layer. Thereby, the fiber formation and structure strongly depend on polymer and solution properties as well as process parameters like the applied voltage, polymer flow rate, or distance between needle and collector [102].

By *droplet-based microfluidic techniques*, spherical microparticles can be produced. In this process, a polymer solution or a two-component system is separated by an inert nonmiscible fluid to obtain droplets in the 10–200 μm range. In most cases, spherical particles are obtained; however, also rods or ellipsoids have been realized [108]. For droplet microfluidics, either glass capillary devices can be used or devices made by lithography techniques, commonly consisting of PDMS. Figure 3.69 shows a flow scheme for the

fabrication of microgel particles with the same size and spherical shape for the encapsulation of bioactive compounds [108].

Three-dimensional printing (*3D printing* or 3DP) is a rapid prototyping (RP) technique that was developed in 1992 at the Massachusetts Institute of Technology (MIT) [109]. In contrast to 3D plotting of hot polymer melts, 3DP uses CAD models that can be obtained with a personal computer [110]. 3DP is a layered fabrication process in which a layer of powder is spread onto the powder bed on which the model will be created. Then a print head ejects

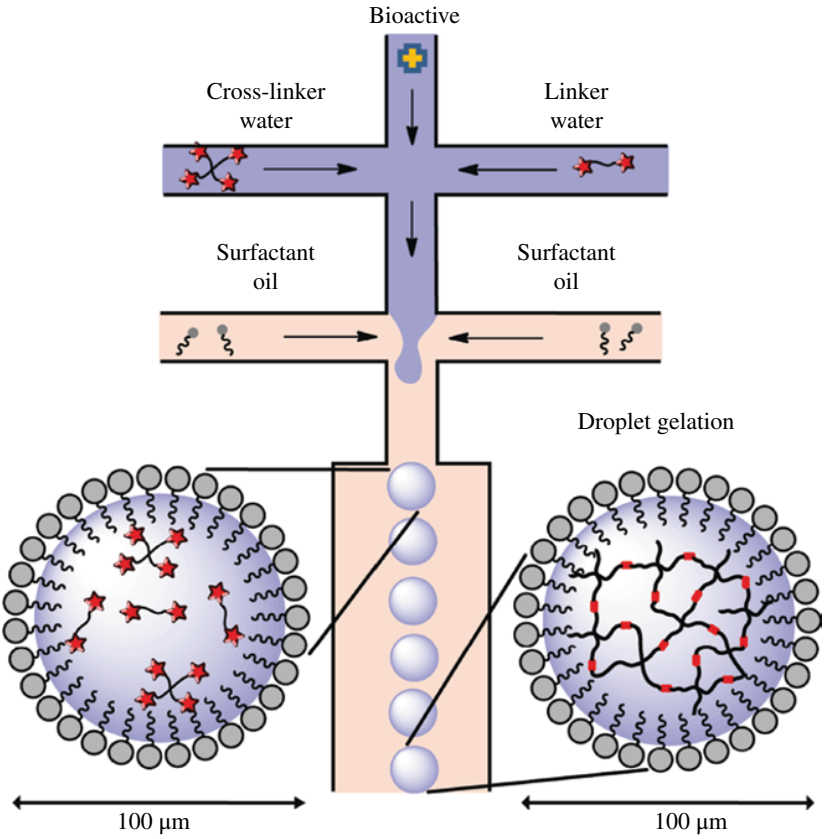

FIGURE 3.69 Schematic representation of microgel formation by microfluidic droplet gelation. At the first cross-junction, these three fluids formed a laminar coflowing stream in the microchannel. This stream is broken to form monodisperse premicrogel droplets at the second cross-junction by flow focusing with immiscible paraffin oil. The droplet formation induces a rapid mixing of all the components inside the droplets, which leads to a subsequent cross-linking of the macromonomers. Source: Seiffert [108]. Reproduced with permission from John Wiley & Sons.

binding materials onto the powder. This print head is similar to those used for ink printing, which makes the process fast, easy, and cheap. After the first layer is completed, another layer of powder is applied and the process is repeated until the desired 3D shape has been constructed. Subsequent removal of the unbound powder and suitable postprocessing gives the final model. 3DP is a very flexible method since many geometrical outlines can be created from many materials, for example, ceramics, metals, polymers, and composites. Additionally, it allows control over the material composition, microstructure, and surface texture.

3DP has a range of potential applications in medicine, for example, in tissue engineering [110, 111] or for the production of DDS [112]. For drug delivery applications, different properties can be installed leading to targeted DDS, oral fast disintegrating DDS, floating DDS, time controlled, and pulse release DDS as well as dosage forms with multiphase release properties and implantable DDS. Additionally, 3DP can help to solve the problematic delivery of poorly water-soluble drugs, peptides, and proteins as well as highly toxic and potent drugs or enable the controlled release of multiple drugs in a single dosage form.

REFERENCES

[1] Odian, G. *Principles of Polymerization*; Wiley Interscience, Hoboken: 2004.

[2] Braun, D.; Cherdron, H.; Rehahn, M.; Ritter, H.; Voit, B. *Polymer Synthesis: Theory and Practice, Fundamentals, Methods, Experiments*; Springer, Berlin, Heidelberg, New York: 2013.

[3] Matyjaszewski, K.; Gnanou, Y.; Leibler, L. *Macromolecular Engineering*, Vol. 1+*2*, Wiley-VCH, Weinheim: 2007.

[4] Matyjaszewski, K.; Dong, H.; Jakubowski, W.; Pietrasik, J.; Kusumo, A. *Langmuir* 2007, *23*, 4528–4531.

[5] Hadjichristidis, N.; Iatrou, H.; Pitsikalis, M.; Sakellariou G. *Chemical Review* 2009, *109*, 5528–5578.

[6] Faust, R.; Kennedy, J. P. *Journal of Polymer Science Part A: Polymer Chemistry* 1987, *25*, 1847–1869.

[7] Puskas, J. E.; Chen, Y.; Dahman, Y.; Padavan, D. *Journal of Polymer Science: Part A: Polymer Chemistry* 2004, *42*, 3091–3109.

[8] Labet, M.; Thielemans, W. *Chemical Society Reviews* 2009, *38*, 3484–3504.

[9] Jäger, M.; Schubert, S.; Ochrimenko, S.; Fischer, D.; Schubert, U. S. *Chemical Society Reviews* 2012, *41*, 4755–4767.

[10] Aoi, K.; Okada, M. *Progress in Polymer Science* 1996, *21*, 151–208.

[11] Adams, N.; Schubert, U. S. *Advanced Drug Delivery Reviews* 2007, *59*, 1504–1520.

[12] Matyjaszewski, K.; Davis, T. *Handbook of Radical Polymerization*; Wiley-Interscience, Hoboken: 2002.

[13] Tsarevsky, N. V.; Matyjaszewski, K. *Chemical Reviews* 2007, *107*, 2270–2299.

[14] Hawker, C. J.; Bosman, A. W.; Harth, E. *Chemical Reviews* 2001, *101*, 3661–3688.

[15] Barner-Kowollik, C.; Perrier S. *Journal of Polymer Science Part A: Polymer Chemistry* 2008, *46*, 5715–5723.

[16] Moad, G.; Rizzardo, E.; Thang, S. H. *Polymer* 2008, *49*, 1079–1131.

[17] Mecking, S. *Angewandte Chemie International Edition* 2001, *40*, 534–540.

[18] Younkin, T. R.; Connor, J. K.; Henderson J. I.; Friedrich, S. K.; Grubbs, R. H.; Bansleben, D. A. *Science* 2000, *287*, 460–462.

[19] Johnson, L. K.; Killian, C. M.; Brookhart, M. *Journal of the American Chemical Society* 1995, *117*, 6414–6415.

[20] Guan, Z.; Cotts, P. M.; McCord, E. F.; McLain S. *Science* 1999, *283*, 2059–2062.

[21] Popeney C. S.; Lukowiak, M. C.; Böttcher, C.; Schade, B.; Welker, P.; Mangoldt, D.; Gunkel, G.; Guan, Z.; Haag, R. *ACS Macro Letters* 2012, *1*, 564–567.

[22] Buchmeiser M. R. "Ring-Opening Metathesis Polymerization" in *Synthesis of Polymers* (eds. Schlüter, A.-D.; Hawker, C.; Sakamoto, J.); Wiley VCH, Weinheim, Vol. *2*: 2012, 547–586.

[23] Yokozawa, T.; Yokoyama, A. *Chemical Reviews* 2009, *109*, 5595–5619.

[24] Yokozawa, T.; Suzuki, H. *Journal of the American Chemical Society* 1999, *121*, 11573–11574.

[25] Yokozawa, T.; Myiakoshi, R.; Yokoyama, A. *Journal of the American Chemical Society* 2005, *127*, 17542–17547.

[26] McCullough, R. D.; Iovu, M. C.; Sheina, E. E.; Gil, R. R. *Macromolecules* 2005, *38*, 8649–9656.

[27] Kiriy, A.; Senkovskyy, V.; Sommer, M. *Macromolecular Rapid Communications* 2011, *32*, 1503–1517.

[28] Iha, R. K.; Wooley, K. L.; Nystrom, A. M.; Burke, D. J.; Kade, M. J.; Hawker, C. J. *Chemical Reviews* 2009, *109*, 5620–5686.

[29] Kolb, H. C.; Finn, M. G.; Sharpless, K. B. *Angewandte Chemie-International Edition* 2001, *40*, 2004–2021.

[30] Barner-Kowollik, C.; Du Prez, F. E.; Espeel, P.; Hawker, C. J.; Junkers, T.; Schlaad, H.; Van Camp, W. *Angewandte Chemie-International Edition* 2011, *50*, 60–62.

[31] Baskin, J. M.; Prescher, J. A.; Laughlin, S. T.; Agard, N. J.; Chang, P. V.; Miller, I. A.; Lo, A.; Codelli, J. A.; Bertozzi, C. R. *Proceedings of the National Academy of Sciences* 2007, *104*, 16793–16797.

[32] Abuchowski, A.; McCoy, J. R.; Palczuk, N. C.; van Es, T.; Davis, F. F. *Journal of Biological Chemistry* 1977, *252*, 3582–3586.

[33] Pasut, G.; Veronese, F. M. *Journal of Controlled Release* 2012, *161*, 461–472.

[34] www.pegasys.com (accessed on October 16, 2015).

[35] https://de.wikipedia.org/wiki/Peginterferon_%CE%B1 (accessed on November 19, 2015).

[36] http://www.rsc.org/chemistryworld/News/2007/January/05010702.asp (accessed on October 16, 2015).

[37] Klaus, W.; Gsell, B.; Labhardt, A. M.; Wipf, B.; Senn, H. *Journal of Molecular Biology* 1997, *274*, 661–675.

[38] Ryan, S. M.; Mantovani, G.; Wang, X.; Haddleton, D. M.; Brayden, D. J. *Expert Opinion on Drug Delivery* 2008, *5*, 371–383.

[39] Wei, Q.; Becherer, T.; Angioletti-Uberti, S.; Dzubiella, J.; Wischke, C.; Neffe, A. T.; Lendlein, A.; Ballauff, M.; Haag, R. *Angewandte Chemie International Edition* 2014, *53*, 8004–8031.

[40] Sharma, S.; Johnson, R. W.; Desai, T. A. *Langmuir* 2004, *20*, 348–356.

[41] Schlaad, H. "Bio-Synthetic Polymer Conjugates" in *Advances Polymer Science* (eds. Abe, A.; Albertson, A.-C.; Dusek, K.; Genzer, J.; Kobayashi, S.; Lee, K.-S.; Leibler, L.; Long, T. E.; Manners, I.; Möller, M.; Trentjev, E. M.; Vicent, M. J.; Voit, B.; Wiesner, U.); Springer Verlag, Berlin-Heidelberg: 2013, 253.

[42] Mao, H. Q.; Roy, K.; Troung-Le, V. L.; Janes, K. A.; Lin, K. Y.; Wang, Y.; August, J. T.; Leong, K. W. *Journal of Controlled Release* 2001, *70*, 399–421.

[43] Alemdaroglua, F. E.; Herrmann, A. *Organic & Biomolecular Chemistry* 2007, *5*, 1311–1320.

[44] Huang, L.; Kerns, R. J. *Bioorganic Medical Chemistry* 2006, *14*, 2300–2313.

[45] Fernández, C.; Hattan, C. M.; Kerns, R. J. *Carbohydrate Research* 2006, *341*, 253–1265.

[46] Hase, S.; Ibuki, T.; Ikenaka, T. *The Journal of Biochemistry* 1984, *95*, 197–203.

[47] Kon, A.; Takagaki, K.; Kawasaki, H.; Nakamura, T.; Endo, M. *The Journal of Biochemistry* 1991, *110*, 132–135.

[48] Strohmeier, G. A.; Pichler, H.; May, O.; Gruber-Khadjawi, M. *Chemical Reviews* 2011, *111*, 4141–4164.

[49] Kobayashi, S.; Makino, A. *Chemical Reviews* 2009, *109*, 5288–5353.

[50] Tran, D. N.; Balkus Jr., K. J. *ACS Catalysis* 2011, *1*, 956–968.

[51] Gross, R. A.; Kalra, B.; Kumar, A. *Applied Microbiology and Biotechnology* 2001, *55*, 655–660.

[52] Mueller, R.-J. *Process Biochemistry* 2006, *41*, 2124–2128.

[53] Dawson, P. E.; Kent, S. B. H. *Annual Review of Biochemistry* 2000, *69*, 923–960.

[54] Young, C. L.; Britton, Z. T.; Robinson, A. S. *Biotechnology Journal* 2012, *7*, 620–634.

[55] Seeberger, P. H. *Carbohydrate Research* 2008, *343*, 1889–1896.

[56] Plante, O. J.; Palmacci, E. R.; Seeberger, P. H. *Science* 2001, *291*, 1523–1525.

[57] Love, K. R.; Seeberger, P. H. *Angewandte Chemie International Edition* 2004, *43*, 602–605.

[58] Codee, J. D. C.; Kröck, L.; Castagner, B.; Seeberger, P. H. *Chemistry—A European Journal* 2008, *14*, 3987–3994.

[59] Hoffman, A. S. *Advanced Drug Delivery Reviews* 2012, *64*, 18–23.

[60] Slaughter, B. V.; Khurshid, S. S.; Fisher, O. Z.; Khademhosseini, A.; Peppas, N. A. *Advanced Materials* 2009, *21*, 3307–3329.

[61] Peppas, N. A.; Hilt, J. Z.; Khademhosseini, A.; Langer, R. *Advanced Materials* 2006, *18*, 1345–1360.

[62] Lin, C.-C.; Metters, A. T. *Advanced Drug Delivery Reviews* 2006, *58*, 1379–1408.

[63] Drury, J. L.; Mooney, D. J. *Biomaterials* 2003, *24*, 4337–4351.

[64] Kopeček, J. *Biomaterials* 2007, *28*, 5185–5192.

[65] Wichterle, O.; Lim, D. *Nature* 1960, *185*, 117–118.

[66] Kolff, W. J.; Berk, H. T. J.; ter Welle M.; van der Ley, A. J.; van Dijk, E. C.; Noordwijjk, J. *Journal of the American Society of Nephrology* 1997, *8*, 1959–1965.

[67] Lagner, R.; Vacanti, J. P.; *Science* 1993, *260*, 920–926.

[68] Święszkowski, W.; Ku, D. N.; Bersee, H. E.; Kurzydlowski, K. J. *Biomaterials* 2006, *27*, 1534–1541.

[69] Jurga, M.; Dainiak, M. B.; Sarnowska, A.; Jablonska, A.; Tripathi, A.; Plieva, F. M.; Savina, I. N.; Strojek, L.; Jungvid, H.; Kumar, A.; Lukomska, B.; Domansky-Janik, K.; Forraz, N.; McGuckin, C. P. *Biomaterials* 2011, *32*, 3423–3434.

[70] Peppas, N. A.; Brenner Jr., R. E. *Biomaterials* 1980, *1*, 158–162.

[71] Burdick, J. A.; Murphy, W. L. *Nature Communications* 2012, *3*, Article number: 1269

[72] Aizawa, Y.; Owen, S. C.; Shoichet, M. S. *Progress in Polymer Science* 2012, *37*, 645–658.

[73] Annabi, N.; Nichol, J. W.; Zhong, X.; Ji, C.; Koshy, S.; Khademhosseini, A.; Dehghani, F. *Tissue Engineering Part B: Reviews* 2010, *16*, 371–383.

[74] Rivest, C.; Morrison, D. W. G.; Ni, B.; Rubin, J.; Yadav, V.; Mahdavi, A.; Karp, J. M.; Khademhosseini, A. *Journal of Mechanics of Materials and Structures* 2007, *2*, 1103–1119.

[75] Kim, T. G.; Shin, H.; Lim, D. W. *Advanced Functional Materials* 2012, *22*, 2446–2468.

[76] Mooney, D. J.; Baldwin, D. F.; Suh, N. P.; Vacanti, J. P.; Langer, R. *Biomaterials* 1996, *17*, 1417–1422.

[77] Freudenberg, U.; Hermann, A.; Welzel, P. B.; Stirl, K.; Schwarz, S. C.; Grimmer, M.; Zieris, A.; Panyanuwat, W.; Zschoche, S.; Meinhold, D.; Storch, A.; Werner, C. *Biomaterials* 2009, *30*, 5049–5060.

[78] Welzel, P. B.; Grimmer, M.; Renneberg, C.; Naujox, L.; Zschoche, S.; Freudenberg, U.; Werner, C. *Biomacromolecules* 2012, *13*, 2349–2358.

[79] Hollister, S. J. *Nature Materials* 2005, *4*, 518–524.

[80] Rivest, C.; Morrison, D. W. G.; Ni, B.; Rubin, J.; Yadav, V.; Mahdavi, A.; Karp, J. M.; Khademhosseini, A. *Journal of Mechanics of Materials and Structures* 2007, *2*, 1103–1119.

[81] Malafaya, P. B.; Pedro, A. J.; Peterbauer, A.; Gabriel, C.; Redl, H.; Reis, R. L. *Journal of Materials Science: Materials in Medicine* 2005, *16*, 1077–1085.

[82] Hutmacher, D. W.; Sittinger, M.; Risbud, M. V. *Trends in Biotechnology* 2004, *22*, 354–362.

[83] Fernandez, J. G.; Khademhosseini, A. *Advanced Materials* 2010, *22*, 2538–2541.

[84] Li, Y.; Rodrigues, J.; Tomás, H. *Chemical Society Reviews* 2012, *41*, 2193–2221.

[85] Tan, H.; Marra, K. G. *Materials* 2010, *3*, 1746–1767.

[86] Tsurkan, M. V.; Chwalek, K.; Prokoph, S.; Zieris, A.; Levental, K. R.; Freudenberg, U.; Werner, C. *Advanced Materials* 2013, *25*, 2606–2610.

[87] Mendes, P. M. *Chemical Society Reviews* 2008, *37*, 2512–2529.

[88] Xia Y.; Whitesides, G. M. *Angewandte Chemie International Edition* 1998, *37*, 550–575.

[89] Decher, G.; Hong J. D.; Schmitt, J. *Thin Solid Films* 1992, *210–211*(Part 2), 831–835.

[90] Nitschke, M.; König, U.; Lappan, U.; Minko, S.; Simon, F.; Zschoche, S.; Werner, C. *Journal of Applied Polymer Science* 2007, *103*, 100–109.

[91] Wei, Q.; Achazi, K.; Liebe, H.; Schulz, A.; Noeske, P.-L. M.; Grunwald, I.; Haag, R. *Angewandte Chemie International Edition* 2014, *53*, 11650–11655.

[92] Wei, Q.; Becherer, T.; Noeske, P.-L. M.; Grunwald, I.; Haag, R. *Advanced Materials* 2014, *26*, 2688–2693.

[93] Friedrich J. *The Plasma Chemistry of Polymer Surfaces—Advanced Techniques for Surface Design*; Wiley-VCH, Weinheim: 2012.

[94] Charlesby, A. *Proceedings of the Royal Society of London Series A, Mathematical and Physical Sciences* 1952, *215*, 187–214.

[95] Heger, A. *Technologie der Strahlenchemie von Polymeren*; Akademie-Verlag, Berlin: 1990.

[96] Tischer, R. Modifizierung von Membranoberflächen zur Verbesserung der Blutkompatibilität. Ph.D. thesis, TU Dresden: 2008.

[97] Qin, D.; Xia, Y.; Whitesides, G. M. *Nature Protocols* 2010, *5*, 491–502.

[98] Rogers, J. A.; Nuzzo, R. G. *Materials Today* 2005, *8*, 50–56.

[99] Heckele, M.; Schomburg, W. K. *Journal of Micromechanics and Microengineering* 2004, *14*, R1–R14

[100] Xu, J.; Wong, D. H. C.; Byrne, J. D.; Chen, K.; Bowerman, C.; DeSimone, J. M. *Angewandte Chemie International Edition* 2013, *52*, 6580–6589.

[101] Agarwal, S.; Greiner, A.; Wendorff, J. H. *Progress in Polymer Science* 2013, *38*, 963–991.

[102] Supaphol, P.; Suwantong, O.; Sangsanoh, P.; Srinivasan, S.; Jayakumar R.; Nair, S. V. *Advances in Polymer Science* 2012, *246*, 213–240.

[103] Bremond, N.; Bibette, J. *Soft Matter* 2012, *8*, 10549–10559.

[104] Seiffert, S. *ChemPhysChem—A European Journal of Chemical Physics and Physical Chemistry* 2013, *14*, 295–304.

[105] Derby, B. *Annual Review of Materials Research* 2010, *40*, 395–414.

[106] Khan, F.; Ahmad, S. R. "Fabrication of 3D Scaffolds and Organ Printing for Tissue Regeneration" in *Biomaterials and Stem Cells in Regenerative Medicine* (eds. Ramalingam, M.; Ramakrishna, S.; Best S.) CRC Press, Boca Raton: 2012, 101–121.

[107] Huck, W. T. S.; Yan, L.; Stroock, A.; Haag, R.; Whitesides, G. M. *Langmuir* 1999, *15*, 6862–6867.

[108] Seiffert, S. *Angewandte Chemie International Edition* 2013, *52*, 11462–11468.

[109] Sachs, E. M.; Cima, M.; Williams, P.; Brancazio, D.; Cornie, J.; *Transaction of the American Society of Mechanical Engineers, Series B* 1992, *114*, 481–488.

[110] Lam, C. X. F.; Mo, X. M.; Teoh, S. H.; Hutmacher, D. W. *Materials Science and Engineering C* 2002, *20*, 49–56.

[111] Malda, J.; Visser, J.; Melchels, F. P.; Jüngst T.; Hennink, W. E.; Dhert, W. J. A.; Groll, J.; Hutmacher, D. W. *Advanced Materials* 2013, *25*, 5011–5028.

[112] Yu, D. G.; Zhu, L.-M.; Branford White, C. J.; Yang, X. L. *Journal of Pharmaceutical Sciences* 2008, *97*, 3666–3690.

4

ANALYTICAL METHODS

In general all characterization methods applied for characterizing large organic molecules and polymers are also relevant in the field of *bio- and multifunctional polymer architectures*. Details on that can be found in common polymer text books [1, 2], and the readers are referred to those since it is impossible to cover all characterization aspects in this book. Especially the field of thermal analysis that allows determining of important features like glass transition temperature, melting temperature, and degradation behavior will not be addressed here, even though these determine significantly the application range of the material. In addition, bulk material property characterization (mechanical properties as well as bulk morphology) will not be addressed with the important exception of gel characterization. However, special aspects like a full structural analysis, verification of meaningful molar masses and dispersities, understanding the solution and aggregation behavior, and, finally, determining surface and biophysical interactions are very essential for any application of synthetic polymers and biohybrids in biomedical application, and hence, the most important characterization techniques will be briefly described from the basic features and their potentials and limitations will be outlined providing some relevant examples.

4.1 MOLECULAR STRUCTURE AND MOLAR MASS DETERMINATION OF POLYMERS AND BIOHYBRIDS

In Table 4.1, the most important characteristics that have to be elucidated for complex polymer structures and suitable analytical methods are listed.

Bio- and Multifunctional Polymer Architectures: Preparation, Analytical Methods, and Applications, First Edition. Brigitte Voit, Rainer Haag, Dietmar Appelhans, and Petra B. Welzel.

TABLE 4.1 Molecular Structure and Molar Mass Determination: Important Polymer Characteristics and Important Analytical Methods for Their Determination

Characteristics	Analytical Methods
Molecular structure	
Chemical composition	NMR, elemental analysis, UV–Vis, IR, pyrolysis–GC–mass spectrometry, MALDI-TOF, LILBID-MS
End groups	Spectroscopy (NMR, UV–Vis, fluorescence, Raman), titration
Branching and cross-linking	NMR, solution viscosity, melt viscosity, light scattering, solubility tests
Stereoregularity, head-to-tail, *cis–trans*	Spectroscopy
Optical isomerism, optical activity	Polarimetry, IR spectroscopy
Refractive index	Refractometry
Molar masses and sizes	
Molar masses Different average values: M_n, M_w	*Absolute methods:* end group analysis, membrane osmometry, vapor pressure osmometry, static light scattering, mass spectrometry (MALDI-TOF, ESI) sedimentation measurements *Relative methods:* solution viscosity, melt viscosity, size-exclusion chromatography exclusion, field-flow fractionation
Dispersity $Đ$ (M_w/M_n)	Fractionation, size-exclusion chromatography
Structure, M_w, and shape	Static light scattering, dynamic light scattering, sedimentation measurements, small-angle X-ray, solution viscosity, imaging methods ((*in situ*) AFM, cryo (HR-)TEM, electron tomography)
Aggregation (in solution)	Dynamic light scattering, field-flow fractionation, small-angle X-ray, fluorescence spectroscopy, UV–Vis spectroscopy, LILBID-MS, imaging ((*in situ*) AFM, (cryo) (HR-)TEM, electron tomography)

4.1.1 Structural Characterization

4.1.1.1 High-Resolution NMR Spectroscopy

Chemical constitution, steric configuration, and, in some cases, details about chain conformation, aggregation, association, and supramolecular self-organization behavior of macromolecular substances can be determined using high-resolution nuclear magnetic resonance (NMR) spectroscopy.

This spectroscopic technique is sensitive towards nuclei with a nuclear spin different from zero. Identical nuclei (e.g., protons) incorporated at different places of a molecule, or bond to different molecules, have different shielding constants s and thus – at constant external field H_0 – different resonance frequencies n_1. This effect is called "chemical shift" d and is usually given relative to that of a standard compound like tetramethylsilane (TMS). Because of the smallness of this shielding constant, the value of the chemical shift of a nucleus i is given in parts per million (ppm). For protons, the chemical shifts d are between 0 and approximately 12 ppm and for ^{13}C between 0 and approximately 220 ppm. Just by analyzing the chemical shifts of the signals found in an NMR spectrum, a first rough analysis of the polymer constitution is possible. Moreover, the intensity of the absorptions of each nucleus is independent of the chemical environment but proportional to their relative concentration. This feature – together with the characteristic chemical shifts – is of special importance for qualitative and quantitative structural elucidation via NMR spectroscopy: Position (d/ppm) and intensity of absorption give clear and direct information about constitution, configuration, and other features of the material to be analyzed. And there is one more dominant effect that consolidates and deepens the structural information obtained from NMR investigations. This is the indirect spin–spin coupling of neighboring, nonequivalent nuclei of a molecule via the bond electrons. It leads to a fine structure (multiplet structure) of the absorption signals, which is caused by the generation of additional small magnetic fields at the locus of the observed nucleus and, thus, provides important information on neighboring molecule groups.

The NMR spectra of dissolved polymers can be interpreted in the same way as those of low molecular weight compounds. Hence, it is a powerful tool for constitutional analyses: The chemical constitution of repeating units and end groups, the content of comonomers, or the steric configuration (tacticity) of macromolecules can be determined in dilute solution using high-resolution NMR spectroscopy. Also, NMR spectra of linear polymers of low molar mass often show unique absorptions due to their end groups. By referencing these absorptions to those of the nuclei in the repeating units, it is possible to obtain the ratio of the number of end groups to the number of repeating units. Thereby it is possible to evaluate the M_n of such a polymer, however, only when the number of end groups per molecule is known, for example, depending on the polymerization method. For branched polymers, NMR absorptions due to the branch point can be identified and reveal the chemical structure of those branch points, thus leading to a better understanding of the mechanism by which the branches form and to information about the relative number of branch points within a macromolecule.

When high-resolution NMR spectra have to be recorded of a polymeric sample, one has to recognize that polymer solutions are in general highly viscous. To prevent excessive signal broadening caused by this restricted mobility of the solution, polymer solutions for NMR studies have to be highly diluted (~1–2 mg/ml). Accordingly, rather long acquisition times are required for readily resolved spectra, in particular for ^{13}C. Nevertheless, despite high dilution, some polymer absorptions may remain broadened, especially those of atoms incorporated directly into the polymer backbone, while absorptions of lateral substituents tend to be well resolved. This broadening even at high dilution is mainly due to the restricted mobility of the polymer backbone, preventing complete averaging of the dipolar environment within the time window of the NMR experiment. Increase of temperature might sharpen some of these signals to a certain extent. Exemplarily, Figures 4.1 and 4.2 present one part of 1D and 2D NMR experiments for analyzing the complex biohybrid structures of maltose-modified hyperbranched poly(ethylene imine) (PEI) to quantify the degree of maltose units attached on the hyperbranched PEI scaffold. Only primary amino (terminal units = T) and secondary amino (linear units = L) groups in the dendritic scaffold can be modified with maltose units, but not the tertiary amino groups (dendritic units = D). This example shows restricted mobility of polymer backbone in the biohybrid structures (Fig. 4.2), while the unmodified hyperbranched PEI shows sharp and easy to differentiate ^{13}C NMR signals for the hyperbranched PEI scaffold (Fig. 4.1).

The limit of accuracy of ^{1}H-NMR experiments carried out in dilute solution is around 1–5%, depending on the resolution of the spectrum, and of approximately 10% for ^{13}C NMR. If the polymer to be investigated proved to be insoluble, solid-state NMR techniques are available for further investigation. Solid-state NMR methods are also very useful for determining bulk properties of polymers such as relaxation behavior of local motions and mutual arrangements of chains and chain segments.

4.1.1.2 IR Spectroscopy

Electromagnetic radiation having wavelengths from approximately $\lambda = 760$ nm ($\nu \triangleq 13{,}000\ cm^{-1}$; near visible light) down to $\lambda \triangleq 1$ mm ($\nu \triangleq 10\ cm^{-1}$), where the microwaves begin, is usually called infrared (IR) light. Thus, IR photons have energies between 1.6 and 0.001 eV. These energies are insufficient to induce electronic transitions but are able to excite vibration motions of molecules and parts thereof in condensed matter. The intensity of interaction between IR radiation and a molecule depends on the molecule's structure, on the symmetry of the molecule's skeleton, and on its electron distribution. This is because a vibration transition of a molecule is IR active only if the dipole moment

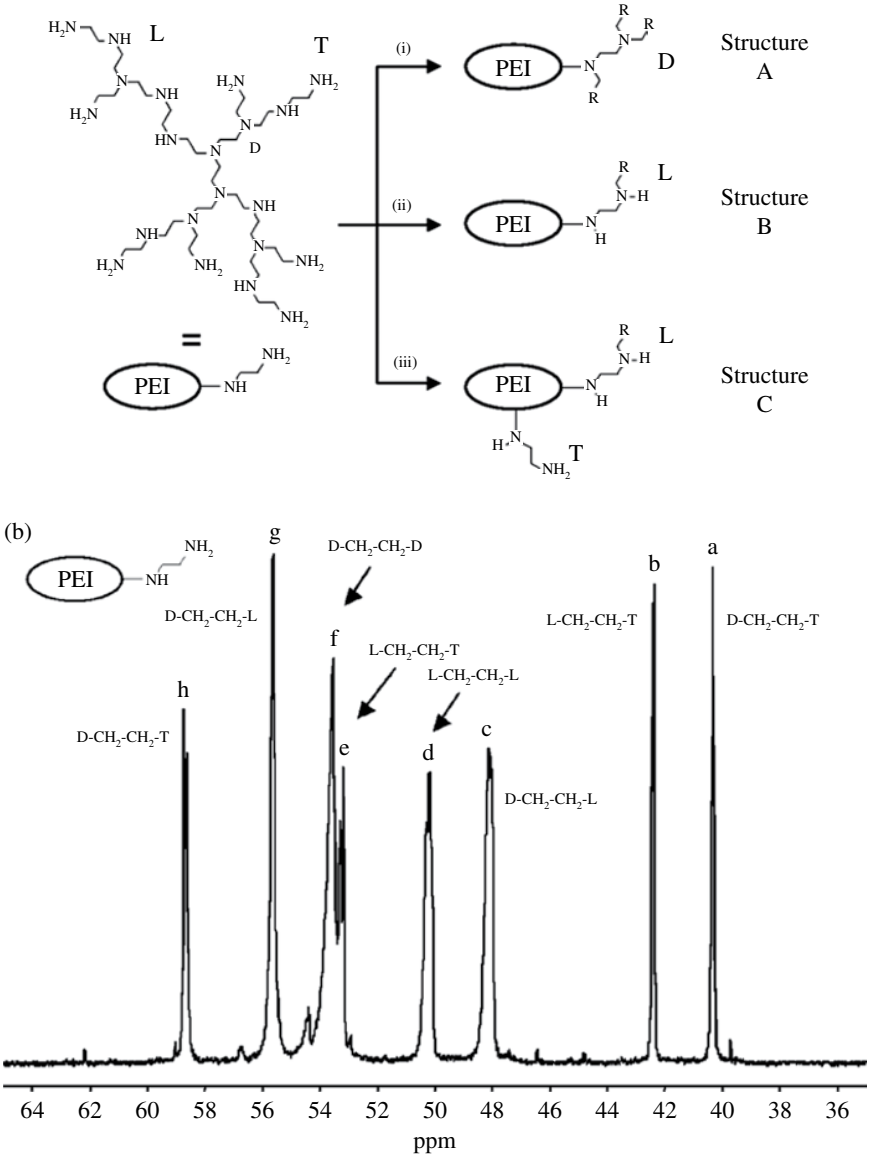

FIGURE 4.1 (a) Synthetic scheme of complex biohybrid structures composed of hyperbranched poly(ethylene imine) (PEI) and maltose units (R). The abbreviations T, L, and D represent terminal (T=—NH_2), linear (L=—NHR), and dendritic (D=—NR_2) units. (b) ^{13}C NMR spectrum of pure PEI in D_2O. The abbreviations T, L, and D represent neighboring terminal (T=—NH_2), linear (L=—NHR), and dendritic (D=—NR_2) units. Source: Appelhans et al. [3]. Reproduced with permission of American Chemical Society.

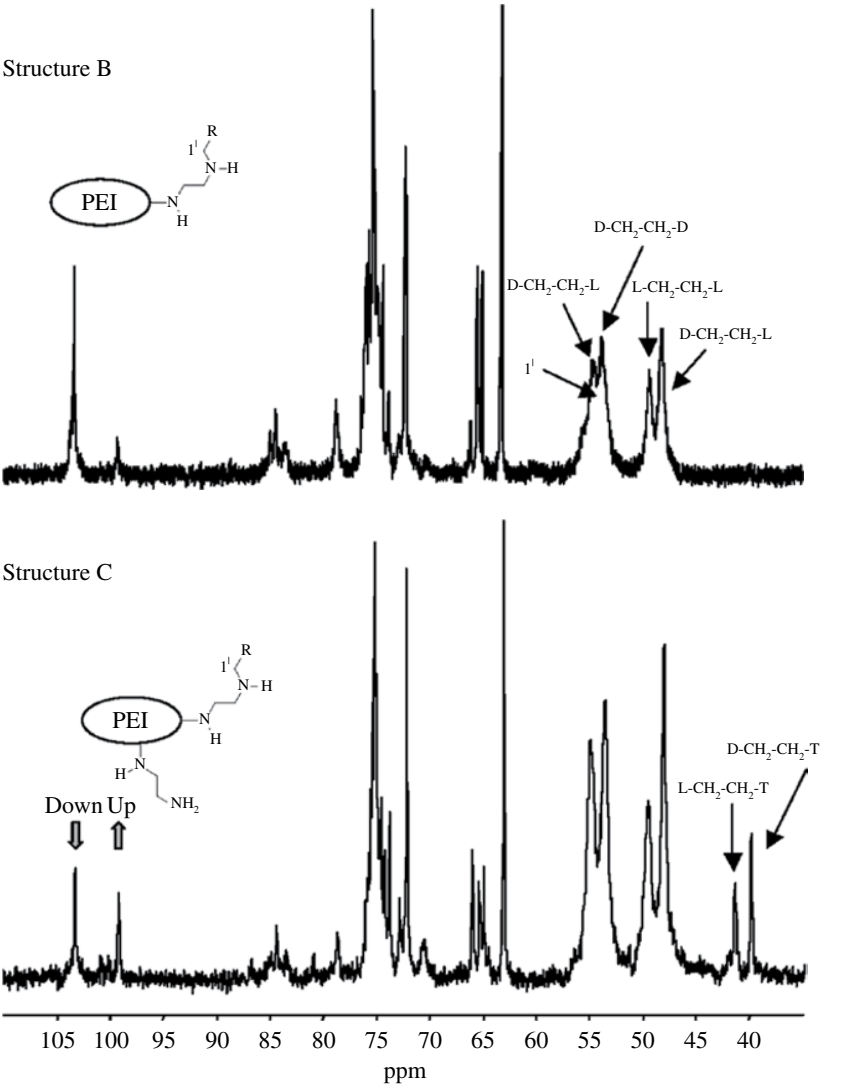

FIGURE 4.2 ^{13}C NMR of structures B and C (Fig. 4.1) of maltose-modified hyperbranched PEI showing the influence of different degrees of maltose attachment on hyperbranched PEI scaffold (Fig. 4.1). Source: Appelhans et al. [3]. Reproduced with permission of American Chemical Society.

changes during the excited vibration motion. Also, the frequency of the absorbed IR radiation as well as the efficiency of IR light absorption strongly depends on the environment of the observed molecule's fragment. Therefore, IR spectroscopy is an important technique in polymer characterization. It allows the analysis of soluble polymers but also of insoluble (cross-linked)

materials. It is sensitive towards structural features like functional groups (carbonyl, aromatics, etc.), chain constitution (1,2-isomerism vs. 1,4-isomerism and *cis–trans* isomerism in polymeric dienes, head-to-tail versus head–head–tail–tail placements in vinyl polymers or branches in polymers like polyethylene, information on conformation), end groups (M_n determination), and copolymer composition.

IR spectroscopy is experimentally much simpler as compared to other methods of vibrational spectroscopy. In order to record an IR spectrum, in most cases, the polymer is brought onto discs of NaCl or KBr either as a thin solid film (made from polymer solution in a volatile solvent or – for low-T_g polymers – from the melt; film thicknesses are typically 30–300 μm) or as a fine and homogeneous suspension in, for example, paraffin oil. Alternatively, solid polymers can be milled together with a large excess of KBr, and the resulting powder can be compressed to a (homogeneous, transparent) disc, or the samples can be dissolved in a solvent and are measured in a solvent IR cell with using the plain solvent as reference. Then, IR radiation is transmitted through the sample, and the absorbance (extinction) is measured as a function of the wavelength l or of the wave number *n* using a detector placed at the opposite site of the sample. In some other cases, the attenuated total reflection (ATR) method is used. Here, the sample is placed as a thin film on the top of an ATR crystal, and the IR spectrum is recorded in reflection geometry. The IR spectra thus obtained provide information on what efficiency IR light is absorbed by the polymer sample at which wavelength l or at which wave number *n*.

Hence, in principle, the identification of local atom groups of polymers proceeds in the same way as for low molecular weight materials, and the position of the respective bands is nearly unchanged. Also, IR spectra of oligomers are hardly different from those of high polymers if a minimum degree of polymerization is exceeded ($P_n > 5–10$). Moreover, characteristic absorption for chain end groups might be observed in the spectra – in particular for strongly IR-active end groups. Then, IR spectroscopy can be used to roughly estimate the degree of polymerization provided that the molar mass is not too high ($M < 10^4$): While qualitative IR analysis is a rather simple technique, quantitative evaluation of the IR spectra is a more complicate matter. The samples have to be prepared very carefully (only measurements in transition are possible, using very homogeneous samples), and some further requirements have to be fulfilled in addition to this. The evaluation of the signal intensities is based on the Lambert–Beer law.

Using data pools and programs that simulate IR spectra, it is possible nowadays to characterize nearly all kinds of polymers very quickly using IR spectroscopy with respect to their constitution and their composition. Also, IR

spectroscopy can be coupled with polymer chromatography (SEC, HPLC). Then it provides detailed chemical information on each individual chromatographic fraction.

IR spectroscopy is not only useful for determining the chemical constitution of polymers. It additionally provides profound information on chain orientation and on the orientation of attached lateral substituents of polymers. In this case, polarized IR radiation is applied that is only absorbed by an IR-active bond if the plane in which the electrical field vector E of the IR beam oscillates is parallel to the transition dipole moment μ of the vibration to be excited.

In addition, IR can show important noncovalent interactions like hydrogen bonding resulting in shifting and broadening of signals of interacting groups.

4.1.1.3 Secondary Structure Analysis of Proteins and Polypeptides

Many polymeric materials used in biomedical research are biohybrids, meaning a combination of synthetic polymers and biological macromolecules. In addition, the interaction of a biomacromolecule like a peptide and any synthetic polymer is of high interest for potential application, for example, if there are conformational changes or denaturation of the proteins in contact with a polymeric surface and, thus, specific characterization tools not only for the synthetic polymers are of need but also for biomacromolecules. Therefore, in the following, specific techniques are described for the characterization of polypeptides as an example for a typical biological macromolecule.

Knowledge of the secondary structure of proteins and polypeptides is still a key task in biochemical, pharmaceutical, and biomedical research. There are four common techniques for the secondary structure analysis of proteins, which are X-ray crystallography, NMR spectroscopy, circular dichroism (CD), and IR spectroscopy.

X-ray Crystallography

X-ray crystallography enables information on the tertiary structure of proteins up to large molar masses close to atomic resolution, so that at least the spatial positions of the constituting amino acids can be given. From these informations, also portions of the typical protein secondary structures α-helix, β-sheet, turns, and random coil can be computed. However, only crystallizable proteins can be analyzed, and the crystal state does not necessarily resemble the solution state, which is closer to its native environment.

NMR Spectroscopy

NMR spectroscopy enables information on the solution state of proteins with a limited molar mass. Observables are distances between amino acids

accessible by the nuclear Overhauser effect (NOE), which serve as input parameters for the computational protein modeling. Like X-ray, from this tertiary structure information, the secondary structure portions can be derived [2].

Circular Dichroism

CD spectroscopy is a classical method to determine secondary structure portions, but no tertiary structure information on the spatial protein folding like the relative positions of α-helical sections or single amino acids can be given. Nevertheless, CD is a powerful tool to determine absolute values of protein secondary structure fractions as well as changes in these values caused by media parameters (e.g., salinity, pH, temperature) or substrate binding of enzymes. Access of CD to protein conformation is provided by their constituting amide units, which are chromophores for the absorption of ultraviolet and visible light (UV–Vis) radiation and result in n–π* and π–π* transitions. Different ordered protein secondary structures give rise to different unit cells, so that these transitions can split into two or four transitions (exciton splitting), which additionally might be both allowed and forbidden. CD spectroscopy uses right- and left-handed circularly polarized light, which is absorbed by optically active molecules to a different extent.

In principle a CD spectrum is the difference between the absorbance spectra recorded by right (R)-handed and by left (L)-handed radiation. CD spectra of optically inactive (macro)molecules result in a flat baseline. Proteins have optical activity based on their chiral C-alpha atoms, and thus their complex CD spectra show CD bands with both negative and positive intensities dependent, if the (split) transition was performed stronger by absorption of L-handed or R-handed radiation. As a consequence different proteins with different secondary structure portions cause different diagnostic signatures in their CD spectra. A random coil polypeptide has a CD spectrum similar to a simple chiral amide featuring a strong negative π–π* transition around 195 nm and a weak positive n–π* transition around 220 nm. Pure α-helical polypeptides and proteins show a strong negative n–α* transition around 223 nm and two split π–π* transitions due to exciton coupling: one positive around 195 nm and one negative around 206 nm. Polypeptides and proteins with dominant antiparallel pleated sheet structure also give rise to two split π–π* transitions: one positive around 195 nm and a negative one at 218 nm.

As a practical example in Figure 4.3, typical CD spectra of lysozyme (LYZ) and concanavalin A (CONA) are shown. The CD spectrum of β-sheet-rich CONA is significantly different from that of α-helix-rich LYZ.

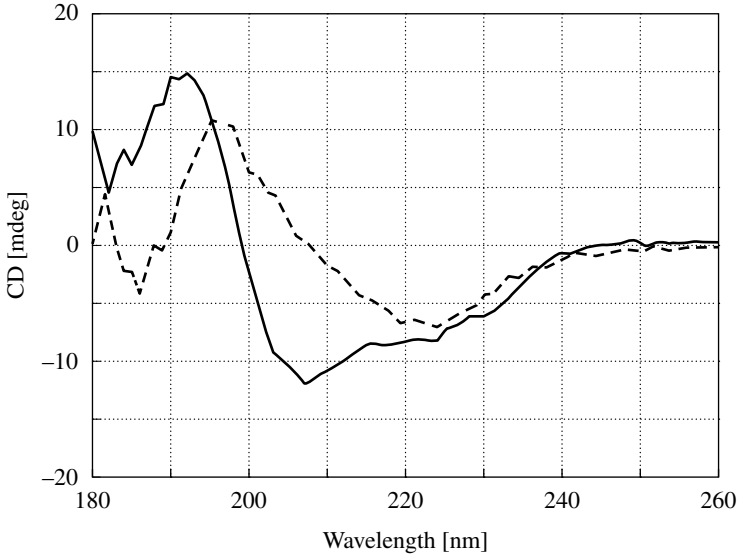

FIGURE 4.3 Typical CD spectra of LYZ (0.1 mg/ml, solid line) and CONA (0.2 mg/ml, broken line).

Infrared (IR) Spectroscopy

IR spectroscopy is also used for the analysis of overall protein secondary structure composition in terms of α-helix, β-sheet, turns, and random coil. A valuable recent review on IR spectroscopy is from Barth [4]. Therefore the use of Fourier transform instruments revolutionized IR spectroscopy with respect to throughput, multiplexing, and fast processing. Additionally, the application of techniques like ATR enabled *in situ* studies at the solid/water interface and biological environment. Similar to CD also in IR spectra of proteins, the amide groups serve as prominent chromophores and give rise to a series of diagnostic amide bands. Based on experimental and theoretical force field studies on small crystalline model secondary amides, nine different amide modes could be identified. Among those the most important are Amide A (3300 cm^{-1}); Amide I (1650 cm^{-1}), which is mainly composed of the ν(C═O) (80%); Amide II (1560 cm^{-1}), which is composed of both ν(C─N) (40%) and ν(N─H) (60%); and Amide III (1300 cm^{-1}) mode.

Significant differences had been identified between the positions and shapes of Amide I and Amide II bands of proteins whose differences in secondary structures were known from X-ray diffraction. Thus, proteins rich in α-helical structure revealed Amide I maximum positions in the range 1652–1657 cm^{-1} and Amide II bands in the range 1545–1551 cm^{-1}. Proteins rich in β-sheet structure revealed Amide I bands centered within 1628–1635 cm^{-1} and Amide II bands within 1521–1525 cm^{-1}.

TABLE 4.2 Assignment of Diagnostic CD [5] and IR Spectral Data [6, 7] on Protein Solutions (H_2O) to Typical Secondary Structure Fractions

Secondary Structure	α-Helix	β-Sheet		Turn	Random Coil
		Antiparallel	Parallel		
CD (nm)	192 (+, s)	195 (+, m)		187 (−, s)	195 (−, s)
				198 (+, w)	223 (+, w)
	206 (−, s)	218 (−, w)		223 (+, m)	
	222 (−, s)				
IR (cm^{-1})	1648–1655	1630–1636 (s)	1630 (s)	1665–1675 (m)	1656–1660
		1690–1693 (w)	1645 (w)		(m,br)

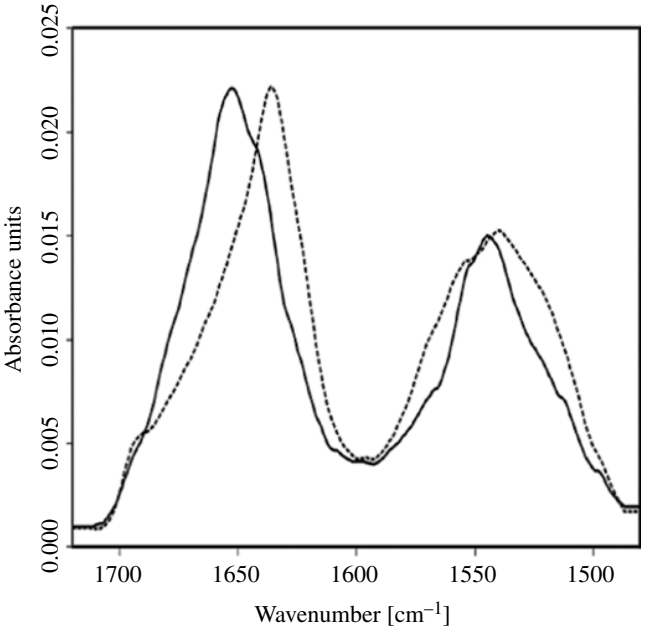

FIGURE 4.4 Typical FTIR spectra of LYZ (10 mg/ml) and CONA (10 mg/ml).

Amide I and II bands are very sensitive to molecular geometries and hydrogen bonding typical for secondary structures like α-helix or β-sheet, so that they can be used diagnostically. In Table 4.2, wavenumber ranges of Amide I positions and their assignments to respective secondary structures are given. In Figure 4.4, typical FTIR spectra of LYZ and CONA are shown. The FTIR spectrum of β-sheet-rich CONA, with an Amide I maximum at 1635 cm^{-1}, is significantly different from that of α-helix-rich LYZ (1653 cm^{-1}).

In practice FTIR spectra on protein solutions or layers may reveal a featureless broad band, since several secondary structure portions prevail and the amide absorptions of each of these portions spectral overlap. Therefore, various numerical methods on the spectral and interferogram level have to be used to significantly deconstruct, resolve, and identify individual Amide I band components.

4.1.1.4 UV–Vis Spectroscopy

Like IR spectroscopy, UV–Vis spectroscopy are important optical methods for polymer characterization. The basis is the interaction of electromagnetic radiation (UV: ~6.7–3.35 eV, Vis: ~3.35–1.6 eV) with organic or inorganic matter. Due to this interaction, an electron of a binding or nonbinding molecular orbital is excited into an antibonding molecular orbital. This electronic transition is caused by energy absorption, which can be detected in a UV–Vis spectrometer. The excitation energy depends on the nature of the excited electrons and is highest for electrons in σ-bonds. Observed electronic transitions are usually overlaid by vibrational transitions. Absorption spectra can be recorded in both transmission and reflection mode and characterize the energy uptake of the sample as function of the excitation wavelength. For reflectance measurements, special accessories (e.g., integrating sphere, praying mantis) are required. Both specular reflectance and diffuse reflectance may be measured. Standard UV–Vis spectrometer covers excitation wavelengths between 185 and 900 nm, and more sophisticated instruments are usable in the vacuum UV (<185 nm; spectrometer has to be flushed with inert gas) and/or near IR (up to 3000 nm).

The transmission at a given wavelength is the ratio of the intensities of the light beam before (I_0) and after passing the sample (I):

$$T = \frac{I_0}{I}$$

The absorbance A is defined as logarithm of T:

$$A = \log_{10}\left(\frac{1}{T}\right)$$

For infinite dilute solutions, the Lambert–Beer law states that the absorbance of a sample is directly proportional to the concentration c of the absorbing compound:

$$A = \varepsilon \times c \times d$$

Here, d is the optical path length and ε is the wavelength dependent molar extinction coefficient, which is characteristic for this compound. Often, ε is additionally dependent on the molecular environment (solvent). Interactions with molecules other than solvent may lead to spectral changes and therefore limit the validity of the Lambert–Beer law at higher concentrations. Absorbancies > 5 are a challenge even for very sophisticated instruments. Standard spectrometers are able to measure in a range of 0.001–3 absorbance units. Assuming a molar extinction coefficient of a (very good) chromophore of about 50,000 l/mol cm, concentrations between 2×10^{-8} and 6×10^{-5} mol/l can be quantitatively determined. Otherwise, evaporating 1 ml of a solution on an area of 1 cm^2 would lead to an ultrathin film with the same absorbance as the solution. Turbidity of solutions or films limits the power of transmission measurements. However, with an integrating sphere, one can overcome these limitations.

Spectral changes due to the interaction of two compounds can be used in order to understand the underlying reactions. Under good circumstances, like during the formation of complexes between PPI dendrimers with transition metals, new peaks in the absorbance spectra give direct information about the formed complexes. For the formation of the avidin/biotin complex, only small spectral shifts can be observed. A quantitative treatment is then much more difficult. Often, conformational changes are accompanied by spectral changes, which allow their investigation.

Polymers and biopolymers often show only small and unspecific absorption. Then the use of special chromophores offers an alternative way to get additional information. Probes for, for example, pH (indicator molecules) or polarity (e.g., pyridinium betaine dyes) might be attached by chemical bonds (label) or physical interactions on the systems under investigation.

The absorption intensity depends on the angle between the electric vector of exciting light and the direction of the transition moment of the excited bond. Typically, the light beam in standard spectrometers is not (or little) polarized so this does not matter. By using polarized light, the study of optical anisotropy becomes possible.

With time-resolved measurements, it is possible to follow the kinetics of chemical reactions. Standard spectrometers allow resolutions in the millisecond range. Of course, the other end is open. More special instruments work with a resolution in the microsecond range and below. This technique allows the investigation of transient intermediates like radicals or triplet states.

In comparison with NMR and IR spectroscopy, UV–Vis spectroscopy is not so specific. Its main advantages are:

- Liquid, solid, and gaseous samples can be measured.
- High sensitivity.
- Time resolution from microsecond and below up to years.
- Remote measurements are possible.
- Nondestructive (exception: Photoreactions may occur).
- Usable for separation and complexation process, when, for example, noncomplexed/nonseparated or complexed molecules are specifically detectable by its chromophore or aggregated molecules are not any more optically detectable.

Giving one example, UV–Vis spectroscopy can be used very easily to determine interaction capability of dendrimers towards biological entities. Thus, carbohydrate-functionalized dendrimers were used to investigate the predictable tunability of multivalent interactions against the lectin CONA [8].

4.1.1.5 Fluorescence Spectroscopy

Fluorescence spectroscopy is commonly used to characterize fluorescence effects in the UV and visible range of the electromagnetic spectrum. Such fluorescence is caused by the fact that the absorption of UV or visible light of specific wavelengths causes excitation of electrons to states with higher energy (Fig. 4.5).

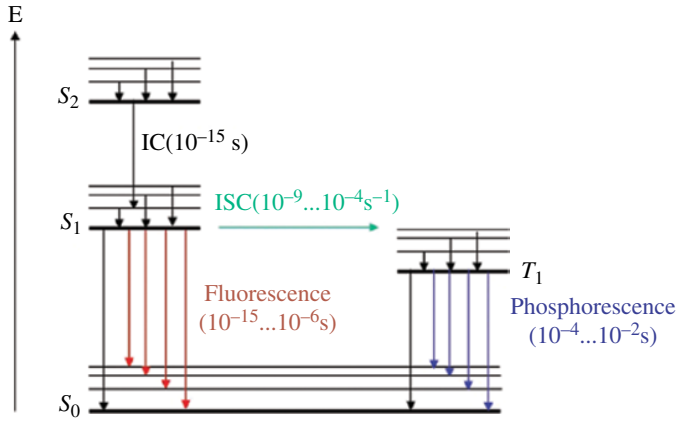

FIGURE 4.5 Jablonski diagram. (*See insert for color representation of the figure*.)

Generally, excitation leads to excited singlet states (S_1, S_2, etc.), which may be overlaid by vibrational energy levels. Higher excited singlet states usually deactivate by internal conversion (IC) very fast (within femtoseconds) to the lowest excited singlet state S_1. These S_1 states are still very instable and have lifetimes in the nanosecond and picosecond range. Three photophysical processes of the S_1 state are typical:

1. Fluorescence (red; S_1 state) is characterized by the emission of a photon and leads to the electronic ground state. The emitted light has lower energy (i.e., longer wavelengths) compared to the absorbed light. This fluorescence can be measured; the spectral distribution of its intensity is the fluorescence emission spectrum. Fine splitting of fluorescence bands is caused by vibrational states.
2. Radiationless IC (black in the Jablonski diagram) leads to the electronic ground state S_0: the excitation energy is converted to thermal energy. This process is often addressed as thermal relaxation, too.
3. Intersystem crossing (ISC, green) is a radiationless process leading to an electronic state with different spin multiplicity (here: the triplet state T_1). ISC is a spin-forbidden process, so the rate constants are generally lower than those for fluorescence and thermal relaxation to the ground state.

For standard fluorescence spectra, the fluorescence intensity is measured perpendicular to the excitation beam. Two types of spectra may be obtained:

1. The *fluorescence emission spectra*, due to their predominant use often simplified addressed as fluorescence spectra, exhibit the spectral distribution of fluorescence intensities at a fixed excitation wavelength.
2. For *fluorescence excitation spectra*, the fluorescence intensity at a fixed emission wavelength is measured in dependence on the excitation wavelength. They correspond to the absorbance spectra.

Typical fluorescence spectrometers deliver relative fluorescence intensities: They are altered by both the wavelength-dependent throughput of optical elements (lenses, mirrors, gratings, lamps) and spectral sensitivity of the detector. Often, these relative spectra are sufficient. In order to obtain corrected spectra, one may use quantum counters or integrating spheres, for instance.

Fluorescence emission spectra contain information that may be valuable for the investigation of polymeric, biohybrid, or aggregated systems:

- In diluted solution, *fluorescence intensities* are proportional to the fluorophore concentration and can therefore be used to determine these concentrations. The method is very sensitive: For good chromophores

like fluorescein, concentrations in the range of 10^{-9} mol/l and below may be quantified with standard instruments.

- *Spectral position and form of fluorescence bands* are dependent on the molecular environment (neighbored molecules) and can be used to investigate adsorption, complexation, interaction, or aggregation processes. Special fluorophores like pyrene and 1-anilinonaphthalene-8-sulfonic acid (ANS) exhibit dramatic changes of their fluorescence spectra when changing the polarity of their environment and were therefore often applied as fluorescence probes.
- The *polarization of emission bands* may give information on the orientation of immobilized molecules or their mobility (fluorescence depolarization).

Besides the earlier addressed monomolecular processes of the S_1 state, bimolecular processes are also important. Interaction of an excited molecule M^* with another molecule mostly leads to the reduction of its fluorescence (quenching). Different quenching processes are possible, for instance:

- *Collisional processes*:

$$M^* + Q \rightarrow M + Q$$

Collision processes are widely used phenomenon in polymer research, for example, for the investigation of adsorption onto fluorescing polymers or surfaces. Here the polymer may be fluorescing by itself or labeled with an appropriate fluorophore.

For collisional quenching, the Stern–Volmer equation may be applied:

$$\frac{I_0}{I} = 1 + \left(k_q \times \tau \times [Q]\right),$$

where

I_0 fluorescence intensity in the absence of Q

I fluorescence intensity in the presence of Q

k_q rate constant of quenching

Q quenching molecule (e.g., dye or (complexed) metal ion)

- *Molecular rearrangements:*

A specific molecular arrangement can lead to changes in the molecular environment of fluorescing moieties and therefore alter fluorescence

emission. Both intermolecular and intramolecular processes may be responsible. The use of fluorescence probes offers a way for the investigation of conformations of even nonfluorescing polymers, complexes, or aggregates.

- *Fluorescence resonance energy transfer* (FRET):

$$M^* + A \rightarrow M + A^*$$

$$A^* \rightarrow A + h\nu$$

Here, the excited acceptor molecule A^* exhibits also fluorescence. This opens a way to investigate spatial properties in polymeric, complexes, and aggregated systems. DNA analysis is a field where FRET has been widely used to identify their location on surface or the interaction with other biological entities.

- *Exciplex* (**exci**ted com**plex**) formation:

$$M^* + Q \rightarrow (M \ldots Q)^*$$

Exciplex or excimer (**exci**ted di**mer** $(M \ldots M)^*$) fluorescence has been extensively used in order to investigate polyelectrolyte, biological, or aggregated systems.

- *Photochemical reactions*: Quenching/formation of fluorescence may give kinetic information.

In addition to the steady-state experiments, time-resolved experiments may provide further information. Microscopic techniques can give structural information up to the molecular level (see Sections 4.3.3.4 and 4.4.7).

4.1.1.6 Mass Spectrometry

Since the development of soft ionization mass spectrometry [9], which allows to analyze large organic molecules without fragmentation, various polymer architectures were characterized by mass spectrometry. In principle, different parameters tailoring polymeric material properties such as molar mass (M_n), architecture (linear, branched, cyclic, star, etc.), monomer composition, degree of functionalization, end groups, and the presence of impurities or additives can be evaluated by mass spectrometry, however, with some limitations. The determination of molar masses of polymers by mass spectrometry is only possible for reasonable low dispersity polymeric architectures, which can be achieved by using controllable polymerization techniques such as anionic or

controlled radical (ATRP, RAFT, etc.) polymerization techniques, but also by defined iterative multistep reactions as for the synthesis of dendritic macromolecules. In multidisperse materials, however, overlapping of molecules with different ionization charges but same molar mass inhibits mostly a reasonable evaluation of the data. From the historical point of view, monodisperse proteins and peptides have been first analyzed by mass spectrometry due to their well-defined molar mass than polymeric materials.

Soft ionization MS techniques [9] like electrospray ionization (ESI) and soft laser desorption, often known as matrix-assisted laser desorption/ionization (MALDI), facilitated the polymer analyses over the last years. The advantage of the soft ionization techniques is the transformation of dissolved liquid or solid sample into the gas phase, where no change in the molecular composition/structure of the sample will be induced, while hard ionization in mass spectrometry (e.g., electron ionization (EI) or fast atom bombardment (FAB)) preferentially destroys the chemical and molecular structure into fragments prior to the detection of the molar mass fragments of the sample by mass spectrometry.

Figure 4.6 presents shortly the ionization mechanism in MALDI-MS. Ionization of (polymeric) sample is realized by shouting a laser beam into the

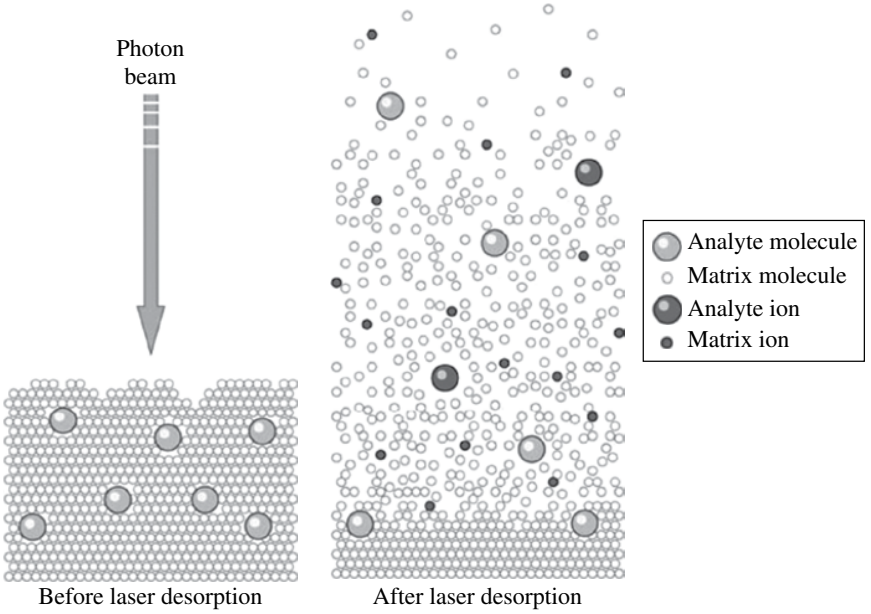

FIGURE 4.6 Schematic outline of ionization mechanism in MALDI-MS. Source: Henderson and McIndoe [10], figure 1. Reproduced with permission of John Wiley & Sons.

matrix with incorporated analyte molecules. The matrix has the function to adsorb most of the laser energy for inducing ionization of the matrix, lowering the energy transfer to analyte molecules, and initiating a gentle ionization of those. Moreover, the matrix should also protect analyte molecules from the direct energy of the laser. This reduces and suppresses degradation and fragmentation processes in the analyte molecules. MALDI-MS is often connected to a time-of-flight (TOF) mass spectrometer analyzing the ionized analyte molecules desorbed by single or collected laser shots on the matrix sample.

For that, after the ionization process, matrix and analyte molecules have to pass a drift region in vacuum where no electric or magnetic field is applied. This only occurs when charged ions of various sizes are generated on the sample slide, as shown in Figure 4.7. A potential difference V_0 between the sample slide and ion source (matrix with analyte molecules) attracts the ions in the direction of drift region and detector (Fig. 4.7). The velocity of the attracted ions v is determined by the law of conservation of energy. As the potential difference V_0 is constant with respect to all ions, ions with smaller m/z value (lighter ions) and more highly charged ions move faster through the drift region until they reach the detector. Consequently, the time of ion flight differs according to the mass-to-charge ratio (m/z) value of the ion. Thus, each matrix and analyte molecule move individually with constant velocity towards the detector (mass analyzer = TOF).

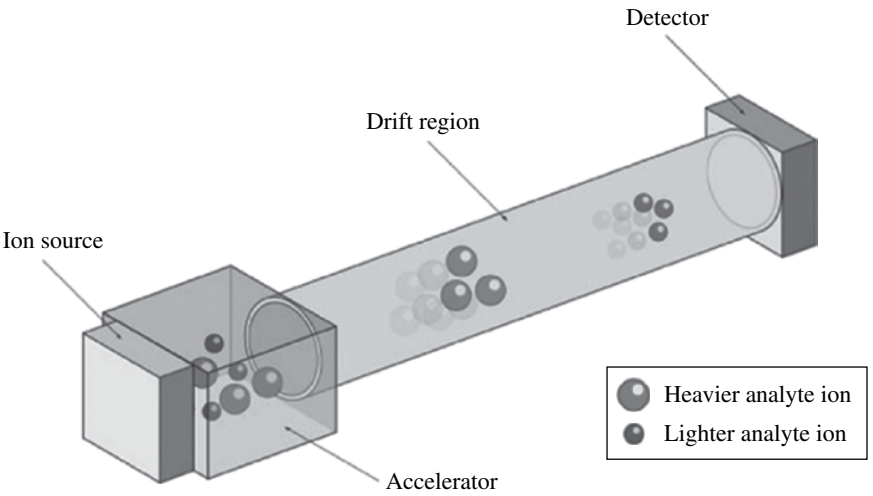

FIGURE 4.7 Simplified TOF process of mass analysis. Ion source (matrix with analyte molecules) and sample slide (opening to drift region) possess a potential difference for accelerating different charged analyte ions. Source: Harth-Smith and Barner-Kowollik [11], figure 1. Reproduced with permission of John Wiley & Sons.

The ionization process of ESI-MS is carried out by spray capillary and repulsive electric forces to disperse sample solutions in a bath gas into smaller aerosol particles. These particles undergo further solvent evaporation under an annealing step to reach unstable smaller droplets. Then bursting droplets will form charged jets in coulomb fission process followed by final formation of gas phase ions to enter the mass spectrometer via two possible mechanisms (ion evaporation model and charge residue model). Different types of mass analyzer have been applied for ESI: TOF, ion trap, quadrupole, etc. With this analysis method, a high resolution (within 2 ppm) is given for determining molar mass. ESI-MS has some limitations allowing the determination of molar masses lower than 10,000 g/mol, while MALDI-MS allows the evaluation of several 100,000 g/mol.

In addition to ESI, a relative new laser desorption mass spectrometry method termed laser-induced liquid bead ion desorption mass spectrometry (LILBID-MS) has been established [12]. Here, preferentially monodisperse macromolecules, especially biomolecules, dissolved in microdroplets are desorbed/ablated by a mid-IR laser into vacuum [12, 13]. Two modes of desorption are addressable: an ultrasoft mode at lower laser intensity in which, for example, a macromolecule complex is desorbed into vacuum and a harsher mode at higher laser intensity by which it is dissociated into its covalent subunits. A broad range of molar masses of biohybrid structures and transmembrane protein complexes, etc. can be determined up to 1,000,000 g/mol, as long as the to be analyzed macromolecular structures can be dissolved in water or in buffer solution with low ionic strength. With this LILBID-MS molar masses of water-soluble glycodendrimers and their complexes with inorganic Re clusters are determinable (Fig. 4.8) [14].

4.1.2 Determination of Molar Mass and Molar Mass Distribution

The degree of polymerization, P, and the molar mass (or molecular weight), M, are some of the most important characteristics of a macromolecular substance. They indicate how many monomer units are linked to form the polymer chain and what their molar mass is. In the case of homopolymers, the molar mass of a macromolecule is given by

$$M = P \times M_{\mathrm{ru}}$$

with M_{ru} being the molar mass of the constitutional repeating unit. However, while low-molar-mass substances consist, by definition, of molecules of identical structure and size, this is generally not the case for polymers. Synthetic macromolecular substances are nearly always composed of macromolecules

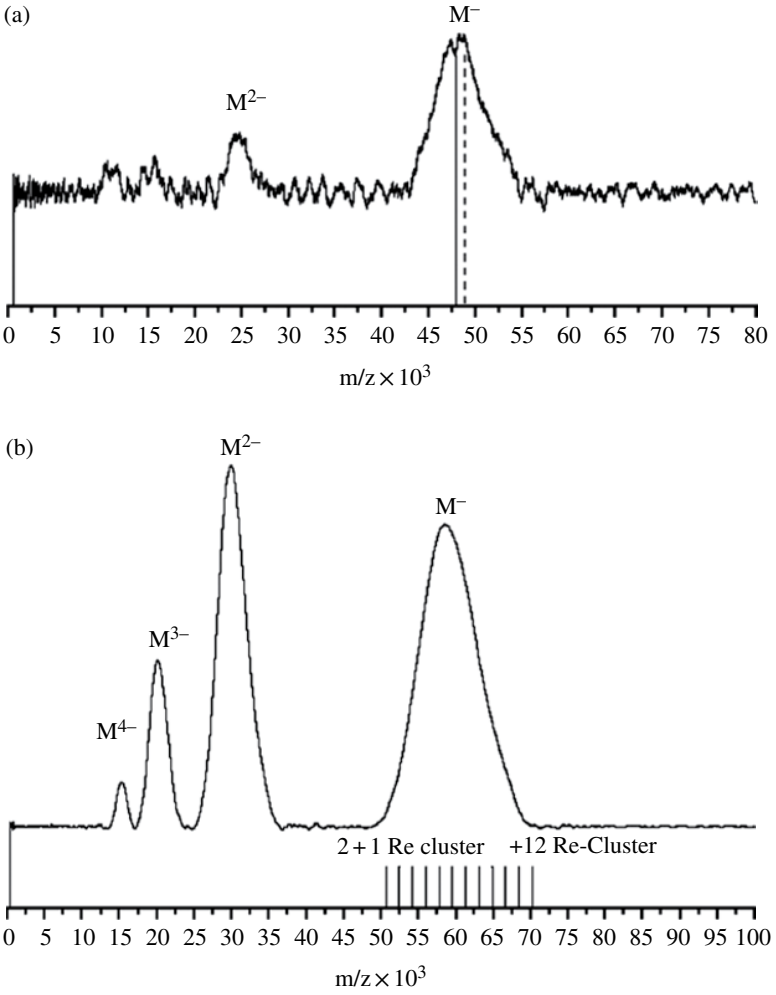

FIGURE 4.8 LILBID mass spectra of fifth-generation glycodendrimer (a) and its complexes with Re clusters (b) for determining complexation ratio between Re cluster and fifth-generation glycodendrimers (as 2 in b) using LILBID-MS technique. Molecules with differing number of negative charges appear as separate peaks in (a and b). In (b), M^- presents the mass distribution where glycodendrimer can complex x-fold Re clusters from twofold up to twelvefold. Source: Kuhlbeil et al. [14]. Reproduced with permission of John Wiley & Sons.

of similar structure but different molar masses. These materials are therefore called *disperse*. As a consequence, chemical formulas of polymers are generally given in a way where the constitutional repeating unit is drawn in square brackets, bearing an index *n* indicating the average number of repeating units

tied together to give the polymer chain. Full characterization of a macromolecular substance is not an easy task, therefore, and quite often statistical methods are required: Because of dispersity $Đ$, the values of P and M are mean values only, and the macromolecular chain molecules of a synthetic polymer are characterized by a (more or less) well-defined chain-length distribution (or molar mass distribution). The respective molar mass distribution is the direct consequence of chain formation statistics and, moreover, in many cases very characteristic for the respective chain growth process.

The number averaged molecular weight (M_n) can be calculated as shown in the succeeding text:

$$M_n = \frac{\sum_i n_i M_i}{\sum_i n_i}$$

where M_i is a particular molecular weight and n_i is the corresponding number of macromolecules with this weight. The number averaged molecular weight is especially sensitive to smaller molecules, whereas the weight averaged molecular weight M_w is more influenced by fractions of higher molecular weight. M_w gets calculated as shown in the following equation:

$$M_w = \frac{\sum_i n_i M_n^2}{\sum_i n_i M_i}$$

The quotient of M_w and M gives the molecular weight dispersity ($Đ_M$):

$$Đ_M = \frac{M_w}{M_n}$$

For an ideal uniform polymer, M_w equals M_n (as there is no distribution) and the $Đ_M$ is 1.0; the higher the $Đ_M$, the broader the molecular weight distribution. In general, a weight distribution is assumed to be "narrow" when $Đ_M \approx 1.1$.

Knowledge of the molar mass and of the molar mass distribution of a polymeric material is indispensable for scientific studies and for many technical applications of polymers. They affect the solution and melt viscosity, the self-assembly behavior, the processability, and the resulting mechanical properties tremendously. Therefore, we will give a short introduction into methods that allow us to determine the required information. Roughly, the methods developed for the determination of molecular weights are subdivided into absolute and relative methods:

Absolute methods provide the molar mass and the degree of polymerization without any calibration. Their calculation from the experimental data

requires only universal constants such as the gas constant and Avogadro's number, apart from readily determinable physical properties such as density, refractive index (RI), etc. The most important methods in use today are mass spectrometry, osmometry, light scattering, and, to some extent, sedimentation and diffusion measurements. Also, some chemical and spectroscopic methods (determination of end groups) are important because of their relative simplicity.

Relative methods measure properties that depend clearly on molar mass, for example, the hydrodynamic volume of the polymer coils (SEC, viscometry) or their solubility as a function of chain length. However, these measurements can only be evaluated with respect to the molecular weight of the macromolecules if experimental calibration curves are available, which were generated by comparison with an absolute method of molar mass determination.

A necessary prerequisite for the application of the aforementioned methods is that the polymer is soluble in a suitable solvent. Moreover, one must ensure that the dissolved macromolecules exist as isolated species and do not form associates or aggregates. Proof of this can be obtained by carrying out reactions on functional groups of the polymer that do not lead to cleavage of the polymer chains. If the degree of polymerization of the original polymer agrees with that of the modified polymer, association can be excluded. Values of molar masses determined in different solvents should also be in agreement if association is absent.

Size-Exclusion Chromatography

The generally applied chromatographic technique for the characterization of (bio)polymers is the size-exclusion chromatography (SEC also known as gel permeation chromatography, GPC). In SEC, the molecules that shall be separated and analyzed are dissolved in a liquid mobile phase, which is pumped through a stationary phase (a solid porous bed packed in a column) where the actual separation takes place. Different to other chromatographic techniques like high-performance liquid chromatography (HPLC) or gas chromatography (GC), no enthalpic interactions occur between stationary phase and dissolved polymer, thus having purely steric separation based on the hydrodynamic volume of the polymers. The packed column material is composed of a porous gel with pores of particular size. Large macromolecules do not fit into small pores; their volume is excluded for this column. On the other hand, a small molecule can permeate into all pores; the accessible column volume is much higher. In this way, sample components are retained by the stationary phase in means of their size. The theoretical description of the size-exclusion effect

predicts that not only the "size" of the macromolecule and pore has to be taken in account; additionally, the geometric conditions and the conformation of the polymer become important. Depending on the column packing material, the separation range usually is between 100 and 10^7 g/mol.

Limitations for the applicability of SEC for certain molecules are the high shear forces due to the dense column packing, which may influence molecular assemblies and lead to degradation. Furthermore, the column packing material can induce unwanted interactions between the stationary phase and the molecules, thus shifting the separation mechanism from pure size exclusion towards separation by enthalpic interactions. Especially in cases of multifunctional polymers like dendritic molecules with a high number of end groups, delayed elution or complete adsorption can be observed.

After the separation step, there is a need of a detection system to monitor the presence of polymers in the column effluent and to give further data for molecular weight calculation. For *relative determination*, a concentration-sensitive detector (RI or ultraviolet (UV)) and defined polymer standards with different molecular weights are necessary. The concept is to establish a correlation of retention volume and molecular weight of standards. Taking the logarithm of the molecular weight and plotting it against the elution volume, a calibration curve will be received. With this curve, the retention volumes of unknown samples can be converted into molecular weights. However, for this molecular weight determination, equal molecular and chemical properties of calibration standard and sample are required. For polymers that cannot be considered to be similar to the standard in chemical composition and/or molecular architecture, the approach of *universal calibration* can be used. In 1967, Grubisic et al. [15] proposed to use the logarithm of the product of intrinsic viscosity ($[\eta]$) and molecular weight (M) for calibration as it is directly proportional to the hydrodynamic volume of a given polymer. However, universal calibration fails if the segmental density of the polymers is strongly deviating from usual linear chains. In this case, *absolute molecular weight determination* should be performed.

Size-Exclusion Chromatography with Light Scattering

Coupled to a SEC system, a static light scattering (SLS) detector allows online determination of molecular weight of polymers. An SLS detector measures the scattered light under multiple detection angles, which results by passing a flow cell.

In contrary to small polymers that scatter light isotropically in all directions, sufficiently large molecules ($d > \lambda/20$; λ is the wavelength of the

applied laser light) scatter light with different intensity under different angles. This is caused by the interference phenomena that occur if there is more than one scattering center per molecule. The scattering intensity $R(q)$ for an angle q is connected with the weight-averaged molar mass (M_w) in the following equation:

$$K^* = \frac{c}{R(q)} = \left[1/M_w + P(q)\right] + A_2 c$$

where c is the polymer concentration and A_2 is the second viral coefficient. $P(q)$ describes the angular dependency of the scattered light. The optical constant K is defined as

$$K^* = 4\pi^2 n_0^2 \left(dn/dc\right)^2 / \lambda_0^4 N_A$$

where n_0 is the RI of the solvent, dn/dc the RI increment, λ_0 the wavelength of the laser, and N_A Avogadro's constant. By plotting $K^* \cdot c/R(q)$ versus $\sin^2(q/2)$, the interception of the y-axis is characterized by MW and the radius of gyration (r_g) is given by the slope.

The light scattering intensity is strongly dependent on the particle size, which leads to rather low sensitivity for smaller molecules. SEC in combination with SLS detection with multiple angles enables the possibility to obtain additional information about the conformation and scaling properties and aggregation behavior of the molecules.

4.2 CHARACTERIZATION OF AGGREGATES AND ASSEMBLIES

The aggregation of natural and synthetic (bio)polymers is commonly based on noncovalent interactions. There are numerous analytical techniques for the characterization of molecular aggregation. Comprehensive studies require gentle and well-controlled analysis conditions without destroying weak bonds between molecules like H bonding, π–π, dipole, or hydrophobic interactions, which may also be strongly concentration and solvent dependent. Any ionic interactions are in addition dependent on ionic strength and pH. Depending on the measurement principle, it is possible to obtain average (e.g., via light scattering) and discrete values (e.g., microscopic techniques) for the aggregate size. In addition, fractionated samples (e.g., achieved by SEC or AF4 with light scattering detection) can be analyzed to achieve information on the aggregate size distribution.

4.2.1 Dynamic Light Scattering

Dynamic light scattering (DLS, also known as photon correlation spectroscopy, PCS) can be used in order to determine the diffusion coefficient (D) and thus the hydrodynamic size of particles.

A laser beam passes though the sample solution where the light gets partially scattered by the particles with certain intensity. Brownian molecular motion of the particles leads to interferences of scattered rays from different molecules. This can be observed as a time-dependent fluctuation of the scattered light. This fluctuation is of higher frequency for smaller particles with higher diffusion coefficients and of lower frequency for larger particles with lower D. For the evaluation of these fluctuations, they can be processed into physical parameters by using a correlator producing an autocorrelation function. In principle, the correlator compares the signal (light scattering intensity) at time t with the signal at time $(t+\tau)$, where τ is as time increment that is being increased from less than 1 µs up to several seconds. If the signals are similar, the correlator gives a high value; if the signals are more different, the value will be lower. Typically, the correlation is high at short time scales (small τ) and decreases exponentially at larger time scales. For monomodal sample, the autocorrelation function can be expressed with an exponential decay function, whereas for a multimodal sample, a superposition of multiple exponential functions has to be established. The experimental data points need to be fitted by theoretical curves that can be expressed by

$$g(\tau) = 1 + \beta \cdot \exp\left(-2Dq^2\tau\right)$$

where $g(\tau)$ is the correlation function, β the amplitude of the function, D the diffusion coefficient, q the scattering vector (dependent on RI of solution, wavelength of the applied laser light, and the observed scattering angle), and τ the time increment.

Making use of the Stokes–Einstein relation, the diffusion coefficient can be converted into the hydrodynamic diameter:

$$d_h = \frac{k_B \cdot T}{3\pi \cdot \eta \cdot D}$$

Besides d_h as the hydrodynamic diameter and D as the diffusion coefficient, the equation contains Boltzmann's constants k_B, the temperature T, and the solvent viscosity η.

In contrast to SLS, DLS allows analysis of smaller particles. For the characterization of mixtures with different components, for example, single

molecules and aggregates, it is necessary to perform a previous separation. Otherwise only an average value will be obtained.

4.2.2 Pulsed Field Gradient and Electrophoretic Nuclear Magnetic Resonance

NMR is an indispensable tool for the structure characterization of new organic polymers, dendrimers, and other complex (macro)molecules utilizing the chemical shift and indirect dipolar couplings, so-called J couplings [16] (see Section 4.1.1.1). However there are various other possibilities to apply NMR for the characterization of materials. In particular pulsed field gradient (PFG) NMR can be used to measure translational displacements of molecules in solution or dispersed systems [17]. Magnetic field gradients are magnetic fields depending on their position in space. Usually constant gradients are applied in which the field has a linear dependence on the position. Because the Larmor frequency is proportional to the field that the nucleus under study experiences in a magnetic field gradient, the Larmor frequency becomes position dependent. This is the basis of magnetic resonance imaging (MRI), a standard diagnostic technique in medicine as well as in materials science. While magnetic field gradients are used to encode spatial positions finally to encode images in NMR signals, pairs of magnetic field gradient pulses can be used to encode displacements in PFG NMR [18].

In a PFG NMR experiment, the first radio-frequency pulse excites the magnetization, which evolves under the interactions present. After a certain time τ, there is a so-called echo pulse that refocuses the evolution so that after the same τ an echo is formed. If after the excitation and after the echo pulse short gradient pulses are applied, the first echo pulse encodes the position of the molecule in the phase of the NMR signal and the second one refocuses this encoding, if the spins are at the same position during each gradient pulse. If the spins change position, two cases are distinguished: If random displacement like diffusion or Brownian motion takes place, there will be a random phase distribution between the spins, which in the average over the entire sample results in an in-phase signal that is attenuated. From the attenuation, the *diffusion coefficient* is determined using the Stejskal–Tanner equation. If on the other hand, there is a coherent motion, the phase difference is the same for all spins resulting in an in-phase signal of full amplitude. The different signatures' amplitude modulation of phase modulation for diffusion or flow can be used to distinguish both in the PFG NMR experiment and allows to *measure coherent motion* resulting in displacements as small as those from diffusion.

There is a general interest to have a measure of the size of nano-objects in solution, because the size has an impact on possible interactions with other molecules or complexes. Size is one important factor controlling, for example, the applicability of dendrimers for transfection. On the other hand, because they are monodisperse, dendrimers offer opportunities to probe fundamental physical concepts. From the dependence of a characteristic length on the molecular weight, scaling exponents (Fig. 4.9: ν) or the fractal dimension as the inverse of the scaling exponent is derived. The hydrodynamic radius, which is derived from the diffusion coefficient with knowledge of the viscosity of the solution using the Stokes–Einstein equation, has been chosen as a characteristic length. As example for AB_2 branched dendrimers, lysine dendrimers have been used [19]. For a single dendron, nearly the same fractal dimension of 1.7 has been observed as for a dendrimer with a bifunctional core. This fractal dimension is nearly that of a planar object. If the same dendrons are linked by a tetrafunctional core, a fractal dimension of 3.7 is observed as shown in Figure 4.9.

Furthermore, the concentration dependence of the apparent diffusion coefficient has been investigated. The determination of the hydrodynamic radius from the diffusion coefficient is valid only when pure self-diffusion is measured, that is, when the experiment is performed in the dilute concentration range. In the semidilute or concentrated regime, interactions between individual solute molecules have to be considered. Whether interactions

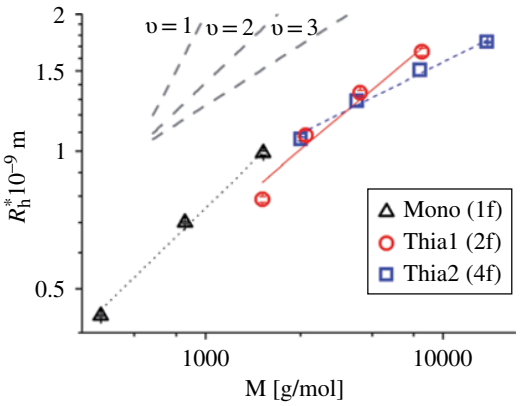

FIGURE 4.9 Dependence of the hydrodynamic size on the molecular weight for lysine dendrimers. Mono = first-, second-, and third-generation monodendron, Thia1 = thiacalixarene core decorated with two monodendrons, Thia2 = thiacalixarene core decorated four monodendrons. The dashed lines indicate the theoretical slopes for the scaling exponents 1, 2, and 3. Source: Fritzinger et al. [19]. Reproduced with permission of John Wiley and Sons.

between molecules have to be considered strongly depends on the internal mobility of the solute molecules. Flexible molecules like linear polymers in a good solvent probe a rather large volume. Inflexible molecules like globular protein tend to probe the hydrodynamic size plus displacements form diffusion only. Investigating the dependence of the concentration dependence of the apparent diffusion coefficient of PAMAM dendrimers, it has been found to be close to that of globular proteins. This means that the flexibility in dendrimers is rather of a short length scale [20]. If in a solution an electric field is applied, charged species will move along the electric field; this motion is called electrophoretic motion. This coherent motion can be investigated using PFG NMR as well, which is called electrophoresis NMR or electrophoretic NMR. To perform such experiments, dedicated equipment is required. It needs a probe head, in which a high voltage can *in situ* be applied to the sample solution. Several factors need to be taken into account: possible electrochemical reactions like electrolysis of the water and resulting gas formation, disturbances of the resolution of the NMR experiment, and the Joule heating of the sample, when currents as a result of the high voltage flow in the sample. These are discussed in detail in the dedicated NMR literature [21]. Applying data processing, a 2D electrophoresis NMR spectrum is obtained correlating chemical shift identifying the molecular species with the electrophoretic mobility as depicted in Figure 4.10.

If the electric field is applied in a solution, there is force acting on a charged object, which will accelerate the charged object. Hydrodynamic friction is counteracting the force of the electric field. The hydrodynamic friction is proportional to the velocity, and the friction coefficient according to Einstein's equation can be determined from the diffusion coefficient [23]. Eventually both forces will be balanced and the object/molecule will move with a constant velocity. This steady state is reached very quickly on the time scale of the PFG NMR experiment, which is on the order of tens of milliseconds. Therefore it is justified to assume this force balance for the entire experiment and to calculate from the force balance the effective number of charges per molecule or complex [22].

For macromolecules like proteins and polyelectrolytes, this effective charge usually is significantly lower than the nominal charge, because the high charge density on the macromolecule creates an electric field, which is so strong that the thermal energy of the counterions is insufficient to escape it. As a result, a fraction of the counterions condenses on the macromolecule shielding a fraction of the charge, so that the rest of the counterions experience an electric field sufficiently low, so that they can escape [24]. There is continuous exchange between condensed and free counterions, so that on the NMR time scale, only an average is observed.

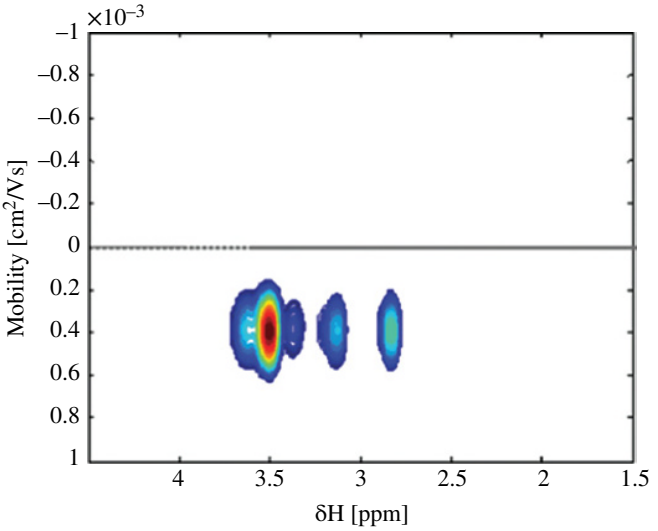

FIGURE 4.10 2D electrophoresis NMR spectrum of PAMAM G2 at pH 3.4. Protonated part structures of dendrimer show the same mobility in average and also confirming the monodisperse property of G2 dendrimer in electric field. Source: Böhme and Scheler [22]. Reproduced with permission of Elsevier.

Thus, in addition to the well-received applications of NMR for structure characterization, there are additional physicochemical aspects of complex macromolecular architectures, biohybrid structures, and aggregates and complexes, which can be investigated using NMR. In particular the measurement of displacements based on PFG NMR for either measuring diffusion or the electrophoretic mobility offers additional information on the size and charge of these various macromolecular architectures and compositions. The inherently available chemical shift information allows the identification of the moving species, which is important in multicomponent systems or when the formation of complexes is studied.

4.2.3 Field-Flow Fractionation

In the last years, the separation method of field-flow fractionation (FFF) comes more into the focus of size determination and separation of polymer mixtures consisting of different components, for example, aggregates, gels, or defined assemblies. Here, the separation takes place in a long and narrow channel, where a carrier liquid transports the molecules. Perpendicular to the main flow direction, a force field will be applied, which influences the sample molecules in order to separate them. Caused by the channel architecture, the

laminar flow generates a parabolic flow profile with fastest flows in the middle and lowest near the walls of the channel. The vertical force field transports the molecules near the accumulation wall, while the contrary diffusion force shifts the molecules into the faster regions of the flow profile. An exponential concentration profile is formed after equilibrium state of force field and diffusion (see Fig. 4.11a). Depending on their diffusion coefficient (D) and hydrodynamic diameter (d_h), based on the Stokes–Einstein equation, the molecules will be separated.

Smaller components move into the faster flows farther away from the accumulation wall and therefore elute before large molecules. This normal elution mode is reverse to that observed in SEC. The separation can be performed with different force fields. In thermal FFF, the separation is based on thermal diffusion between temperature difference of top and bottom wall. In case of electric FFF, the separation is driven by charge differences and electrophoretic mobility of the molecules applying an electrical field. Another way to separate components depending on their density properties is sedimentation FFF, where a circular channel rotates and generates a gravitational force field.

The group of flow FFF is the most improved separation technique within the FFF family. Particularly the asymmetrical flow field-flow fractionation (AF4) provides a broad range of application possibilities. In this case, the separation is caused by different diffusion coefficients (D) by inducing a flow field with a perpendicular liquid flow. A permeable wall (porous frit covered with an ultrafiltration membrane; see Fig. 4.10b) allows the cross flow to act as force field. The retention time (t_r) is given by the following equation:

$$t_r = \frac{w^2 \eta t_0 \pi \tilde{v}}{2V_0 kT} d_h$$

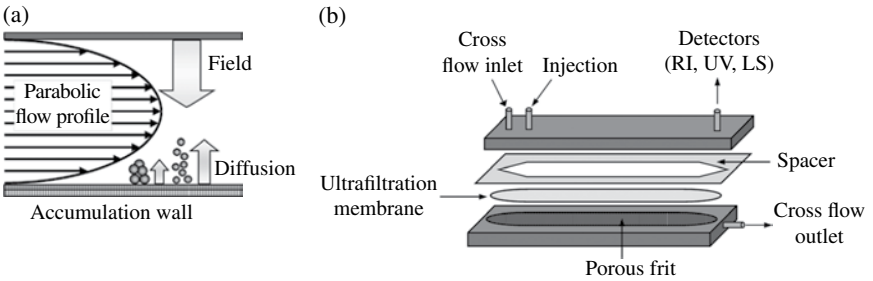

FIGURE 4.11 (a) Scheme of channel profile with perpendicular forces during the separation of a sample mixture and (b) AF4 separation channel setup with specific components.

where w is the channel height, η is the carrier fluid viscosity, t_0 is the void time, $\tilde{V}_c$ is the cross flow rate, V_0 is the void volume, k is Boltzmann's constant, and T is the temperature.

Compared to SEC, AF4 possesses numerous benefits. The most important fact is a very broad molar mass application range (10^3 up to 10^9 g/mol), where single molecules and aggregates or microgels can be separated simultaneously only limited by the molecular weight cutoff of the ultrafiltration membrane. But this ultrafiltration effect can be applied either for the purification of sample solution (no previous sample filtration is necessary) or otherwise for the quantification of small molecules, for example, free components in polymeric host-guest systems. Additionally to high separation force of AF4, this feature makes it very promising for the characterization of drug delivery systems. Due to the lack of column material, interactions are minimized and, for example, multifunctional polymers can be studied comprehensively. Furthermore reduced shear forces facilitate, for example, aggregation studies or the analysis of biohybrid structures, where it is important that weak bonds will not be destroyed. Furthermore due to the channel design, fast changes of eluents/buffers without preconditioning times as known from SEC columns are possible.

AF4 coupled with static and DLS detectors enables comprehensive information about structural and branching characteristics of biopolymers (e.g., starches), synthetic polymers, proteins, etc. [25, 26]. Especially in case of branched polymer structures like dendronized glycopolymers, the separation and characterization with AF4-LS lead to comprehensive information and understanding in molecular structures and aggregation behavior [27]. Furthermore, studies of uptake studies of dendritic glycopolymers and dye molecules were performed for the first time by AF4-LS (see Fig. 4.12). Here, a good correlation was obtained between the increase of molar mass and the quantified amount of dye molecules, which were encapsulated by the glycopolymers [28].

4.2.4 UV–Vis Spectroscopy and Fluorescence Spectroscopy

As aforementioned interaction, complexation or aggregation phenomenon but also the fabrication of supramolecular (biohybrid) structures can be proven by using UV–Vis and fluorescence spectroscopy where the corresponding prerequisites have to be considered. Most important prerequisites are solubility of starting components and final structures, concentration range, nonoverlapping absorption, or emission properties of molecular functions or conjugated substructures for the differentiation starting and aim structures.

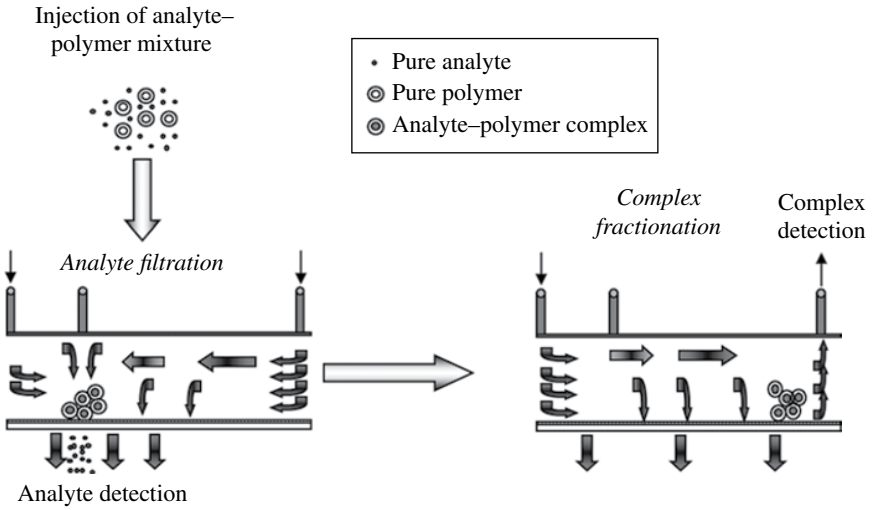

FIGURE 4.12 Principle of AF4 method for analyte filtration and analyte@polymer complex fractionation. Source: Boye et al. [28]. Reproduced with permission of Elsevier.

4.2.5 Electron Microscopy

Electron microscopy techniques are widely used for imaging objects smaller than the resolution of light microscope (200 nm). Thus the shape, size, size distribution, and assembling properties of nano-objects (various polymer architectures, for example, into micelles or polymersomes; proteins or polymer–protein conjugates) can be observed directly. Observations in electron microscope often complement findings of indirect methods (light scattering and X-ray crystallography). Modern transmission electron microscopes (TEM) can routinely achieve 0.1 nm resolution allowing for determining the conformation of large molecules [29] with a resolution of approximately 0.4 nm, where the resolution is hereby limited by the radiation damage of the specimen and not by the resolving power of the microscope.

There are many similarities but also crucial differences between light microscopy and electron microscopy. The basic setup of a TEM is the same as of a familiar light microscope. Illumination system consisting of a source, which emits the electrons (a sharp hot tungsten tip or LaB6 crystal), accelerator that accelerates the electrons to a desired energy, and few condenser lenses provide an illuminating beam of desired size and intensity. The beam is transmitted through the specimen mounted in a goniometer, which allows moving the specimen in three dimensions and tilting it around one or two axes. An image is formed by the objective lens and further magnified by a series of projector lenses onto a viewing screen or a digital camera.

The mechanism of image formation is different from the light microscopy. It is not absorption, reflection, or fluorescence but scattering of the electrons on the atoms forming the specimen. Elastic scattering on the atomic cores provides information about the specimen structure, morphology, and crystallinity. Inelastic scattering on the atomic shells provides information about its chemical composition and even oxidation state. A comprehensive theory and many examples and practical hints can be found in Refs. 30 and 31.

Albeit being a powerful tool, TEM has also limitations such as necessity of observing the specimen in vacuum and damage of the specimen by the electron beam. The specimens for TEM must be very thin (typically 10–500 nm depending on the specimen nature and goal of the investigation), which often poses a serious problem on how to prepare them. Bulk polymers are usually cut by a diamond knife into slices of dimensions roughly 0.1 mm × 0.1 mm × 100 nm and placed on fine-meshed metal grid. Solid particles dispersed in solvents are prepared by putting a drop of the dispersion on a thin (20 nm) supporting carbon film stretched over a fine-meshed metal grid and letting the solvent evaporate. The drop casting preparation often leads to serious artifacts (like agglomeration, shrinkage, loss of shape) in case of soft objects (like microgel particles, polymersomes). Despite the mentioned artifacts, TEM can be used for the successful visualization of, for example, the assembly of amphiphilic block copolymers into the larger nano-objects of polymersomes (Fig. 4.13) and other soft objects under suited conditions. The

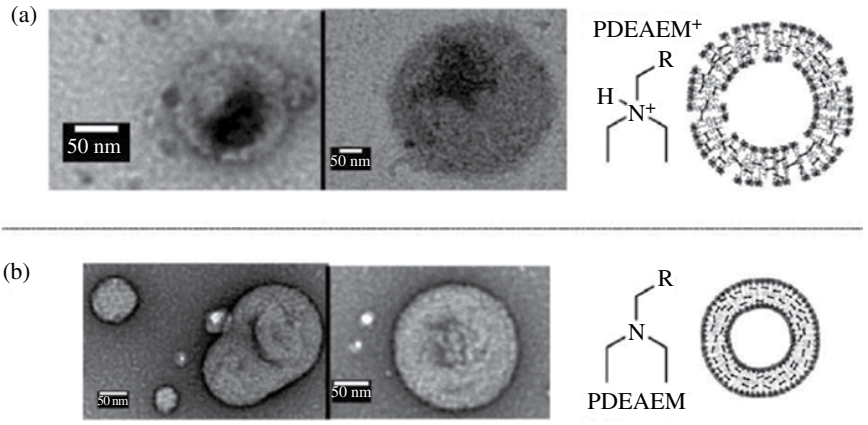

FIGURE 4.13 TEM of polymersomes at pH 3 (a) and 10 (b). Membrane consists of protonable poly(diethylaminoethyl methacrylate) (PDEAEM), which is responsible for the swelling/deswelling properties of polymersome. Source: Gaitzsch et al. [32]. Reproduced with permission of John Wiley & Sons.

way of preserving the original state of the objects in solution is the cryogenic TEM (cryo-TEM): vitrification, that is, rapid freezing, of a thin film of the solution and observing the frozen film inside the TEM. The freezing is so fast (thousands of Kelvins per second) that the morphology of thermoresponsive polymers is preserved during the freezing and original state below and above the transition temperature can be observed [33], when the solution is vitrified from the respective temperature. The effect of pH or the presence of salts on the polymer chain conformation can be observed as well.

The inherent shortcoming of the TEM is the fact that a 2D image of a 3D object is recorded. The true 3D shape of the object cannot be deduced from a single image. Tomographic techniques reconstruct the 3D shape from 2D projections of the object viewed in different directions. In case of a tilt series tomography, an object is selected, the specimen holder is tilted in small steps (1 or 2°) in as wide range of angles as possible (typically from −70 to +70°), while a 2D image of the object is recorded at each holder tilt. The resulting sequence of the 2D projections is aligned and numerically back-projected in a computer to create virtual 3D object [34]. Single particle analysis is applicable for 3D reconstruction of *identical* objects (such as proteins). Thousands to tens of thousands of images of these identical randomly oriented objects are properly oriented and aligned, sorted into classes representing projections in different viewing directions, and the 3D shape is reconstructed by fitting a suggested 3D model to the image classes.

4.3 CHARACTERIZATION OF HYDROGEL NETWORKS

Polymer networks (e.g., elastomers and gels) can be described on the microscopic scale by typical structural parameters like mesh size but also on the macroscopic scale by their bulk properties like swelling (uptake of liquids) or mechanical behavior. As the most important polymer networks used in bionanotechnology and biomedicine are hydrogel networks, we will focus on experimental methods and theories that are commonly used to analyze such hydrogel networks.

The network structure of a hydrogel plays a key role not only for swelling and mechanical properties but also for the diffusion of solutes through the hydrogel matrix. Diffusion characteristics are, for example, important for nutrient supply in cell-seeded hydrogel scaffolds or for the release of drugs from hydrogel matrices. Mechanical properties have been shown to be another crucial parameter in various hydrogel applications [35], for example, in designing cell-instructive tissue engineering scaffolds.

4.3.1 Network Structure of Hydrogels

The structure of hydrogel networks is usually characterized by the following microscopic parameters (Fig. 4.14):

- Cross-linking density (ν_c), that is, the amount (mol) of active polymer chain segments (bounded on both ends by cross-links) in a given volume of the polymer network
- Average molar mass of a polymer chain segment between two adjacent cross-links (M_c)
- The corresponding average mesh size (ξ), that is, the linear distance between two adjacent cross-links

These parameters are related to one another and can be determined theoretically or through the use of a variety of experimental techniques. Usually they are calculated from typical macroscopic network properties, like swelling degree Q or Young's modulus E (for tensile or compression strain) or shear modulus G (for shearing strain), which can be determined by physical methods as will be shown in Sections 4.3.2–4.3.4.

Simple models assume ideal networks. However, real polymer networks contain network defects, like free chain ends (dangling ends), rings, and entanglements (Fig. 4.14), which sensitively affect mechanical properties and also swelling behavior.

4.3.2 Swelling Degree

One of the most important properties of hydrogel networks is their swelling degree. Due to water absorption into the network, the macroscopic dimensions of the cross-linked bulk polymer increase until an equilibrium is reached at which the decrease in free energy due to mixing of the polymer chains with

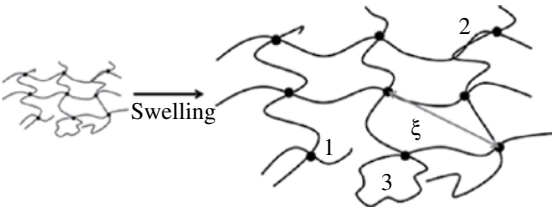

FIGURE 4.14 Swelling of a cross-linked bulk polymer and network structure of the swollen hydrogel characterized by the average mesh size ξ. Network defects: 1. dangling end, 2. entanglement, 3. ring.

the solvent is perfectly balanced by the increase in free energy accompanying the stretching of the chains (elasticity, Flory–Rehner theory). The equilibrium swelling degree for a given temperature is defined as the ratio of the swollen polymer volume to the volume of the dry polymer:

$$Q_v = \frac{V_{swollen}}{V_{nonswollen}} = \frac{1}{\text{volume fraction of polymer in the swollen sample}}$$

The volume degree of swelling Q_v of cross-linked polymers is simply the inverse of the polymer volume fraction. For a cylindrical sample, Q_v can be obtained from the diameter of the swollen $d_{swollen}$ and the dry cylinder d_{dry} as follows:

$$Q_v = \left(\frac{d_{swollen}}{d_{dry}} \right)^3$$

Alternatively, the equilibrium swelling degree can be defined as the ratio of the swollen polymer mass to the mass of the dry polymer:

$$Q_m = \frac{m_{swollen}}{m_{dry}}$$

Thus, swelling ratios can be measured using either a gravimetric or a volumetric method. The diameter and the mass of the dry sample are determined before it is immersed in the swelling medium at a given temperature. The swelling medium is exchanged several times until equilibrium is reached. The final diameter and weight of the swollen samples are measured immediately after removal of excess swelling medium from the surface.

The hydrophilic/hydrophobic balance of the polymer network and the degree of cross-linking are the important parameters, which control the equilibrium swelling (Fig. 4.15).

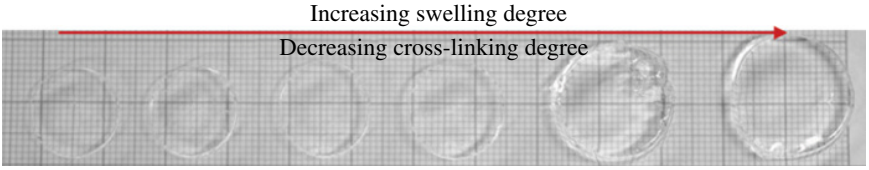

FIGURE 4.15 The degree of cross-linking is an important parameter that controls the equilibrium swelling: The image shows a series of biohybrid hydrogels synthesized by covalent cross-linking of four-arm poly(ethylene glycol) and heparin using carbodiimide chemistry. With decreasing molar ratio of poly(ethylene glycol) to heparin, the cross-linking degree decreases, which results in increased swelling of the networks.

In the case of ionic hydrogels, the equilibrium swelling of the polymeric matrix is more complicated as it heavily depends also on the ionization degree of the polymer chains and ionic strength of the external solution. Increasing number of ionic groups in polymer networks is known to increase their swelling capacities in aqueous solution. This is mainly due to the simultaneous increase of the number of counter ions inside the network, which produces an additional osmotic pressure that swells the polymeric matrix. The excess swelling over the swelling of the corresponding nonionic matrix can be suppressed with increasing salt concentration in the external solution, which decreases the concentration difference of the counterions between the inside and outside of the network.

Swelling of environmentally sensitive hydrogels can be additionally affected by specific stimuli, as already discussed in Section 3.8.

To analyze swelling of immobilized hydrogel surface layers, spectroscopic ellipsometry or QCM-D can be utilized, as described in Section 4.4.7.

4.3.3 Mechanical Properties

Usually the bulk mechanical behavior of a polymer network is characterized by its stress–strain properties describing the deformation and fracture of the network under stress.

4.3.3.1 Uniaxial Tensile and Compression Tests

Static mechanical testing involves applying a constant stress or strain to a gel sample in tension or compression.

For uniaxial tensile testing, dog bone-shaped samples are placed between two clamps and stretched at constant extension rates. Similarly, for unconfined compression tests, cylindrical specimens are compressed between two parallel plates. From these experiments, three important quantities can be determined (Fig. 4.16):

From the initial region of the stress–strain curve, Young's modulus E and the shear modulus G can be obtained. Both are a measure of the stiffness of a given material, which mirrors the resistance of an elastic body against deflection of an applied force. The point where the stress–strain curve abruptly falls down is known as the fracture point where the sample ruptures. Fracture stress and fracture strain are defined as the maximal stress and deformation (elongation or compression) that a sample can withstand. Material toughness can also be calculated from the area under the stress–strain curve up to ultimate fracture point. It is defined as amount of energy per unit volume required to cause a fracture in a material.

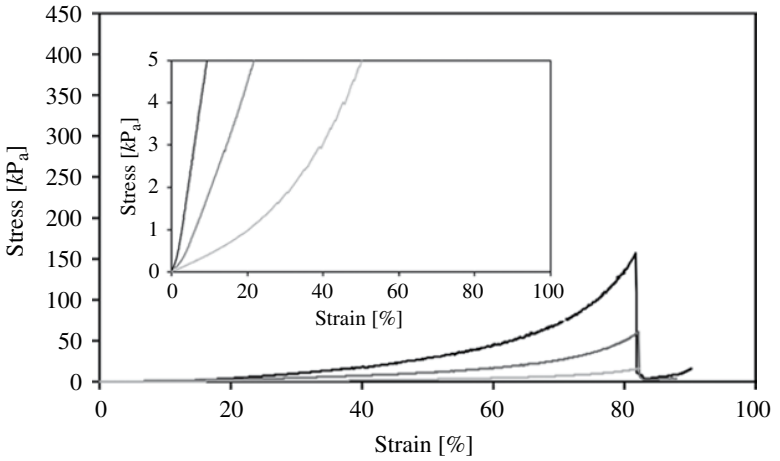

FIGURE 4.16 Uniaxial compression stress–strain curves obtained for star-(poly-ethylene glycol)-heparin hydrogels with three different cross-linking degrees. Black: high. Dark gray: medium. Light gray: low cross-linking degree. Source: Welzel et al. [36]. Reproduced with permission of American Chemical Society.

4.3.3.2 Dynamic Mechanical Analysis (DMA): Storage and Loss Modulus

Dynamic mechanical analysis (DMA) is typically performed to measure the viscoelastic behavior of polymer networks. A sinusoidal force (stress) is applied to a material and the resulting displacement (strain) is measured, allowing one to determine the complex modulus.

For example, oscillatory shear experiments can be performed on a rotational rheometer (Fig. 4.17), where the polymer network is placed between two parallel plates in order to obtain the complex shear modulus G:

$$G = G' + iG''$$

The storage modulus G' measures the stored energy, representing the elastic portion (solid-like behavior), and the loss modulus G'' measures the energy dissipated as heat, representing the viscous portion (liquid-like behavior) (Fig. 4.18).

The bulk measurements described so far do not allow for the detection of local differences in the mechanical material properties. However, several applications of hydrogel networks require characterization methods with high spatial resolution, for example, when hydrogels should be used for tissue engineering as cells respond to spatial variations in the substrate stiffness. Two methods, atomic force microscopy (AFM) and magnetic resonance elastography (MRE), will be highlighted in the next two paragraphs.

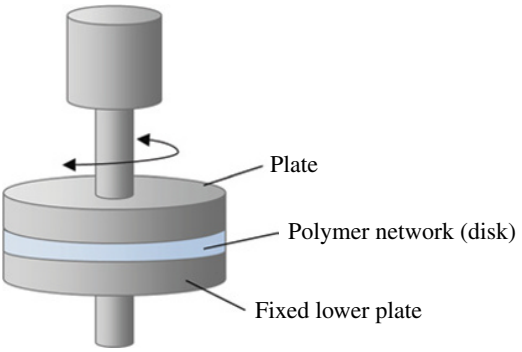

FIGURE 4.17 Oscillatory shear experiments can be performed on a rotational rheometer, where the polymer network is placed between two parallel plates.

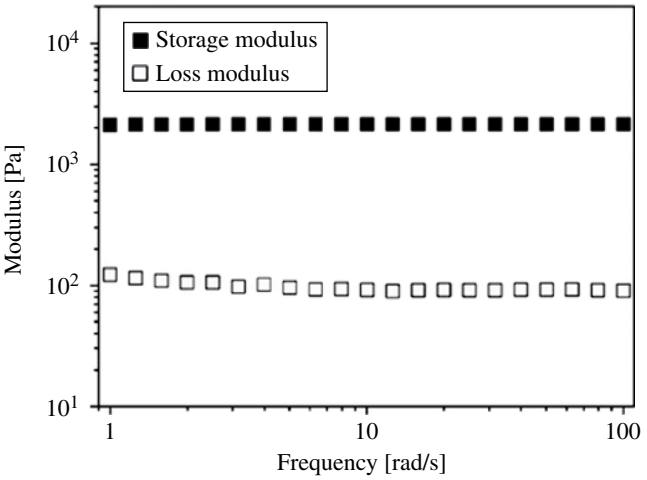

FIGURE 4.18 Frequency dependence of storage und loss modulus for star-(polyethylene glycol)-heparin hydrogel obtained by means of oscillatory rheometry. Reproduced with permission from Ref. 37.

4.3.3.3 Atomic Force Microscopy

AFM can be used not only for imaging the topography of surfaces but also for measuring local mechanical properties, as it will be described in Section 4.4.5.

4.3.3.4 Magnetic Resonance Elastography

MRE is a noninvasive and nondestructive technique that visualizes spatial changes in mechanical properties. It is used to characterize the elastic properties of tissue *in vitro* and *in vivo* but also of hydrogel samples.

Shear waves are generated in the sample under consideration, and their propagation within the sample is imaged using an MRI system. Processing the

resulting data allows to generate a quantitative map displaying the viscoelastic parameters at each location of the sample [35].

4.3.4 Deriving Microscopic Network Parameters from Macroscopic Hydrogel Properties

As already mentioned earlier, the structure of a polymer network can be elucidated from its macroscopic network properties, like swelling or mechanical characteristics. The most prominent methods used are the equilibrium swelling theory and the rubber elasticity theory (RET).

The structure of hydrogels that do not contain ionic moieties can be analyzed by the equilibrium swelling theory of Flory–Rehner: Based on the degree of swelling Q_v (or its reciprocal, i.e., the volume fraction of polymer in the swollen sample), the molar volume of the swelling medium (solvent) and the so-called Flory polymer–solvent interaction term, which expresses the quality of the solvent and is known for many polymer–solvent pairs, the cross-linking density ν_c can be calculated. The presence of ionic moieties in hydrogels makes the theoretical treatment of swelling much more complex. For more details, the reader is referred to the special literature, for example, [38, 39].

Alternatively, measurement of the mechanical properties of the polymer network, for example, the shear modulus G, provides a method for the determination of the cross-linking density ν_c through the use of the RET:

$$\nu_c = \frac{G}{RT}$$

where R is universal gas constant and T is the absolute temperature.

As network parameters are linked via (N_A: Avogadro's constant, ρ_B: density of the polymer network)

$$M_c = \frac{\rho_B}{\nu_c}$$

$$\xi = \left(N_A \nu_c\right)^{-1/3}$$

average molar mass of a polymer chain segment between two adjacent cross-links (M_c) and mesh size (ξ) consequently may be determined in the same way.

There are also some direct experimental techniques to study the molecular structure of hydrogel networks. For instance, the uptake of fluorescence-labeled tracer molecules (solutes) of different size into the networks can be investigated by confocal laser scanning microscopy (CLSM). Theoretically,

diffusion of molecules within the hydrogel matrix strictly requires mesh sizes larger than the hydrodynamic radii of these molecules. In this context, the mesh size of the network can be compared with the dimensions of tracer molecules. Furthermore, small-angle neutron scattering (SANS) has proven to be an effective method in providing structural information for a number of gel systems. The general approach for probing the mesoscale structure is to compare the excess scattering intensity from gels with respect to the corresponding semidilute solution [38].

4.4 SURFACE CHARACTERIZATION

A very important aspect when characterizing polymers especially for potential application in biomedicine or biotechnology is the surface characterization since the surface properties of the materials define largely any biological interactions. Again we will focus on some essential methods with special focus on their importance for polymer film in contact with the biosystems and hydrogels.

Information that can be gained by the various methods cover:

- Chemical information
- Film thickness, homogeneity, topology, and morphology
- Physical properties with regard to their interactions

Table 4.3 summarizes the methodologies, and in the following, some methods will be outlined in more detail.

4.4.1 X-Ray Photoelectron Spectroscopy

X-ray photoelectron spectroscopy (XPS) is an extremely surface-sensitive technique that allows one to quantify the atomic composition of a sample and to identify the binding states of the atoms. Monochromatic X-ray irradiation with a given photon energy is therefore used to release photoelectrons. The kinetic energy of the photoelectrons, as determined by the energy analyzer of the instrument, can be employed to calculate the binding energy. The electron count rate as a function of the binding energy is called the X-ray photoelectron spectrum. In a wide scan spectrum, distinct peaks can be assigned to the respective elements, for example, the signal of the carbon 1s electron. Quantitative elemental compositions are determined from the peak areas while considering the relative sensitivity factors and transmission function of

TABLE 4.3 Surface Characterization Methods and Information Gained

Chemical Information	
ATR-FT-IR (with and without imaging)	Information on structural units, verification of chemical structure, binding states, H bonding and other noncovalent interactions, lateral resolution micrometer range (see Section 4.1)
Raman spectroscopy and surface-enhanced Raman spectroscopy	Information on structural units, verification of chemical structure, binding states, H bonding and other noncovalent interactions, lateral resolution 100 nm range (see Section 4.1)
UV–Vis spectroscopy	Presence of chromophores (see Section 4.1)
Laser scanning fluorescence microscopy	Presence of fluorophores, lateral resolution in micrometer range
XPS	Elemental analysis of the surface (topmost layer as well as down to 10 nm)
Film Thickness, Homogeneity, Topology, and Morphology	
Surface force microscopy	Surface topology, homogeneity local differences in modulus of the film, nanostructure
Spectroscopic ellipsometry	Film thickness, homogeneity, refractive index
Scanning electron microscopy (SEM)	Morphology, homogeneity
Physical Properties with Regard to Their Interactions	
Contact angle measurements	Wetting behavior, surface hydrophilicity and hydrophobicity
Electrokinetic measurements	Electrokinetic effects, streaming potential and current, charge formation at interfaces; this provides also chemical information
Spectroscopic ellipsometry, flow cell	*In situ* adsorption measurements, swelling, and deswelling
ATR-FTIR, flow cell	*In situ* adsorption measurements
Quartz crystal microbalance, flow cell	*In situ* adsorption measurements
Surface plasmon resonance, flow cell	*In situ* adsorption measurements
Surface force microscopy	Topological and conformational information on adsorbed macromolecules and species
ESEM	Topological and conformational information on adsorbed macromolecules and species

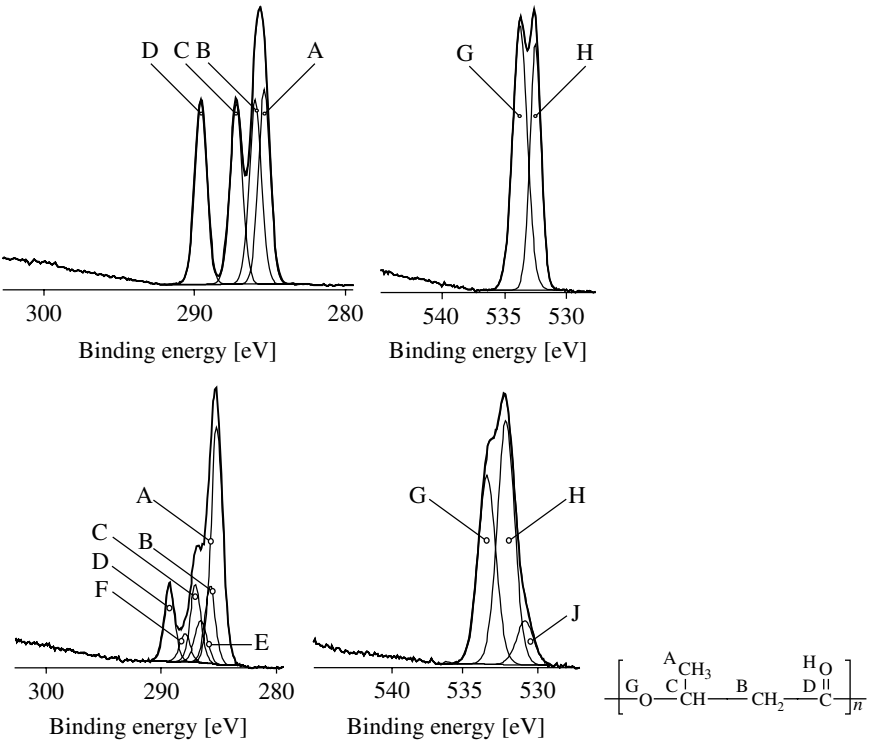

FIGURE 4.19 XPS $C1_s$ (left) and $O1_s$ spectra (right) of poly(3-hydroxybutyrate) before (top) and after NH_3 plasma treatment (bottom). Source: Nitschke et al. [40], figures 3 and 8. Reproduced with permission of John Wiley & Sons.

the spectrometer. High-resolution spectra, for example, of the C_{1s} signal can be deconvoluted into different energetic components (Fig. 4.19). These components correspond to nonequivalent atoms of the particular element in different chemical environments. The separation of the components on the binding energy scale is called the chemical shift. Since different chemical environments may have similar chemical shifts, the procedure allows one to extract some but not all information on the chemical structure of a polymer sample. In this situation, the significance of XPS analysis can be further improved by labeling techniques. A selective chemical reaction attaches a label molecule to a particular functional group and introduces a new element to the sample. This element appears with a new peak in the wide scan spectrum and can be taken as a measure for the abundance of the functional group.

The surface selectivity of XPS arises from the fact that only photoelectrons released very close to the surface can escape from a solid material without inelastic collisions and can subsequently contribute to the spectral information.

For an electron takeoff perpendicular to the sample surface, the mean free path of photoelectrons of about 10 nm directly corresponds to the information depth. Collecting only photoelectrons with grazing takeoff geometry allows one to further decrease the information depth. With this technique, which is called angle resolved XPS, a depth profile for the composition of the uppermost few nanometers of the sample material can thus be acquired.

4.4.2 Contact Angle Measurements by Axisymmetric Drop Shape Analysis

The sessile drop (or captive bubble) technique is the most common approach for characterizing the wetting behavior of a flat surface. The contact angle between a liquid drop or gas bubble and a solid surface is determined by using a tangent that has been aligned with the drop or bubble's profile at the contact point with the solid surface. Measurements can be dynamically performed by increasing and decreasing the droplet or bubble's volume to determine the advancing and receding contact angles, respectively. These values are usually different (contact angle hysteresis). Possible reasons for this effect are heterogeneous or rough surfaces. The accuracy of the earlier described method is about ±2°.

For even better results, drop profile analysis can be applied instead of measuring the contact angle directly (axisymmetric drop shape analysis, ASDA; Fig. 4.20). This technique extracts experimental drop profiles from video images while slowly increasing or decreasing the droplet volume [42, 43]. The best fit of experimental data with theoretical assumptions based on the Laplace equation of capillarity allows one to calculate the surface/interfacial tension and subsequently the contact angle. Also droplet radius, droplet volume, and the contact area are computed. ADSA can therefore reveal

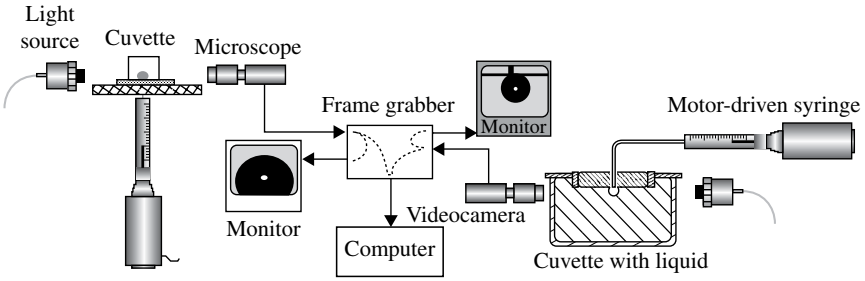

FIGURE 4.20 Scheme of the experimental setup for sessile drop experiments (left) and for captive air bubble measurements (right) using ADSA. Source: Uhlmann et al. [41]. Reproduced with permission of American Chemical Society.

phenomena like slip/stick behavior or time-dependent changes in the contact angle. Irregular or inconsistent values can be easily identified. An accuracy of ±0.2° is achieved.

4.4.3 Electrokinetic Measurements

To characterize charge formation processes at the interface between planar polymer surfaces and aqueous solutions, electrokinetic effects, namely, streaming potential and streaming current, are used. In the case of hard (impermeable) surfaces without any roughness and lateral inhomogeneity, the results can be converted into the electrokinetic or zeta potential by applying the Smoluchowski theory [44]. The zeta potential is defined as the electrical potential of an imaginary hydrodynamic shear plane that separates the inner region in the direct vicinity of the surface without any fluid motion from the outer region where fluid motion occurs. However, for soft (permeable) coatings, no sharp boundary exists. Liquids and ions can penetrate the coating and the charge distribution is strongly influenced by the distribution of ionizable groups along the polymer chains. Consequently, an appropriate treatment for streaming potential/current data obtained from soft (permeable) surfaces requires a more complex model that goes beyond the classical concept of zeta potential. Towards this goal, the theoretical formalism suggested by Duval et al. [45] covers diffuse, permeable, and charged hydrogel films that have been immobilized on charged rigid surfaces. With this theoretical approach, experimental streaming current data from immobilized poly(*N*-isopropylacrylamide)-co-*N*-(1-phenylethyl) acrylamide thin films above and below the transition temperature were successfully reproduced for the whole range of pH and ionic strength investigated. A similar approach that takes into account also surface conductivity was suggested by Zimmermann et al. [46]. It was applied to a negatively charged thermoresponsive coating of poly(*N*-isopropylacrylamide-co-carboxyacrylamide), and a clear evidence for a heterogeneous swelling below the transition temperature was found. The idea of a consistent derivation of electrohydrodynamic and structural properties of immobilized swollen coatings was further developed and applied to materials with high densities of dissociable groups like poly(acrylic acid) films [47] and polyelectrolyte multilayers [48]. Thus, electrokinetic measurements combined with an advanced theory for soft surfaces have proven to be an effective tool for the comprehensive characterization of soft hydrogel coatings. The physicochemical parameters accessible by this approach like the distribution of polymer segment density, the charge density, the hydrodynamic softness, and the interphasial diffuseness complement the results obtained by other techniques like ellipsometry or indentation experiments.

4.4.4 Spectroscopic Ellipsometry

Ellipsometry is an optical technique that detects the change of the polarization state when light is reflected from a surface. For rather simple systems like transparent films on reflecting substrates, film thickness and refractive index can be determined with high accuracy. More complicated samples (e.g., multilayer structures or layers with a graded index of refraction on a reflective carrier) can be characterized with a sufficient set of independent experimental data obtained for multiple angles of incidence and/or multiple wavelengths (spectroscopic ellipsometry). With a liquid cell, ellipsometry can be performed also in aqueous environments.

In the example illustrated in Figure 4.21, spectroscopic ellipsometry is employed to characterize the switching behavior of a thermoresponsive coating on a reflecting substrate in water. Based on proper model assumptions, physical values like the thickness and the optical properties of the swollen polymer film can be calculated. The plot of the film thickness versus temperature allows to determine the degree of swelling in the expanded and collapsed state, respectively. Also the phase transition temperature can be evaluated from the data set. After the first heating/cooling cycle, the switching behavior

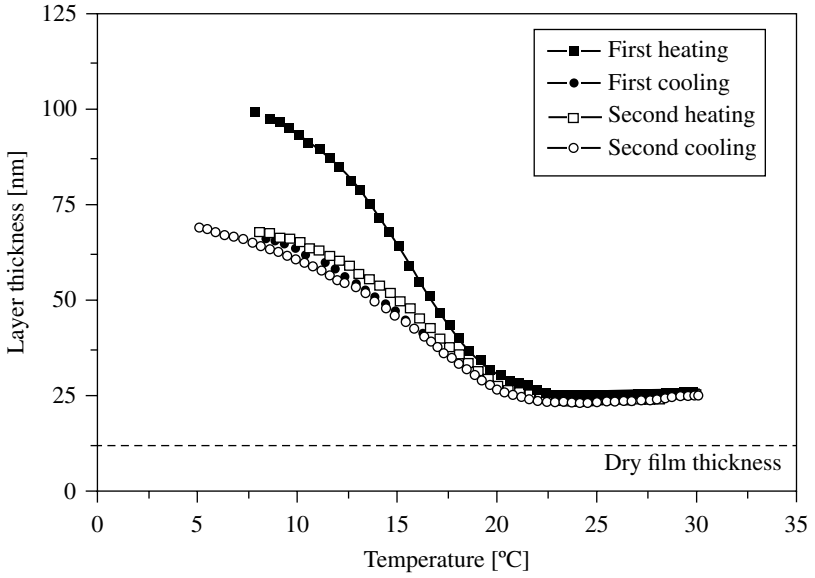

FIGURE 4.21 Poly(*N*-isopropylacrylamide-co-*N*-(1-phenylethyl) acrylamide) film thickness versus temperature during first and second heating/cooling cycles in distilled water (heating/cooling rate 1 K/min). Source: Cordeiro et al. [49]. Reproduced with permission of Royal Society of Chemistry.

of the system becomes fully reversible. The hysteresis between subsequent heating and cooling curves can be understood in terms of the kinetics of the interaction mechanism. Furthermore, it becomes obvious that the solvent is not fully expelled from the thermoresponsive layer above the transition temperature, that is, the system keeps a certain amount of water regardless of the actual temperature.

Beyond the working principle described so far, ellipsometry can also provide laterally resolved information. This is possible in a scanning process but also directly by imaging ellipsometry. The latter approach is illustrated, for example, by the work of Schmaljohann et al. [50] who exemplified the advantages of this technique for a micropatterned thermoresponsive coating.

4.4.5 Quartz Crystal Microbalance with Dissipation Monitoring

The working principle of a quartz crystal microbalance (QCM) is based on a quartz crystal that oscillates at its resonance frequency. The shift of the resonance frequency Δf that is caused by the deposition of a thin film on the quartz surface allows one to calculate the mass per unit area. In an extended concept, also the decay of the quartz oscillation when switching off the ac excitation is observed (QCM-D). This provides additional information on the viscoelastic properties of the coating. In particular, the change of dissipation ΔD introduced by the thin film can be calculated. The technique also works in liquid environments, which makes QCM-D a powerful tool to study phenomena like protein adsorption or denaturation on solid surfaces. In the case of surface immobilized thin hydrogel films in contact with an aqueous medium, QCM-D also senses the mass of water molecules that are bound to the hydrogel due to hydration. Together with the capability to monitor viscoelastic properties of the hydrated layer, QCM-D can comprehensively characterize the phase transition behavior of thermoresponsive polymer coatings.

This is shown in Figure 4.22. The QCM-D plot illustrates the typical behavior of Δf and ΔD of a thermoresponsive PNiPAAm-based coating upon temperature variation [51]. Increasing temperature leads to a gradual dehydration of the hydrogel and finally to a collapse of the film. Consequently, the observed frequency increases due to the expelled amount of water. On the other hand, the collapse of the hydrogel causes a change in the viscoelastic properties. The film becomes more dense and compact above the phase transition temperature, which results in less energy dissipation (ΔD) compared to the extended and flexible state below the phase transition temperature.

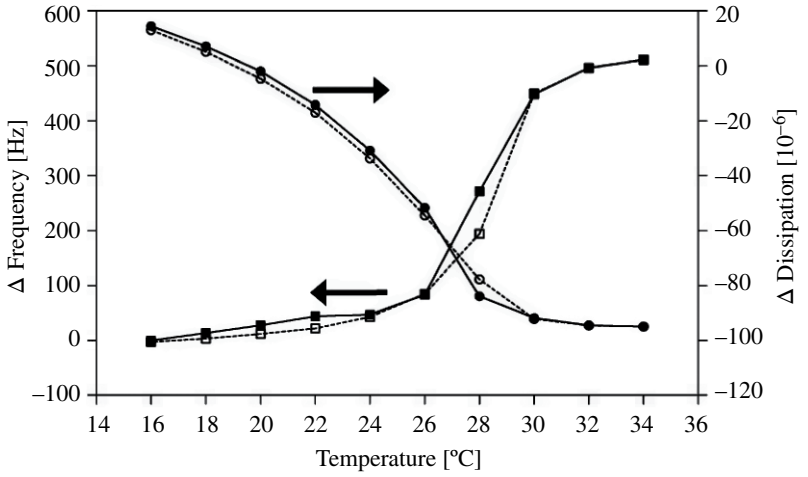

FIGURE 4.22 QCM-D data of a PNiPAAm-based copolymer film at temperatures around the phase transition. Solid lines correspond to data obtained ramping up temperature, while dashed lines correspond to ramping down temperature. Source: Alf et al. [51]. Reproduced with permission of John Wiley & Sons.

4.4.6 Surface Plasmon Resonance

The surface plasmon resonance (SPR) is the analytical technique widely applied in the field of characterizing adsorption to surfaces. The big advantage of this method is the high sensitivity in detecting substances adsorbed on a surface (1 pg/μm^2 of protein molecules) and the possibility of label-free measurements also in the *in situ* mode. The resulting graph is presented in the arbitrary units and called sensogram.

In general, the system comprises the light source, detector, optical system (mostly prism), and a sensor chip (mostly thin gold film) (Fig. 4.23). The sensor chip, depending on the method, can stay in direct contact with the prism surface (Kretschmann configuration) or close to the surface (Otto configuration).

On a metal surface, free electron constellations are present, so-called surface plasmons. In the distinct conditions, the light wave can interact with the surface plasmons and transfers them to the surface plasmon polaritions, which are surface electromagnetic waves propagating along the metal interface. The absorption of light photons results in the decrease of the intensity of the light wave, which reflects from the prism surface. To evoke the SPR phenomenon, the energy and the angle of incident light must match.

The SPR is operated under total internal reflection conditions. It means no light is transmitted through the reflecting surface and all light is reflected. To achieve total reflection condition, the RI of the crystal has to be significantly

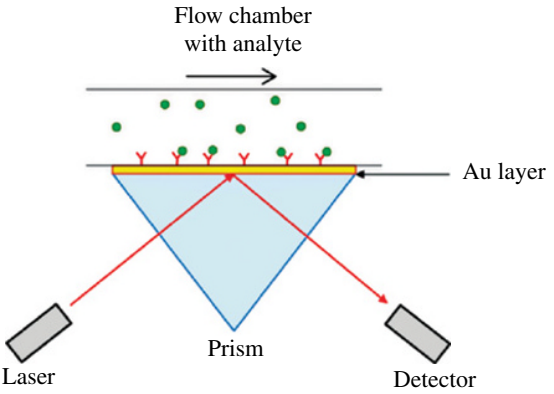

FIGURE 4.23 Setup and principle of surface plasmon resonance (Kretschmann configuration).

greater than that of the sample; otherwise the incident light will be also partly transmitted to the sample. Although the light reflects from the prism surface, the reflected photons create an electric field, a so-called evanescent wave, on the opposite side of the interface. This evanescent wave penetrates only a few microns (0.5–5 μm) beyond the crystal surface and into the sample. The evanescent wave can excite surface plasmons, inducing SPR. SPR triggers a dip in the light intensity and, hence, the angle where the maximum of the intensity loss is registered is the SPR angle. When the optical properties (the RI) in the close vicinity of the sample surface change, for example, by the adsorption of biomolecules or simple swelling in water, it influences the angle at which SPR is induced. Thus, the adsorption of molecules at the sample surface and, namely, the changes in the RI close to the surface induces a shift of the SPR angle and that is registered and presented as an outcome.

4.4.7 Scanning Force Techniques

Direct visualization of nano- and micrometer-sized objects is the most straightforward way for their analysis in surface and polymer science, biomaterial research, and biology. Rapid progress in engineering and microtechnology has led to numerous techniques that allow observation and mechanical manipulation of microscopic objects of various natures. AFM [52] is the most commonly used of these techniques. In AFM, a sample surface is mechanically scanned with a tiny probe—a sharpened stylus fixed at the end of a flexible cantilever. When the stylus interacts with the samples, the resulting force acts on the stylus and causes deflection of the cantilever. This deflection is detected via an optical lever system, that is, a laser beam reflected from the end of the

cantilever changes its position on a position-sensitive photodetector. The information from the photodetector can then be assembled into a topographical as well as phase image of the sample surface. AFM images can be taken from solid films, usually prepared on a smooth surface like silica wafer or mica via spin coating, as well as in liquids. Depending on the setup of the instrument, measuring conditions, and the quality of the tip, up to atomic resolution is possible (scanning tunneling microscopy under ultrahigh vacuum). Polymer films are usually assessed with a lateral accuracy down to a few nanometers under ambient conditions. In topology mode information on film homogeneity and surface roughness is given, whereas phase images that are providing information on the local module of the surface allow also conclusions on variations in chemistry, for example, in a nanophase-separated block copolymer film (see, e.g., examples in Section 5.1).

AFM provides a number of unique features in experiments on biotic and abiotic specimens. Firstly, visualizing the surface topography of the sample does not require additional staining or labeling that could potentially harm or alter the sample. Secondly, measurements can be carried out in various conditions either in vacuum, in air, or in water solutions, and environmental factors such as temperature, pH, and electrolyte concentration can be adjusted within a wide range. Mimicking biological conditions ensures that fragile samples retain intact in AFM experiments, which provides reliable data on structure, stability, and function. Remarkably, AFM is characterized under these conditions by an exceptionally high signal-to-noise ratio.

AFM is frequently applied for the characterization of polymeric biomaterials. Recently, it was used to characterize the formation, structure, and function of nanopatterned collagen matrices [53]. These nanoscopic matrices are composed of highly ordered fibrils assembled from collagen type I molecules (Fig. 4.24a). High-resolution AFM topographs of the matrices allowed a correlation between the ultrastructure of the self-assembled collagen fibrils and collagen fibrils assembled *in vivo*. AFM was furthermore applied to study the interaction of cells with the nanopatterned matrices (Fig. 4.24b) [54], which revealed that the structural and mechanical anisotropy of the matrices enabled the cells to bundle collagen fibrils into large fibers. This bundling favored the development of a unidirectional traction along the fibers and led to cell polarization.

A scanning force instrument also allows for the acquisition of force–distance curves to characterize the local mechanical properties of the sample. Well-defined indentation experiments on soft surfaces like swollen hydrogels in aqueous media are possible with the colloidal probe technique. Raw data are assessed, for example, according to the Hertz model, with the assumption

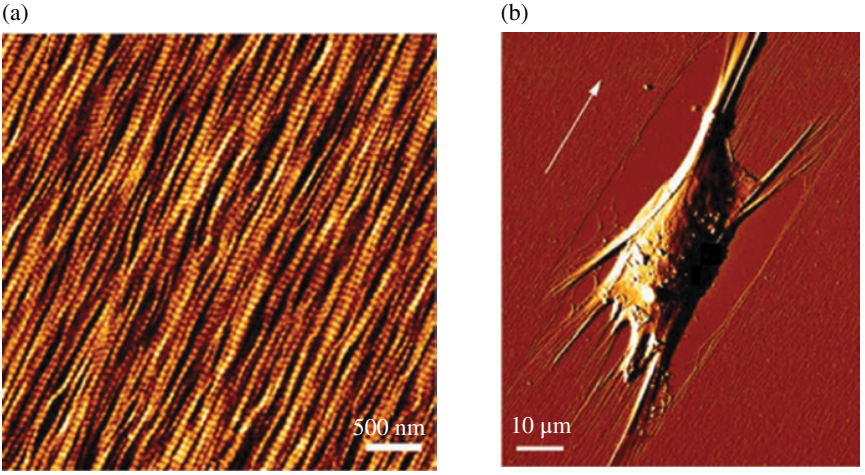

FIGURE 4.24 (a) High-resolution AFM topograph of a nanopatterned matrix composed of aligned collagen type I fibrils. (b) Cells seeded onto the collagen matrices strongly polarize along the direction of the fibrils (white arrow) and deform matrix perpendicular to the fibril direction. Collagen fibrils are bundled at the front and back of the cell without rupturing. Source: Friedrichs et al. [54]. Reproduced with permission of Elsevier.

that an infinitely hard sphere is indenting a flat surface. When the material under investigation is a soft hydrogel layer, the indentation should be small compared to the total film thickness. A hard surface (e.g., mica) is used as a reference to account for the properties of the experimental setup. This approach has been illustrated by the work of Matzelle et al. [55]. For thermoresponsive PNiPAAm coatings immersed in water above and below the phase transition temperature, force–distance curves were obtained (Fig. 4.25). In this experiment, a variation of Young's modulus of more than two orders of magnitude between the swollen and the collapsed state was found.

4.4.8 Environmental Scanning Electron Microscopy

Scanning electron microscopy (SEM) requires high vacuum conditions. To image wet or biological samples, these materials are subject to complex preparation procedures, which usually introduce additional artifacts. This limits the applicability of conventional SEM in this field and leads to the concept of environmental scanning electron microscopy (ESEM) [56]. The technique's most remarkable feature is that it allows the acquisition of scanning electron micrographs under gaseous atmospheres with pressure magnitudes higher than in SEM instruments. Depending on the experimental purpose, the atmosphere can consist of various gases. However, water vapor is the most

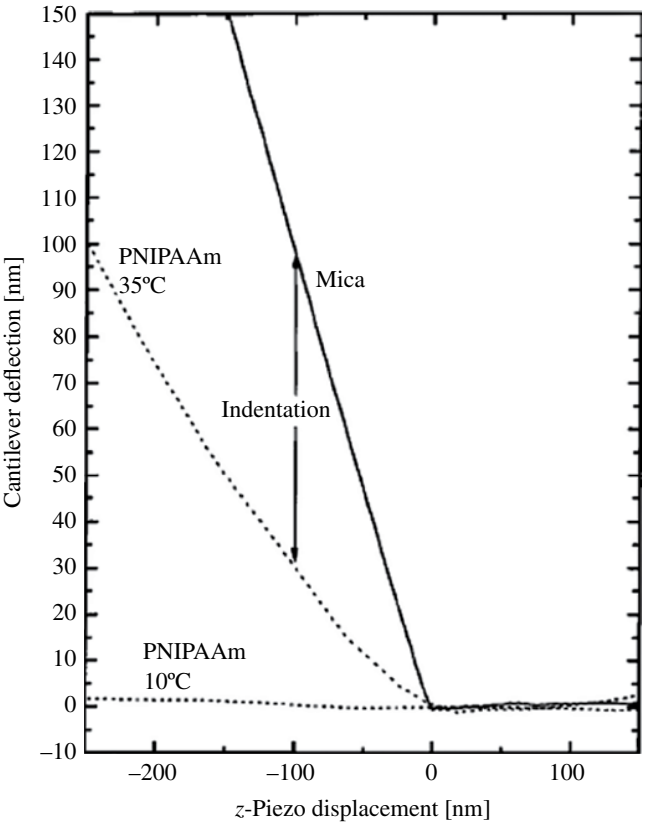

FIGURE 4.25 Force versus displacement curves on PNiPAAm gel in pure water at 10 and 35°C and on mica in pure water at room temperature. The same *z*-piezo displacement results in a smaller cantilever deflection on the soft gel surface in comparison with the hard mica sample because of elastic indentation. Source: Matzelle et al. [55]. Reproduced with permission of American Chemical Society.

common working gas used in ESEM. In this case, the appropriate pressure and temperature conditions allow one to maintain samples in a wet state from minutes to hours.

Due to small effective cross-sections between water molecules and high energetic electrons, the primary electron beam (5–30 keV) penetrates the atmosphere almost without scattering. In contrast, low energetic secondary electrons released from the sample surface (<50 eV) strongly interact with the water molecules and produce additional secondary electrons. The atmosphere works as a cascade amplifier and the signal is amplified before the electrons reach the detector. Furthermore, the ionized gas neutralizes surface charges of insulating samples. As a result, there is no need to provide a conductive surface as in conventional SEM.

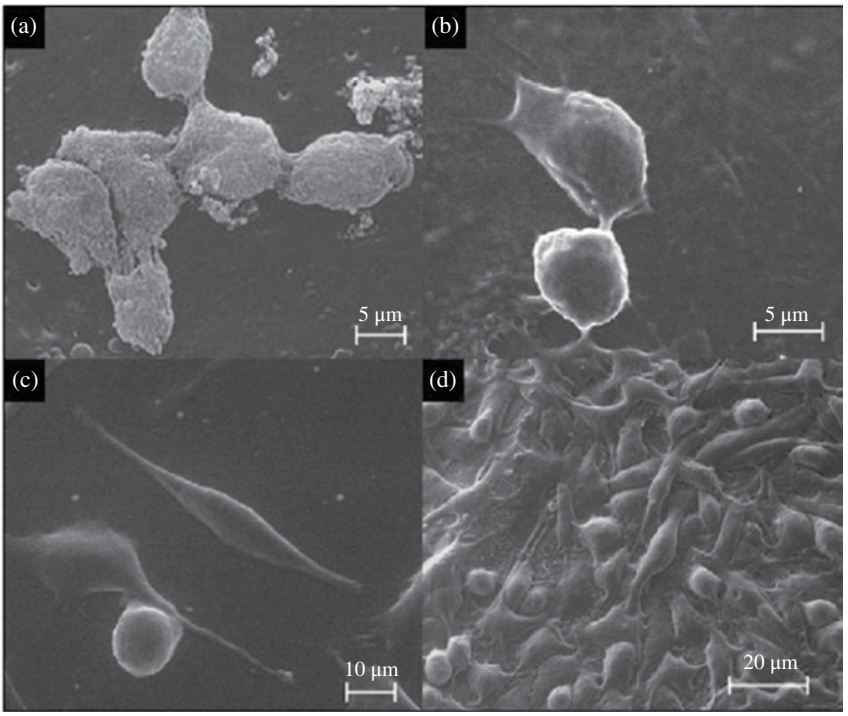

FIGURE 4.26 SEM/ESEM images of mouse fibroblast cell morphology. (a) SEM images of 3T3 mouse fibroblasts (20 kV). (b–d) ESEM images of 3T3 mouse fibroblasts adhesion and proliferation on biomaterials (4.60 Torr, 5°C, 7 kV). Source: Muscariello et al. [57]. Reproduced with permission of John Wiley & Sons.

The potential of ESEM—to study the interaction between cells and material surfaces under hydrated conditions after minimal sample preparation procedures—is illustrated in Figure 4.26. This predestines the ESEM technique for biomaterial and tissue engineering research. However, optimal working conditions for imaging wet samples are far from standardized and have to be determined empirically. Furthermore, a range of technical limitations have to be considered in the data analyses [57].

4.5 BIOPHYSICAL CHARACTERIZATION AND BIOCOMPATIBILITY

Artificial materials designed for applications in biotechnologies and in medicine interact with the biological environment at their surface, making accurate biophysical characterization of the surface crucially important for understanding

subsequent biological effects. Physical and chemical properties of the material surface, protein adsorption, and cellular and tissue response are all considered to be interrelated and ultimately determine the biocompatibility of materials.

In the following, we will focus on biophysical characterization of material surfaces, especially on quantifying their interaction with proteins and cells, and on biological evaluation of biomaterials and medical devices by *in vitro* tests as a first step towards ensuring their biocompatibility.

4.5.1 Biophysical Characterization

Biophysics in general studies life at every level, from atoms and molecules to cells, organisms, and environments. It aims to find out how biological systems work by looking for pattern in life and analyzing them with mathematics and physics.

This chapter concentrates on biophysical characterization of material surfaces in biological environments and just highlights some examples. Especially, the quantification of protein adsorption and/or cell adhesion is important in order to evaluate the potential of a biomaterial for a given application.

4.5.1.1 Adsorbed Proteins

It is well described that materials in contact with biofluids are immediately coated with proteins. Protein adsorption is influenced by the underlying substrate surface properties including surface chemistry, charge, and free energy. After cell adhesion on top of this primary protein layer, the formation of secondary protein layers can take place due to nonspecific adsorption of cell-secreted proteins (Fig. 4.27).

A large spectrum of methods is utilized to characterize adsorbed proteins (Table 4.4), regarding the adsorption dynamics, the adsorbed amount and the composition of the protein layer, the lateral (or 3D) distribution, orientation

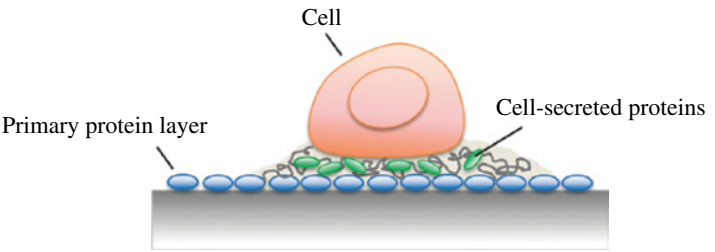

FIGURE 4.27 Cell adhesion on a primary protein layer and the formation of secondary protein layers by cell-secreted proteins.

TABLE 4.4 Characterization of Adsorbed Proteins

Information on Proteins at Biomaterials (Readout)	Method
Adsorbed amount	• Fluorescence spectroscopy and microscopy (including immunofluorescence, total internal reflection fluorescence) • Detection of radiolabeled proteins • Immunosorbent assays (e.g., enzyme-linked immunosorbent assay(ELISA)) • Acid hydrolysis and subsequent amino acid quantification by high-performance liquid chromatography (HPLC) • Attenuated total reflection Fourier transform infrared spectroscopy (ATR-FTIR) • X-ray photoelectron spectroscopy • Surface plasmon resonance • Quartz crystal microbalance • Waveguide interferometry • (Spectroscopic) ellipsometry
Identification/layer composition	• Fluorescence spectroscopy and microscopy (including immunofluorescence, total internal reflection fluorescence) • Detection of radiolabeled proteins • Mass spectrometry (electrospray ionization, matrix-assisted laser desorption, ionization) • Gel electrophoresis (2D polyacrylamide gel electrophoresis) • Acid hydrolysis and subsequent amino acid quantification by high-performance liquid chromatography (HPLC) • X-ray photoelectron spectroscopy • Surface plasmon resonance
Lateral and spatial distribution of proteins in adsorbed layer, morphology/topography of protein layer	• Fluorescence spectroscopy and microscopy (including immunofluorescence, total internal reflection fluorescence) • Environmental scanning electron microscopy • Atomic force microscopy
Orientation	• Fluorescence spectroscopy and microscopy (including immunofluorescence, total internal reflection fluorescence)

TABLE 4.4 (continued)

Information on Proteins at Biomaterials (Readout)	Method
Adsorption dynamics	• Fluorescence spectroscopy and microscopy (including immunofluorescence, total internal reflection fluorescence) • Attenuated total reflection Fourier transform infrared spectroscopy (ATR-FTIR) • Quartz crystal microbalance • (Spectroscopic) ellipsometry • Reflectometric interference spectroscopy
Layer thickness (structure)	• (Spectroscopic) ellipsometry • X-ray/neutron reflectivity • Reflectometric interference spectroscopy
Conformation/adsorption-induced conformational changes: • Secondary structure (on planar surfaces) • Secondary structure (on dispersed solids) • Thermal stability (on dispersed solids) • Activity	• Quartz crystal microbalance • Attenuated total reflection Fourier transform infrared spectroscopy (ATR-FTIR) • Circular dichroism • High sensitivity differential scanning calorimetry (micro-DSC) • Fluorescence microscopy (immunofluorescence)
Surface charge/charge density of proteins: • On flat surfaces • On dispersed solids	Electrokinetic measurements Potentiometric titration
Interfacial free energy and heterogeneity of protein layers	• Wetting measurements
Adsorption and displacement enthalpy (proteins on dispersed solids)	• Isothermal titration calorimetry (ITC)
Separation/characterization of net charge (dissolved proteins; depletion method)	• Capillary electrophoresis (CE)
Separation/mass characterization (dissolved proteins; depletion method)	• Ultracentrifugation

and clustering, adsorption-induced conformational changes, functional alterations, and availability. They include physicochemical methods (e.g., layer thickness measurement), biochemical methods (e.g., antibody binding), and application-oriented testing (e.g., cell or bacteria adhesion).

Besides direct surface analysis methods, indirect solution depletion methods can be applied to study protein adsorption. Solution depletion methods use solids of known large surface area (usually dispersed solids) that are placed into a solution of known protein concentration. After incubation, the concentration of the protein in the supernatant is measured. From the depletion, the adsorbed protein amount can be calculated.

Several methods listed in Table 4.4 are also used for characterizing material surfaces in general and have thus been described in Section 4.3.3.4. In this context, also the potential of AFM and ESEM for investigating the interaction of proteins and/or cells with material surfaces was already reported.

Here, only a selected method and its application for biophysical characterization of material surfaces will be briefly highlighted in more detail. Electrokinetic measurements for the characterization of charge formation processes at solid/liquid interfaces can be combined with different optical methods in order to get deeper insights in protein adsorption processes. For instance, adsorption of the plasma protein fibrinogen (FGN) at poly(octadecene-*alt*-maleic acid) thin films at different protein solution concentrations was studied by the combination of streaming current measurements and reflectometric interference spectroscopy (Fig. 4.28) [58]. Both the streaming current versus pressure gradient and the optical layer thickness immediately responded to the variation of the protein solution concentration. While the optical layer thickness d correlates with the adsorbed amount of FGN, the streaming current versus pressure gradient dI_s/dp reflects the variation of the interfacial charge during the adsorption process. The introduced methodology was found suitable to follow electrosurface characteristic of proteins *in situ* and to investigate the relevance of surface charge for the adsorption and orientation of proteins at interfaces.

4.5.1.2 Adherent Cells

Cell adhesion to artificial surfaces plays a key role in a wide variety of demanding products and technologies such as medical implants or bioreactor systems. Adhesion of eukaryotic and bacterial cells to a biomaterial surface can be a major factor mediating its biocompatibility. For a proper integration of an implant into tissue, cell adhesion may be desired, whereas bacterial cell adhesion to medical devices must be prevented in order to minimize the risk of infections and toxicity.

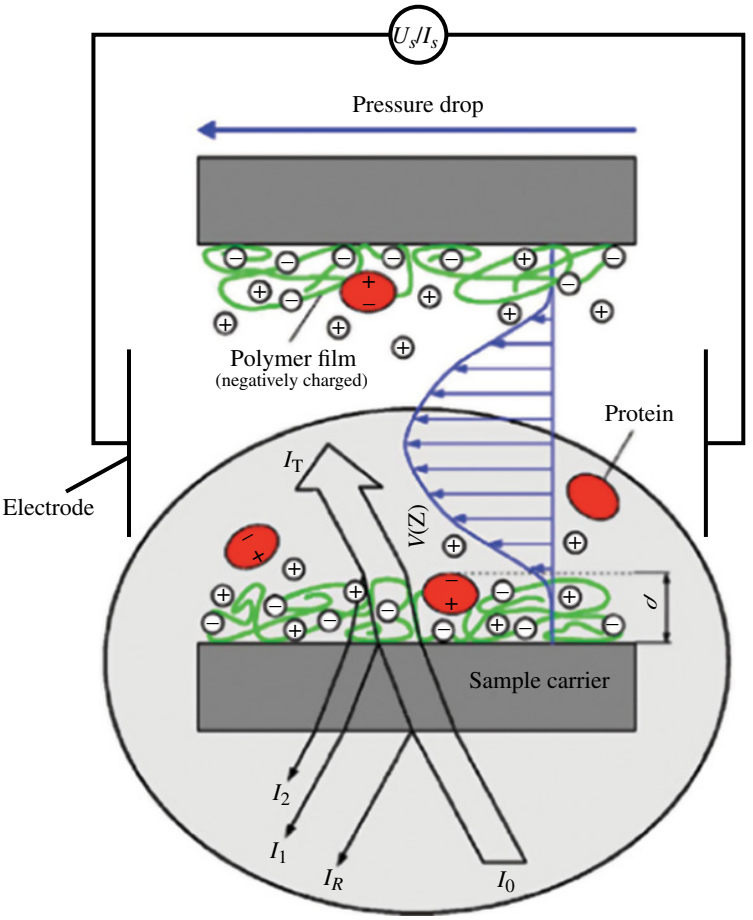

FIGURE 4.28 Principle of streaming potential/current measurements combined with reflectometric interference spectroscopy. The charge of the polymer film is determined by streaming potential and streaming current measurements via nonpolarizable electrodes positioned at the inlet and outlet of the channel. Structural variations of the polymer layer and adsorption or desorption processes are followed simultaneously through the evaluation of the interference pattern resulting from the interference of the partial beams I_1 and I_2. The relative dimensions in the scheme are not in scale. Source: Zimmermann et al. [58]. Reproduced with permission of AIP Publishing LLC.

Different assays have been developed to qualitatively and quantitatively study cell adhesion. Usually, these assays probe the ability of cells to remain attached to an adhesive substrate when *exposed to a certain detachment force*. They can be classified into single-cell assays and bulk assays that analyze the average behavior of large cellular populations (an overview is given in Ref. 59).

The most common bulk adhesion assay, the plate-and-wash assay, relies on seeding cells onto surfaces of interest, washing off "nonadherent" cells with physiological buffers, and counting the remaining cells (e.g., by using colorimetric assays like the MTT assay (cf. Section 4.5.1.1) or flow cytometry after trypsinizing the cells from the surface). Plate-and-wash assays have enabled the identification of key adhesion components and generated valuable insights into mechanisms regulating adhesion. However, these assays provide no information on adhesion strength and report only the initial rate of attachment of cells to the material surface.

Several semiquantitative adhesion assays, including flow chamber assays, spinning-disc assays, and centrifugation assays, apply controlled shear stress to adherent cells.

To quantitatively determine the interaction forces of cells with given surfaces, sensitive single-cell force spectroscopy (SCFS) assays are used [59]. SCFS assays allow adhesive interaction forces and binding kinetics to be measured in physiologically relevant conditions from the cellular level down to the contribution of single molecules. Among all of these assays, including micropipette-based manipulation assays and optical tweezers, AFM-based SCFS is currently the most versatile method to study adhesive interactions of cells with other cells, proteins, and surfaces. This is because AFM-based SCFS offers a large range of detectable forces, from 10 pN to ≈ 100 nN, and offers precise spatial (≈1 nm to ≈100 μm) and temporal (≈0.1 s to >10 min) control over the adhesion experiment and the experimental parameters. Figure 4.29 illustrates the principles of AFM-based SCFS [59, 60].

In the standard setup, a single cell is captured by gently pressing an AFM cantilever functionalized with an adhesive protein onto it. This converts the living cell into a probe, which is brought into contact with functionalized surfaces or other cells at a set force and for a specific adhesion time (Fig. 4.29a). Subsequently, the cantilever is withdrawn at a constant speed, detaching the cell from its binding place. During this separation process, the cantilever deflection, which is proportional to the vertical force between the cell and the substrate, is recorded in an *F–D* curve (Fig. 4.29b). This curve provides the signature of the cell adhesion.

Alternatively to force-based approaches, cell adhesion can be quantified by *measuring the intersurface distance* between the cell and a planar transparent substrate (Fig. 4.30). Reflection interference contrast microscopy (RICM) is ideally suited for studying cell adhesion characteristics and dynamics in aqueous environment, as it allows for nanometer precise determination of intersurface distances with milliseconds' time resolution [62]. It has the added

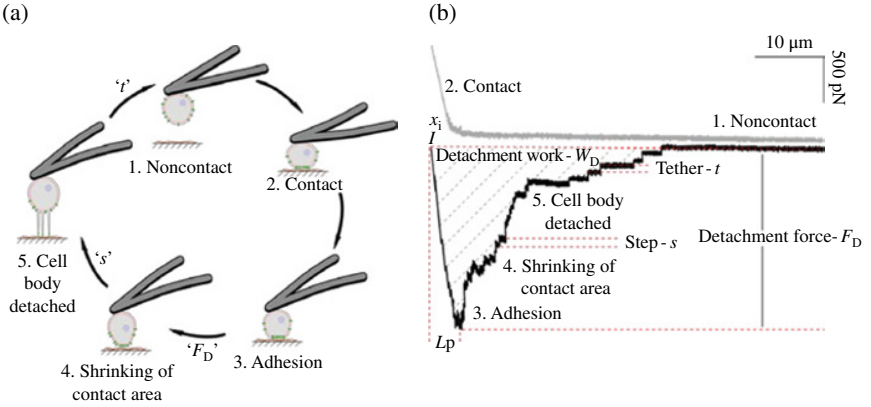

FIGURE 4.29 Schematic illustration of an SCFS experiment and of the adhesion events detected. (a) A single cell is attached to an AFM cantilever (1) and approached to a substrate (1 and 2). Once in contact, cell adhesion molecules diffuse into the contact zone (2). The adhesive strength between cell and substrate increases. After a predefined contact time, the cell is retracted and the cantilever bends because of the adhesive strength between the cell and the substrate (3). Once the restoring force of the cantilever exceeds the strength of the interactions between cell and substrate, the cell starts to detach (3 and 4). The force detected at this point corresponds to the maximum detachment force (F_D). During further retraction of the cantilever, the contact area between the cell and the substrate shrinks (4) and the cell sequentially detaches from the substrate (5) until the cell and the substrate are completely separated (1). (b) Force–distance (*F–D*) curve showing steps (1–5) corresponding to those outlined in A. During approach (gray line) and retraction (black line), the force exerted on the cantilever, which is proportional to cantilever deflection, is recorded in an *F–D* curve. The retraction *F–D* curve is characterized by the maximum detachment force (F_D). This force is generally followed by steplike events that correspond to the unbinding single cell adhesion molecules from the substrate (*s* and *t* events). Source: Lyubchenko et al. [60]. Reproduced with permission of Elsevier.

advantage of directly visualizing cell adhesion areas without influencing the cell culture by additional fluorescent staining methods. Implementation of RICM on a standard inverted microscope is possible with relative ease and very little investment. Combination with other microscopic techniques or micromanipulations is possible.

An incident beam is partially reflected at the substrate surface and partially transmitted through the buffer solution to be reflected by the cell membrane (Fig. 4.30). A constructive or destructive interference pattern formed by the superposition of the object beam (cell membrane) and the reference beam (substrate surface) is observed through the objective as

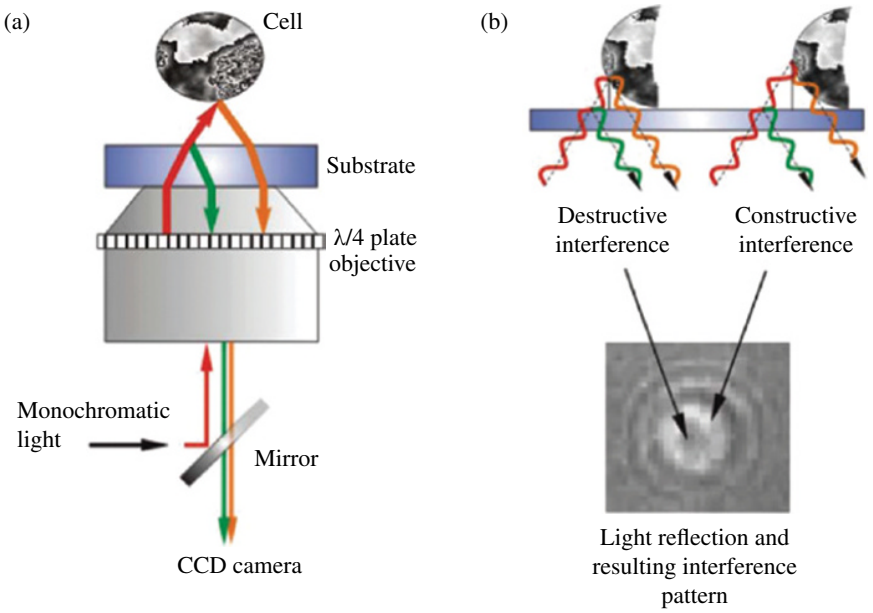

FIGURE 4.30 Optical principle of reflection interference contrast microscopy (RICM). The optical path (a) and the formation of constructive and destructive interference with the resulting reference pattern (b) are depicted on Ref. 61.

circular interference fringes, which depend on the vertical distance between the cell and the surface.

The following example illustrates the power of RICM to reveal effective matrix coatings, which can provide anchorage of hematopoietic progenitor cells (HPC) to artificially designed microenvironments [63]. Therefore, the adhesion characteristics of HPCs to a set of ECM biopolymer coatings covalently attached to thin films of maleic anhydride copolymers were investigated using RICM. 10 s after taking the RICM image, the differential interference contrast (DIC) image was taken with the same microscope at the same position. Figure 4.31 shows separately RICM images as well as overlaid with DIC images in order to visualize the adhesion areas as well as the overall cell circumference. If the adhesion area detected by RICM was central below the cell shape in DIC image, the cell was assumed to be adherent (Fig. 4.31a) or vice versa (Fig. 4.31b). Intense cell–matrix interactions were found on surfaces coated with fibronectin (Fig. 4.31a), heparin, and heparan sulfate and on collagen I-based cofibrils. Insignificant adhesion was found for tropocollagen I (Fig. 4.31b) and hyaluronic acid. In addition, RICM was used in this study to analyze adhesion areas and fractions of adherent cells.

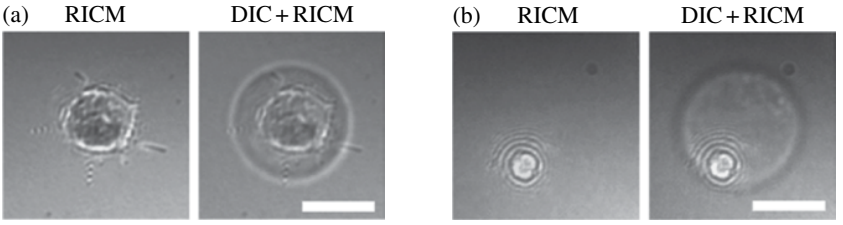

FIGURE 4.31 Adhesion characteristic of HPC after 24 h of cultivation on matrix coatings is shown by RICM images and an overlay of RICM and DIC images taken at the same objective position. RICM images show adhesion areas; DIC images visualize the cell above. Surfaces: (a) fibronectin, (b) tropocollagen I. Scale bar, 5 μm. Source: Adapted from Franke et al. [63], figure 3. Reproduced with permission of Elsevier.

4.5.2 Biocompatibility

Biocompatibility as defined in Section 2.5 is a main prerequisite for the proper and safe use of medical devices consisting of a single material or material composition. In Section 4.5.1, it was demonstrated that the biophysical characterization of material surfaces only draws attention to some aspects of their response to biological systems. In order to assess biocompatibility for a device or a material, it is necessary to do a battery of tests depending on its intended use, with body contact ranging from transient skin contact to contact with blood to permanent implantation. Biocompatibility is usually examined with three types of biological tests: *in vitro* tests, animal experiments (*in vivo* tests), and clinical tests.

Currently, the key basis of the biological evaluation of medical devices is a set of standards developed by the International Organization for Standardization (ISO), known as ISO Standard 10993. These tests do not prove the biocompatibility of a material, which can be described only if the precise context of material usage is known. However, this standard serves as a structured framework (Table 4.5), which allows for planning an effective biological evaluation of a material for potential biological risks arising from its use as a medical device. Thus, ISO 10993 constitutes an important step towards clinical trials that will finally determine the biocompatibility of the material in a given application.

In Germany ISO 10993 was published as norm DIN EN ISO 10993.

In the following, we will focus on *in vitro* tests for cell compatibility and blood compatibility. In this context, we will also discuss ISO 10993-5 (tests for *in vitro* cytotoxicity) and ISO 10993-4 (selection of tests for interactions with blood). Finally, the risk of pyrogens in the biomaterial context, especially of bacterial toxins (endotoxins), will be briefly highlighted and selected methods for determining pyrogens/endotoxins (cf. also ISO 10993-11) will be presented.

TABLE 4.5 Structure of ISO 10993

Part	Title
1	Evaluation and testing within a risk management process
2	Animal welfare requirements
3	Tests for genotoxicity, carcinogenicity and reproductive toxicity
4	Selection of tests for medical devices that interact with blood
5	Tests for *in vitro* cytotoxicity
6	Tests for local effects after implantation
7	Ethylene oxide sterilization residuals
8	Selection and qualification of reference materials for biological tests
9	Framework for identification and quantification of potential degradation products
10	Tests for irritation and skin sensitization
11	Tests for systemic toxicity
12	Sample preparation and reference materials
13	Identification and quantification of degradation products from polymeric medical devices
14	Identification and quantification of degradation products from ceramics
15	Identification and quantification of degradation products from metals and alloys
16	Toxicokinetic study design for degradation products and leachables
17	Establishment of allowable limits for leachable substances
18	Chemical characterization of materials
19	Physico-chemical, morphological and topographical characterization of materials
20	Principles

4.5.2.1 Tests for In Vitro *Cytotoxicity and Other Cell Culture-Based Assays for Cell/Tissue Compatibility*

Although cell culture experiments do not reproduce *in vivo* situations, they can give some idea of how different cell types might respond to a biomedical device. By this the number of surfaces that have to be tested in animal experiments can be reduced. In addition, products that are already on the market can be tested regularly with regard to cytotoxicity.

ISO 10993-5 Biological Evaluation of Medical Devices—Part 5: Tests for In Vitro *Cytotoxicity*

Testing for cytotoxicity (quality of being poisonous against cells) is a good first step towards ensuring the biocompatibility of a medical device. ISO 10993-5:2009 describes test methods to assess the in vitro cytotoxicity of medical devices. These methods specify the incubation of cultured cells in contact with a device and/or extracts of a device either directly or through diffusion. These methods are designed to determine the biological response of mammalian cells *in vitro* using appropriate biological parameters.

ISO 10993 states: "Cytotoxicity tests employing cell culture techniques shall be used to determine the lysis of cells (cell death), the inhibition of cell growth, colony formation, and other effects on cells by medical devices, materials and/or their extracts…":

- Direct contact: Cell cultures are grown to a standard monolayer. The test material is placed in direct contact with the cell layer for 24 h. Subsequently, the monolayers are examined microscopically for the presence of morphological changes, reduction in cell density, or lysis induced by the test material.
- Agar diffusion (Direct Contact or Saline Extract): The cell monolayer is overlaid with agar (protects the cells from mechanical damage while allowing the diffusion of leachables) and stained before treatment with the test material or extract. After 24 h, the cells are scored microscopically for decolorization and lysis.
- MEM Elution (Test on Extracts): The test material is extracted for 24 h in Minimum Essential Medium (MEM). An extract is prepared from the test material, which is then placed on cell monolayers. The cells are examined for morphologic changes and cytolysis to determine a toxicity score.

The qualitative evaluation of cytotoxicity is usually done by microscopy evaluation. Cells are observed for visible signs of toxicity, such as changes in the size or appearance of cellular components or a disruption in their configuration, in response to test and control materials.

For a quantitative evaluation of cytotoxicity, the cell viability/proliferation can be determined, for instance, by means of the MTT assay. This colorimetric assay measures the metabolic activity of viable cells, once the dissolved MTT (3-(4,5-dimethylthiazol-2-yl)-2,5-diphenyltetrazolium bromide) can be converted to a water-insoluble purple formazan by mitochondrial dehydrogenase enzymes of living cells. The number of viable cells correlates to the color intensity determined by photometric measurements after dissolving the formazan.

Other Cell Culture-Based Assays for Cell/Tissue Compatibility

In addition biocompatibility behavior can be evaluated by seeding cells directly on the test material (similar to the wash-and-plate assay described in Section 4.4.8) and subsequent analysis of cell adhesion, cell proliferation, cell morphology, and cytoskeletal organization and the presence of cell-secreted extracellular matrix (ECM). A proper cell adhesion and the formation of ECM proteins, like fibronectin, are, for instance, essential steps for successful tissue integration of biomaterials.

Immunofluorescence staining combined with CLSM can be applied to visualize cell components (e.g., nucleus-DAPI (6-diamidino-2-phenylindole) or actin filaments–phalloidin) and ECM molecules.

The number of adherent cells and cell viability/proliferation can be determined by means of the MTT assay as already described earlier.

If the biomaterial is biodegradable, its biological evaluation becomes even more complex since the degradation (by)-products need to prove general biocompatibility as well as cytocompatibility to the transplanted cells.

4.5.2.2 In Vitro *Tests for Blood Compatibility*

Blood-contacting materials have to fulfill particular requirements, as they are immediately exposed to all host defense mechanisms of the body. Thus, the contact of blood with foreign surfaces induces several cascade reactions and activation phenomena. These complex and highly interconnected reactions potentially create clinically significant side effects in the application of medical devices (e.g., cardiovascular implants, extracorporeal circulation, catheters) and interfere with the success of the medical treatments [64]. In certain cases, even the formation of thromboemboli or systemic inflammatory reactions were reported to occur as a consequence of the activation of coagulation enzymes and thrombocytes and/or the activation of the complement system and leukocytes (immune response) at the biointerfaces of the applied materials [65].

Part 4 of ISO 10993 (Biological evaluation of medical devices—Part 4: Selection of tests for interactions with blood) deals with the requirements of evaluating interactions of medical devices with blood.

However, there is no standard yet concerning size, design, and type of *in vitro* test systems for blood compatibility (hemocompatibility). In consequence, a wide variety of different test systems are currently applied in the development of new materials. As the dependence of the *in vitro* alteration of blood on several experimental conditions is rather complex, the comparison of results from hemocompatibility tests performed in different setups and by different incubation procedures remains ambiguous and may even lead to contradicting conclusions depending on the type of experimental approach used [66].

In the following, a set of incubation systems and procedures, suitable for both fundamental and application-oriented studies of blood–material interactions, are described.

The use of freshly drawn whole blood anticoagulated with heparin and strict prevention of blood–air contact are prerequisites for reliable testing. Additionally, the choice of the incubation system should be oriented towards

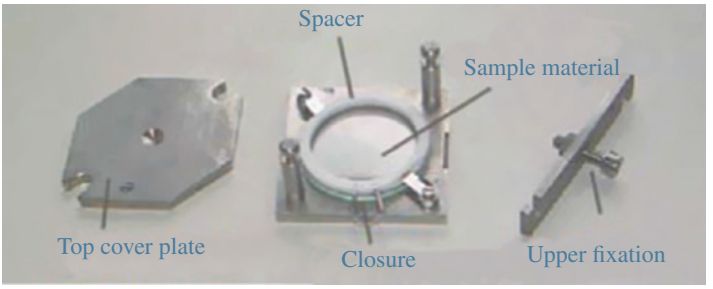

FIGURE 4.32 Screening chamber: Two stainless steel cover plates (left and middle) that fix the test surfaces are pressed together by a screw (right). The PTFE spacer forms a cavity. Blood is filled into the mounted chamber through holes in the PTFE spacer, which are sealed with a closure. Source: Streller et al. [66]. Reproduced with permission of John Wiley & Sons.

the intended use of the device. Perfusion systems are utilized to model the blood flow upon incubation, whereas screening chambers (Fig. 4.32) are applied to compare a higher number of sample materials. Glass and poly(tetrafluoroethylene) are suitable as reference materials for hemocompatibility tests [66]. The parameters to be analyzed after incubation of the samples with blood (up to 3 h at 37°C) were chosen to reflect the levels of cellular and humoral blood components in the fluid phase (blood/plasma) as well as on the surfaces of the materials to characterize the activation of selected aspects of coagulation, thrombogenicity, and immune responses (complement system) (Table 4.6) [66, 67].

4.5.2.3 Pyrogenicity and Pyrogen/Endotoxin Contamination

Contamination of liquids and surfaces with pyrogenic substances is a major concern with respect to biomedical applications and life science research [68]. The presence of pyrogen contamination of medical devices and parenteral drugs represents a serious risk for the patients but also may affect the scientific evaluation of biomaterials, for instance, regarding their hemocompatibility. Pyrogenicity testing is one aspect of evaluating the acute systemic toxicity of a material (ISO 10993-11), especially its potential to cause a fever-like response. Most exogenic pyrogens are of microbial origin, like components of bacteria (e.g., lipopolysaccharides (LPS), lipoteichoic acid, and peptidoglycan), viruses, or fungi, which can induce a complex inflammatory response in the human body. They cause release of endogenous pyrogens in the body, which are cytokines, for example, interleukin-1 or interleukin-6, produced by activated immune cells. However, the material itself can cause similar febrile responses, too (material-mediated pyrogenicity).

TABLE 4.6 ***In Vitro*** **Hemocompatibility Assays**[a]

Analyzed Parameter		Method
Blood Analysis		
Activation marker (in plasma)		
• For coagulation	TAT, FXIIa	ELISA
	Individual coagulation factor activities	Chromogenic enzyme kinetic assay/photometry
• For complement activation (immune response)	C5a, C5b-9, C3b	ELISA
• For thrombogenicity	PF4, βTG	ELISA
Blood cell number (decay due to adhesion or cell death)	Leucocytes Thrombocytes Erythrocytes	Cell counter
Activation status of cells (quantification of surface antigen)		
• Leucocytes (immune response)	CD11b	Flow cytometry
• Thrombocytes	CD41a	
Plasma clotting (global assay for clotting)		Coagulometry
Surface Analysis		
Activation status of cells		Immunostaining and fluorescence microscopy and/or CLSM
• Leucocytes (immune response)		
• Thrombocytes		
Adherent cells (hematocytes in general)		SEM (Fig. 4.33)
Protein aggregates (fibrin meshwork)		SEM

[a] From Refs. 66 and 67.

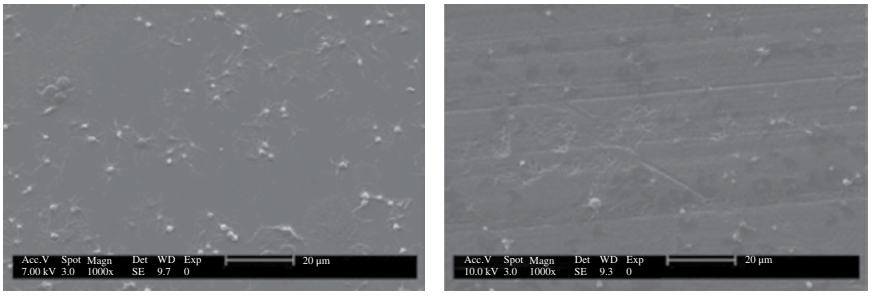

FIGURE 4.33 The number of adherent thrombocytes on glass surface (left) after 3 h incubation with blood in a screening chamber is higher than on PTFE surface (right). Source: Streller et al. [66]. Reproduced with permission of John Wiley & Sons.

The best investigated exogenous pyrogens are bacterial endotoxins that are a part of the outer cell membrane of Gram-negative bacteria. Endotoxins are shed upon cell death but also during growth and division. They can be present even when viable bacteria are not. Most critically, even small amounts of bacterial endotoxins can have very strong biological effects in humans and animals when entering the bloodstream or the spinal fluid with symptoms ranging from fever and shivering to hypotension, adult respiratory distress syndrome, disseminated intravascular coagulation, and endotoxin shock [69]. Structurally these endotoxins are LPS that consist of a polysaccharidic O-antigen, the negatively charged core oligosaccharide, and the hydrophobic lipid A. Lipid A is the most conserved part of endotoxin and is responsible for most of the biological activities of endotoxin. Due to their amphiphilic structure, endotoxins tend to form aggregates; thus the size of endotoxin species ranges from about 10–20 kDa (monomer) to over 1000 kDa (vesicles). This structure also favors the adsorption of the molecule to positively charged or hydrophobic surfaces.

Endotoxins are highly heat stable and hence are not destroyed under regular sterilizing conditions. In the sterilization process, the bacteria on a material are killed but not removed and the dead bacterial components are recognized by the body resulting in responses as described earlier. Thus, sterile does not necessarily mean endotoxin- or pyrogen-free, and endotoxin or pyrogenicity testing is not to be confused with sterility testing. The importance of endotoxin testing and removal in determining the biocompatibility of biomaterials, for example, their toxicity or the inflammatory potential, has been demonstrated, for instance, by Beenken-Rothkopf et al. [70]. Endotoxin contamination can significantly affect the biological response observed and hence completely superpose the impact of the biomaterial characteristics. Maitz et al. [68] pointed out that a clear distinction between properties of the materials and effects due to surface contamination by adsorbed endotoxins is also essential when evaluating the blood compatibility of new materials. They reported that biological reactions at *in vitro* blood exposure were found to be only minimally influenced by adsorbed endotoxins during the time window of 2 h, allowing for a straightforward discrimination between materials and endotoxin-dependent reactions. It should be noted that contamination of the finished product with bacterial endotoxins is not a biocompatibility issue of the material itself, but rather a manufacturing control issue.

The classic test for measuring pyrogenicity used to be the *in vivo* rabbit pyrogen test (European Pharmacopoeia 2.6.8; United States Pharmacopeia <151>; ISO 10993-11), which measures the rise in body temperature (an increase of 0.5°C or more indicated pyrogenicity) following an intravenous injection of the sample or the aqueous extract (typically with 40 ml water)

of the sample, for example, of a medical device, to the animals (sensitivity 0.5 EU/ml; 1 endotoxin unit (EU) of the WHO International Standard Endotoxin *E. coli O113:H19:K* corresponds to 100 pg of endotoxin). This test does not only detect bacterial endotoxins but also material-mediated pyrogens.

As an alternative to this animal test, an *in vitro* quality control was established with the limulus amoebocyte lysate (LAL) test (European Pharmacopoeia 2.6.14; United States Pharmacopeia <85>). It is based on the LPS-sensitive coagulant system of the horseshoe crab *Limulus polyphemus*. Different versions of the assay are available: the gel-clot assay or the chromogenic substrate method, which is more sensitive (0.005 EU/ml) than the older gel-clot assay (0.03 EU/ml). The LAL test only detects endotoxins but fails to recognize, for example, Gram-positive or fungal contaminants or viral antigens and is not sensitive to material-mediated pyrogens. In recent years, it has largely replaced the rabbit pyrogen test to confirm the absence of bacterial endotoxin contaminants in individual production lots. The US Food and Drug Administration (FDA) gives some recommendations for endotoxin elution from biomedical devices with water. This FDA approach of LPS elution was, for instance, extended by the use of organic solvents and detergent solutions [68].

Recently, the monocyte activation test (MAT) has been validated and recently accepted by European Pharmacopoeia and US FDA. This human *in vitro* pyrogen test has been also been included in the draft ISO guideline for biological testing of medical devices (ISO/TC194, working group on pyrogen testing) [71]. The MAT (e.g., the commercially available PyroCheck®) exploits the reaction of monocytes/macrophages for the detection of pyrogens. Therefore, human whole blood is incubated in the presence of the test sample at 37°C. If pyrogens are present, the monocytes/macrophages are activated to release the important inflammatory mediator interleukin-1β, which can be quantified by means of an ELISA assay. Recently, Stang et al. reported the detection of very small amounts of pyrogens directly on the surface of medical devices [72] by combining a modified MAT protocol and a dynamic incubation system. However, as already mentioned earlier, a clear distinction of effects due to material properties and due to pyrogen/endotoxin surface contamination is often difficult.

Current FDA limits are such that eluates from medical devices may not exceed 0.5 EU/ml, unless the device comes into contact with cerebrospinal fluid where the limit is then 0.06 EU/ml [69].

As already mentioned, standard autoclaving will not destroy endotoxin. A temperature of over 180°C is necessary to inactivate endotoxins. Unfortunately, few polymers can withstand these conditions. There are some washing procedures that can effectively remove adsorbed endotoxin, at least from solid materials that

can withstand these strong solutions. Different methods, such as ultrafiltration, extraction, and adsorption, are available to remove endotoxin from contaminated solutions.

Since endotoxin is very difficult to remove from a biomaterial, finding a supplier that offers an endotoxin-free product and preventing biomaterial contamination in the first place is often the only solution. Using endotoxin-free water is strongly recommended. Glassware or equipment are also potential sources of endotoxin [69].

REFERENCES

[1] Braun, D.; Cherdron, H.; Rehahn, M.; Ritter, H.; Voit, B.; *Polymer Synthesis: Theory and Practice, Fundamentals, Methods, Experiments*, 4th Edition, Springer, Berlin, Heidelberg, New York: 2005.

[2] Campbell, D.; Pethrick, R. A.; White, J. R. *Polymer Characterization: Physical Techniques*, 2nd Edition, CRC Press, Boca Raton: 2001.

[3] Appelhans, D.; Komber, H.; Abdul Quadir, M.; Loos, A.; Schwarz, S.; Richter, S.; Aigner, A.; Müller, M.; Haag, R.; Voit, B. *Biomacromolecules* 2009, *10*, 1114–1124.

[4] Barth, A. *Biochimica et Biophysica Acta, Bioenergetics* 2007, *1767*, 1073–1101.

[5] Kauppinen, J. K.; Moffat, D.; Mantzsch, H. H.; Cameron, D. G. *Applied Spectroscopy* 1981, *35*, 271–276.

[6] Jackson, M.; Mantzsch, H. H. *Critical Reviews in Biochemistry and Molecular Biology* 1995, *30*, 95–120.

[7] Arrondo, J. L. R.; Muga, A.; Castresana, J.; Goni, F. M. *Progress in Biophysics and Molecular Biology* 1993, *59*, 23–56.

[8] Wolfenden, M. L.; Cloninger, M. J. *Bioconjugate Chemistry* 2006, *17*, 958–966.

[9] Soeriyadi, A. H.; Whittaker, M. R.; Boyer, C.; Davis, T. P. *Journal of Polymer Science Part A: Polymer Chemistry* 2013, *51*, 1475–1505.

[10] Henderson, W.; McIndoe, J. S. *Mass Spectrometry of Inorganic, Coordination and Organometallic Compounds: Tools-Techniques-Tips*; John Wiley & Sons, Ltd, Chichester: 2005.

[11] Harth-Smith, G.; Barner-Kowollik, C. *Macromolecular Chemistry and Physics* 2010, *211*, 1507–1529.

[12] Morgner, N.; Barth, H.-D.; Brutschy, B. *Australian Journal of Chemistry* 2006, *59*, 109–114.

[13] Morgner, N.; Barth, H.-D.; Brutschy, B.; Scheffer, U.; Breitung, S.; Göbel, M. *Journal of the American Society for Mass Spectrometry* 2008, *19*, 1600–1611.

[14] Kuhlbeil, M.; Stephan, H.; Pietzsch, H.-J.; Geipel, G.; Appelhans, D.; Voit, B.; Hoffmann, J.; Brutschy, B.; Mironov, Y.; Brylev, K. A.; Fedorov, V. E. *Chemistry, an Asian Journal* 2010, *5*, 2507–2514.

[15] Grubisic, Z.; Rempp, P.; Benoit, H. A. *Journal of Polymer Science, Part B: Polymer Letters* 1967, *5*, 753–759.

[16] Berger, S.; Braun, S. *200 and More NMR Experiments*; Wiley-VCH, Weinheim: 2004.

[17] Callaghan, P. T. *Principles of Nuclear Magnetic Resonance Microscopy*; Oxford University Press, Oxford: 1993.

[18] (a)Stejskal, E. O.; Tanner, J. E. *The Journal of Chemical Physics* 1965, *42*, 288–292. (b)Heil, S. R.; Holz, M. *Angewandte Chemie* 1996, *15*, 1801–1804.

[19] Fritzinger, B.; Appelhans, D.; Voit, B.; Scheler, U. *Macromolecular Rapid Communications* 2005, *26*, 1647–1650.

[20] Sagidullin, A.; Skirda, W. D.; Tatarinova, E. A.; Muzafarov, A. M.; Krykin, M. A.; Ozerin, A.; Fritzinger, B.; Scheler, U. *Applied Magnetic Resonance* 2003, *25*, 129–156.

[21] Scheler, U. "Electrophoretic NMR" in *Encyclopedia of Magnetic Resonance*; John Wiley & Sons, Inc., New York: 2012.

[22] Böhme, U.; Scheler, U. *Colloids and Surfaces A: Physicochemical and Engineering Aspects* 2003, *222*, 35–40.

[23] Einstein, A. *Annalen der Physik* 1905, *17*, 549–560.

[24] Manning, G. S. "Limiting Laws for Equilibrium and Transport Properties of Polyelectrolyte Solutions" in *Polyelectrolytes* (eds. Sélégny, E.; Mandel, M.; Strauss, U. P.) D. Reidel Publishing Company, Dordrecht: 1974, 9–34.

[25] Williams, S. K. R.; Lee, D. *Journal of Separation Science* 2006, *29*(12), 1720–1732.

[26] Messaud, F. A.; Sanderson, R. D.; Runyon, J. R.; Otte, T.; Pasch, H.; Williams, S. K. R. *Progress in Polymer Science* 2009, *34*, 351–368.

[27] Boye, S.; Appelhans, D.; Boyko, V.; Zschoche, S.; Komber, H.; Friedel, P.; Formanek, P.; Janke, A.; Voit, B. I.; Lederer, A. *Biomacromolecules* 2012, *13*, 4222–4235.

[28] Boye, S.; Polikarpov, N.; Appelhans, D.; Lederer, A. *Journal of Chromatography A* 2010, *1217*, 4841–4849.

[29] Liao, M.; Cao, E.; Julius, D.; Cheng, Y. *Nature* 2013, *504*, 107–112.

[30] Williams, D. B.; Carter, C. B. *Transmission Electron Microscopy: A Textbook for Materials Science*; Springer US, New York: 2009.

[31] Michler, G. H. *Electron Microscopy of Polymers*; Springer US, New York: 2010.

[32] Gaitzsch, J.; Appelhans, D.; Wang, L.; Battaglia, G.; Voit, B. *Angewandte Chemie International Edition* 2012, *51*, 4448–4451.

[33] Crassous, J. J.; Ballauff, M.; Drechsler, M.; Schmidt, J.; Talmon, Y. *Langmuir* 2006, *22*, 2403–2406.

[34] Midgley, P. A.; Dunin-Borkowski, R. E. *Nature Materials* 2009, *8*, 271–280.

[35] Brandl, F.; Sommer, F.; Goepferich, A. *Biomaterials* 2007, *28*, 134–146.

[36] Welzel, P. B.; Grimmer, M.; Renneberg, C.; Naujox, L.; Zschoche, S.; Freudenberg, U.; Werner, C. *Biomacromolecules* 2012, *13*, 2349–2358.

[37] Welzel, P.; Prokoph, S.; Zieris, A.; Grimmer, M.; Zschoche, S.; Freudenberg, U.; Werner, C. *Polymers* 2011, *3*, 602–620.

[38] Arndt, K. F.; Müller, G. *Polymercharakterisierung*; Hanser Verlag, München: 1996.

[39] Peppas, N. A.; Hilt, J. Z.; Khademhosseini, A.; Langer, R. *Advanced Materials* 2006, *18*, 1345–1360.

[40] Nitschke, M.; Schmack, G.; Janke, A.; Simon, F.; Pleul, D.; Werner, C. *Journal of Biomedical Materials Research* 2002, *59*, 632–638.

[41] Uhlmann, P.; Skorupa, S.; Werner, C.; Grundke, K. *Langmuir* 2005, *21*, 6302–6307.

[42] Kwok, C. D. Y.; Lam, N. C.; Li, A.; Leung, A.; Wu, R.; Mok, E.; Neumann, A. W. *Colloids and Surfaces A* 1998, *142*, 219–235.

[43] Grundke, K. "Characterization of Polymer Surfaces by Wetting and Electrokinetic Measurements – Contact Angle, Interfacial Tension, Zeta Potential" in *Polymer Surfaces and Interfaces: Characterization, Modification and Applications* (ed. Stamm, M.) Springer, Berlin, Heidelberg: 2008, 103–138.

[44] Delgado, A. V.; Gonzalez-Caballero, E.; Hunter, R. J.; Koopal, L. K.; Lyklema, J. *Pure and Applied Chemistry* 2005, *77*, 1753–1805.

[45] Duval, J. F. L.; Zimmermann, R.; Cordeiro, A. L.; Rein, N.; Werner, C. *Langmuir* 2009, *25*, 10691–10703.

[46] Zimmermann, R.; Kuckling, D.; Kaufmann, M.; Werner, C.; Duval, J. F. L. *Langmuir* 2010, *26*, 18169–18181.

[47] Duval, J. F. L.; Küttner, D.; Nitschke, M.; Werner, C.; Zimmermann, R. *Journal of Colloid and Interface Science* 2011, *362*, 439–449.

[48] Duval, J. F. L.; Küttner, D.; Werner, C.; Zimmermann, R. *Langmuir* 2011, *27*, 10739–10752.

[49] Cordeiro, A. L.; Zimmermann, R.; Gramm, S.; Nitschke, M.; Janke, A.; Schäfer, N.; Grundke, K.; Werner, C. *Soft Matter* 2009, *5*, 1367–1377.

[50] Schmaljohann, D.; Nitschke, M.; Schulze, R.; Eing, A.; Werner, C.; Eichhorn, K. J. *Langmuir* 2005, *21*, 2317–2322.

[51] Alf, M. E.; Godfrin, P. D.; Hatton, T. A.; Gleason, K. K. *Macromolecular Rapid Communications* 2010, *31*, 2166–2172.

[52] Binnig, G.; Quate, C. F.; Gerber, C. *Physical Review Letters* 1986, *56*, 930–933.

[53] Cisneros, D. A.; Hung, C.; Franz, C. A.; Müller, D. J. *Journal of Structural Biology* 2006, *154*, 232–245.

[54] Friedrichs, J.; Taubenberger, A.; Franz, C. M.; Müller, D. J. *Journal of Molecular Biology* 2007, *372*, 594–607.

[55] Matzelle, T. R.; Ivanov, D. A.; Landwehr, D.; Heinrich, L. A.; Herkt-Bruns, C.; Reichelt, R.; Kruse, N. *Journal of Physical Chemistry B* 2002, *106*, 2861–2866.

[56] Stokes, D. J. *Philosophical Transactions of the Royal Society of London, Series A: Mathematical, Physical and Engineering Sciences* 2003, *361*, 2771–2787.

[57] Muscariello, L.; Rosso, F.; Marino, G.; Giordano, A.; Barbarisi, M.; Cafiero, G.; Barbarisi, A. *Journal of Cellular Physiology* 2005, *205*, 328–334.

[58] Zimmermann, R.; Osaki, T.; Gauglitz, G.; Werner, C. *Biointerphases* 2007, *2*, 159–164.

[59] Friedrichs, J.; Zieris, A.; Prokoph, S.; Werner, C. *Macromolecular Rapid Communications* 2012, *33*, 1453–1458.

[60] Lyubchenko, Y.; Friedrichs, J.; Legate, K.R.; Schubert, R.; Bharadwaj, M.; Werner, C.; Müller, D.; Benoit, M. *Methods* 2013, *60*, 169–178.

[61] Franke, K. Adhesion and Single Cell Tracking of Hematopoietic Stem Cells on Extracellular Matrices, Ph.D. Thesis, TU Dresden: 2011.

[62] Limozin, L.; Sengupta, K. *A European Journal of Chemical Physics and Physical Chemistry ChemPhysChem* 2009, *10*, 2752–2768.

[63] Franke, K.; Pompe, T.; Bornhäuser, M.; Werner, C. *Biomaterials* 2007, *28*, 836–843.

[64] Cazenave, J. P.; Davies, J. A.; Kazatchkine, M. D.; van Aken, W. G., eds., *Blood-Surface Interactions: Biological Principles Underlying Hemocompatibility with Artificial Materials*; Elsevier, Amsterdam/New York/Oxford: 1986.

[65] Ragaller, M.; Werner, C.; Bleyl, J.; Adam, S.; Jacobasch, H. J.; Albrecht, D. M. *Kidney International. Supplement* 1998; *64* 84–90.

[66] Streller, U.; Sperling, C.; Hübner, J.; Hanke, R.; Werner, C. *Journal of Biomedical Materials Research, Part B: Applied Biomaterials* 2003, *66*, 379–390.

[67] Sperling, C.; Fischer, M.; Maitz, M. F.; Werner, C. *Biomaterials* 2009, *30*, 4447–4456.

[68] Maitz, M. F., Teichmann, J., Sperling, C. Werner, C. *Journal of Biomedical Materials Research, Part B: Applied Biomaterials* 2009, *90B*: 18–25.

[69] Gorbet, M. B.; Sefton, M. V. *Biomaterials* 2005, *26*, 6811–6817.

[70] Beenken-Rothkopf, L. N.; Karfeld-Sulzer, L. S.; Zhang, X.; Kissler, H.; Michie, S. A.; Kaufman, D. B.; Fontaine, M. J.; Barron, A. E. *Journal of Biomaterials Applications* 2013, *28*, 395–406.

[71] Schindler, S.; von Aulock, S.; Daneshian, M.; Hartung T. *ALTEX* 2009, *26*, 265–277.

[72] Stang, K.; Fennrich, S.; Krajewski, S.; Stoppelkamp, S.; Burgener, I. A.; Wendel, H. P. *Journal of Materials Science: Materials in Medicine* 2014, *25*, 1065–1075.

5

MULTIFUNCTIONAL POLYMER ARCHITECTURES

5.1 MULTIFUNCTIONAL (BLOCK) COPOLYMERS

5.1.1 Multifunctionality through Copolymerization

Copolymer formation is ideal to introduce multifunctionality (see Section 2.2) into polymeric materials. Whereas the base polymer backbone structure defines major material properties like solubility, thermal properties, film formation ability, degradability or stability, and hydrophilicity or hydrophobicity, an additional functionality can be introduced by copolymerization with a second or even a third monomer. In the easiest case, random copolymerization of the selected monomers in a defined ratio is carried out, for example, by free radical polymerization. Thus, for example, copolymerization of methyl methacrylate (MMA) with a few mol% glycidyl methacrylate or of styrene with maleic acid anhydride provides very stable, film forming polymers with some reactive groups for polymer analogous reactions or immobilization on surfaces. Copolymers of MMA with (oligoethylene oxide) methacrylate or sugar-containing (meth)-acrylates enhance the biocompatibility of a standard polymer. Styrene or (meth)acrylates can be copolymerized with monomers containing adamantane or cyclodextrin units that allow for specific host–guest interactions. Of course, there is a huge multitude of such kind of copolymers reported, many of them commercially available. It has to be noted that the properties of these materials even when composed of the same comonomers can vary widely depending on the comonomer ratio and the polymerization method. Furthermore, the polymeric microstructure in a copolymer governed

Bio- and Multifunctional Polymer Architectures: Preparation, Analytical Methods, and Applications, First Edition. Brigitte Voit, Rainer Haag, Dietmar Appelhans, and Petra B. Welzel.

by the sequence of the comonomers can have a significant influence on the interactions of that copolymer, for example, in a biological environment. It was, for example, demonstrated that a poly(acrylamide) where hydrophobic comonomers were randomly distributed within the polymer chain shows a better cellular uptake than corresponding block copolymers of identical composition due to a different aggregation behavior [1].

The efficiency and randomness of the incorporation of a second monomer depend on the copolymerization parameters (see Section 3.1) and the type of chain growth method applied. For each monomer pair these factors have to be evaluated and considered for defining structure and functionality. In addition, basic polymer properties like solubility and thermal properties defined by the major monomer are strongly influenced by a second monomer of different functionality; thus, in any random copolymerization process, it is usually not possible to introduce a second functionality without compromising the properties of the parent homopolymer, and this is enhanced with increasing the comonomer ratio.

A specific example for a multifunctional random copolymer prepared by free radical polymerization that is of special interest for the preparation of coatings with antibacterial properties is given in Figure 5.1 [2]. Here, MMA provides stability and film forming ability and is used as the major monomer; methacrylates with long semifluorinated side chains have a high hydrophobicity and tend to surface segregate providing low fouling surfaces (reduced adsorption of bacteria and proteins); the acetylacetonato side chain can complex with metal ions like iron or silver, and thus, active antibacterial properties are achieved; benzophenone side groups are photoactive and produce radicals

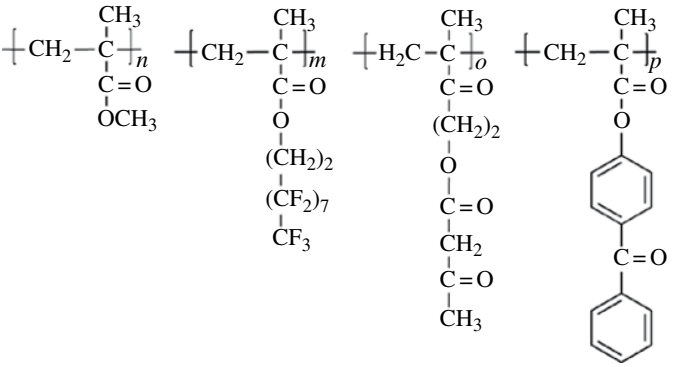

FIGURE 5.1 Multifunctional random copolymer of four monomers: methyl methacrylate (MMA), semifluorinated methacrylate (sfMA-H2F8), acetylacetonato methacrylate (AAMA), and benzophenone methacrylate (BPMA) [2].

during UV irradiation that cross-link the polymer film providing very high stability and long-livingness of a coating also under harsh conditions.

5.1.2 Multifunctionality by Polymer Analogous Reactions

Multifunctionality can be introduced not only through copolymerization but also by polymer analogous reactions in a postpolymerization modification step, often in combination with the introduction of additional comonomers during the polymerization process. Well-known technical examples are copolymers of polyvinyl alcohol and polyvinyl acetate with different amounts of vinyl acetate (see Section 3.1.3), which all derive from homopoly(vinyl acetate) and are the result of acetate hydrolysis to a different extent. The content of remaining vinyl acetate groups defines the hydrophilicity/hydrophobicity of the copolymer and thus the amphiphilic and stabilizing character of the material.

A famous example of multifunctionality in polymeric materials for biomedical applications is the concept of polymer–drug conjugates as introduced by Ringsdorf in 1975 [3] (Fig. 5.2). The various functionalities are introduced by a combination of copolymerization and polymer analogous reactions. It has to be noted that for drug delivery carrier polymers, not only the functionality but also the molar mass are of high importance for the application since it defines not only the solubility but also the half-life time in blood and the uptake in specific cells and the excretion from the kidneys.

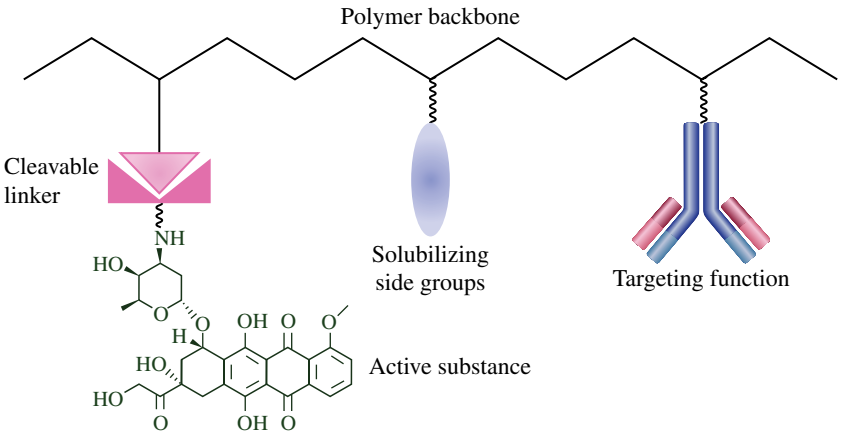

FIGURE 5.2 Ringsdorf model of polymer therapeutics [3], showing a polymer chain with a given biocompatible backbone where the solubility is fine-tuned by the solubilizing groups incorporated by copolymerization. Targeting groups and cleavable prodrugs (here: doxorubicin) can be introduced by polymer analogous reactions.

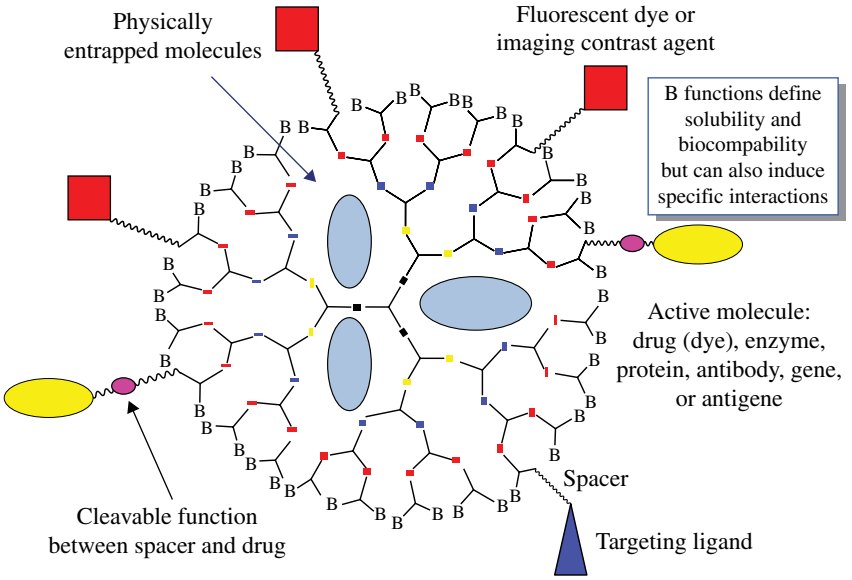

FIGURE 5.3 Schematic representation of a dendritic multifunctional carrier molecule.

Polymer analogous reactions are also of special interest with regard to end group functionalization often achieved after the polymerization process. The end group effect can be strongly enhanced in polymer architectures with a multitude of end groups as they are found in star polymers, graft copolymers, and dendritic polymer structures (see Section 5.2). In those cases, also various end groups of different functionality can be introduced within a single, highly functional macromolecule in combination with three-dimensional (3D) scaffold features and physical binding of active molecules (see Fig. 5.3).

5.1.3 Spatially Defined Multifunctionality by Phase Separation and Self-Assembly of Segmented Copolymers

The use of controlled polymerization methods (see Section 3.2), also in combination with efficient polymer analogous reactions (see Section 3.3), allows to spatially define the arrangement of any second functionality in a copolymer structure. Different functionalities can be arranged randomly along the polymer chain, in a gradient fashion, as specific end groups, or selectively in segments as achieved in block and graft copolymers (Fig. 5.4). First attempts are made for full monomer sequence control also in synthetic polymers [4–6], but so far rare and only very specific examples exist for that.

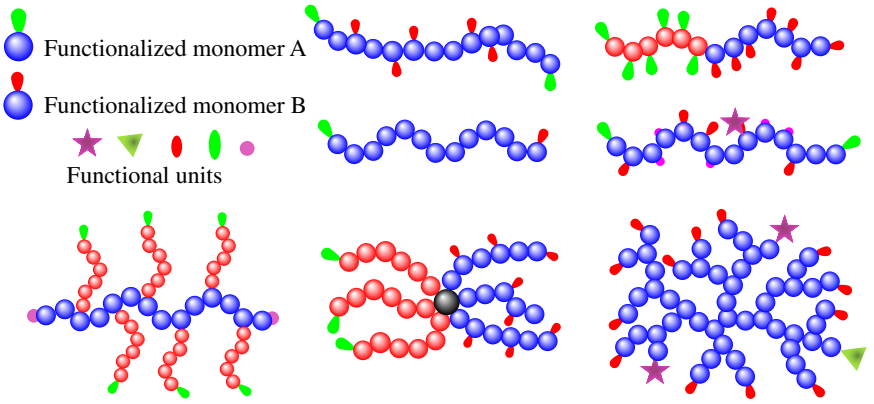

FIGURE 5.4 Schematic representation of multifunctionality in various polymer architectures.

The preparation of functional block copolymers furthermore allows for the formation of nanodomains in which an individual functionality can be confined and thus fine-tuned independently, which is very different from random copolymer formation. Polymers of different nature tend to phase-separate. However, when polymer segments are chemically bound like in a block or graft copolymer, macroscopic phase separation is not possible, and thus, a nanodomain morphology is obtained where the domain size depends on the block length of the individual polymer segments and the block ratio defines the morphological structure (Fig. 5.5a). This is even more pronounced when the different segments in polymers are of different polarity like in amphiphilic block copolymers. Phase separation and morphologies of block copolymers are very well studied [7, 9, 10], and the highest-ordered nanostructures are observed when the dispersity of the blocks is very low as it can be achieved by living anionic polymerization. Of special interest are ordered nanodomains in thin polymer films, which are used to provide spatially defined functionality on a surface or act as templates for selective metallization or as nanostructured masks (Fig. 5.5b). Here, a long-range order in a large film area is often aimed for which can be achieved by special techniques as slow dip coating, vapor and solvent annealing, application of an electric or magnetic field, substrate pretreatment, and structuring [11, 12].

Similarly, well-ordered bulk nanostructures can also be achieved by triblock copolymers as shown impressively, for example, by Abetz for styrene–butadiene–*tert*-butyl methacrylate triblock copolymers [13] (Fig. 5.6).

The individual segments in block copolymers are usually of different chemical nature and thus of different functionality. This allows for the creation

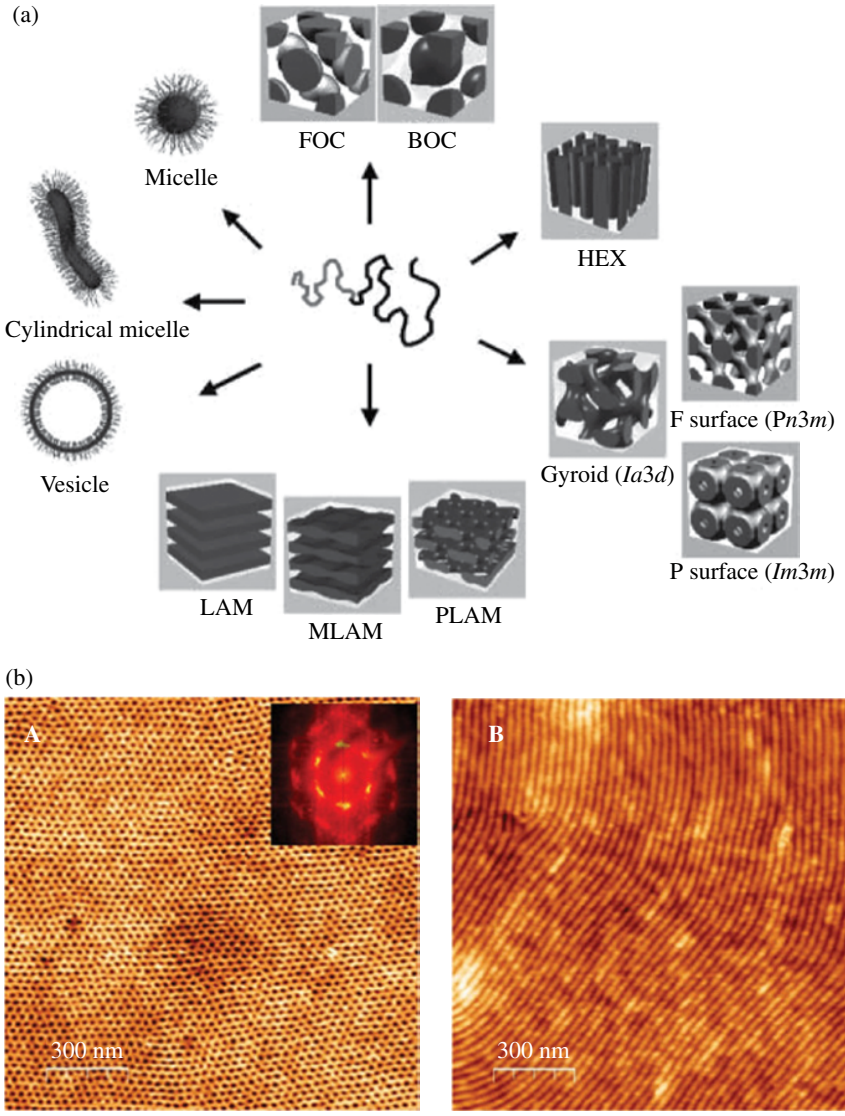

FIGURE 5.5 (a) Self-organization structures of block copolymers and surfactants: spherical micelles, cylindrical micelles, vesicles, foc- and boc-packed spheres (FOC, BOC), hexagonally packed cylinders (HEX), various minimal surfaces (gyroid, F surface, P surface), simple lamellae (LAM), as well as modulated and perforated lamellae (MLAM, PLAM). Source: Förster and Plantenberg [7], figure 13. Reproduced with permission from John Wiley & Sons. (b) AFM pictures (insert: SAXS analysis) of phase-separated poly(styrene-*b*-4-vinylpyridine) diblock copolymer films containing a low molar mass additive 2-(4-hydroxyphenylazo)benzoic acid (HABA) and showing in vapor-annealed films standing up (A) (dioxane) and laying down (B) (chloroform) cylinders, suitable for templating. Source: Adapted from Kuila and Stamm [8]. Reproduced with permission from the Royal Society of Chemistry.

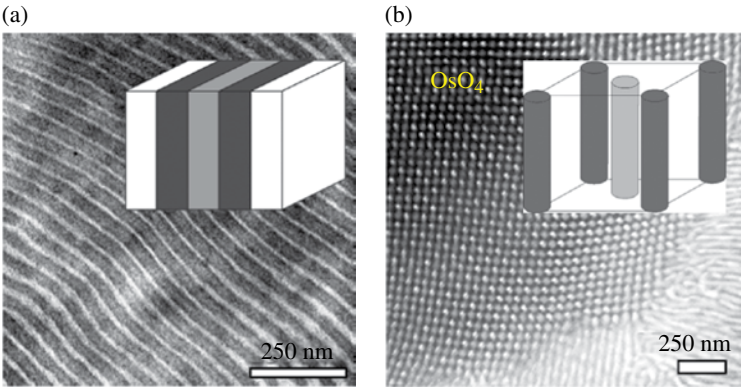

FIGURE 5.6 Nanomorphologies (TEM pictures, OsO_4 stained) in styrene–butadiene–*tert*-butyl methacrylate triblock SBT copolymers of different compositions (numbers indicate repeating units of the blocks). (a) $S_{27}B_{29}T_{44}$: triphasic lamellae. (b) $S_{19}B_{57}T_{24}$: two phases from cylinders; one phase forms the matrix. Source: Adapted from Abetz et al. [14], figure 1. Reproduced with permission from John Wiley & Sons.

of nanodomains in a thin nanostructured block copolymer film, for example, showing different wetting behavior or binding ability. The method has also been used for block copolymer lithography [11, 12, 15]. A special example has been given by Spatz et al. [16] who used the self-assembly of the block copolymer (poly(styrene-*b*-2-vinylpyridine)) into micelles with a metal ion binding core (2-vinylpyridine) and a nonpolar corona (styrene) acting as spacer of different dimension to deposit nanoparticles spatially defined on a substrate by a simple spin-coating or dip-coating process of the metal-loaded block copolymer solution. After reduction of the metal salts to metal nanodots in the film, the organic block copolymer is removed by plasma etching (Fig. 5.7). The deposited gold nanodots can further be used to bind specific biologically active components like integrins, which guide cell binding ability (Fig. 5.8).

The phase separation of block copolymers in bulk is also the driving force for their self-assembly. Self-assembly of amphiphilic block copolymers in specific solvents leads to a vast variety of aggregates where functionality can be compartmentalized like in micelles and various types of vesicles like polymersomes (Fig. 5.5a). The type of vesicle formed depends on the hydrophobic/hydrophilic ratio and the block length of the block copolymers (Fig. 5.9; see also Section 6.1). Different functionalities, like a metal binding group, complexation units, bioactive groups, or pH or salt concentration-sensitive units, can then be placed selectively into one of the phases, for example, at the inner part of a micellar structure or in the corona.

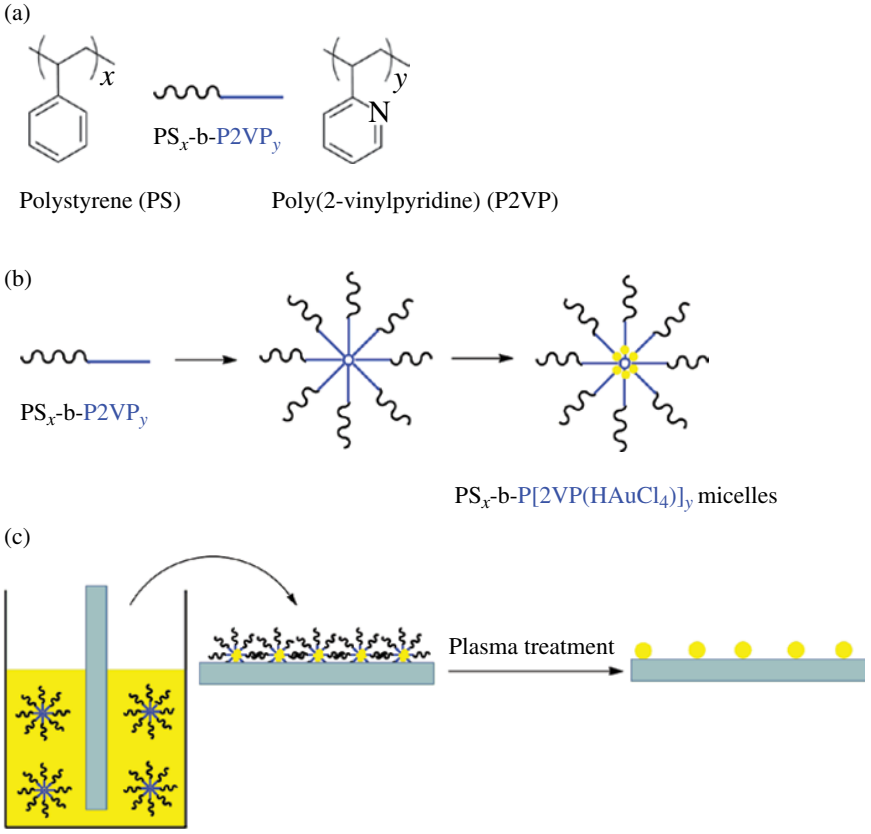

FIGURE 5.7 Principle of block copolymer lithography for spatially defined placing of gold nanoparticles on surfaces [16]. (a) Block copolymer structure, (b) formation of micelles with a metal ion core, and (c) formation of thin films by dip coating and plasma treatment to remove organic layer. (*See insert for color representation of the figure.*)

Müller et al. [18] demonstrated that by carefully choosing the composition of triblock copolymers and adjusting the preparation techniques, precise hierarchical self-assembly of multicompartment micelles can be achieved, which can "polymerize" into micrometer structures (Fig. 5.10).

With this knowledge also dual-stimuli-responsive micellar aggregates with a compartmentalized shell have been formed in aqueous solution from ABC triblock terpolymers with tunable hydrophilicity: polybutadiene-*block*-poly (*tert*-butyl methacrylate)-*block*-poly(2-(dimethylamino)ethyl meth-acrylate) (PB-*b*-P*t*BMA-*b*-PDMAEMA) and, after modification by hydrolysis to poly(methacrylic acid) (PMAA) or quaternization to PDMAEMAq, PB-*b*-PMAA-*b*-PDMAEMAq terpolymers. Control over micellar shape, size, and charge was achieved by self-assembly in water, depending on pH and

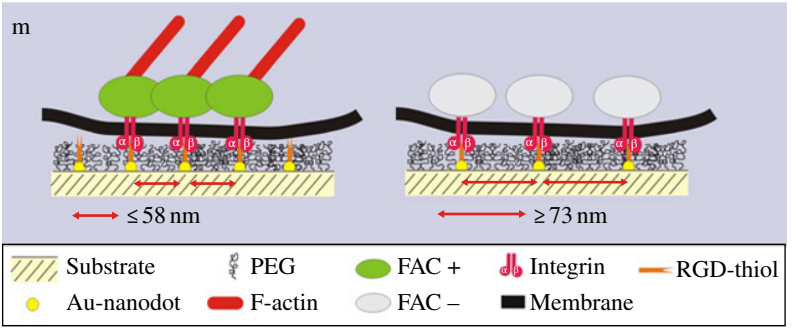

FIGURE 5.8 Scheme for the control of cell's integrin clustering at nanostructured and biofunctionalized substrates (based on spatially defined deposition of gold nanodots through block copolymer lithography). Source: Adapted from Arnold et al. [17], figure 2. Reproduced with permission from John Wiley & Sons. (*See insert for color representation of the figure*.)

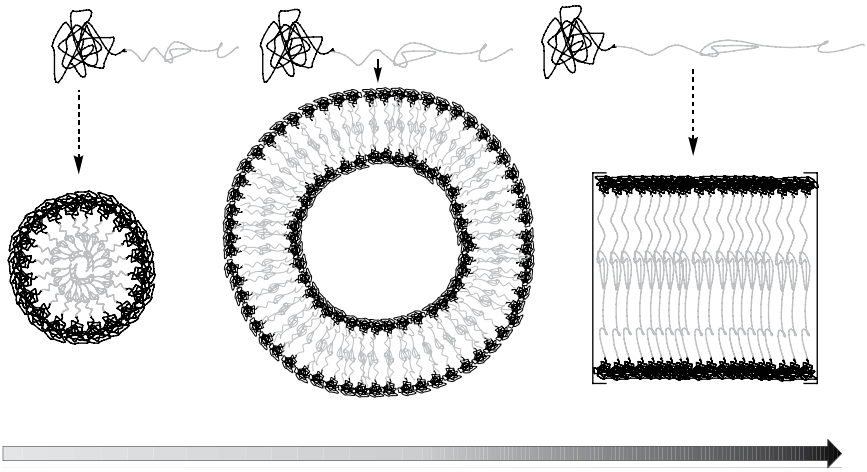

FIGURE 5.9 Amphiphilic block copolymers form different structures with increasing length of the hydrophobic segment. The resulting curvature forces the formation of micelles, polymersomes, or wormlike structures.

temperature as well as rearrangements in both the shell and the corona in response to external stimuli like pH or salinity [19].

The potential of self-assembly of functional block copolymers with the aim to confine functionality in a specific compartment is well demonstrated by the formation of functional polymersomes (Section 6.1.1.2). As an example, Meier et al. [20] prepared polymersomes composed of poly(dimethylsiloxane)-*block*-poly(2-methyloxazoline) diblock copolymers that had been modified

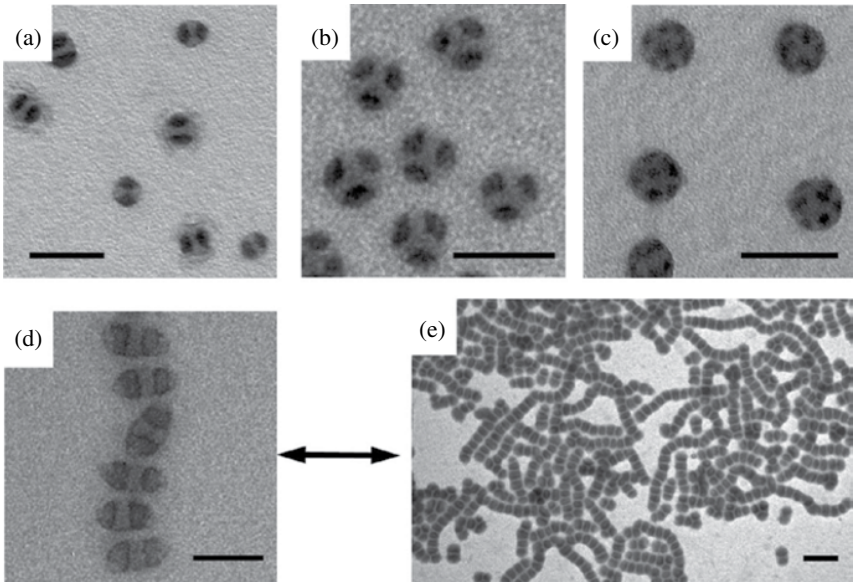

FIGURE 5.10 TEM pictures showing examples of spherical and linear multicompartment micelles formed by poly(styrene-block-2-butadiene-block-methylmethacrylate) (SBM) triblock copolymers with various core volume ratios (*V*PS/*V*PB) resulting in the structures shown in (a–e). Staining was achieved with OsO_4 (B black, S gray, M corona not visible) [18]. Scale bars correspond all to 100 nm. Source: Gröschel et al. [18]. Reproduced with permission from Nature Publishing Group.

with 4-formylbenzoate groups that allowed the conjugation of 6-hydrazinonicotinate acetone hydrazone-functionalized antibodies on the polymersome surface (Fig. 5.11).

The phase-separating and assembly behavior of functional copolymer architectures with longer functional polymer segments of one kind is the base of today's high importance of self-assembly of synthetic multifunctional macromolecules and biohybrids in bionanotechnology. Functionality can be confined in specific compartments of nanometer size, and further self-assembly in specific solvents can lead to micrometer-sized objects (see further examples in Section 6.1.1.2).

5.2 DENDRITIC POLYMERS

Trees, roots, snowflakes, river deltas, corals, circulation systems, and many other natural structures all demonstrate a characteristic highly branched architecture in the macro world. Descending into the nanoscale, we find

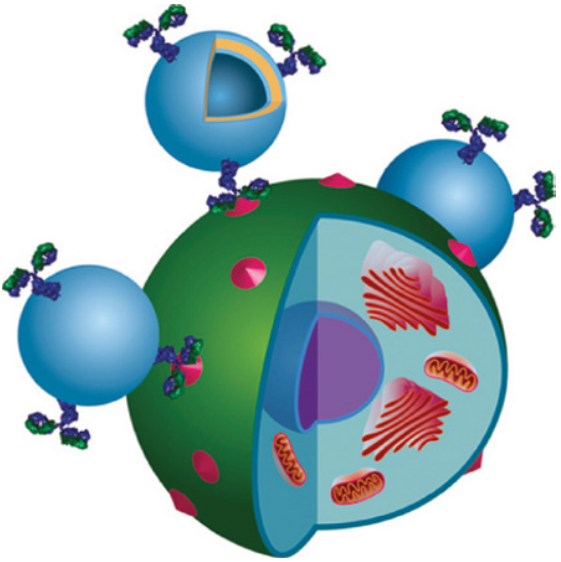

FIGURE 5.11 Schematic representation of a multifunctional polymersome able to interact with a cell. Source: Egli et al. [20]. Reproduced with permission from American Chemical Society.

naturally occurring polysaccharides like dextran, glycogen, and amylopectin that also possess this unique structure. Four main classes of polymers may be distinguished: (i) linear, (ii) cross-linked, (iii) branched, and (iv) dendritic (see Section 2.1). The last class comprises dendrimers, hyperbranched polymers, linear dendritic hybrids, as well as dendrigrafted and hypergrafted polymers (Fig. 5.12) [21]. Only the first two classes will be briefly described in the following. Dendrimers are characterized by a perfect structure consisting of a core, shell interior, and terminal functional groups of the shell. The structure of hyperbranched polymers, in comparison to dendrimers, is not perfect. They are statistically branched and more flexible. An ideal dendrimer possesses only dendritic (D) and terminal (T) units, whereas hyperbranched polymers possess additional linear units (L) obtained by incomplete branching.

The degree of branching (DB), which determines the ratio of branched, terminal, and linear units in the polymer structure, is 100% for dendrimers and much less than 100% for hyperbranched polymers, usually about 50% for AB_2 monomer-based structures.

In 1952, Flory described random AB_x polycondensation theoretically and showed that highly branched polymers can be synthesized without gelation by polycondensation of an AB_x monomer ($x \geq 2$) in which A functional groups can react with B groups [22]. In 1988, the term "hyperbranched polymer" was

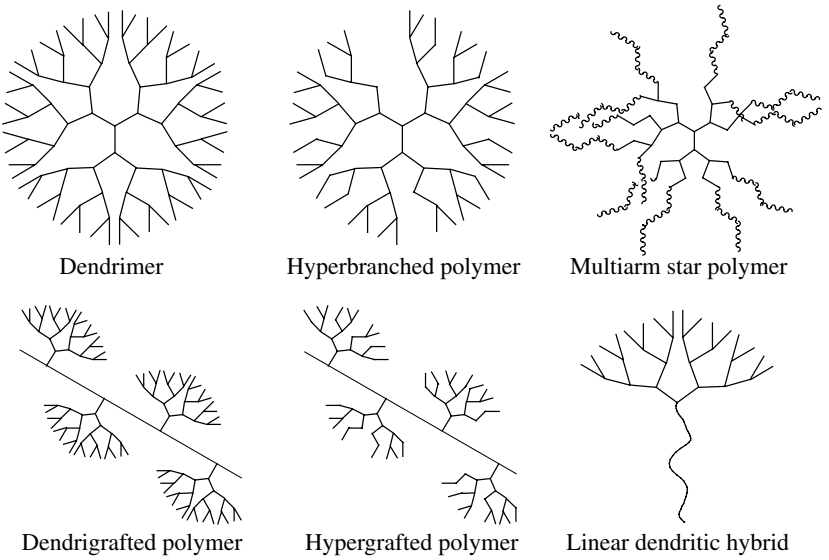

FIGURE 5.12 Examples of dendritic polymer structures.

introduced by Kim and Webster, who published their results on the synthesis of soluble hyperbranched polyphenylene [23]. Since then, a huge variety of hyperbranched structures has been realized [24].

In 1979, while working for Dow Chemical Co., Donald A. Tomalia discovered Starburst® dendrimers, which are poly(amidoamine) (PAMAM) dendrimers prepared by a so-called divergent synthesis [25]. These structures are some of the best characterized and most extensively utilized dendritic polymers in the field of bioscience. Other widely known dendrimer structures are polyethers, which were reported in 1990 by Fréchet [26], and poly(propylene imine) (PPI) dendrimers from the groups of Wörner and Mülhaupt [27] and de Brabander-van den Berg and Meijer [28]. Smaller PPI dendrons were described by Vögtle et al. already in 1978 [29].

5.2.1 Synthesis of Dendrimers and Hyperbranched Polymers

For the synthesis of dendrimers, mainly the divergent and the convergent methods are used (Fig. 5.13). In the divergent method, a dendritic macromolecule is synthesized that starts from the core and is expanded in a stepwise fashion. Further generations (G) are built with well-defined core–shell structures in iterative stages. A basic example of the divergent

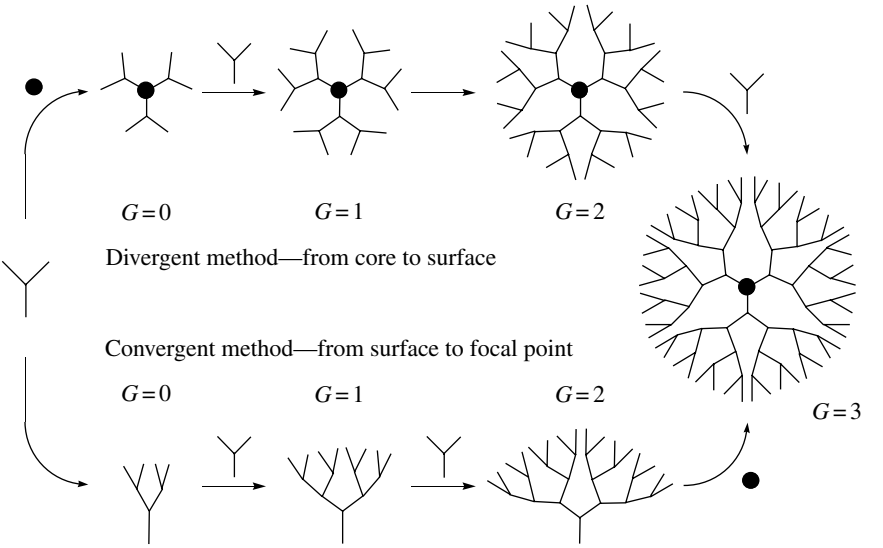

FIGURE 5.13 Divergent and convergent synthetic routes toward dendrimers. G: generation.

method is the synthesis of PAMAM dendrimers, where ethylenediamine (EDA) is chosen as the core, followed by alkylation with methyl acrylate by Michael addition and subsequent amidation of the created esters with EDA (Fig. 5.14). In the convergent method (Fig. 5.13), a dendritic molecule is constructed by synthesizing branches, which are then later connected together to the core (focal point). There are fundamental advantages and disadvantages of both methods. The divergent method is structurally limited because of the number of steps required. The great excess of reagents and purification steps also causes problems in the divergent method. However, the divergent approach allows more generations to form, whereas the development of larger molecules is sterically hindered in the convergent method. Despite resulting in smaller macromolecules, the convergent method ensures a better control of molecular weight and structure.

Hyperbranched polymers are synthesized in a one-step method, often from AB_x monomers but also by combining $A_2 + B_x$ ($x \geq 3$) monomers or variations of those. Polymerization methods have been applied that involve polycondensation, polyaddition, and ring-opening or self-condensing vinyl polymerization. Even though the one-pot synthetic approach leads to imperfectly branched structures because of uncontrolled growth, it is more suitable for the preparation on a larger scale and thus for commercial use. Nowadays, different

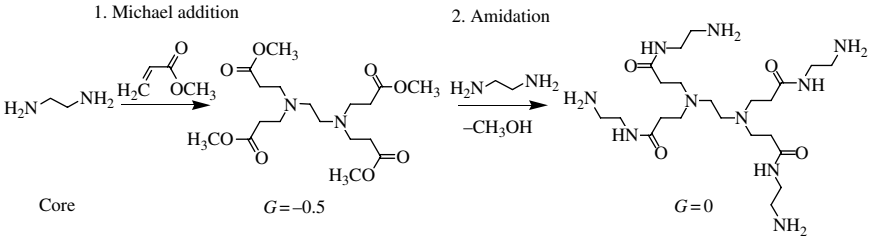

FIGURE 5.14 Synthetic steps toward PAMAM dendrimers by the divergent method.

hyperbranched polymers are commercially available, that is, Lupasol® (poly(ethylene imine) (PEI)) by BASF AG, Hybrane® (poly(ester amides)) by DSM Fine Chemicals, Boltorn® (aliphatic polyesters) by Perstorp Group, and Polyglycerol® (aliphatic polyethers) by Nanopartica GmbH.

5.2.2 Properties and Applications

The most important and characteristic feature of dendritic structures is their great number of terminal functional groups and an excellent solubility with low solution viscosity. The functionalization of these groups is a simple way to tailor the properties of dendritic macromolecules (solubility, toxicity, specific interactions, etc.). Therefore, such structures are highly interesting because of their potential applications, especially in the field of bio- and nanomedicine. Dendrimers have been investigated, for example, in the transfer of genetic material and in drug and dye delivery, as imaging agents or as nanoscale containers and biocides. The most studied dendrimer, PAMAM, was also investigated as a microbiocide to treat herpes simplex virus infections [30].

Dendritic PAMAM gadolinium polychelates have been used as magnetic resonance imaging (MRI) contrast agents [31, 32]. The sixth-generation gadolinium dendrimer displayed a significantly better performance compared to a monomeric chelate or a linear polymeric analog.

PAMAM dendrimers have also been used to transfer biomolecules into several mammalian cell lines [33]. Since PAMAM dendrimers are positively charged at physiological pH and are therefore able to interact with biologically relevant anions, for example, nucleic acids, they are particularly suited for applications as transfection agent. Transfection of various cell lines can be achieved with high efficiency but strongly depends on the dendrimer generation as well as on the cell line.

Hyperbranched polymers exhibit some properties of linear polymers like isomerism as well as structural and molecular weight dispersity. On the other hand, they have lower viscosity and higher solubility than their linear analogs.

Perfectly branched dendrimers have potentially better properties for applications in the field of biomedicine than hyperbranched polymers due to their well-defined and predictable structure and narrow mass distribution, which is important for *in vitro* and *in vivo* applications. However, hyperbranched polymers have one very significant advantage, which is their easier preparation by a one-step synthesis. Therefore, hyperbranched polymers are also used in technical applications, for example, as additives, blends, or coating components and as multifunctional cross-linkers. But both, dendrimers and hyperbranched polymers, have been extensively studied in the fields of encapsulation and delivery of drugs, dyes, and genes because of their original branched architecture (Fig. 5.15). Small molecules of interest can be incorporated in the interior cavities of dendritic molecules or bound to their outer functional groups.

An interesting representative of this class is hyperbranched polyglycerol (hPG) due to its high biocompatibility and water solubility (Fig. 5.16).

For example, Sunder et al. [34] presented the uptake of the water-soluble guest dye Congo red into nanocapsules based on amphiphilic hPG. Kurniasih et al. studied the uptake of small molecules (drugs and dyes) by hPG with a poly(ethylene glycol) (PEG) shell attached to the dendritic scaffold with or without hydrophobic linkers [35]. This resulted in the enhanced encapsulation of polar and nonpolar guest molecules, respectively, depending on the hydrophobicity of the spacer between hPG and PEG.

Another easily accessible hyperbranched polymer is PEI (Fig. 5.16), which is widely used, for example, for coatings and paper treatment but also has found wide application in biomedicine despite its high cytotoxicity [36]. Hyperbranched polyethylene imine (hPEI) is one of the most efficient nonviral transfection agents for *in vitro* and *in vivo* gene delivery. The high potential of hPEI as a gene carrier lies in the fact that every nitrogen atom in the polymer structure may be protonated. Therefore, hPEI possesses a high cationic charge density and can easily interact with negatively charged nucleic acids to form

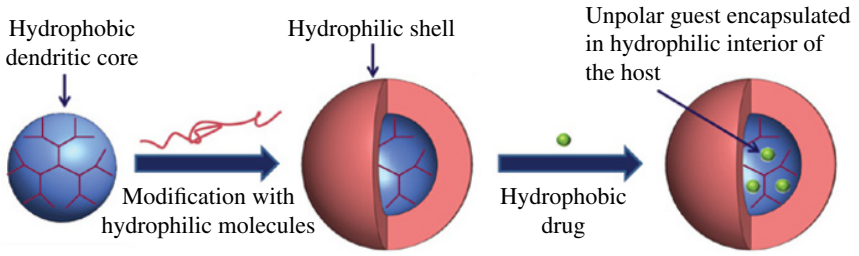

FIGURE 5.15 General scheme of a unimolecular amphiphilic core–shell dendritic architecture as drug carrier.

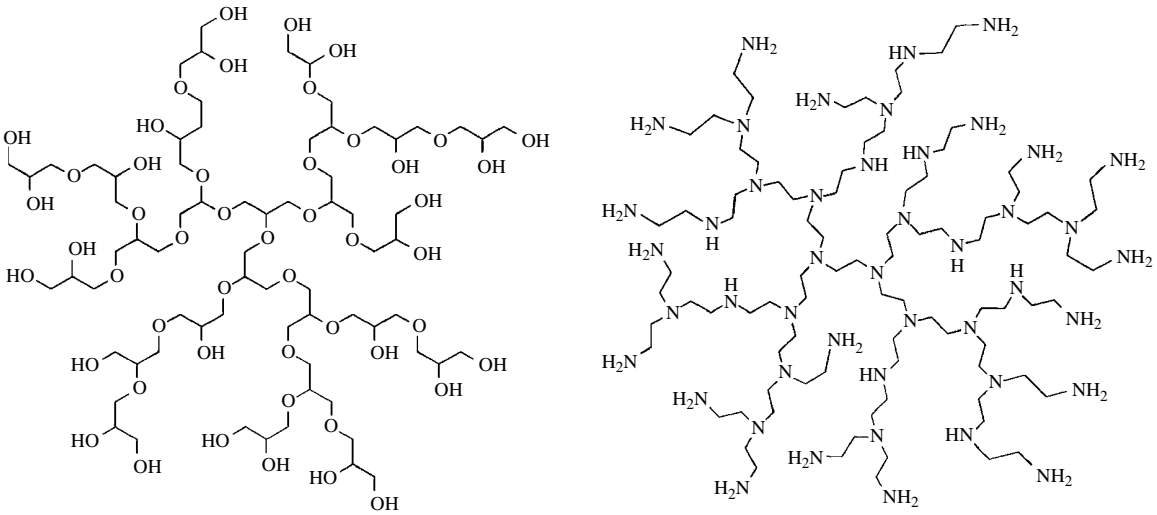

FIGURE 5.16 Hyperbranched polyglycerol (hPG) and poly(ethylene imine) (PEI).

polyplexes with them. The transfection efficiency depends on the molecular weight of hPEI, among others. The biggest problem is, however, the cytotoxicity of hPEI. Although it was reported that the complex hPEI/DNA is less toxic, hPEI itself can disrupt the cell membrane or interact with cell nuclei inducing cell lysis or cell death. In order to overcome or reduce the toxicity of hPEI, this polymer was extensively modified by functionalization of the amine end groups, for example, with PEG, hyaluronic acid, poly(*g*-benzyl-L-glutamate), polyether, and poly(vinylpyrrolidone). The broad scope of modification also contains carbohydrates like chitosan, galactose, and mannose (see also Sections 3.5 and 5.3.2). hPEI was also investigated for the preparation of nanoparticles, for cell immobilization, for inducing antimicrobial activity on cotton fabric, and for long-term storage of proteins as a stabilizer. Its technical applications include usage as flocculation agent in paper production, for heavy metal ion complexation, and as adhesive.

5.3 GLYCOPOLYMERS

Natural saccharides (carbohydrates) are highly important as biomass, food, and raw materials. As a result, their chemical modification has been investigated from early on to develop a variety of industrial products like fibers. Due to their high biocompatibility and biodegradability, carbohydrate-based materials (Fig. 5.17) have also been widely used for pharmaceutical and medical applications.

Sugars play a key role in biological processes. Besides structural scaffolds, carbohydrates are the space-filling matrices between cell membrane proteins, and they transmit information in a plethora of biological processes. In recent years, even new fields like *chemical glycobiology* have been developed [37]. As the understanding of the highly complex interactions of multivalent carbohydrates increases, their medical importance as active components also increased. The automated synthesis of carbohydrates developed by Seeberger [38] is a key element in the design of synthetic polysaccharides (see also Section 3.7.1.3) and has led to carbohydrate-based vaccines, to carbohydrates for targeted drug delivery, and to various approaches in the field of tissue engineering due to their selective cell binding capacities.

Synthetic carbohydrate polymers, so-called glycopolymers, also exhibit specific interactions with lectins and proteins. Thus, synthetic polymers containing sugar units can mimic functions similar to those found in biological interactions of natural carbohydrates. Figure 5.18 schematically highlights possible interactions of glycopolymer architectures with cell membranes.

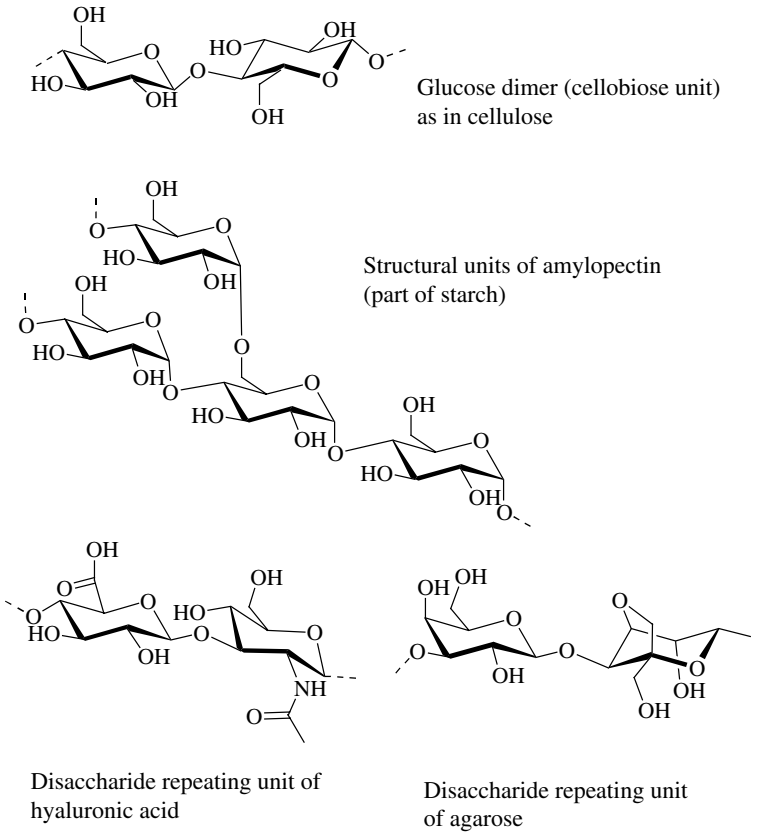

FIGURE 5.17 Common carbohydrate-based materials.

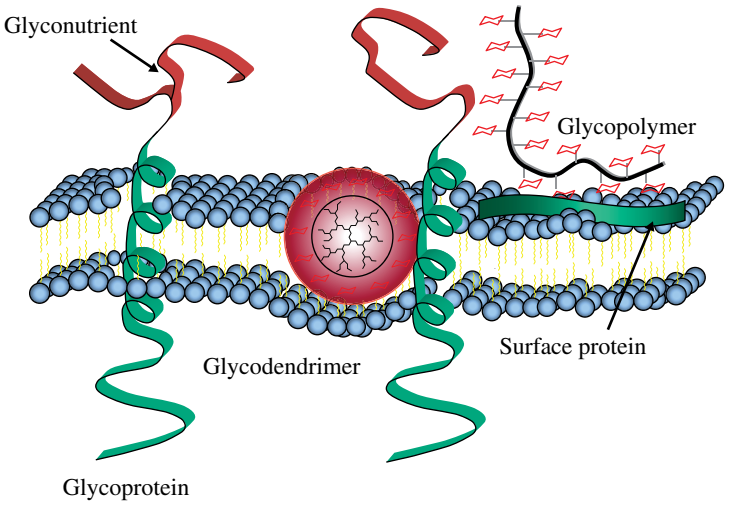

FIGURE 5.18 Schematic representation of a cell membrane decorated with glycopolymers indicating their specific biointeractions. Source: Voit and Appelhans [39a], figure 1. Reproduced with permission from John Wiley & Sons.

Synthetic glycopolymers of various architectures have been prepared in recent years using the fast development of controlled polymerization techniques and the very efficient coupling reactions in polymer analogous approaches. Both, linear and globular polymer structures that have been obtained by synthesizing dendritic, starlike, or micelle-like structures or nanogels have received much attention.

Glycodendrimers are mainly considered in various biomedical fields [39b] because of their high biocompatibility in combination with multivalency and specific interactions that are important, for example, for protein and cell membrane binding and recognition processes. The use of glycopolymers as viral and bacterial antiadhesion drugs and for inhibition of infections is very prominent (see also Sections 6.2 and 6.3).

The most important synthetic approaches toward linear and globular/branched glycopolymers will be highlighted here. Two main approaches are addressed: preformation of reactive polymers, which can be further modified by polymer analogous reaction with sugar moieties, and direct incorporation of glyco units during the polymer formation process.

5.3.1 Linear Glycopolymers

Extensive reviews on different synthetic strategies for glycopolymers have been provided by Okada in 2001 [40] and Haddleton et al. in 2004 [41] and others [39]. Especially, the various approaches toward linear glycopolymers by vinyl polymerization (radical, cationic, anionic) and through ring-opening (NCA and metathesis) polymerizations have been summarized. From early on, glycopolymers have been prepared by free radical polymerization of sugar-bearing vinyl monomers of increasing complexity and bioactivity. ROMP has also been very popular because NCA or unprotected norbornene monomers can be polymerized in a controlled manner. Anionic and cationic polymerization that could only be performed on protected glycomonomers has allowed control of the architectures and provided block copolymers.

With the development of controlled radical polymerization techniques like *nitroxide-mediated radical polymerization* (NMRP), *atom transfer radical polymerization* (ATRP), and *reversible addition fragmentation chain transfer* (RAFT) polymerization (see Section 3.2), the field of linear glycopolymers has significantly flourished, especially as control of molar mass and monomer sequence has become available, even for functionalized monomers. This enables incorporation of new and more complex glycomonomers as well as allows controlled dispersity, end group functionality, and monomer sequences in block, star-shaped, and graft copolymers, and eventually

provides a way to prepare well-defined bioconjugates and to control the self-assembly process of glycopolymers.

Control of chain length and chain functions has turned out to be highly important for glycopolymers, especially regarding their effectiveness in bio-interactions. Kiessling and coworkers [42] used the ROMP methodology to assemble glycopolymers that have been able to act as potent and selective inhibitors of carbohydrate binding proteins. This assessment was performed in terms of functional affinity and chain length using the tetrameric, mannose-binding concanavalin A in a hemagglutination inhibition assay. Up to a degree of polymerization (DP) of 52%, a strong increase in affinity was observed before a plateau value was reached, which demonstrates that multivalency, which is indicated as the number of functional repeating units, is as important in synthetic glycopolymers as in biopolymers [42].

RAFT gained special interest, firstly because this polymerization technique works very well with polar monomers and often allows polymerization of unprotected glycomonomers (Fig. 5.19). The obtained products are usually metal-free, therefore biocompatible, and polymerization in water has been long reported.

The control of the end group in controlled radical processes facilitates chain extension and block copolymer formation as well as new and interesting end functions. In their summary of various bioconjugates, Haddleton et al. [43] pointed out the potential of biotin-labeled glycopolymer structures to open the way for further bioconjugation based on specific noncovalent interactions. An interesting virus–glycopolymer bioconjugate between the cowpea mosaic virus and a glycopolymer was reported by Finn and coworkers [44]. Methacryloxyethyl glucoside was polymerized with

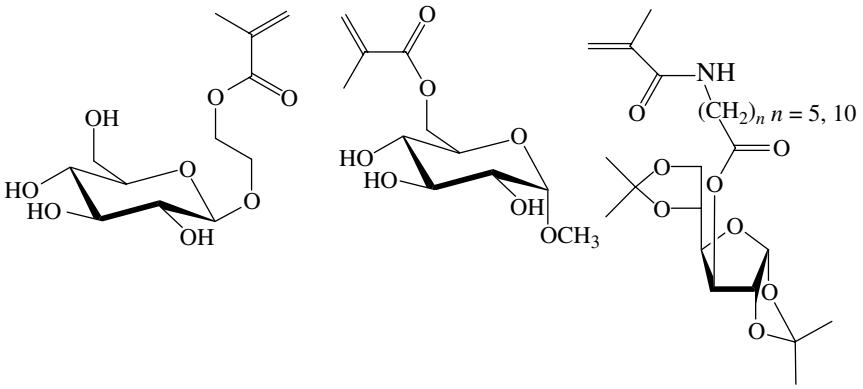

FIGURE 5.19 Examples of glycomonomers used in RAFT polymerization reactions.

ATRP using an azide-modified initiator, whereby this polymer was first coupled with a fluorescent dialkyne and then with the azide-modified virus.

The preparation of block copolymers with segments that carry glyco units and exhibit an amphiphilic character is especially interesting. These well-defined structures can be used for self-assembly processes to access more complex glycostructures.

The *chemical modification of preformed polymers*, which is simpler than using sugar-bearing monomers because the latter often require a multistep synthesis and special reaction conditions during polymerization [40], has been recently revived and performed with highly efficient and selective organic reactions (click reactions), most prominently with the classic alkyne–azide coupling and thiol–ene addition, and by using active esters (see also Section 3.3) [43]. Other examples that may be highlighted are polymers containing pentafluorostyrene units for a thiol-*p*-fluoro "click" glycosylation and thiolated oligosaccharides attached to chloroacetylated poly-L-lysine.

Glycosylated block copolymers, prepared by a thiol–ene radical photoaddition reaction of 2,3,4,6-*tetra*-*O*-acetyl-1-thio-*b*-D-glucopyranose onto 1,2-polybutadiene-*b*-poly(ethylene oxide), have been demonstrated to self-assemble in dilute aqueous solution and spontaneously form vesicles (glycosomes) with sugar-coated asymmetric membranes (Fig. 5.20) [45].

One class of polyreactions that has proven to be especially effective for the preparation of polymers with complex biologically active glyco units interesting as polyvalent ligands for specific interactions with proteins or viruses is the enzymatic modification of synthetic glycopolymers. By using enzymes, it is possible to convert rather simple sugar units into complex stereoregular oligosaccharide units that demonstrate high bioselectivity and activity. As an example, part of a synthetic scheme for preparing a water-soluble polyacrylamide with 3′-sialyl-*N*-acetyllactosamine [Neu5Acα(2->3)Galβ(1->4)GlcNAc], which was reported by Nishimura et al., is depicted in Figure 5.21 [46]. The starting glycopolymer was polyacrylamide with GlcNAc (1-acetamido-2-deoxy-β-D-glucopyranoside) units prepared by free radical copolymerization. *Bovine milk galactosyltransferase* (GalT) was used in the first step for an effective and complete galactosylation. Subsequently, *Trypanosoma cruzi trans-sialidase* (TcTs) was applied for partial sialylation.

5.3.2 Globular Glycomacromolecules

In the last two decades, many synthetic strategies and improvements have been reported for a highly efficient preparation of glycodendrimers (based on PAMAM, PPI, polyester, polyamide, cyclodextrin, etc.) and glycodendrons

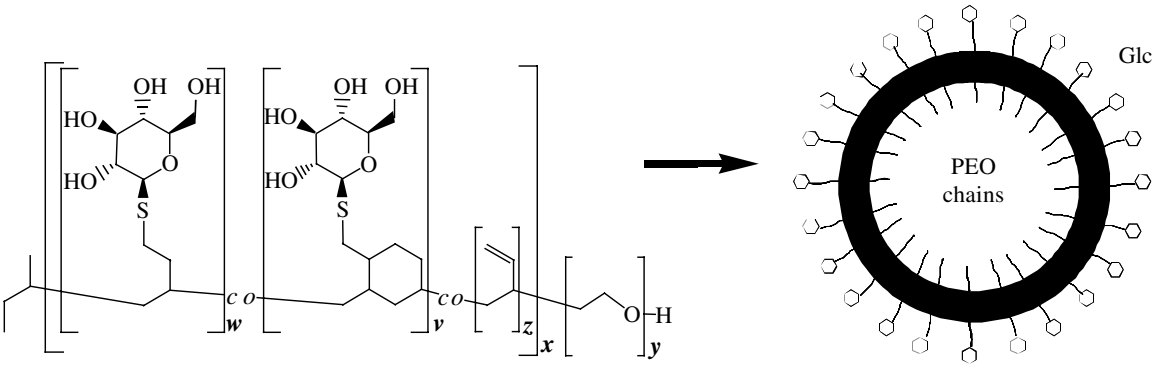

FIGURE 5.20 Amphiphilic glycoblock copolymers that self-assemble into vesicles. Source: Schlaad et al. [45], Reproduced with permission from the Royal Society of Chemistry and American Chemical Society.

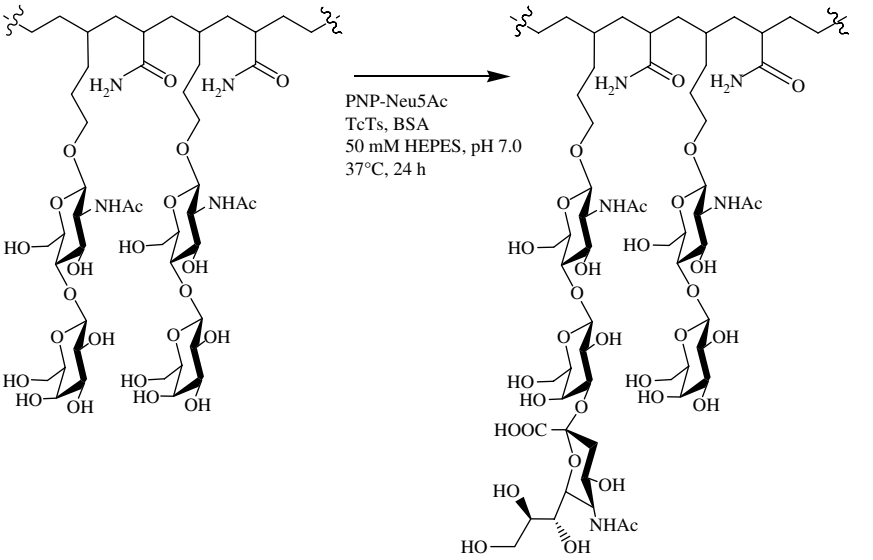

FIGURE 5.21 Enzymatic sugar elongation of a synthetic glycopolymer (only one reaction step is shown [46]; TcTs = *Trypanosoma cruzi trans-sialidase*; PNPNeu5Ac = *p*-nitrophenyl-5-acetamido-3,5-dideoxy-α-D-glycero-D-galacto-2-nonulopyranosidonic acid; BSA = bovine serum albumin; HEPES = *N*-2-hydroxyethylpiperazine-*N*′-2-ethanesulfonic acid). Source: Nishimura [46]. Reproduced with permission from Elsevier.

(based on polylysine, oligosaccharide, etc.) and their structural derivatives. This has been achieved, for example, by introducing peptide sequences (glycopeptides) in order not only to enhance binding affinities to explore biological processes but also to improve their biocompatibility as carrier systems for various drugs and for successful application in analytical devices for diagnostics.

The introduction of mono-, di-, and oligosaccharide units on dendritic surfaces is usually carried out as the final synthetic step in monodendron and dendrimer synthesis. For this purpose, well-known polymer analogous/organic conversion steps are used: amidation, esterification, reductive amination, nucleophilic substitution, addition/elimination, thiol–ene reaction, 1,3-dipolar cycloaddition, and others (Fig. 5.22).

Furthermore, simplicity is the driving force to further reduce the final coupling and deprotection steps on the dendritic surface to obtain the desired (oligo)saccharide-containing dendritic scaffolds. Much research has been focused on synthetic approaches in aqueous solution. As a result, reductive amination is now widely used under acidic and basic conditions, because it

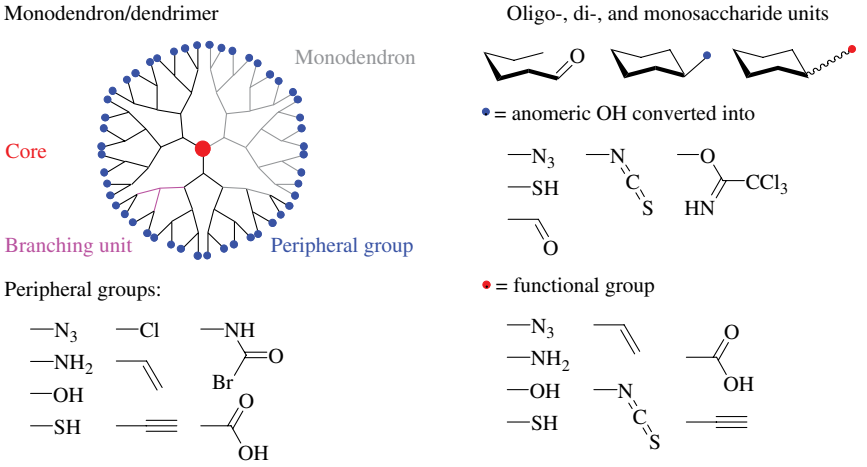

FIGURE 5.22 Main functional groups for the introduction of oligo-, di-, and monosaccharide units on monodendron and dendrimer surfaces. (*See insert for color representation of the figure*.)

allows a simple mixing of the water-soluble dendritic polymer (PPI, polylysine, etc.) with a number of (commercially available) oligo-, di-, and monosaccharides. Also, the introduction of alkyne and azide substituents in both components, the saccharide moiety and dendritic scaffold, enables a facile saccharide decoration of the dendritic scaffold surface that can be carried out in aqueous solution and in mixtures of water/organic solvent. Additionally, enzymatic conversion of simple glycodendrimers allows for a fast introduction of more complex oligosaccharides units in order to avoid additional protection/deprotection steps. As an example, the octameric sialyl Lewis^x antigen, coupled on dendritic poly-L-lysine scaffold, was obtained by combining solid phase peptide synthesis and chemoenzymatic glycosylation reactions [47]. In this context, the use of (solid phase) combinatorial chemistry has been an indispensable working tool in order to establish various glycopeptide dendrimer libraries for exploring and strengthening, for example, the binding affinity toward lectins.

The great interest in realizing different dendritic scaffolds with various (oligo)saccharide shells has been motivated by the need to establish a better understanding of the structure/activity relationship in glycodendrimers regarding the binding capacity of the biological binding unit/space in/on proteins, viruses, bacteria, and cell surfaces. Variations in the composition of the glycodendron and glycodendrimer architectures comprised the core functionality, spacer length between the branching units, and/or spacer length between (oligo)saccharide and branching unit in the outer shell, combined with varying the size of the dendritic scaffold. These variations have allowed,

for example, an effective mimicking of the HIV-1 gp120 surface for binding human HIV-1 antibody [48] and provided a way to inhibit inducible nitric oxide synthase.

Other synthetic efforts have been focused on the formation of heterofunctionalized saccharide shells in the glycodendrimers. In particular, the coupling of at least two different saccharide units or of one saccharide unit with other water-soluble functional groups has been described to enhance the binding affinity to lectins, and the influence of the density of the saccharide shell on binding affinities has been evaluated in this regard.

In contrast to the prominent efforts to realize and use perfectly branched glycodendrons and glycodendrimers, a more moderate role can be assigned to hyperbranched glycopolymers (Fig. 5.23) and other highly branched derivatives (core–shell architectures, starlike structures, formation of defined aggregates/micelles).

The most prominent representatives of hyperbranched glycopolymers are hPEI, which are decorated with different mono-, di-, and oligosaccharide

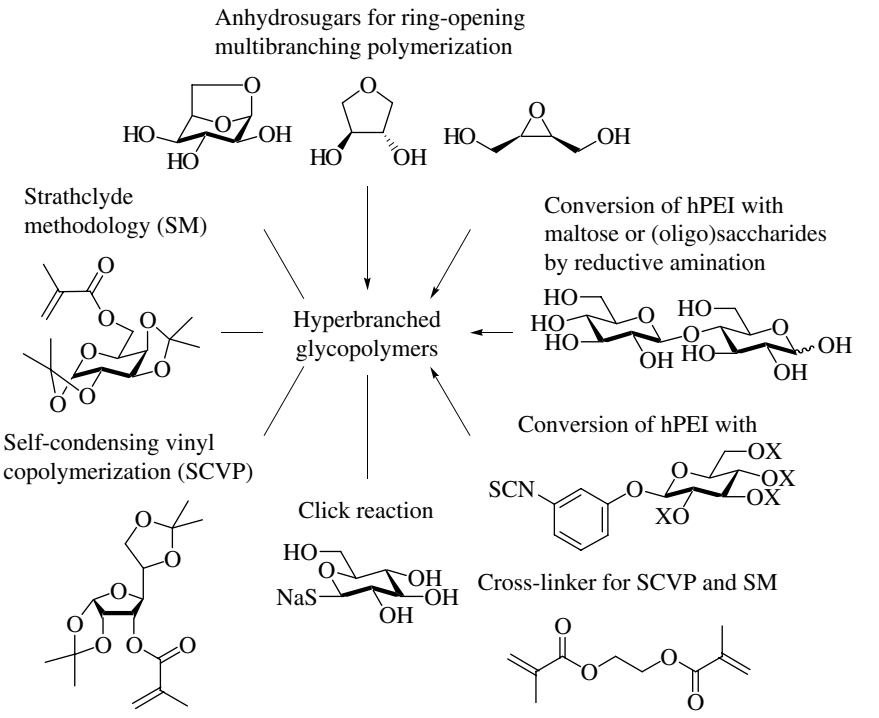

FIGURE 5.23 General synthetic approaches toward hyperbranched glycopolymers and related structures.

units and generally used as carrier systems for poly-, oligo-, and mononucleotide acids [49–51]. The introduction of the various saccharide units on PEI surfaces is preferably achieved by reductive amination or the reaction of thioisocyanate-modified saccharide units with the amino groups of hPEI.

Another very promising material for the preparation of hyperbranched glycopolymers are hPG and their derivatives that have been successfully applied as drug delivery systems. Surprisingly, a direct comparison of a sulfated glycodendrimer decorated with lactose units and sulfated hyperbranched glycopolyglycerol decorated with monosaccharide galactose [52] has revealed that the hyperbranched scaffolds exhibited more sensitive anti-inflammatory properties. Papp et al. [53] reported up to 80% of influenza virus inhibition after interaction with the hPG–sialic acid conjugated nanoparticles when they are of equal size as the virus itself (~60 nm) (Fig. 5.24; see also Section 6.3). These examples outline that perfectly branched dendrimers are not necessarily better than the irregular hyperbranched structures for mimicking, for example, the biologically active units in protein binding.

5.4 PEPTIDE-BASED STRUCTURES

The most important aspect of peptides is their inherent capacity to adopt several secondary structures that can self-assemble into tertiary structures and quaternary assemblies due to noncovalent interactions. In addition, a variety of chemical functionalities is available via naturally occurring and nonnatural amino acids that can be moreover exactly sequenced. Even complex polypeptide molecules can be synthesized rather rapidly and easily by biosynthetic and chemical methods (cf. Sections 3.3, 3.5, and 3.7). Our increasing understanding of peptide and protein folding and hierarchical assembly provides unique opportunities for the design of polymeric materials that are not easily available with traditional synthetic organic molecules and polymers. The availability of peptides with specific motifs or sequences opened up the possibility for engineering novel self-assembling supramolecular structures, for example, extended protein fibers, and other bioinspired materials, for example, hydrogel matrices, in which structure and function can be precisely specified. Such systems, incorporating intelligent features of proteins and peptides, can be potentially applied for the development of new diagnostic devices or for the preparation of scaffolds for tissue engineering that provide cells with physiologically relevant microenvironments [55–57].

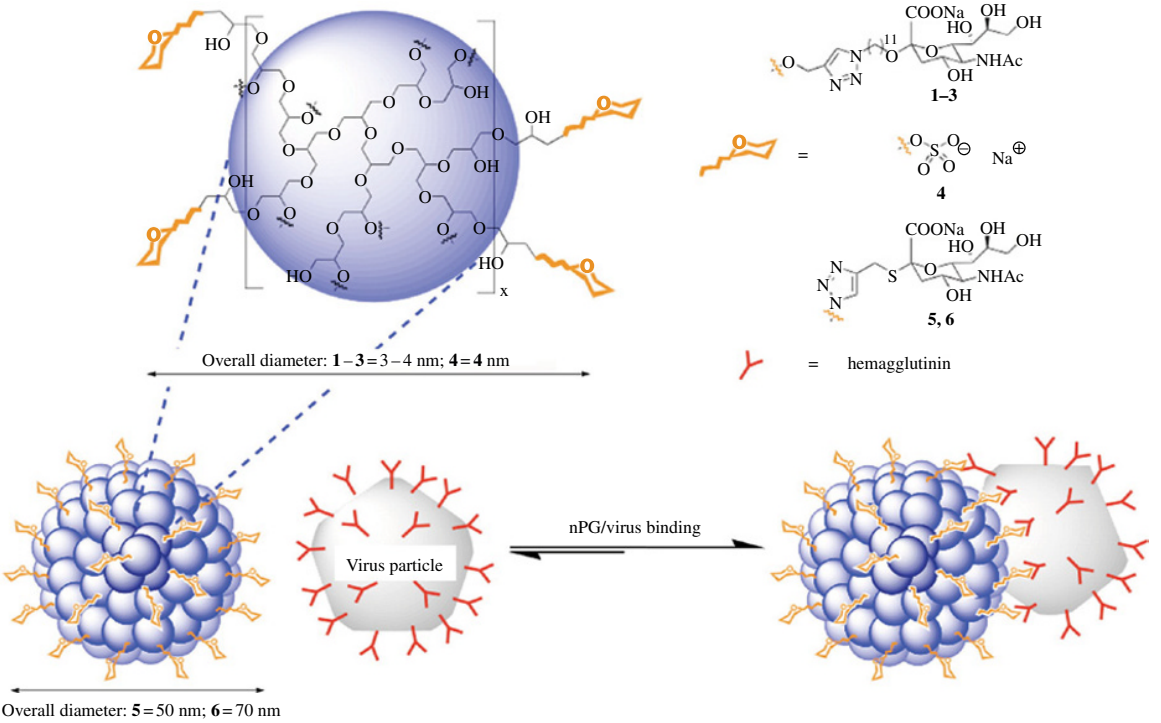

FIGURE 5.24 Sialic acid conjugated dendritic polyglycerol nanoparticles with diameters in the range of 60 nm efficiently block viral infections by polyvalent inhibition of the hemagglutinin in contrast to their smaller multivalent analog. Source: Quadir and Haag [54]. Reproduced with permission from Elsevier.

5.4.1 Hierarchical Self-Assembly of Peptide Molecules

The self-assembly of peptides leading to 3D structures is a hierarchical process (simplified shown in Fig. 5.25).

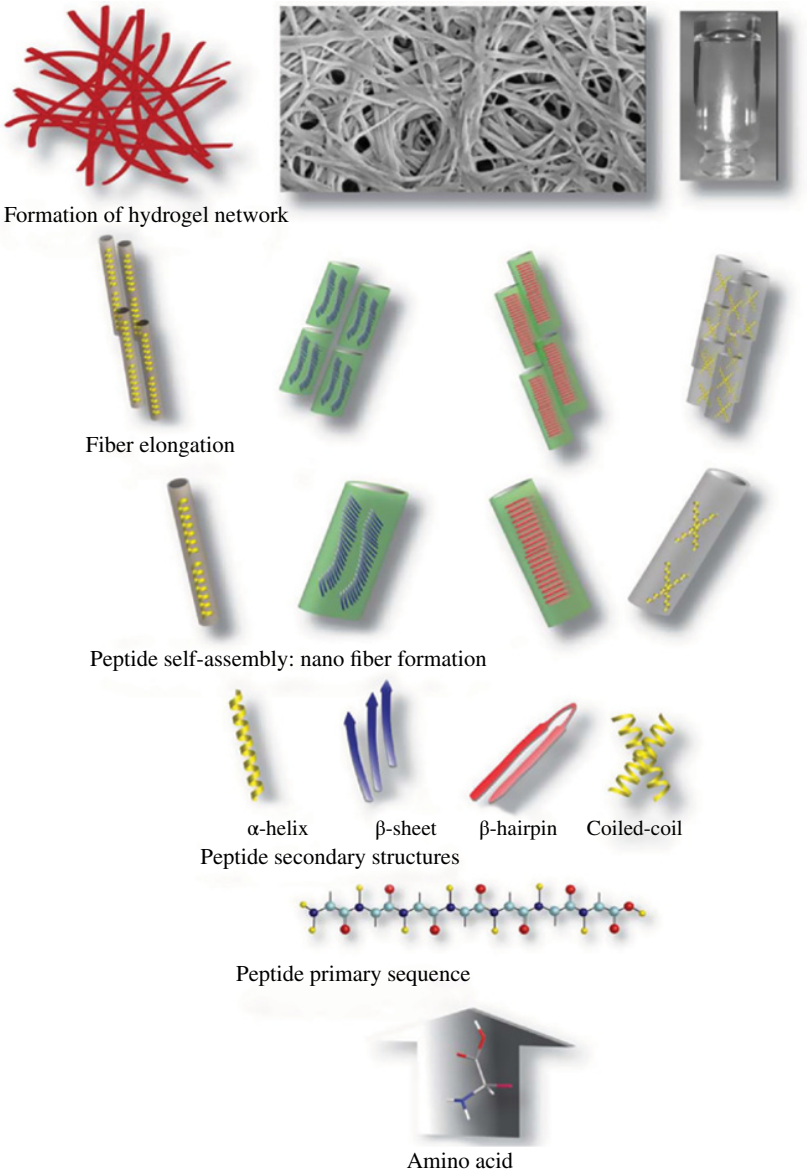

FIGURE 5.25 Simplified schematic illustrations of the hierarchical self-assembly processes involved in the formation of hydrogels from peptide molecules. Source: Dasgupta et al. [55]. Reproduced with permission from the Royal Society of Chemistry.

In solution, peptide molecules adopt a specific secondary conformation, like β-sheet, β-hairpin, α-helix, or the coiled coil (Fig. 5.26). The secondary structures then self-assemble to form nanofibers or physically cross-linked networks. Elongation of the nanofibers in 3D space leads to thicker and longer fibers, which further assemble to fibrillar networks capable of entrapping water (Fig. 5.25) [55]. β-Structured peptides dominate the literature of self-assembled systems, either natural or designed.

The folding and the hierarchical self-assembly processes are governed by hydrophobic interaction, π–π stacking, hydrogen bonding, and electrostatic interaction. Natural amino acids provide all fundamental features that promote these types of intra- or intermolecular interactions.

5.4.2 General Design Concepts for Peptide-Based Structural Materials

The wealth of natural examples provides immense inspiration for the molecular design of novel peptide-based materials that can be potentially applied as devices, sensors, and biomaterials for medical applications. In addition to hierarchical self-assembly, nature uses other mechanisms, for example, enzyme-mediated covalent cross-linking, to build up structural proteins and higher-ordered structures. In the following sections we will focus on man-made peptide-based materials that belong to the three classes listed below. They will be split with respect to the underlying design concept into materials formed by:

1. Mimicking mechanisms that nature uses in naturally occurring structural proteins (collagen, elastin, silk):
   - Self-assembly/physical cross-linking of polypeptides (e.g., triple-helix formation by collagen-derived tripeptides or self-assembly to fibers through silk-derived β-sheet-forming domains)
   - Covalent cross-linking of polypeptides (e.g., enzyme-based cross-linking via lysine-rich segments in the elastin precursor tropoelastin)
2. Self-assembly of polypeptides via other naturally occurring or *de novo* designed self-assembling domains such as coiled coils
3. Self-assembly of short peptide derivates and peptide-based amphiphilic molecules

Besides serving as structural building blocks to provide mechanical strength, peptide-based structures offer numerous possibilities to create novel bioactive and dynamic materials [57]. For instance, peptide sequences that facilitate mineralization and foster cell adhesion can be readily incorporated

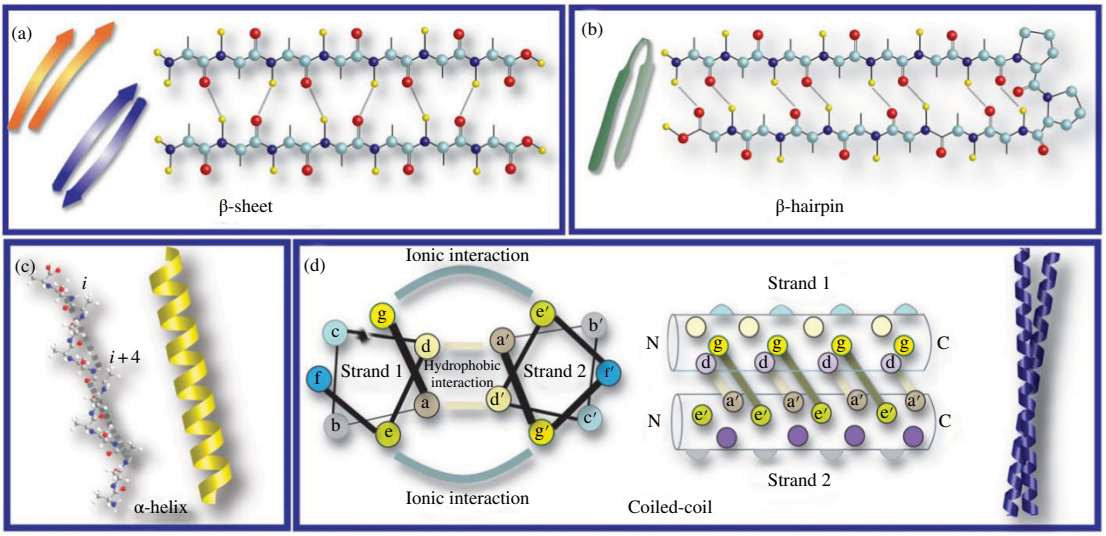

FIGURE 5.26 Schematic illustration of different secondary structures formed by polypeptides: (a) β-sheet, (b) β-hairpin, (c) α-helix, and (d) the supercoiled multistranded protein motif coiled coil. Source: Dasgupta et al. [55]. Reproduced with permission from the Royal Society of Chemistry. (*See insert for color representation of the figure*.)

in lipidated peptide amphiphiles (PA) without compromising their assembly potential [55, 56]. Fibrous materials that display common cell binding epitopes, including RGDS,[1] YIGSR, and IKVAV, are currently under intense study as extracellular matrix (ECM) mimetics due to their dual roles as structural and adhesive frameworks [58]. Molecularly designed customized polypeptide materials can be synthesized both chemically and biosynthetically (see Section 3.7).

In addition to the design principles just mentioned, peptides, proteins, and peptide-based supramolecular structures can be cross-linked into 3D networks via conventional synthetic chemistry (e.g., active ester chemistry or short synthetic cross-linkers) or via bioorthogonal click chemistry (e.g., Michael-type addition), utilizing their inherent multitude of functional groups (─NH_2, ─COOH, ─SH) and/or other additionally introduced functionalities.

Some of these basic strategies can be also adapted to create biohybrid materials consisting of peptides or proteins and synthetic organic polymer units (Section 5.5.3).

5.4.3 Noncanonical Amino Acids in Peptide/Protein Engineering

In nature the 20 proteinogenetic standard (or natural) α-amino acids that are directly encoded by the genetic code are the building blocks of all proteins within humans and other eukaryotes. Amino acids that are not among these standard amino acids are named noncanonical amino acids, nonstandard or unnatural amino acids.

The feasibility of incorporating nonstandard amino acids into peptides/proteins offers valuable options to modulate the functionality and reactivity of the produced molecular structures. Novel amino acids can be introduced in either a residue-specific or site-specific fashion. Integrating these engineered peptides into biomimetic scaffolds facilitates the construction of biomaterials with tunable chemical and mechanical properties.

5.4.4 Peptide-Based Materials Inspired by Naturally Occurring Structural Proteins

Peptide-based structural materials have often been designed by using consensus peptide sequences derived from naturally occurring structural proteins such as collagen, elastin, and silk as building blocks. Most of these building

[1] The amino acids in proteins or peptides are usually listed with their three-letter or one-letter code. Here, the one-letter code is used.

blocks can self-assemble and form higher-order structures. By engineering polypeptides that recapitulate the essential structures and properties of native collagens, elastins, and silks, limitations of animal-derived materials such as batch-to-batch variations, the risk of transmitting infectious diseases, and difficulties in modifying and precisely controlling material properties can be circumvented [57].

5.4.4.1 Collagen-Like Polypeptide Materials

Collagens are the main components of connective tissues and the most abundant proteins in mammals. More than 20 types of native collagens have been identified and proven to play distinct roles during natural tissue development and regeneration processes. They do not only provide mechanical support but also regulate a variety of cellular events, including cell adhesion, migration, proliferation, differentiation, and survival. Native collagens are characterized by the consensus tripeptide sequence GXY, in which the X and Y positions are commonly occupied by proline and post-translationally modified hydroxyproline. This feature of the primary sequence allows interchain hydrogen bonding between hydroxyproline and glycine, providing the primary driving force for the assembly of closely packed triple helices, a structural hallmark of collagens [57] and one of the basic supercoiled multistranded protein motifs [59]. Animal-derived collagen I has been used in a wide variety of tissue engineering applications, for instance, as a scaffold for tissue-engineered skin substitutes for cosmetic and burns surgery.

Collagen-inspired polypeptides composed of either collagen-derived domains or tandem repeats of the collagen-derived consensus tripeptide GXY have been designed and synthesized in order to explore fundamental aspects of peptide self-assembly and to exploit the resulting structures. Engineered polypeptides containing hydroxyproline have been biosynthesized in a variety of expression systems [57]. In this context, peptides that form a sticky-ended collagen-like triple helix by self-assembly in an offset fashion have been developed by the Hartgerink group [60]. Such systems substantially recapitulate the hierarchical self-assembly of natural collagen, as they simultaneously demonstrate triple-helix, nanofiber, and hydrogel formation at sufficient concentrations similar to the natural protein. The same research group has systematically studied the formation of collagen-like helical structures, using single amino acid substitutions in the canonical GXY repeat. Based on pairwise amino acid interactions heterotrimeric helices with far-reaching control over helix structure, assembly mechanism and stability have been prepared [61].

5.4.4.2 Elastin-Like Polypeptide Materials

Another type of important structural ECM proteins, the elastin, is rich in elastic tissues and organs, such as the cardiovascular and pulmonary system and skin, and of extreme importance for their proper function. The precursors of native elastin, the tropoelastins, are composed of alternating hydrophobic domains, enabling hydrophobic interaction, and lysine-rich domains, allowing for covalent cross-linking through the mediation of the enzyme lysyl oxidase.

Recombinant techniques and fragmentation of elastin can yield products that display many important properties of native elastin, such as high elasticity and coacervation behavior. The most common of these polymers are elastin-like polypeptides (ELPs) that have found utility in tissue engineering applications. They are composed of a repetition of the amino acid sequence of the tropoelastin molecule (VPGXG) that can be manipulated by adding any amino acid except proline at the X position [57], affording exquisite control over the final protein functionality. These engineered polypeptides are biocompatible, biodegradable, and nonimmunogenic and exhibit a lower critical solution temperature (LCST). Chemically cross-linkable ELPs have been genetically engineered by introducing lysine residues, mimicking the composition of tropoelastins [57]. Cross-linking was reached by lysyl oxidase-mediated reaction or by using bifunctional amine-reactive chemical reagents, such as glutaraldehyde. Mechanical properties of these materials can be systematically tuned in a wide range by varying the number of lysine residues and their positions along the polypeptide backbone. Applications of ELPs include the replacement of cartilage, intervertebral discs, vasculature, liver, and ocular surface [62]. Using a cell-compatible, amine-reactive cross-linker, a one-pot synthesis was conducted to simultaneously encapsulate cells while precisely controlling the grafting density of small, growth factor-mimetic peptides in the ELP hydrogels in order to provide long-term biological signals [63]. The LCST behavior of ELPs has been exploited to engineer cell sheets, which could be transplanted to repair tissue. For instance, an ELP containing the cell adhesion RGD peptide motif was directly coated on the surface of tissue culture plates [64]. At 37°C these ELP coatings were hydrophobic and presented the RGD sequence, which allowed cells to grow into monolayers. For harvesting the cells the temperature was reduced to lower values, at which the ELPs became hydrophilic. Urry and coworkers [65] demonstrated that the transition temperature of ELPs is proportional to the hydrophobicity of the repeating unit.

5.4.4.3 Silk-like Polypeptide Materials

Silk fibers have been used in textiles for more than 5000 years and as a suturing material for many centuries. Naturally occurring silk proteins are derived from silkworms and spiders [57]. The repetitive and alternating hydrophobic and

hydrophilic domains in silk proteins are responsible for their extraordinary mechanical properties, that is, both high tensile strength and elasticity at the same time. Toughness is due to the hydrophobic domains that assemble into β-sheets and form crystalline regions, whereas the less ordered hydrophilic domains provide elasticity and increase toughness. Moreover, silk is biocompatible and biodegradable and therefore an attractive material for biomedical applications [66], although silk proteins are not native in the human body. In particular, spider silks have been a focus for almost two decades. However, the inhomogeneity of natural spider silk and its low availability are major drawbacks of any application. Recently developed recombinant spider silk proteins and silk-inspired polypeptides ensure constant material properties, as well as scalable production, and further processing into morphologies other than fibers, as illustrated in Figure 5.27. For instance, films, gels, foams, capsules, spheres, and nanofibers can be prepared, thus broadening the range of applications, such as implant coatings, scaffolds for tissue engineering, wound dressing devices, as well as drug delivery systems [66, 67].

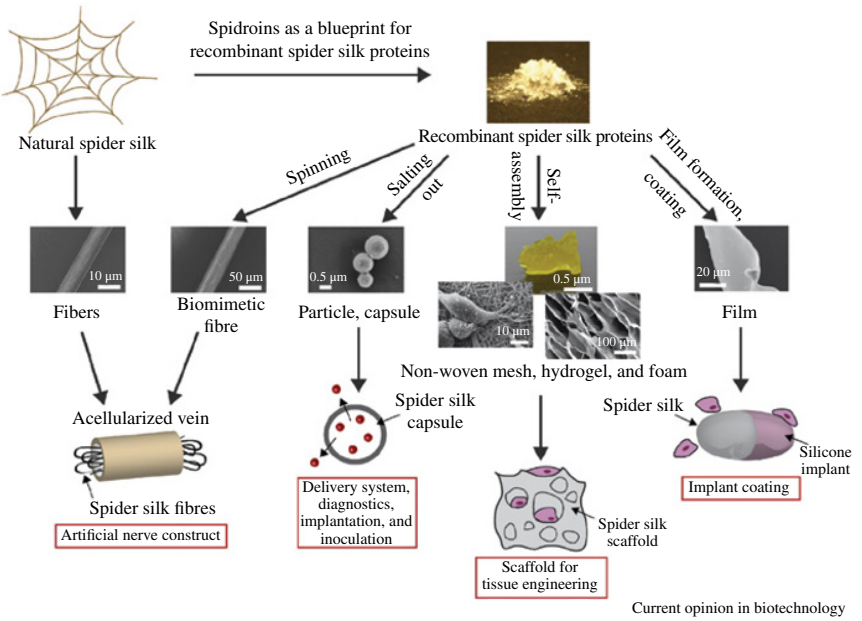

FIGURE 5.27 Possible applications of spider silk materials in biomedicine. Recombinant spider silk proteins can be processed into morphologies other than fibers, broadening the spectrum of possible applications. Source: Schacht et al. [66]. Reproduced with permission from Elsevier.

In addition, synthesis of recombinant spider silks helped to unravel a fundamental understanding of structure–function–property relationships. The relationships between molecular composition, secondary structures and mechanical properties found in different types of spider silks, as well as artificial spinning of these proteins enable a wide range of applications, including directed biomineralization [68, 69]. Molecular engineering approaches allow incorporation of additional functionalities tailored for tissue engineering requirements, such as cell adhesion and biodegradation. For instance, it was shown that materials constructed from recombinant silk-like polypeptides with genetically incorporated cell adhesion motifs, which do not exist in natural silks, significantly enhanced cell adhesion [70].

5.4.5 Polypeptide Materials Based on other Naturally Occurring or *De Novo* Designed Self-Assembling Domains such as Coiled Coils

Besides the peptide motifs discussed in Section 5.4.4, other naturally occurring and *de novo* designed self-assembling domains have been introduced into polypeptide-based polymers to yield fibers and networks. One prominent example is the α-helical coiled-coil motif, which is one of the basic supercoiled multistranded protein motifs like the collagen triple helix. However, whereas the collagen triple-helical structure requires a three-stranded configuration, in the coiled-coil structure, two or more strands of α-helices self-assemble and wrap around each other like the strands of a rope to form superhelical bundles. The primary sequences of coiled coils are characterized by a repeated pattern of seven hydrophobic and charged amino acid residues, referred to as heptad repeats *abcdefg* (Fig. 5.26d). The positions *a* and *d* are occupied by hydrophobic residues. The α-helical structure causes the formation of an amphiphilic structure. Interstrand hydrophobic interactions provide the primary driving force for self-assembly. The positions *e* and *g* of the heptads are occupied by charged residues, which mediate the specificity and stability of molecular association. An extensively studied family of coiled coils is the leucine zipper family, where the *a* and the *d* positions are mainly occupied by leucine residues.

Artificial proteins consisting of terminal leucine zipper domains flanking a central, water-soluble, and flexible polyelectrolyte segment were created by Tirrell and coworkers [71]. These peptide-based triblock copolymers undergo reversible gelation in response to changes in temperature and pH. In near-neutral aqueous solutions the terminal leucine zippers form coiled-coil aggregates and trigger the formation of a 3D polymer network. Dissociation of the

coiled-coil domains through elevation of temperature or pH causes dissolution of the gel leading to a viscous solution. A similar approach was suggested by Kopeček and coworkers [72] to create artificial protein hydrogels. However, they attached rationally designed coiled-coil domains in place of the leucine zippers. The pH- and temperature-dependent self-assembly of the hydrogels was found to be directly correlated to the structural properties of the coiled-coil domains.

Woolfson et al. reported the design of a self-assembling fiber (SAF) system [73] that comprises two complementary *de novo* designed leucine zipper peptides. Due to complementary interactions in the core and flanking ion pairs, the two peptides combine rapidly to form partly helical staggered heterodimers. These heterodimers have "sticky ends" to promote their lateral noncovalent association into extended coiled-coil fibers.

Rational architectural changes in the peptide sequences lead to the formation of fibers with improved stability and altered morphologies, for instance, thicker, thinner, branched, and segmented fibers. Most recently, the SAF system was altered to produce hydrogelating variants (hSAF) that form flexible fiber networks for use in 3D tissue culture or other applications. Since these hSAF systems are dual-peptide-based systems and gelation occurs only upon mixing of the two complementary components, tight control of gelation can be achieved [55, 57, 74].

Schneider et al. [75] described a series of *de novo* designed peptides consisting of alternating hydrophobic (valine) and hydrophilic (lysine) residues flanking a central tetrapeptide having a high type II β-turn propensity. These amphiphilic strands show stimuli-driven intramolecular folding to a β-hairpin conformation that undergoes rapid self-assembly.

5.4.6 Self-Assembly of Short Peptide Derivates and Peptide-Based Amphiphilic Molecules

5.4.6.1 Fmoc- and Boc-Protected Short Peptides

Aromatic fluorenylmethoxy carbonyl (Fmoc) dipeptides can self-assemble to form nanofibrous matrices. Gelation occurs through the formation of antiparallel β-sheets that are stabilized via the fluorenyl groups by aromatic interactions (π–π-stacking). For instance, cell-adhesive hydrogels were engineered by Gazit et al. [76] by means of self-assembly of the Fmoc-protected peptide adhesion motif RGD. Banerjee et al. reported the formation of thermoreversible pH-sensitive hydrogels from *tert*-butyloxycarbonyl (Boc)-protected di- and tripeptides [77]. These nanofibrillar networks are suitable for dye removal from industrial waste water, for example.

5.4.6.2 Peptide-Based Amphiphilic Molecules

Peptide-based amphiphilic molecules can be divided into:

- Purely peptidic systems with amphiphilic properties arising from sequences of hydrophobic and hydrophilic residues (amphiphilic peptides)
- Lipidated PA [55] in which hydrophobic lipid chains are attached to hydrophilic peptide sequences containing charged residues

Amphiphilic Peptides

Amphiphilic peptides can be in turn divided into two subclasses. One of them comprises peptide sequences formed by alternating polar and apolar residues that exhibit both hydrophilic and hydrophobic domains only when the peptide is appropriately folded. Some examples have been already discussed in Section 5.4.5. The other subclass of amphiphilic peptides contains a hydrophobic amino acid stretch attached to a number of hydrophilic amino acids that constitute the polar head group. In this context diblock copolypeptide amphiphiles consisting of the hydrophobic domain poly(L-leucine) connected to a hydrophilic polyelectrolyte domain such as poly(L-lysine) or poly(L-glutamic acid) have been reported [78]. Both domains are indispensable for hydrogel formation, and their molecular characteristics determine the properties of the resulting hydrogels. Even dilute solutions of these copolypeptides formed hydrogels with good biocompatibility that retain their mechanical strength up to temperatures of about 90°C and recover rapidly after stress.

Lipidated PA

As lipidated peptides are very common in nature and have some specific role in biological systems, synthetic lipidated peptides are of immense importance as biomaterials and therapeutic agents [55]. Grafting a hydrophobic alkyl tail onto specially designed peptide sequences allows for additional hydrophobic interaction between the peptide molecules that facilitates their self-organizing ability. Stupp and coworkers have extensively studied such lipidated PA [56] and showed that this class of molecules spontaneously forms high-aspect-ratio cylindrical nanofibers. Self-assembly of PA molecules occurs through hydrophobic collapse of the hydrophobic tails in concert with the formation of a hydrogen bonding network between the amino acid residues down the long axis of the nanofiber. Covalent coupling between neighboring cysteine residues was introduced to stabilize the resulting fibrous structure. Gelation of the nanofibers into networks can be triggered by charge screening through the addition of electrolytes or a change in pH. Cells have been successfully encapsulated in these 3D nanofibrous matrices. Bioactive epitopes can be presented in high

densities on the surface of the nanofibers to optimize cell signaling for regeneration and guide differentiation of stem cells. Macroscopically aligned constructs may be a good template for highly aligned tissue, such as muscle fibers, the spinal cord, and parts of the brain [56].

In sum, peptide-based materials offer numerous possibilities to integrate bioactive sequences, order, and dynamics in order to achieve function. Especially, due to their capability to self-assemble, peptides are, for instance, exiting materials for producing bioinspired hydrogels that enable the culture of cells within a dynamic structure. Such hydrogels are beneficial as they can mimic the heterogeneous structure and temporal changes of the native ECM. As monomer design allows fine-tuning of the self-assembly and function, customized materials for a wide range of possible applications can be obtained.

5.5 BIOHYBRID HYDROGELS

This chapter will introduce polymer systems containing either naturally occurring macromolecules (polysaccharides, proteins, DNA) or their subunits (bioanalogous molecules, amino acids, short peptides and peptide derivatives, polypeptides, polynucleotides), respectively. The natural building blocks can be connected by covalent bonds or by self-assembly and either can be used alone (see, e.g., Section 5.4) or in combination with synthetic polymer units (biohybrids). Alternatively the building block itself may be a hybrid of a natural and synthetic molecule (bioconjugate; cf. Section 3.5), as, for instance, a PEG–peptide conjugate.

Macromolecules occurring in biological systems are often highly target adapted to accurately enable specific functions. Importantly, polymer-based structures in living organisms are in general multifunctional and often gain functionality through biomolecular recognition and/or structural features due to hierarchical assembly across scales. Moreover, they afford high degrees of dynamic adaptation to varying environmental conditions. Implementing these features in engineered polymer system defines challenges of ongoing research. It is the basis of a plethora of biomimicry strategies and of paramount interest for various different applications, including the development of customized, cell-instructive scaffolds for new medical therapies to direct regeneration of tissues and organs.

In the subsequent sections, the current state of related studies will be briefly summarized focusing on basic principles and selected examples of biohybrid hydrogels.

5.5.1 Composition, Basic Principles, and Formation of Biohybrids

Whereas traditional composites consist of two or more constituents at the macroscopic (micrometer to millimeter) level, the constituents in hybrid materials are at the nanometer or molecular level.

Biohybrid materials seek to integrate both synthetic and natural components into the same system. To keep focus, we will not discuss here the related rich work on materials where one constituent is inorganic in nature (e.g., bone substitutes) and systems made of synthetic polymers with pendant amino acids or sugar residues (cf. Section 5.3). In this chapter we will concentrate on biohybrid hydrogels that are built up from biomolecules (e.g., peptide sequences, proteins, polysaccharides, polynucleotides) and synthetic organic polymers (e.g., PEG, PVA, PHEMA, poly(acryl amide)), utilizing the biomolecules as a cross-linker and/or as a building block. Such materials aim to combine the advantageous properties of the two components, namely, biological function, biomolecular recognition, chirality, degradability, and highly controlled assembly properties of the biomolecules and versatility of synthetic matter, which can result in new characteristics with unforeseen relevance. They are consequently highly suited for applications related to bioactivity, structural features, and stimuli responsiveness and dynamics, for instance, as artificial ECM for tissue engineering, for sustained and feedback-controlled drug delivery or as biosensor materials. Recent developments concern the design of biohybrid hydrogels with multiple functions, hydrogels sensitive to several stimuli, hydrogels with programmable responses, and hydrogels translating substrate recognition into mechanical action, enabling the construction of machinelike devices [79]. Some biohybrid systems have been already introduced in Sections 3.8 and 5.4, and some more examples will be given in Section 6.4.

Biohybrid hydrogels can be formed by noncovalent or covalent interactions (cf. Section 3.8). As already introduced in Section 3.8, physical networks are held together by noncovalent interactions like hydrophobic forces, hydrogen bonds, chain entanglement, crystallinity, electrostatic interactions, or highly specific biological interactions, using interacting pairs well-known from natural systems, for example, protein/ligand, peptide/peptide (cf. Section 5.4), oligosaccharide/protein, oligosaccharide/peptide, or polynucleotide/polynucleotide pairs. Reversible biomimetic cross-linking and self-assembly mediated by biorecognition of biological motifs allow for including both structural organization and dynamics in biohybrid materials as already exemplarily shown for peptide-based systems in Section 5.4 Stimulus-sensing biomaterials based on specific interactions between proteins, between proteins and

small molecules, and between complementary DNA strands have recently been reviewed by Hotz [80]. A special type of physical biohybrid networks is the so-called interpenetrating polymer networks (IPNs), that is, polymers consisting of two or more different networks (formed by either synthetic or natural precursors) that are interlaced on the polymer scale but not covalently bound to each other. For instance, alginate–polyacrylamide IPNs have been shown to form hydrogels that are both stiff and tough, making them ideal candidates for further development of load-bearing materials for cartilage replacement and soft robotics [81].

In chemical biohybrid hydrogels the building blocks are cross-linked via covalent bonds. Therefore, copolymerization schemes using photoinduced polymerization or active ester chemistry have often been employed. Photocross-linkable hydrogels are commonly prepared by UV-induced radical polymerization of reactive species containing double carbon-bonded functional groups (e.g., vinyl, acrylic, and methacrylic) [82, 83]. Materials with both synthetic and natural origins have been modified with photocross-linkable functional groups. For instance, hyaluronic acid, a polysaccharide component of natural ECM, was methacrylated to yield photocurable hydrogels with PEG [84]. Photocross-linking offers a number of advantages over other types of cross-linking schemes, as it enables generation of micro- and nanostructures, as well as easily tuning the chemical, biological, and mechanical properties of the hydrogel materials. Despite these attractive features, photocross-linkable hydrogels have also demonstrated some drawbacks, for example, DNA damage due to the formation of free radicals upon UV exposure. In addition, *in vivo* gelation of photocross-linkable hydrogel is challenging due to the limited light penetration through the tissues [85]. 3D biohybrid networks were also achieved using active ester chemistry, for instance, by cross-linking amino end-functionalized synthetic starPEG with 1-ethyl-3-(3-dimethylaminopropyl)carbodiimide/*N*-hydroxy-sulfosuccinimide (EDC/sulfo-NHS)-activated carboxylic groups of natural heparin [86] (cf. also Section 3.8).

Recent approaches have aimed at forming covalent biohybrid hydrogel networks in the presence of cells in culture or even in living tissue [87], which requires more biocompatible and selective chemical reactions. The reactions must be bioorthogonal, meaning the reagents used should not cross-react or interact in noticeable ways with the biological system and they and their products must be stable and nontoxic in physiological settings. Especially, (bioorthogonal) click chemistry (cf. Sections 3.3 and 3.4) is a synthetic strategy inspired by nature's use of simple, rapid, and powerful connecting reactions that renders it possible to generate cross-links quickly, selective and

reliable by joining small units together. In particular, the recent development of copper-free click chemistry such as strain-promoted alkyne–azide cycloaddition, Diels–Alder cycloaddition, or Michael-type addition has allowed the formation of biohybrid networks without the use of potentially toxic catalysts. For example, DeForest et al. utilized the copper-free click chemistry to create PEG–polypeptide-hybrid hydrogels [88]. The reaction between tetrazide-functionalized 4-arm PEG and bis(difluorocyclooctyne)-functionalized polypeptide resulted in hydrogel formation under physiological conditions. Another powerful reaction is the Michael-type addition reaction, as it does not require a catalyst, has no side products, and proceeds rapidly under physiological conditions [89]. A very common synthetic scheme for the formation of PEG–peptide hydrogels utilizes the thiol groups of cysteine-containing peptides as nucleophile to react with PEG polymers carrying electron-deficient double bonds at the terminal groups. Recently, Michael-type reaction schemes were applied for the formation of customized, cell-embedding, PEG–glycosaminoglycan (GAG) hydrogels with precisely adjusted polymer network properties and independently tunable signaling characteristics [90]. These *in situ* curing biohybrid hydrogel materials have been already highlighted in Section 3.8.2.5.

Alternatively, the use of enzymes has gained increasing attention particularly for the synthesis of injectable *in situ* forming biohybrid hydrogels, because enzymes usually react under physiological conditions and are mostly regarded as biocompatible [91] (cf. also Sections 5.4.4 and 3.6). Enzyme-based cross-linking reactions can often be controlled by modifying temperature, pH, or ionic strength. However, enzymatic cross-linking is only possible if the target amino acids are accessible, that is, at a surface-exposed position. As the enzyme itself may potentially serve as substrate for the cross-linking reaction, its undesired incorporation into the cross-linked network may occur. Transferases, hydrolases, and oxidoreductases can be employed as catalysts for the synthesis of biohybrid networks via oligopeptide building blocks. For instance, the activated transglutaminase enzyme factor XIIIa was utilized for cross-linking of hydrogel networks from factor XIIIa substrate-modified multiarm PEG macromers involving the formation of covalent isopeptide bridges between glutamine and lysine residues [92].

In the following we will briefly describe some selected examples of biohybrid structures and networks consisting of synthetic organic polymers and polynucleotides, polypeptides/proteins, and/or polysaccharides with focus on biomedical applications. In order to provide multifunctional biohybrid materials with the optimal combination of mechanical, biological, and structural properties for particular purposes, different design aspects must be considered.

5.5.2 Polynucleotide Biohybrids

Similar to polypeptides, oligo- and polynucleotides (single-stranded DNAs (ssDNAs)) have been used for the creation of nanoscale structures that offer a large variety of design parameters (e. g., sequence, self-assembly, and specific interaction with other biomolecules). With the solid phase synthesis method (cf. Section 3.7.1.2), oligonucleotides that share similar properties with their natural counterparts have been generated. Recently, advances in combinatorial chemistry have enabled widespread research in artificial oligonucleotides, particularly the introduction of a novel class of synthetic oligonucleotides known as aptamers. Aptamers are single-stranded short DNA or RNA oligonucleotides that bind to specific targets (e.g., small molecules, proteins, and even whole cells). They have found numerous applications in biosensing, biomedicine, and functional materials [93].

Due to their programmable sequences and precise recognition properties, oligonucleotides have received broad attention as cross-linker in hybrid hydrogels with synthetic organic polymers. Such materials are beneficial, as dramatic physical and chemical properties changes can be achieved at the macrolevel by simply changing the design parameters at the nanoscale DNA structures [94]. The highly specific base-pairing interactions of polynucleotide molecules and the reversible nature of DNA hybridization in response to external stimulus do not only allow for designing static polynucleotide-based materials but also enable the construction of biocompatible stimuli-responsive systems like sensing devices or materials for controlled release of therapeutic agents [95].

Polynucleotides can be incorporated into hydrogel networks mainly through two different strategies. The first uses dual-functionalized ssDNA, such as polynucleotides with amino groups on both ends, as permanent linker groups to induce covalent cross-linking of functionalized polymer backbones. In the second approach, duplex DNA formed by DNA hybridization serves as the noncovalent cross-linker for the hydrogels [93].

5.5.2.1 Covalent Cross-Linking by Dual-Functionalized DNA

Using the first strategy, that is, dual-functionalized polynucleotides as covalent cross-linkers, Murakami designed a new DNA-responsive hydrogel structure (Fig. 5.28) [96]. A DNA–polymer hybrid hydrogel was prepared by copolymerization of acrylamide and single-stranded polynucleotides modified with methacryloyl groups on both 3′ and 5′ ends. The addition of particular complementary polynucleotide sequences could trigger the shrinkage or expansion of the hybrid hydrogel, depending on the structure of the cross-linker, which can

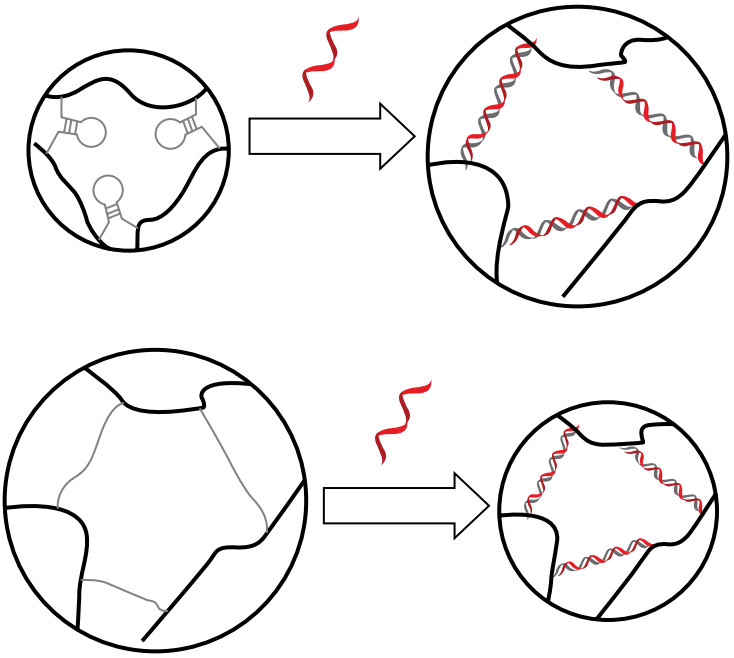

FIGURE 5.28 Target ssDNA-induced volume change of hairpin DNA (top) and DNA without secondary structure cross-linked polymer hydrogels. Source: Peng et al. [93]. Reproduced with permission from the Royal Society of Chemistry.

lead to the rational design of hydrogels with desired responsiveness for DNA sensing applications. When the polynucleotide cross-linker was designed as a hairpin, the hydrogel swelled upon the addition of a complementary polynucleotide sequences. This volume increase was explained by the hybridization-induced elimination of hairpin structure and longitudinal extension of the DNA cross-linkers. In contrast, when a polynucleotide cross-linker without secondary structure was used, the addition of the complementary polynucleotide resulted in a volume shrinkage.

5.5.2.2 Noncovalent Cross-Linking by DNA Hybridization

Nagahara and Matsuda [97] used the second approach to form a polyacrylamide/DNA hybrid hydrogel. They grafted complementary ssDNA onto polyacrylamide. Upon mixing, cross-linking based on duplex formation due to DNA hybridization occurred.

Alternatively, polyacrylamide chains were functionalized with two different noncomplementary ssDNAs. Cross-linking was then achieved with a third ssDNA ("cross-linker") that had terminal complementary sequences to the

two ssDNAs functionalized on the polyacrylamide chains. By carefully designing another ssDNA, also called "removal" DNA that can hybridize with the "cross-linker" oligonucleotide, one is able to reverse the cross-linking process [98].

The reversible nature of DNA hybridization in response to an external stimulus causes this type of DNA–polymer hydrogels to have special properties, such as sol–gel phase transition and responsive releasing capability [93]. Thus, potential applications of these materials as label-free DNA sensing device or for controlled drug delivery have been discussed. Just a small portion of DNA is needed to achieve hydrogel responsiveness.

Tierney and Stokke [99] used a slightly different approach for label-free sensing of polynucleotides. They designed a covalently cross-linked polyacrylamide hydrogel with additional noncovalent junction points based on hybridized oligonucleotides grafted to the polyacrylamide backbone. Addition of a target sequence that destabilized the junction points in competitive displacement-hybridization, induced swelling of the functional hydrogel. This swelling is sensitive to the concentration of the probe, the sequence, and the matching length between probe and sensing oligonucleotide. An interferometric readout platform was used to determine changes in the optical length of the DNA hybrid hydrogel.

To further expand the functionality of polypeptide hybrid hydrogels, aptamers that bind specifically to various small molecules and protein transcription factors (operator/promoter sequences) have been integrated in their network. Polyacrylamide main chains were branched with polynucleotide strands, which could be gelatinized by DNA base pairing with a second thrombin-bound polynucleotide strand ("cross-linker"). A third DNA strand that can form a duplex with the "cross-linker" strand was used to dissolve the hydrogel and to release the thrombin [100].

A similar system was developed for detection and separation of adenosine. Linear polyacrylamide polymers grafted with two different single polynucleotide strands were cross-linked via a third cross-linker ssDNA. The cross-linker strand included segments that are complementary to the two polynucleotide strands for hydrogel formation. Moreover, it contained a toehold segment for the initiation of DNA displacement to enable a reversible hydrogel transition and an adenosine aptamer segment. By target recognition of the aptamer in the cross-linker strand, the DNA hydrogel system acts as a molecular hook to fish out specific molecules in a pool of different molecules. A subsequent target separation step was realized by first washing away the nonspecific targets from the hydrogel and then dissolving the hydrogel by adding a fourth strand, fully complementary to the cross-linker strand, to the system [101].

5.5.3 Polypeptide or Protein Biohybrids

Due to their unique properties that have been already discussed in Section 5.4, polypeptides and proteins are useful building blocks also for constructing biohybrid hydrogels. Such hybrid materials combine synthetic organic polymers with, for instance, natural ECM proteins, cellular recognition sequences, growth factors, or their functional subunits, enzyme sensitive peptides, and/or peptide ligands with high affinity to other biomolecules.

Often well-defined peptide–polymer bioconjugates (cf. Section 3.5) have been used as precursors for polypeptide biohybrid materials due to their capability to undergo biorecognition-driven spontaneous self-assembly and self-organization into highly organized nanoscale and higher-order structures and networks via noncovalent interactions. By using similar design concepts as introduced for peptide-based systems in Section 5.4, multifunctional fibrous materials and dynamic biohybrid hydrogel systems, which respond to endogenous stimuli, including pH or specific binding of a biochemical ligand, have been created. For instance, the Kopeček group [102] has utilized the coiled-coil motif (cf. Section 5.4) quite extensively as cross-linker for synthetic polymers to create hybrid hydrogels that are both pH and salt responsive. Alternatively to interactions between peptide secondary structure elements, high-affinity molecular interactions between proteins or peptides and other biomolecules can be employed to form noncovalently cross-linked biohybrid networks. Some examples for protein/peptide/GAG interactions will be discussed in Chapter 6 dealing with polysaccharide-based biohybrid materials. Physical peptide–synthetic polymer hybrid hydrogels formed by noncovalent interactions appear, for instance, as suitable biocompatible materials for injectable *in vivo* gelling tissue engineering scaffolds [103], for cell delivery and controlled drug delivery, as well as for biosensors.

Covalent protein/peptide biohybrid hydrogels have been prepared by enzyme-mediated reaction and by (bioorthogonal) chemical cross-linking (e.g., Michael-type addition and other types of click chemistry, photochemical cross-linking, ester or amide formation using the carboxyl or amino groups of the peptides/proteins and functional groups of the synthetic polymers). Some examples for peptide–organic polymer biohybrid hydrogels have already been mentioned in Section 5.5.1. Several studies aimed to incorporate ECM proteins in synthetic networks in order to serve as a quasinatural microenvironment for encapsulated cells. In hydrogels formed from collagen or gelatin (derived from hydrolyzed collagen) and synthetic organic polymer like PEG, PVA, or PHEMA, the ECM proteins retained their adhesive properties of and their susceptibility to enzymatic remodeling. This was demonstrated, for

instance, by the formation of capillary vessel-like networks in PEG–collagen hydrogels after photoencapsulation and *in vitro* coculture of endothelial cells and fibroblasts within this biohybrid material [104], indicating their potential to support the formation of vascularized tissue constructs for application in regenerative medicine. Such hybrid hydrogel scaffolds often overcome the limitations of pure protein scaffolds, for example, low mechanical stability or lack of flexibility. Proteins can be further chemically cross-linked with synthetic polymers bearing multiple maleimide residues via their thiol groups using Michael-type addition. However, free thiol groups occur rather rarely in proteins as cysteine has a low relative abundance. Moreover, most inherent cysteine residues in proteins are not accessible to chemical reactions due to the formation of intramolecular disulfide bonds or being buried in the inner part of proteins [105]. Thus, there have been some attempts to genetically introduce cysteine residues to proteins to allow for gelation through thiol–maleimide addition reaction.

In order to mimic the enzymatic remodeling of the natural ECM, not only ECM proteins have been used as natural building block for biohybrid hydrogels. Alternatively, oligopeptide cross-linkers sensitive to cleavage by matrix metalloproteases (MMP) have been introduced in many synthetic gels, thus permitting the degradation and remodeling of the material by cells secreting this enzymes. One example of such an MMP-responsive biohybrid hydrogel that can be expected to support the vascularization of engineered tissues will be presented in Section 6.4.5 [106]. The concrete design of the peptide sequence is an important feature. For instance, the rate of degradation can be further controlled by utilizing peptides with different enzymatic sensitivities. Moreover rational peptide design allows for the synthesis of hydrogels that are responsive to other enzymes. As an example, a thrombin-cleavable network will be discussed in more detail in Section 6.4.2. This material may be applied as heparin delivery system with feedback-control and consequently as “intelligent” material for anticoagulant coatings.

5.5.4 Polysaccharide Biohybrids

Highly specific interactions between polysaccharides and proteins or peptides have been utilized for the design of noncovalently bound biohybrid hydrogels. Incorporation of polysaccharides into biomaterials has been moreover employed as a method of presenting and delivering proteins and other bioactive substances in various biomedical applications. Furthermore, polysaccharides are susceptible to enzymatic cleavage and have therefore been used as degradable cross-linker in covalently bound networks with synthetic building blocks.

Here, we will concentrate on polysaccharide biohybrid hydrogels that have been developed for application in tissue engineering. Among those, biohybrid materials based on GAGs and synthetic polymers allow for a fargoing recapitulation of signaling characteristics of ECM, including the reversible conjugation of a wide variety of soluble growth factors (e.g., [107–113]) due to their high affinity to the GAG component [114]. The sequestration of growth factors is an important trigger of morphogenesis and tissue regeneration. Moreover, GAG-based biohybrid matrices were successfully applied for the feedback-controlled delivery of bioactive substances (Section 6.4).

In the following, we limit ourselves on biohybrid hydrogels containing the highly sulfated GAG heparin as a base for the reversible binding and sustained delivery of multiple growth factors. For instance, heparin has been incorporated into noncovalently assembled, polymeric hydrogel networks based on its interactions with known heparin-interacting basic peptides and proteins, as excellently reviewed in Ref. [111]. Four-arm PEG polymers (starPEG) functionalized with heparin-binding peptide motifs on each arm were reported to assemble with heparin into viscoelastic solutions with tunable properties (e.g., [107]). Recently a library of peptides was synthesized, and starPEG–peptide conjugates were screened for hydrogel formation with heparin in order to study the structure–function relationship of oligosaccharide-dependent macromolecular noncovalent assembly [112]. It was shown that both basic residues and the heparin-induced α-helix formation of the peptides are important for the gelation process (Fig. 5.29). Simple rules enabled tuning various aspects of the matrix system such as gelation rates, biodegradability, rheological properties, and biofunctionality. The hydrogels can encapsulate cells and support cell survival.

Alternatively, starPEG–peptide conjugates can be mixed with starPEG–heparin conjugates to form physically cross-linked hydrogels capable of growth factor delivery via hydrogel erosion (e.g., [108]). Such erosion strategies, although passive, may offer opportunities to modulate the growth factor activity via corelease of the growth factor with the heparinized macromolecules. In addition, physical networks were formed through direct association of similar PEG–heparin conjugates with dimeric heparin-binding growth factors (specifically vascular endothelial growth factor (VEGF)) [115]. These hydrogels degrade through receptor-mediated erosion as VEGF is delivered to the cells.

Other authors reported the covalent incorporation of heparin into hydrogel networks: Anseth and coworkers [110] have copolymerized methacrylated high molecular weight heparin and dimethacrylated PEG to yield hydrogels of varying composition. These gels were analyzed as a possible delivery vehicle

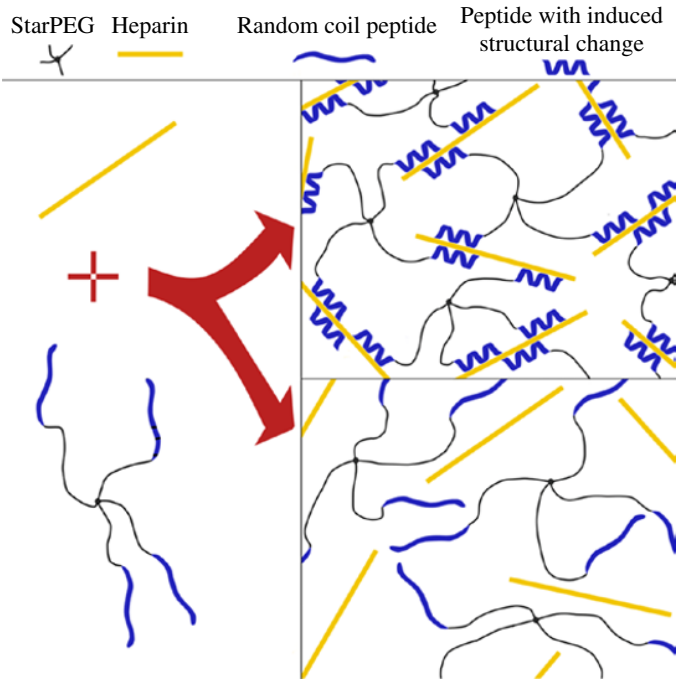

FIGURE 5.29 Screening of peptide motifs coupled to starPEGs that can form hydrogels with 14 kDa heparin. Source: Wieduwild et al. [112]. Reproduced with permission from American Chemical Society.

for basic fibroblast growth factor (FGF-2) and as a synthetic ECM for the osteogenic differentiation of human mesenchymal stem cells. In another approach [109] heparin was modified with a dihydrazide and cross-linked to the *N*-hydroxysuccinimidyl ester of PEG-bis-butanoic acid.

Kiick [116] suggested the combination of noncovalent assembly strategies with covalent cross-linking methods for the formation of mechanically tunable, biodegradable heparinized hydrogels. They investigated methods to functionalize heparin with chemically reactive groups at controlled degrees of substitution and demonstrated the rapid *in situ* cross-linking of this multifunctional heparin with thiol-derivatized PEGs of various molecular weights and polymer structures. The gels can be used as a controlled delivery vehicle for growth factors with activities useful for tissue regeneration and vascularization.

Recently, a modular hydrogel platform based on starPEG and heparin was developed utilizing a rational design strategy [113]. Carboxylic groups of heparin were activated with carbodiimide/sulfo-NHS to create a hydrogel network by the formation of amide bonds, with *N*-terminal amino groups of

starPEG. These materials allow the decoupling of their mechanical and biomolecular characteristics, which is considered a prerequisite for *in vitro* assays suitable for dissecting the cell-instructive roles of biochemical and physical cues. This work was further extended by using cell-compatible Michael-type reaction schemes for cell-embedding and *in vivo* gelation [90, 106] (Section 3.8). The heparin component allows for the versatile biomimetic functionalization of the obtained materials with a plethora of GAG-binding growth factors and for the covalent conjugation of adhesion ligands via carbodiimide or click chemistry. Network formation through enzymatically cleavable peptide linkers creates cell-responsive environments (cf. Sections 5.5.2.1 and 6.4), which also facilitated delivery of growth factors. These bioactive multifunctional materials are expected to become instrumental in medical technologies aimed at regenerating diseased or injured tissues. A further option to modulate the release profiles of growth factors from GAG-based hydrogels is the substitution of the native heparin compound in the biohybrid network by selectively desulfated heparin derivatives, as the sulfation patterns of GAGs govern the electrostatic complexation of biomolecules [117].

Summarizing, biohybrid materials represent significantly more than the sum of the individual building blocks. The combination of biological (signaling) molecules and synthetic organic polymers has opened the door to novel applications, not only in biomedicine for tissue engineering or drug delivery but also in medical and environmental analytics [80].

REFERENCES

[1] Barz, M.; Luxenhofer, R.; Zentel, R.; Kabanov, A. V. *Biomaterials* 2009, 30, 5682–5690.

[2] Pospiech, D.; Starke, S.; Bünker, T.; Müller, F.; Frenzel, R.; Simon, F.; Grundke, K.; Oertel, U.; Opitz, M.; Kruspe, R.; Voit, B. *Proceedings of International Conference on Heat Exchanger Fouling and Cleaning* 2013, 10, 210–215.

[3] Ringsdorf, H. *Journal of Polymer Science: Polymer Symposia* 1975, 51, 135–153.

[4] Lutz, J. F.; Ouchi, M.; Liu, D. R.; Sawamoto, M. *Science* 2013, 341, 628–636.

[5] Hibi, Y.; Ouchi, M.; Sawamoto, M. *Angewandte Chemie International Edition* 2011, 50, 7434–7537.

[6] McKee, M.; Milnes, P.; Bath, J.; Stulz, E.; Turberfield, A. J.; O'Reilly, R. K. *Angewandte Chemie International Edition* 2010, 49, 7948–7951.

[7] Förster, S.; Plantenberg, T. *Angewandte Chemie International Edition* 2002, 41, 688–714.

[8] Kuila, B. K.; Stamm, M. *Journal of Materials Chemistry* 2011, 21, 14127–14134.

[9] Bates, F. S. *Science* 1991, 251, 898–905.

[10] Hamley, I. W., ed., *Developments in Block Copolymer Science and Technology*, John Wiley & Sons, Ltd, Chichester: 2004.

[11] Bratton, D.; Yang, D.; Dai, J.; Ober, C. K. *Polymers for Advanced Technology* 2006, 17, 94–103.

[12] Nandan, B.; Stamm, M. "Self-assembled polymer supermolecules as templates for nanomaterials" in *Supramolecular Chemistry: From Molecules to Nanomaterials* (eds. Steed, J. W.; Gale, P. A.), Wiley-VCH, Weinheim: 2012, 3563–3586.

[13] Abetz V. *Encyclopedia of Polymer Science and Technology* (ed. Kroschwitz, J. I.) Wiley VCH, Hoboken, vol. 1, 2003, 482–523.

[14] Abetz, V.; Markgraf, K.; Rebizant, V. *Macromolecular Symposium* 2002, 177, 139–146.

[15] Park, C.; Yoon, J.; Thomas, E. L. *Polymer* 2003, 44(22), 6725–6760.

[16] Glass, R.; Moller, M.; Spatz, J. P. *Nanotechnology* 2003, 14, 1153–1160.

[17] Arnold, M.; Cavalcanti-Adam, E. A.; Glass, R.; Blümmel, J.; Eck, W.; Kantlehner, M.; Kessler, H.; Spatz, J. P., *ChemPhysChem* 2004, 5, 383–388.

[18] Gröschel, A. H.; Schacher, F. H.; Schmalz, H.; Borisov, O. V.; Zhulina, E. B.; Walther, A.; Müller, A. H. E. *Nature Communications* 2012, 3, Article number: 710.

[19] Betthausen, E.; Drechsler, M.; Förtsch, M.; Schacher, F. H.; Müller, A. H. E. *Soft Matter* 2011, 7, 8880–8891.

[20] Egli, S.; Nussbaumer, M. G.; Balasubramanian, V.; Chami, M.; Burns, N.; Palivan, C.; Meier, W. *Journal of the American Chemical Society* 2011, 133, 4476–4483.

[21] Voit, B.; Lederer, A. *Chemical Reviews* 2009, 109, 5924–5973.

[22] Flory, P. J. *Journal of the American Chemical Society* 1952, 74, 2718–2723.

[23] Kim, Y. H.; Webster, O. W. *Macromolecules* 1992, 25, 5561–5572.

[24] Yan, D.; Gao, C.; Frey H., eds. *Hyperbranched Polymers: Synthesis, Properties, and Applications, Wiley Series on Plastics Engineering and Technology*, John Wiley & Sons, Inc., Hoboken, NJ: 2011.

[25] Tomalia, D. A.; Fréchet, J. M. J. *Journal of Polymer Science Part A: Polymer Chemistry* 2002, 40, 2719–2728.

[26] Hawker, C. J.; Fréchet, J. M. J. *Journal of the American Chemical Society* 1990, 112, 7638–7647.

[27] Wörner, C.; Mülhaupt, R. *Angewandte Chemie International Edition in English* 1993, 32, 1306–1308.

[28] de Brabander-van den Berg, E. M. M.; Meijer, E. W. *Angewandte Chemie International Edition in English* 1993, 32, 1308–1311.

[29] Buhleier, E.; Wehner, W.; Vögtle, F. *Synthesis* 1978, 155–158.

[30] Frey, H.; Haag, R. *Reviews in Molecular Biotechnology* 2002, 90, 257–267.

[31] Wiener, E. C.; Brechbiel, M. W.; Brothers, H.; Magin, R. L.; Gansow, O. A.; Tomalia, D. A.; Lauterbur, P. C. *Magnetic Resonance in Medicine* 1994, 31, 1–8.

[32] Wiener, E. C.; Auteri, F. P.; Chen, J. W., Brechbiel, M. W.; Gansow, O. A.; Schneider, D. S.; Belford, R. L.; Clarkson, R. B.; Lauterbur, P. C. J. *American Chemical Society* 1996, 118, 7774–7782.

[33] (a) Haensler, J.; Szoka, F. C., Jr. *Bioconjugate Chemistry* 1993, 4, 372–379; (b) Kukowska-Latallo, J.; Bielinska, A. U.; Johnson, J.; Spindler, R.; Tomalia, D. A.; Baker, J. R., Jr. *Proceedings of the National Academy of Sciences of the United States of America* 1996, 93, 4897–4902.

[34] Sunder, A.; Krämer, M.; Hanselmann, R.; Mülhaupt, R.; Frey, H. *Angewandte Chemie International Edition* 1999, 38, 3552–3555.

[35] Kurniasih, I. N.; Liang, H.; Möschwitzer, V. D.; Quadir, M. A.; Radowski, M.; Rabe, J. P.; Haag, R. *New Journal of Chemistry* 2012, 36, 371–379.

[36] Jäger, M.; Schubert, S.; Ochrimenko, S.; Fischer D.; Schubert, U. S. *Chemical Society Reviews* 2012, 41, 4755–4767.

[37] Maheshwari, R.; Liu, S.; Polizzotti, B. D.; Wang, Y.; Kiick, K. L. *American Chemical Society Symposium Series* 2008, 990, 288–305.

[38] Seeberger, P. H. *Carbohydrate Research* 2008, 343, 1889–1896.

[39] (a) Voit, B.; Appelhans, D. *Macromolecular Chemistry and Physics* 2010, 211, 727–735; (b) Appelhans, D.; Klajnert-Maculewicz, B.; Janaszewska, A.; Lazniewsk L.; Voit, B. *Chemical Society Review* 2015, 44, 3968–3996.

[40] Okada, M. *Progress in Polymer Science* 2001, 26, 67.

[41] Ladmiral, V.; Meia, E.; Haddleton, D. M. *European Polymer Journal* 2004, 40, 431.

[42] Gestwicki, J. E.; Cairo, C. W.; Strong, L. E.; Oetjen, K. A.; Kiessling, L. L.; *Journal of the American Chemical Society* 2002, 124, 14922.

[43] Nicolas, J.; Mantovani, G.; Haddleton, D. M. *Macromolecular Rapid Communications* 2007, 28, 1083.

[44] Gupta, S. S.; Raja, K. S.; Kaltgrad, E.; Strable, E.; Finn, M. G. *Chemical Communications* 2005, 15, 954.

[45] (a) Schlaad, H.; You, L.; Sigel, R.; Smarsly, B.; Heydenreich, M.; Mantione, A.; Masic, A. *Chemical Communications* 2009, 1478–1480; (b) You, L.; Schlaad, H.; *Journal of the American Chemical Society* 2006, 128, 13336–13337.

[46] Nishimura, S.-I.; Lee, K. B.; Matsuoka, K.; Lee, Y. C. *Biochemical and Biophysical Research Communications* 1994, 199, 249–254.

[47] Palcic, M.; Li, H.; Zanini, D.; Bella, R. S.; Roy, R. *Carbohydrate Research* 1998, 305, 433–442.

[48] Wang, J.; Li, H.; Zou, G.; Wang, L.-X. *Organic & Biomolecular Chemistry* 2007, 5, 1529–1540.

[49] Diebold, S. S.; Kursa, M.; Wagner, E.; Cotten, M.; Zenke, M. *The Journal of Biological Chemistry* 1999, 274, 19087–19094.

[50] Kunath, K.; von Harpe, A.; Fischer, D.; Kissel, T. *Journal of Controlled Release* 2003, 88, 159–172.

[51] Appelhans, D.; Komber, H.; Quadir, M. A.; Richter, S.; Schwarz, S.; van der Vlist, J.; Aigner, A.; Müller, M.; Loos, K.; Seidel, J.; Arndt, K.-F.; Haag, R.; Voit, B. *Biomacromolecules* 2009, 10, 1114–1124.

[52] Calderon, M.; Gräser, R.; Kratz, F.; Haag, R. *Bioorganic & Medicinial Chemistry Letters* 2009, 19, 3725–3728.

[53] Papp, I.; Sieben, C.; Sisson, A. L.; Kostka, J.; Böttcher, C.; Ludwig, K.; Herrmann, A.; Haag, R. *ChemBioChem—A European Journal of Chemical Biology* 2011, 12, 887–895.

[54] Quadir M. A.; Haag, R. *Journal of Controlled Release* 2012, 161, 484–495.

[55] Dasgupta, A.; Mondal, J.-H.; Das, D. *RCS Advances* 2013, 3, 9117–9149.

[56] Matson, J. B.; Stupp, S. I. *Chemical Communication (Camb)* 2012, 48, 26–33.

[57] Burdick, J. A.; Mauck, R. L. *Biomaterials for Tissue Engineering Applications. A Review of the Past and Future Trends*, Springer, Wien: 2010.

[58] Jung, J. P.; Moyano, J. V.; Collier, J. H. *Integrative Biology* 2011, 3, 185–196.

[59] Beck, K.; Brodsky, B. *Journal of Structural Biology* 1998, 122, 17–29.

[60] O'Leary, L. E. R.; Fallas, J. A.; Bakota, E. L.; Kang, M. K.; Hartgerink, J. D. *Nature Chemistry* 2011, 3, 821–828.

[61] Jalan, A. A.; Hartgerink J. D. *Current Opinion in Chemical Biology* 2013, 17, 960–967.

[62] Nettles, D. L.; Chilkoti, A.; Setton, L. A. *Advanced Drug Delivery Reviews* 2010, 62, 1479–1485.

[63] Cai, L.; Dinh, C. B.; Heilshorn, S. C. *Biomaterials Science* 2014, 2, 757–765.

[64] Zhang, H. L.; Iwama, M.; Akaike, T.; Urry, D. W.; Pattanaik, A.; Parker, T. M.; Konishi, I.; Nikaido, T. *Tissue Engineering* 2006, 12, 391–401.

[65] Urry, D. W.; Harris, R. D.; Long, M. M.; Prasad, K. U. *International Journal of Peptide and Protein Research* 1986, 28, 649–660.

[66] Schacht, K.; Scheibel, T. *Current Opinion in Biotechnology* 2014, 29, 62–69.

[67] Seib, F. P.; Kaplan, D. L. *Israel Journal of Chemistry* 2013, 53, 756–766.

[68] Cranford, S. W.; Tarakanova, A.; Pugno, N. M.; Buehler, M. J. *Nature* 2012, 482, 72–76.

[69] Tokareva, O.; Jacobsen, M.; Buehler, M.; Wong, J.; Kaplan, D. L. *Acta Biomaterialia* 2014, 10, 1612–1626.

[70] Bini, E.; Foo, C. W. P.; Huang, J.; Karageorgiou, V.; Kitchel, B.; Kaplan D. L. *Biomacromolecules* 2006, 7, 3139–3145.

[71] Petka, W. A.; Harden, J. L.; McGrath, K. P.; Wirtz, D.; Tirrell, D. A. *Science* 1998, 281, 389–392.

[72] Xu, C.; Breedveld, V.; Kopeček, J. *Biomacromolecules* 2005, 6, 1739–1749.

[73] Banwell, E. F.; Abelardo, E. S.; Adams, D. J.; Birchall, M. A.; Corrigan, A.; Donald, A. M.; Kirkland, M.; Serpell, L. C.; Butler, M. F.; Woolfson, D. N. *Nature Materials* 2009, 8, 596–600.

[74] Castillo, J.; Sasso, L.; Svendsen, W. E. *Self-Assembled Peptide Nanostructures: Advances and Applications in Nanobiotechnology*, CRC Press, Boca Raton: 2012.

[75] Schneider, J. P.; Pochan, D. J.; Ozbas, B.; Rajagopal, K.; Pakstis, L.; Kretsinger, J. *Journal of the American Chemical Society* 2002, 124, 15030–15037.

[76] Orbach, R.; Adler-Abramovich, L.; Zigerson, S.; Mironi-Harpaz, I.; Seliktar, D.; Gazit, E. *Biomacromolecules* 2009, 10, 2646–2651.

[77] Adhikari, B.; Palui, G.; Banerjee, A. *Soft Matter* 2009, 5, 3452–3460.

[78] Deming, T. J. *Soft Matter* 2005, 1, 28–35.

[79] Kopeček J.; Yang J. *Angewandte Chemie International Edition* 2012, 51, 7396–7417.

[80] Hotz, N.; Wilcke, L.; Weber, W. *Macromolecular Rapid Communications* 2013, 34, 1594–1610.

[81] Li, J.; Illeperuma, W. R. K.; Suo, Z.; Vlassak, J. J. *ACS Macro Letters* 2014, 3, 520–523.

[82] Jia, X.; Kiick, K. L. *Macromolecular Bioscience* 2009, 9, 140–156.

[83] Ifkovits, J. L.; Burdick, J. A. *Tissue Engineering* 2007, 13, 2369–2385.

[84] Leach, J. B.; Schmidt, C. E. *Biomaterials* 2005, 26, 125–135.

[85] Annabi, N.; Tamayol, A.; Uquillas, J. A.; Akbari, M.; Bertassoni, L. E.; Cha, C.; Camci-Unal, G.; Dokmeci, M. R.; Peppas, N. A.; Khademhosseini, A. *Advanced Materials* 2014, 26, 85–124.

[86] Freudenberg, U.; Hermann, A.; Welzel, P. B.; Stirl, K.; Schwarz, S. C.; Grimmer, M.; Zieris, A.; Panyanuwat, W.; Zschoche, S.; Meinhold, D.; Storch, A.; Werner, C. *Biomaterials* 2009, 30, 5049–5060.

[87] Werner, C. *eXPRESS Polymer Letters* 2013, 7, 805.

[88] DeForest, C. A.; Polizzotti, B. D.; Anseth, K. S. *Nature Materials* 2009, 8, 659–664.

[89] Phelps, E. A.; Enemchukwu, N. O.; Fiore, V. F.; Sy, J. C.; Murthy, N.; Sulchek, T. A.; Barker, T. H.; García, A. J. *Advanced Materials* 2012, 24, 64–70.

[90] Tsurkan, M.; Chwalek, K.; Prokoph, S.; Zieris, A.; Levental, K.; Freudenberg, U.; Werner, C. *Advanced Materials* 2013, 25, 2606–2610.

[91] Heck, T.; Faccio, G.; Richter, M.; Thöny-Meyer, L. *Applied Microbiology and Biotechnology* 2013, 97, 461–475.

[92] Ehrbar, M.; Rizzi, S. C.; Schoenmakers, R. G.; Miguel, B. S.; Hubbell, J. A.; Weber, F. E.; Lutolf, M. P. *Biomacromolecules* 2007, 8, 3000–3007.

[93] Peng, L.; Wu, C.; You, M.; Han, D.; Chen, Y.; Fu, T.; Ye, M.; Tan, W. *Chemical Science* 2013, 4, 1928–1938.

[94] Jiang, F. X.; Yurke, B.; Verma, D.; Previtera, M.; Schloss, R.; Langrana, N. A. "Development of DNA Based Active Macro–Materials for Biology and Medicine: A Review" in Biomaterials Science and Engineering, (ed. R., Pignatello), InTech: 2011. Available from: http://www.intechopen.com/books/biomaterials-science-and-engineering/development-of-dna-based-active-macro-materials-for-biology-and-medicine-a-review.

[95] Liu, D.; Cheng, E.; Yang, Z. *NPG Asia Materials* 2011, 3, 109–114.

[96] Murakami, Y.; Maeda, M. *Biomacromolecules* 2005, 6, 2927–2929.

[97] Nagahara, S.; Matsuda, T. *Polymeric Gels Networks* 1996, 4, 111–127.

[98] Lin, D. C.; Yurke, B.; Langrana, N. A. *Journal of Biomechanical Engineering* 2004, 126, 104–110.

[99] Tierney, S.; Stokke, B. T. *Biomacromolecules* 2009, 10, 1619–1626.

[100] Wei, B.; Cheng, I.; Luo, K. Q.; Mi, Y. L. *Angewandte Chemie International Edition* 2008, 47, 331–333.

[101] He, X.; Wei, B.; Mi, Y. *Chemical Communications*, 2010, 46, 6308–6310.

[102] Wang, C.; Stewart, R. J.; Kopeček, J. *Nature* 1999, 397, 417–420.

[103] Morell, M.; Puiggalí, J. *Polymers* 2013, 5, 188–224.

[104] Singh, R. K.; Seliktar, D.; Putnam, A. J. *Biomaterials* 2013, 34, 9331–9340.

[105] Wang, H.; Han, A.; Cai, Y.; Xie, Y.; Zhou, H.; Long, J.; Yang, Z. *Chemical Communications* 2013, 49, 7448–7450.

[106] Tsurkan M. V.; Chwalek, K.; Levental, C. R.; Freudenberg, U.; Werner, C. *Macromolecular Rapid Communications* 2010, 31, 1529–1533.

[107] Seal B. L.; Panitch, A. *Biomacromolecules* 2003, 4, 1572–1582.

[108] Yamaguchi, N.; Kiick, K. L. *Biomacromolecules* 2005, 6, 1921–1930.

[109] Tae, G.; Scatena, M.; Stayton, P. S. et al. *Journal of Biomaterial Science Polymer Edition* 2006, 17, 187–197.

[110] Benoit, D. S. W.; Durney, A. R.; Anseth, K. S. *Biomaterials* 2007, 28, 66–77.

[111] Baldwin, A. D.; Kiick, K. L. *Biopolymers* 2010, 94, 128–140.

[112] Wieduwild, R.; Tsurkan, M.; Chwalek, K.; Murawala, P.; Nowak, M.; Freudenberg, U.; Neinhuis, C.; Werner, C.; Zhang, Y. *Journal of the American Chemical Society* 2013, 135, 2919–2922.

[113] Freudenberg, U.; Sommer, J.-U.; Levental, K. R.; Welzel, P. B.; Zieris, A.; Chwalek, K.; Schneider, K.; Prokoph, S.; Prewitz, M.; Dockhorn, R.; Werner, C. *Advanced Functional Materials* 2012, 22, 1391–1398.

[114] Capila, I.; Linhardt, R. J. *Angewandte Chemie International Edition* 2002, 41, 391–412.

[115] Yamaguchi, N.; Zhang, L.; Chae, B. S. et al. *Journal of the American Chemical Society* 2007, 129, 3040–3041.

[116] Kiick, K. L. *Soft Matter* 2008, 4, 29–37.

[117] Zieris, A.; Dockhorn, R.; Röhrich, A.; Zimmermann, R.; Müller, M.; Welzel, P. B.; Tsurkan, M. V., Sommer, J.-U.; Freudenberg, U.; Werner, C. *Biomacromolecules* 2014, 15, 4439–4446.

6

FUNCTIONAL MATERIALS AND APPLIED SYSTEMS

6.1 ORGANIC NANOPARTICLES AND AGGREGATES FOR DRUG AND GENE DELIVERY

6.1.1 Polymeric Micelles, Polymersomes, and Nanocapsules

6.1.1.1 Polymeric Micelles

In contrast to micelles of small surfactant molecules, polymeric micelles (Fig. 6.1) are generally more stable and can retain the loaded drug for a longer period [1]. Block copolymer micelles form spontaneously by self-assembly in water when the concentration of the amphiphilic block copolymer is above the critical micelle concentration (CMC). The driving forces can be either hydrophobic interactions of the inner block, for example, a nonpolar poly(ε-caprolactone) block (PCL), or ionic interactions, for example, a poly(aspartate) block (PAsp), complexed to a negatively charged polymer, such as DNA, to form a polyion micelle [2]. The outer hydrophilic block consists in many cases of a polar poly(ethylene oxide) (PEO) block, which will form the shell of the nanocarrier and protect the core by steric stabilization. It has also been demonstrated that PEO prevents the adsorption of proteins and hence forms a biocompatible polymeric nanocarrier shell. The size of these block copolymer micelles is determined by thermodynamic parameters, yet partial size control is possible by variation of the block length. Typically, these block copolymer micelles are several tenths of nanometers in diameter with a relatively narrow distribution and therefore have a similar size as viruses, lipoproteins, and other naturally occurring transport systems. A major

Bio- and Multifunctional Polymer Architectures: Preparation, Analytical Methods, and Applications, First Edition. Brigitte Voit, Rainer Haag, Dietmar Appelhans, and Petra B. Welzel.

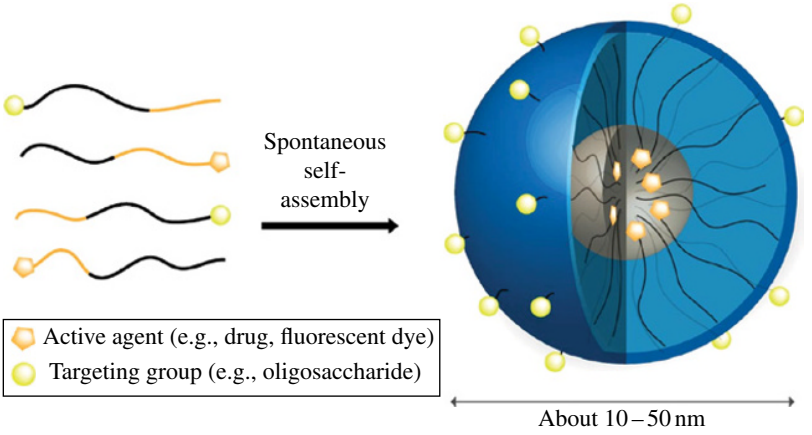

FIGURE 6.1 Formation and architecture of block copolymer micelles, which spontaneously form by self-assembly in water. The characteristic features are a pronounced core–shell architecture, which can be controlled by the individual polymer blocks. Typical examples for block copolymers are PEO-*b*-PPO, PEO-*b*-PCL, and PEO-*b*-PAsp. Source: Kataoka et al. [1], figure 1. Reproduced with permission of Elsevier. (*See insert for color representation of the figure.*)

obstacle for such nanocarrier systems is their nonspecific uptake by the reticuloendothelial system (RES). In order to achieve long blood circulation times and to reach their target, the size and the surface properties of such block copolymer-based nanocarriers require a careful design [3]. The polarity and functionality of each block allow the control of the spontaneously formed core–shell architecture. While terminal functionalities on the outer block, "the shell," control the biocompatibility and might incorporate possible targeting functionalities of these nanocarriers, the inner block can be used to complex or covalently couple active drug molecules (cf. Fig. 6.1). Especially for nonpolar drugs with limited solubility in water, this concept is frequently used to solubilize these drugs in water (e.g., using Pluronics®: PEO-*b*-PPO).

6.1.1.2 Polymersomes and Polymeric Nanocapsules

General Synthesis and Preparation Schemes

An important class of polymeric nanocarriers is based on nanocapsules with a polymeric membrane. As outlined earlier, in aqueous solutions, for example, of specific amphiphilic block copolymers above the CMC, self-assembly to spherical micelles takes place in the simplest case. However, depending on the polymer structure and architecture, block length, and hydrophilic/hydrophobic balance, the formation of more complex vesicular structures can also take place (see Section 5.1; Figs. 5.5a and 5.9).

As a result of their unique structure comprising different compartments, nano- and micrometer-size hollow vesicles are of high interest and promising applications can be envisioned in different fields including materials science, biomedicine, and catalysis. The research activities of the last decade brought a flourishing progress regarding these vesicular structures ranging from the well-known liposomes to block copolymer-based polymersomes and polymeric capsules.

Besides cells, cell organelles and cellular vesicles are also surrounded by membranes, which are composed of a double layer formed by amphiphilic molecules. These amphiphiles are mostly phospholipids and therefore the resulting vesicles are called "liposomes." Similarly, amphiphilic polymers can form a lipid-like double layer that forms the membrane of a polymeric vesicle, the so-called polymersome [4]. In contrast to micelles, the inner and outer parts of the membrane of polymersomes are in contact with water.

A polymeric capsule has a polymersome-like structure, with a hollow core domain and a polymeric shell. Differing from polymersomes of which the shell is strictly composed of amphiphilic polymers, the composition of polymeric capsules can be freely tailored by choosing a variety of polymers for different purposes. This inherent advantage of polymeric capsules allows a rapid development of divers polymeric nanocarriers.

So far, a large number of different functional capsules were constructed; for example, some of them demonstrate a wide range of external stimuli responsiveness including sensitivity toward pH, temperature, light, ions, sugar, reducing agents, etc. Additionally, a variety of fabrication methods were described, such as layer-by-layer (LbL) assembly, emulsion-based polymerization, and surface-initiated polymerization (SIP) (Fig. 6.2). Some of the constructed polymeric capsules have already been approved as promising candidates in diagnostic applications, tissue engineering, and drug delivery and as nanoreactors.

Regardless of the construction procedure, the constructed polymeric capsules are generally classified into three types based on the arrangement of polymers in the shell. As shown in Figure 6.2, the polymer chains arrange either vertically (type I), horizontally (type II), or irregularly (type III) on the core/droplet surface.

Polymersomes

Various amphiphilic polymers with a defined block length ratio of about 1:2 polar/nonpolar have so far been applied to the preparation of polymersomes (Fig. 6.3) [6, 7].

With suitable polymers in hand, these macromolecular structures only need to self-assemble into the desired vesicle structure. For that purpose, a number

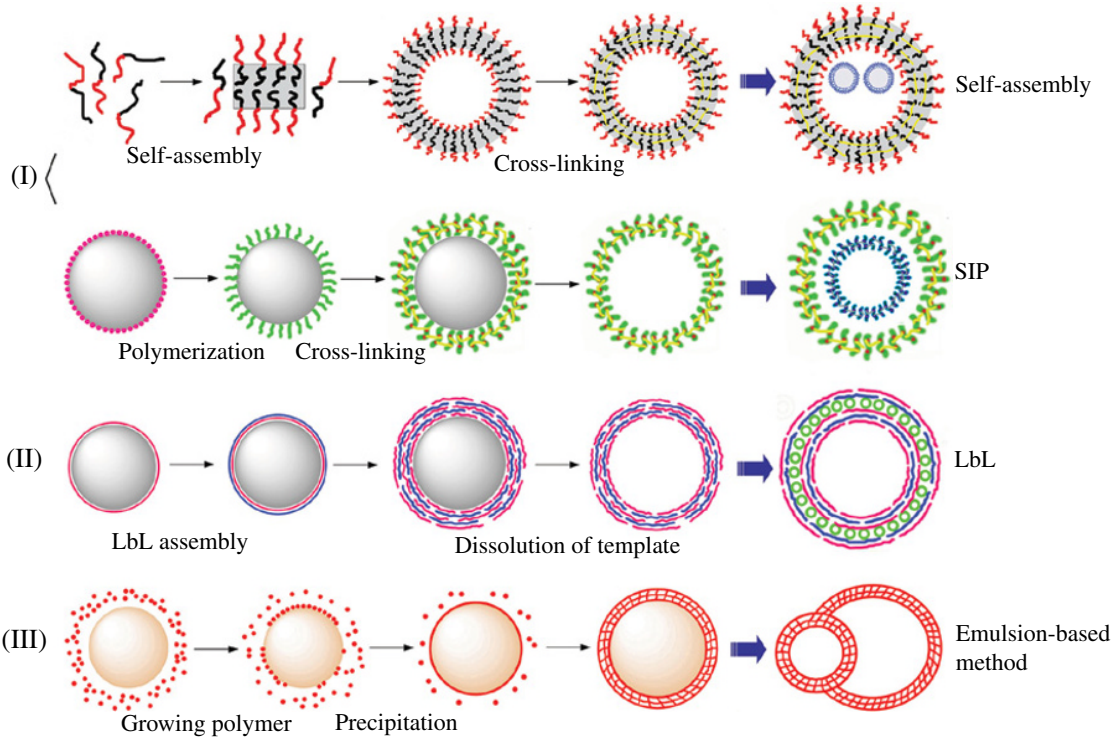

FIGURE 6.2 Preparation methods for polymeric capsules that can be used for multicompartmentalization: in type I, the polymer in the shell is arranged vertically along the core surface. These systems can be obtained by self-assembly of amphiphilic copolymers into polymersomes and subsequent cross-linking or by surface-initiated polymerization (SIP) from the surface of nanoparticle templates; in type II, the polymer in the shell arranges horizontally along the core surface, mainly synthesized by layer-by-layer (LbL) assembly of polyelectrolytes onto a particle; in type III, the polymer in the shell arranges disorderly along the droplet surface, commonly synthesized by an emulsion-based method where a polymer is deposited at an aqueous/organic interface, yielding a polymer wall around a stabilized droplet. Source: Reproduced with permission from Ref. 5. (*See insert for color representation of the figure*.)

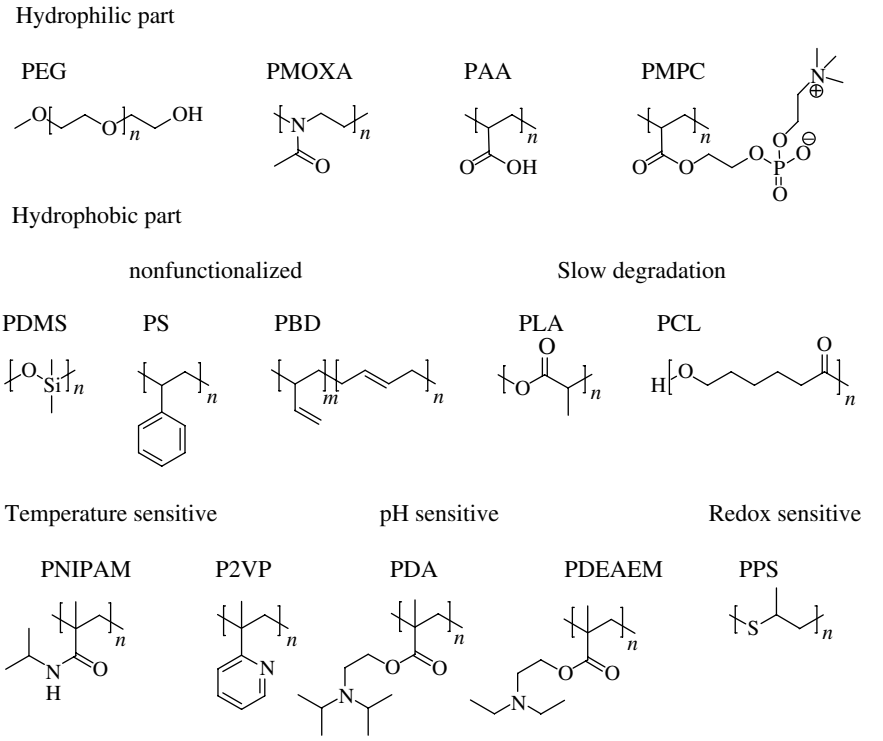

FIGURE 6.3 Polymeric units used in block copolymers for polymersome preparation.

of strategies have been developed such as film rehydration, solvent inversion, pH switch, and electroformation (Fig. 6.4), which can also be applied for liposome formation.

For the solvent inversion method the whole block copolymer has to be completely dissolved in a solvent before polymersome formation is initiated. Once the solvent containing the dissolved polymer is poured into an excess of water, the hydrophobic block becomes insoluble and polymersome formation is induced. Here, the created vesicles are typically between 100 and 200 nm in diameter. Besides solvent inversion, film rehydration also relies on dissolving the amphiphilic block copolymer in a solvent other than water. In contrast to solvent inversion, the solvent is slowly evaporated during this method to produce a thin film of precipitated polymer at the wall of the jar used. Once the film is created, the jar is filled with water and the self-assembly starts from the precipitated polymer film. Eventually, polymersomes are formed and the film is totally removed. If the jar surface is chemically altered, vesicles of up to 20 μm can be achieved. Otherwise, film rehydration yields the same vesicle sizes as solvent inversion.

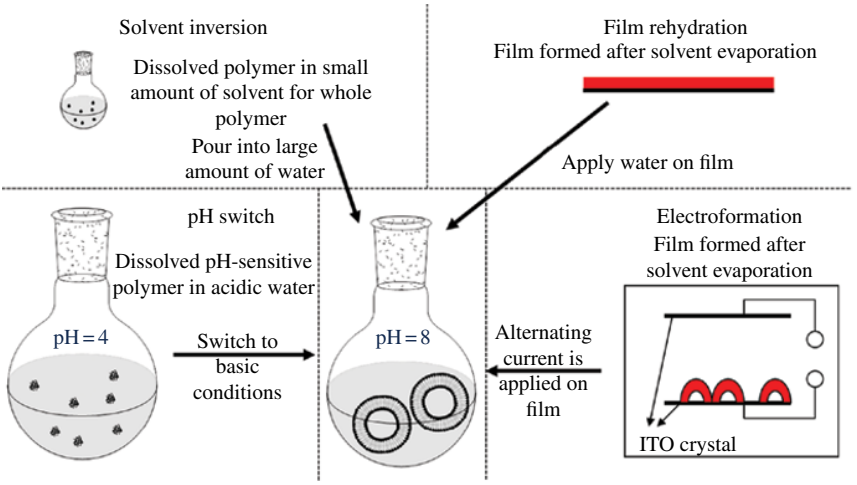

FIGURE 6.4 Mechanisms of polymersome formation from block copolymers. For solvent inversion, film rehydration, and electroformation, the polymer is first dissolved in an organic solvent and polymersomes are initiated after water is added to the system. In contrast, pH-sensitive polymers are dissolved in acidic water and polymersomes are formed by switching to basic conditions.

Besides simply pouring water over the film, the vesicles can also be produced using an external stimulus like a constantly changing electrical field. This method is called electroformation and is widely used for liposome production. Upon a change in the frequency of the changing electrical field applied, the vesicles eventually detach from the surface, yielding giant polymersomes of several micrometers in diameter.

All methods discussed earlier at some point require the exchange of solvent. However, if a pH-sensitive material is used, polymersome formation can be initiated by only changing the solvent conditions with regard to the pH of the solvent. A great advantage of this method over the previously mentioned ones is that the solution does not need to be cleaned afterward and no solvent exchange is necessary. While for solvent inversion, vesicles of about 100–200 nm can be obtained by the pH switch method.

A biomedical or biotechnological application of such polymersome structures is obvious because of their similarity to liposomes. On the one hand, hydrophobic drugs (e.g., doxorubicin (DOX) or paclitaxel) and hydrophilic bioactive molecules (e.g., proteins, siRNA, DNA) can be encapsulated and then transported to and delivered at the target area (drug delivery system). On the other hand, they can carry catalysts (e.g., enzymes) that are stabilized and protected by the polymersome membrane and selectively addressed when needed. Polymersomes, however, differ a lot from liposomes. Firstly, with

regard to size, they are usually smaller, and secondly, they are chemically and mechanically significantly more stable.

Due to its high stability, the membrane of polymersomes has low fluidity, which leads to a very limited transport through the membrane. Thus, in order to allow for transmembrane transport, specific efforts are necessary. One option is the use of responsive polymer blocks, which allow a switching of the block from hydrophilic to hydrophobic, or vice versa. This can be achieved with thermo-responsive poly(*N*-isopropylacrylamide) (PNIPAM), pH-sensitive amino-functionalized methacryl derivatives (e.g., poly(diethylaminoethyl methacrylate) (PDEAEM)), or the redox-sensitive poly(propylene sulfide) (PPS).

By changing the hydrophilic/hydrophobic equilibrium via an external trigger, a polymersome is no longer stable and disintegrates. This allows the delivery of the cargo such as drugs; however, it is not useful for nanoreactors. In that case, an enhanced transmembrane transport of small molecules is required that should not destroy the polymersome. The passive exchange of small molecules from outside to inside and vice versa has to be allowed, for example, to interact with an encapsulated enzyme. In analogy to nature this can be realized by incorporating transmembrane proteins in the membrane, which can further govern the direction of the transport by controlling the orientation of the transmembrane protein (realized, e.g., using the triblock copolymer PMOXA-*b*-PDMS-*b*-PMOXA). Thus, in polymersomes, enzymes such as, nucleoside hydrolase, HRP, β-lactamase, or acid phosphatase have been successfully encapsulated and activated. Often, the encapsulated enzymes exhibit even higher stability and lifetime.

Polymersomes can be further applied as synthetic cell organelles for the modeling of simple cell processes. For example, it was possible to prepare polymersomes with the integrated membrane protein LamB, which allowed the docking of the bacteriophage lambda at the polymersome surface. This system enabled the study of DNA transfer from the bacteriophage into the polymersome via the membrane protein [8].

Another concept is the preparation of responsive polymersome membranes, which are further cross-linked for stabilization. This concept allows for preservation of the general polymersome capsule structure upon switching polarity but leads to a more leaky membrane structure, resulting in enhanced membrane transport (Fig. 6.5).This can be achieved by incorporating pH-sensitive blocks, for example, in photo-cross-linkable polymersomes. The membrane of the vesicle is then formed spontaneously as double layer at suitable pH from the block copolymer containing the photo-cross-linkable units and is subsequently cross-linked in the collapsed state. Upon acidification, the non-polar blocks are protonated and transformed into a polar block. Therefore, the polymersome would like to disintegrate but is linked by chemical bonds, and

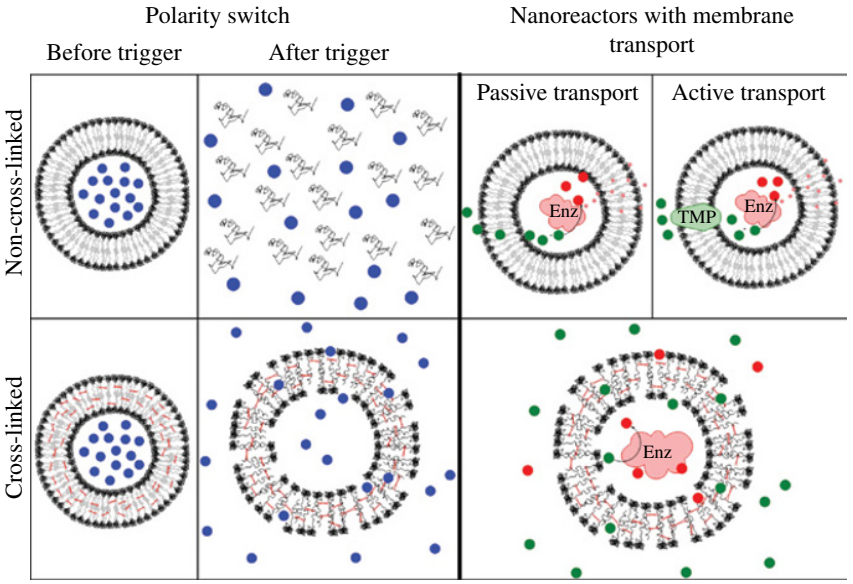

FIGURE 6.5 Schematic representation of polymersomes, with non-cross-linked and cross-linked membranes. Only in cross-linked polymersome membranes, transport can be reversibly activated upon polarity switch. (*See insert for color representation of the figure.*)

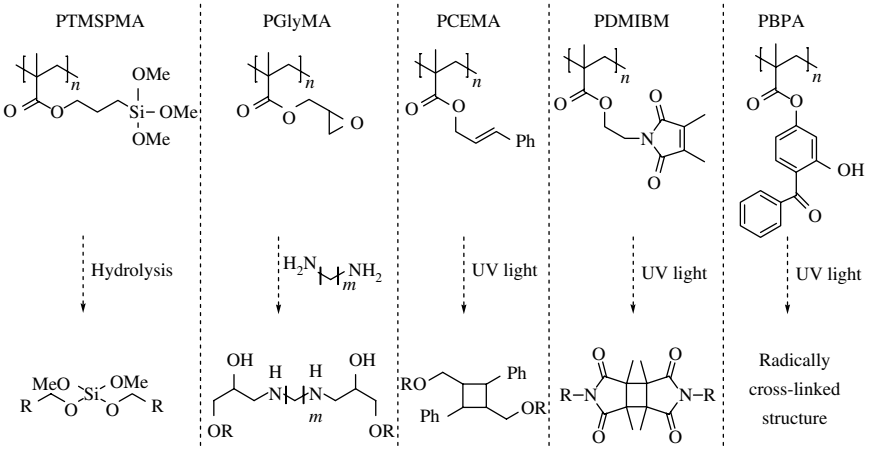

FIGURE 6.6 Cross-linking units that have been integrated in block copolymers used for polymersome formation.

thus, only swelling of the membrane is possible, which allows enhanced membrane transport. A variety of possible cross-linking units are given in Figure 6.6.

Using this concept the enzyme myoglobin was successfully encapsulated by a photo-cross-linked polymer membrane and the pH-dependent activity was reported [9]. This principle offers a high potential for biotechnological applications. Similarly, pH-sensitive swelling of the cross-linked membrane can also be used for controlled drug release systems.

For any biomedical application one has to consider aspects of cell and blood compatibility of polymersomes. This has been successfully documented for a variety of polymersomes by integrating well-known bioinert structural units like PEG or poly(methyl oxazoline) (Fig. 6.3). In addition, for effective cell internalization, polymersomes are constructed mimicking natural compartments as closely as possible. Viruses and bacteria, for example, do not have a smooth, homogenous surface but a rough, patchy structure, which favors cell interaction. This can be mimicked by polymers using block copolymer mixtures, leading to phase-separation effects in the polymersome membrane. The resulting island structure is very similar to that of natural vesicles and exhibits a 10–20 times faster cell internalization compared to polymersomes from a single block copolymer component [10].

Another common approach is the integration of biologically active molecules, peptide sequences, or proteins via bioconjugation and chemical binding onto the polymersome surface, which are known to allow active interaction with cell membranes. In addition to the well-known "biotin–avidin" bioconjugation, efficient polymer analogous reactions (see Section 3.3) are successfully employed to fix those active units at the block copolymer chain end. One example is the binding of dendritic glycostructures via 1,3-dipolar cycloaddition at the polymersome surface for selective cell internalization [11].

Polymeric and Multicompartment Capsules

Inspired by cells that are able to perform multiple complex reactions within confined environments owing to their internal subcompartment structure, the development of multicompartment vesicles fulfilling simple predefined cell activities or acting as multifunctional nanoreactors or drug carriers is gaining more and more attention [5]. Currently, the successfully created multicompartment capsules include vesosomes, liposomes in liposome structure formed by smaller vesicles encapsulated within a bigger vesicle; polymer vesosome, where a polymersome in a polymersome structure is formed by using different polymersomes for the carrier and subcompartment structures; and dendrimersomes, which are formed by the self-assembly of Janus dendrimers in solution. However, the topic of multicompartment polymeric capsules (capsosomes) is still in its initial stage. So far, the LbL method, self-assembly, emulsion-based

polymerization, or SIP methods have been used to construct these kind of structures. Depending on the methods (Fig. 6.2), capsules in the nano- to micrometer range can be prepared.

Self-Assembly

In the first case (type I of polymeric capsules in Fig. 6.2), the shell of polymeric capsules is composed of polymers that arrange vertically along the core surface. The spontaneous self-assembly of amphiphilic polymers into higher-order, discrete supramolecular assemblies and the use of amphiphilic block copolymers to obtain nanomaterials with distinct compartments are well established and exploited, for example, for polymersome formation (see earlier text and also Section 5.1.3). Depending on the block copolymer structure, a wealth of different self-assembled morphologies are reported, for example, hollow concentric vesicles, onions, and vesicles with tubes in the wall. Furthermore, the controlled generation of multicompartment polymersomes was demonstrated recently, where the capsule content and wall properties can be modulated. For example, Eisenberg et al. [12] reported a vesicle system with a pH-induced "breathing" feature that consisted of a three-layered wall structure formed by a triblock copolymer (PEO_{45}-*b*-PS_{130}-*b*-$PDEA_{120}$) as building block. Due to the pH-sensitive PDEA layer in the middle of the vesicle wall, a change of pH led to great changes of both the vesicle size and the thickness of all three layers, which allowed the vesicle to demonstrate a "breathing" feature by diffusion of species in and out of the vesicles. Another interesting example was described by Lecommandoux et al. [13] who synthesized multicompartment polymersomes by combining nanoprecipitation and emulsion–centrifugation techniques. As shown by the authors, the synthesized multicompartment polymersomes can encapsulate different nanosize polymersomes inside larger ones and are able to encapsulate molecules and (bio)macromolecules in at least three different compartments (in the membrane/lumen of the inner nanosize polymersomes, in the cavity, and in the membrane of the giant vesicles). Importantly, by measuring the release profile of DOX as a model drug, a double-membrane diffusion barrier effect had been demonstrated. For the construction of multicompartment polymeric capsules, also a method was developed that utilizes UV light to cross-link the preformed polymersome with encapsulated dendrimers inside the core [9]. The controlled release of globular dendritic glycopolymers of different sizes was demonstrated by tuning the shear rate (Fig. 6.7). The natural multicompartment structure in dendrimers bestows a multicompartment behavior to the synthesized polymeric capsules after encapsulating dendritic glycopolymers inside the core.

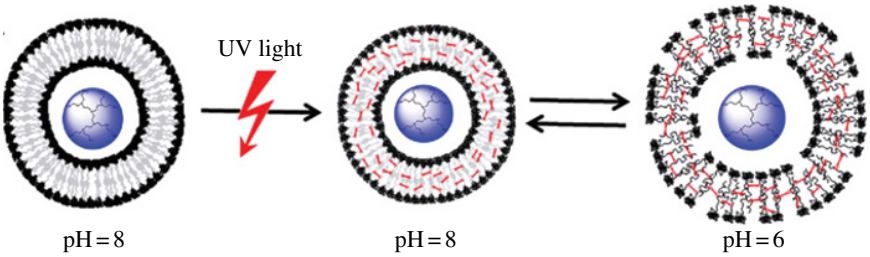

FIGURE 6.7 Schematic illustration of the constructed pH-sensitive polymeric capsule with a dendritic glycopolymer inside the core and the formation of a porous wall by switching the pH to 6 or lower, which can lead to the release of the encapsulated dendritic glycopolymer tuned by the shear rate [9] (for TEM images of collapsed and swollen membrane, cf. Fig. 4.13). Source: Gaitzsch et al. [9], figure 1. Reproduced with permission of John Wiley & Sons.

Surface-Initiated Polymerization

Another frequently used strategy to synthesize polymeric capsules (type I in Fig. 6.2) is the SIP method where polymers are directly grown from the surface of nanoparticle templates. The polymeric capsule is then obtained after cross-linking the shell and removing the core. The obvious advantages of this method are as follows: (i) the size of the capsules can be easily tuned by choosing different sizes of nanoparticles as templates, (ii) the shell thickness can be controlled by controlling the molecular weight of the grafted polymer, (iii) the shell composition can be easily varied by using different functional monomers, (iv) and the post-functionalization of the surface of the polymeric capsules can be continued from active end groups of the grafted polymer chain. The first example on this topic was reported by Hawker et al. [14] who employed surface-initiated controlled nitroxide-mediated radical polymerization to grow polystyrene from the surface of silica nanoparticles and cross-linked the capsules either thermally by the incorporation of vinyl benzocyclobutene groups or chemically by the reaction of maleic anhydride repeat units with a diamino cross-linker. Similarly, surface-initiated RAFT was successfully demonstrated for the synthesis of polymeric capsules (Fig. 6.8) [15]. Here, the silica nanoparticle template was first modified by a RAFT agent, and then block copolymers were grown from the surface via RAFT polymerization. Photo-cross-linkable units were incorporated into the polymer chain to allow cross-linking of the shell and after removal of the templates' polymeric capsules were obtained.

Several soft templates such as emulsion droplets or vesicles are of special interest since they can be readily dissolved under relatively mild conditions

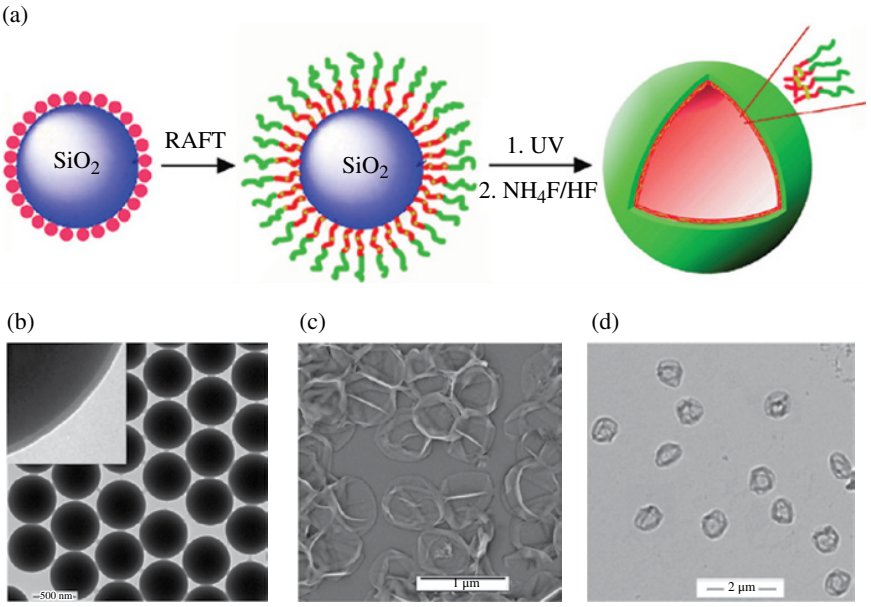

FIGURE 6.8 (a) Schematic illustration of the procedure for the synthesis of polymeric capsules based on surface-initiated RAFT polymerization using silica nanoparticles as templates. (b) TEM image of polymer grafted silica nanoparticles. (c) SEM and (d) TEM images of the synthesized polymeric capsules. Source: Huang et al. [15]. Reproduced with permission of American Chemical Society.

(e.g., aqueous alcohol solutions) and are easily preloaded with substances. For example, Ali et al. employed vesicles as templates to construct polymeric capsules [16]. Due to the colloidal instability, the required vesicle template may not be suitable for the final application, but this soft templating approach still represents a promising method for the synthesis of polymeric capsules because the mild conditions for "core dissolution" and the easy encapsulation of the substances are of interest.

With regard to the preparation of multicompartment polymer capsules based on this SIP method, a successful approach was demonstrated by Kang et al. [17] who used a two-step distillation/precipitation polymerization of methacrylic acid (MAA) and *N*-isopropylacrylamide (NIPAM), respectively, onto silica nanoparticles as templates. More interestingly, due to the PMAA inner shell and PNIPAM outer shell, the hollow structure can respond independently to changes in pH and temperature. After loading DOX into the capsules, temperature- and pH-controlled release of anticancer drug behavior was demonstrated.

Layer-by-Layer (LbL) Assembly

In contrast to type I, type II polymeric capsules exhibit a horizontal arrangement of the polymer in the shell along the core surface. In order to construct this type of polymeric capsules, the most popular method is LbL assembly, where the polymeric capsules are generated via sequential deposition of two interacting polymers onto a sacrificial particle template followed by the removal of the template, which results in hollow polymeric capsules (Fig. 6.2). More than 10 years have passed since this method was developed by Möhwald and Caruso [18]. Nowadays, a great number of polymeric capsules have been reported based on various interactions between the two polymers including electrostatic interactions, hydrogen bonding, DNA–DNA hybridization, or covalent linking (i.e., click chemistry). It has been demonstrated that a range of materials, from small molecule drugs to plasmid DNA, can be loaded into these polymeric capsules. In order to yield low-fouling capsules or to allow targeting by binding antibodies, the surface of the capsules can be modified by the adsorption of a poly(ethylene glycol) (PEG) layer or by binding antibodies.

For a further development of this method i.e., the preparation of multifunctionalized capsules, a series of multicompartment polymeric capsules were successfully constructed. For example, Städler et al. [19] synthesized multicompartment polymeric capsules with embedded liposomes in the shell via the LbL technique by using poly(styrene sulfonate) (PSS) and poly(allylamine hydrochloride) (PAH) as the polyelectrolytes and 50 nm zwitterionic 1,2-dioleoyl-*sn*-glycero-3-phosphocholine (DOPC) liposomes as the cargo. The TEM images (Fig. 6.9) clearly show the encapsulated liposomes in the polymeric shell.

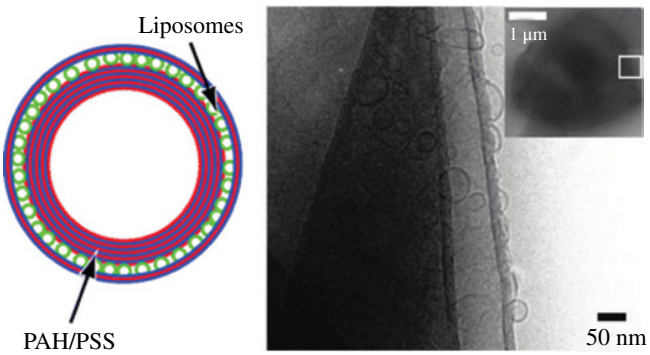

FIGURE 6.9 Schematic illustration of the morphology of liposomes embedded in a multicompartment polymeric capsule (left) and cryo-TEM image of a $(PAH/PSS)_4/PAH/liposomes_{NBD}/PSS/PAH/PSS$ multicompartment polymeric capsule embedded in ice (inset) and a close-up of the polyelectrolyte shell, which contains intact liposomes (right). Source: Städler et al. [19]. Reproduced with permission of American Chemical Society.

Emulsion-Based Methods

Finally, for type III polymeric capsules (see Fig. 6.2), the polymer in the shell arranges disorderly along the core surface. In order to synthesize this kind of polymeric capsules, a number of methods are employed including emulsion/miniemulsion polymerization, coacervation, internal phase separation, and so on, which also dictate the final size of the capsules. Among them, the emulsion/miniemulsion polymerization method was most commonly exploited, because of its simplicity, versatility, productivity, and ease of application on small scales [20]. The work of the Landfester group was able to prove that miniemulsion polymerization is a versatile tool for the formation of polymeric capsules composed of different kinds of polymers obtained by a variety of polymerization types ranging from radical, anionic, to polyaddition or polycondensation polymerization. By different processes such as emulsion/inverse emulsion, various hydrophilic or hydrophobic substances of interest can be encapsulated inside the core. For example, one report demonstrated that dsDNA (790 bp) was encapsulated via anionic polymerization of *n*-butylcyanoacrylate carried out at the interface of homogeneously distributed aqueous droplets in an inverse miniemulsion. By adopting similar strategies, many polymeric capsules were constructed. The dependence of the nanocapsule morphology on several factors such as the type of surfactant, the type of hydrophilic comonomer, and the surfactant/monomer ratio was investigated. Furthermore, the combination of controlled radical polymerization (ATRP or RAFT) and interfacial miniemulsion polymerization for the synthesis of polymeric capsules was described.

6.1.2 Polymeric Beads and Micro/Nanogels Based on Dendritic Structures

In order to address different length scales in biology (proteins 1–10 nm, viruses 50–1000 nm, bacteria 1–10 μm, and cells 5–50 μm), multifunctional micro- and nanogels are of great need for biomedical applications. In the following sections, the synthetic methodologies and potential applications of micro- and nanogels are highlighted using various polyglycerols (PGs) as examples for biofunctional materials. In this context, several methodologies have been reported in the past for the synthesis of PG hydrogels with dimensions in the micrometer scale [21, 22].

For the preparation of nano- and microgels, reactive monomers and macromonomers are loaded into nano- and microreactors, which are usually emulsion droplets [23] or cavities generated by soft lithography [24]. After cross-linking the macromonomers inside of these nano- and microtemplates

gel particles are formed that have the same size and shape as the template. Additionally, self-assembly of the macromonomers can be used to prepare nano- and microgels [25]. The choice of the templation method is crucial for the encapsulation of sensitive biological systems such as living cells and proteins, because strong mechanical forces might rupture cell membranes and the complex 3D structure of proteins might be destroyed. Additionally, cytotoxic solvents and other harmful additives, such as surfactants, should not get into direct contact with encapsulated guests to avoid detrimental effects. Furthermore, the choice of templation method directly influences the properties of the prepared gels, such as particle size, degree of cross-linking, and distribution of degree of cross-linking. Therefore, a careful selection of the templation method needs to be performed.

6.1.2.1 Polyglycerol Nanogels

In the pioneering work of Sisson et al. [26], hyperbranched PG monomers were converted to their high molecular weight variant using the nanoreactor template, whereas cross-linking was achieved by an easy Huisgen-type alkyne/azide cycloaddition reaction (Fig. 6.10a). It is noteworthy that due to the confinement of space, no copper was needed for this thermal [2 + 3] cycloaddition at only 80°C. Both hydrophilic and hydrophobic nanoparticles could therefore be prepared by a direct and inverse miniemulsion process, yielding nanogels with particles sizes between 25 and 90 nm.

More recently, a new concept was developed by Haag and coworkers in which functional PG nanogels were synthesized by an acid-catalyzed polyaddition of glycerol to triglycidyl glycerol ether utilizing the inverse miniemulsion technique where the polar reactants were dispersed in nonpolar cyclohexane (Fig. 6.10b) [27]. A poly(ethylene-*co*-butylene)-block-poly(ethylene oxide) surfactant was used as a stabilizer, and a small amount of DMSO was used to prevent Ostwald ripening. Alternatively, multifunctional alcohols were used as monomers and di- and triepoxides as cross-linking agents [28]. The properties of these nanogels, that is, size, degree of branching, viscosity, and swelling behavior, could be controlled by varying the functionalities of the monomers and cross-linkers.

In an attempt to extend the length scale of the PG gels and their potential applications, Steinhilber et al. developed a technique to prepare PG megamers on different length scales by extending the size of hyperbranched PGs (3 nm) to nanogels (32 nm) and microgels (140 and 220 mm) [29a]. The authors used a miniemulsion templating system for the preparation of nanogels and microfluidic templation for the preparation of microgels, which were prepared by a free-radical polymerization of hyperbranched PG decaacrylate and PEG diacrylate. Figure 6.11 describes the method utilized to prepare

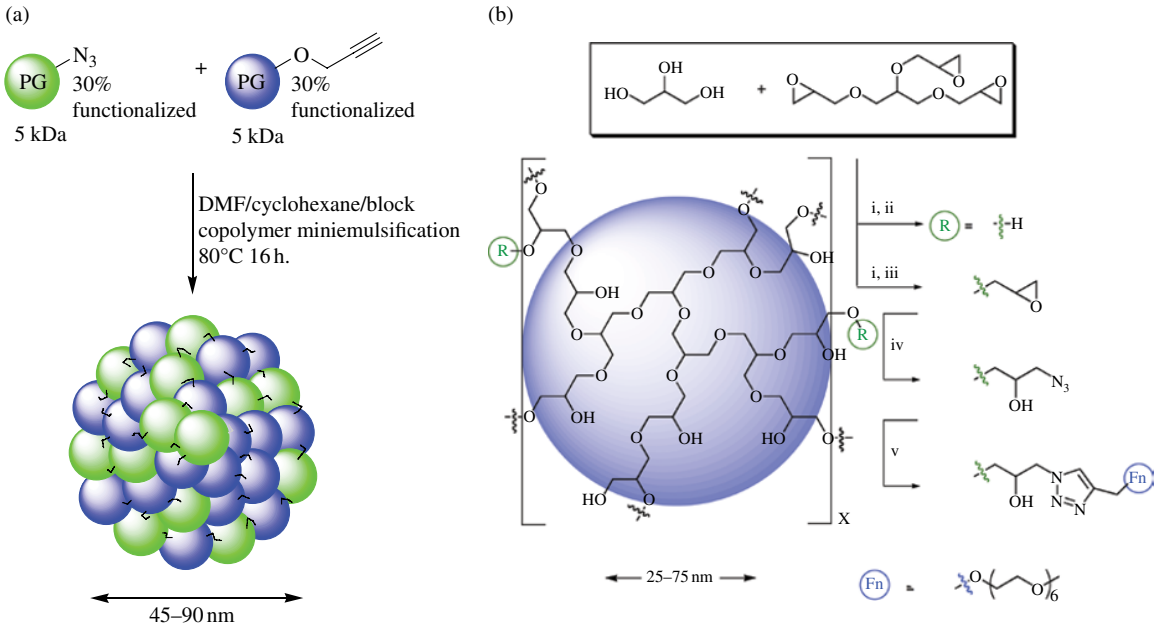

FIGURE 6.10 (a) Synthetic scheme for "thermal click" reaction to form PG megamers. (b) Synthetic pathways toward pure PG-nanogel and surface-functionalized PG-nanogel particles: (i) cyclohexane/DMSO/block copolymer surfactant, sonic tip miniemulsification 4 × 1 min; (ii) *p*-TSA (cat.), 115°C, 16 h; (iii) *p*-TSA (cat.), 115°C, varied time; (iv) NaN_3, DMF, 60°C, 24 h; (v) propargyl derivative, $CuSO_4 \cdot 5H_2O$, sodium ascorbate, H_2O, 24 h. Source: Sisson et al. [26, 27]. Reproduced with permission of American Chemical Society and Angewandte Chemistry.

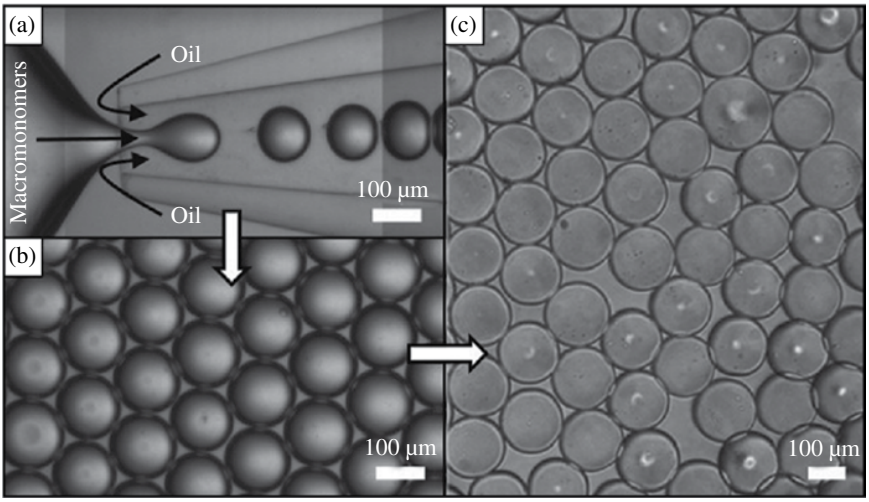

FIGURE 6.11 (a) Droplet microfluidic templating of micrometer-sized droplets using a glass microcapillary device. (b) Pre-microgel emulsion obtained from the experiment in Panel a. (c) Optical micrograph of water-swollen microgel particles formed by gelation of the droplets in Panel b. Source: Steinhilber et al. [29]. Reproduced with permission of Elsevier.

micrometer-sized droplets, as obtained through microfluidic emulsification, that allowed the formation of monodisperse PG microgels with uniform diameters of several tens or hundreds of micrometers. The cross-linking process was performed by free-radical polymerization of PG with MW 14.5 kDa in miniemulsion/microemulsion droplets, initiated by ammonium persulfate/tetramethylethylenediamine. More recently, the even more biocompatible "thiol–ene and copper-free click" chemistry was used to stabilize human cell lines with very high survival rates (up to 90%) [29b,c].

Micro- and nanogel technology has already established itself as a robust platform for the creation of functional materials with optimal size and multifunctionality for different fields of applications. The inherent properties of the PG gels, related to their high hydrophilicity, high biocompatibility, and controllable size/architecture in between 20 nm and several micrometers, enabled their application in several biomedical scenarios. In particular, the easily functionalizable surface equates to nanoscale multivalent substrates, which could have enhanced recognition properties toward biological surfaces [30]. In addition, microgels have been postulated for their potential in the field of tissue engineering, since PG gels might biomimic extracellular matrix (ECM) component proteins [29c].

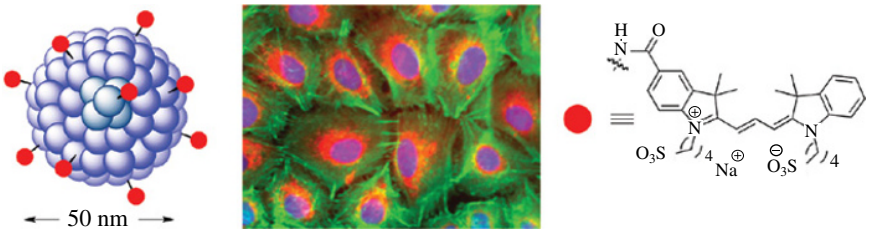

FIGURE 6.12 Fluorescence microscopy shows clear evidence for cellular uptake of fluorescently labeled PG nanogels via an endocytotic pathway. Source: Sisson et al. [27], scheme 1, figure 3. Reproduced with permission of John Wiley & Sons. (*See insert for color representation of the figure*.)

The interest of PG nanogels spearheads from their nontrivial synthesis into their biological implications. For example, nanogels with sizes between 25 and 350 nm have been shown to rapidly internalize into cell, with a preferred localization in the perinuclear region. As shown in Figure 6.12, there is evidence for a size-dependent endocytotic mechanism of cell entry. In addition, such PG gel architectures afforded a safe cytotoxicity profile in the mg/ml range [27].

In an attempt to use PG microgels as scaffolds for the synthesis of cell-laden microparticles, Steinhilber et al. [29] applied the microfluidic approach to fabricate microgels that were highly loaded with yeast cells. The polymer matrix allowed the cells to metabolize so that a good percentage of the cells stayed alive for more than 12 h after the particle formation.

For the design of smart systems, biodegradable PG nanogels and hydrogels were prepared via an acid-catalyzed ring-opening polyaddition of disulfide containing polyols and polyepoxides (Fig. 6.13) [31, 32]. Varying conditions allowed tuning of the particles and the disulfide content within the polymer network, yielding particles with narrow dispersities and diameters in the range from 25 to 350 nm. Interestingly, the disulfide-containing PG nanogels were found to be highly biocompatible and to degrade into small oligomeric subunits in reducing environments. Additionally, a near-infrared fluorescent dye was encapsulated in the hydrogel network that showed complete degradation in reducing environments and a controlled release of the fluorescence dye. In an elegant approach, Groll et al. prepared reductively sensitive hydro- and nanogels by enzymatic cross-linking. Mild reaction conditions allowed the authors to encapsulate proteins and living cells [33, 34].

The fabrication of thermoresponsive PG nanogels was recently developed by Calderòn et al. [35] in an attempt to develop stimuli-responsive materials based on dendritic PG. In this work, the precipitation polymerization method

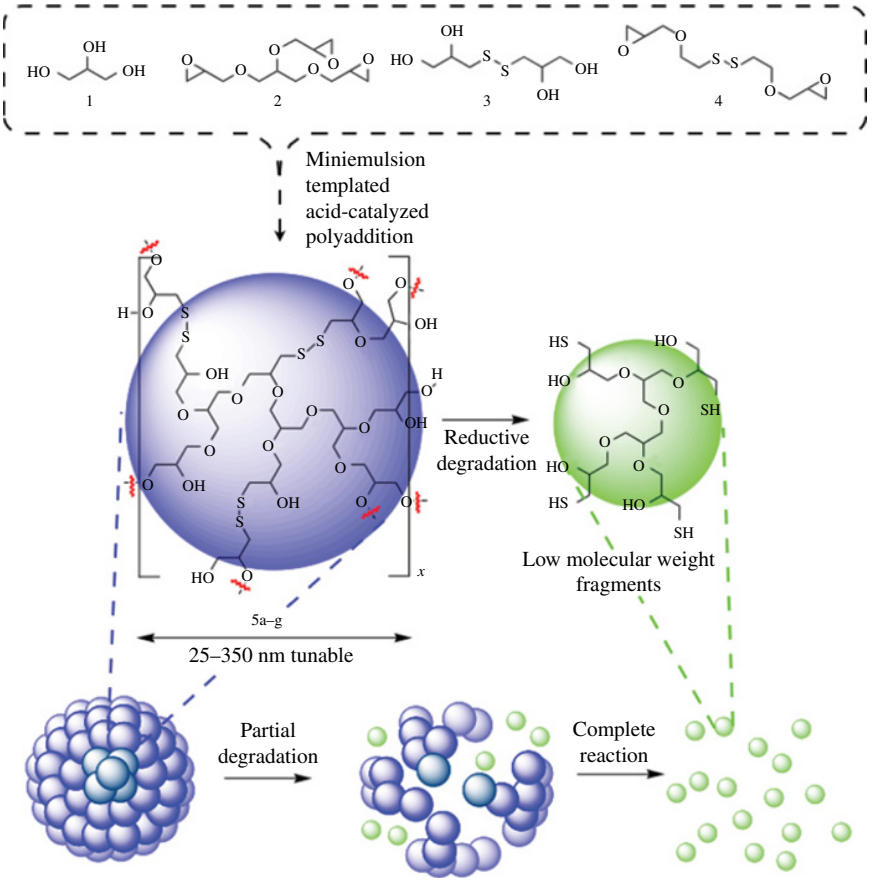

FIGURE 6.13 Synthetic route to biodegradable polyglycerol nanogels, showing a generalized depiction of a nanogel and degradation fragments [31, 32]. Source: Steinhilber et al. [31], scheme 1. Reproduced with permission of John Wiley & Sons. (*See insert for color representation of the figure*.)

was used to cross-link NIPAM and hyperbranched PG to yield monodisperse nanogels with sizes between 50 and 200 nm (Fig. 6.14). The incorporation of PG as cross-linking agent enhanced the water solubility of the nanogels, improved their biocompatibility profile, and allowed a fine-tuning of the thermoresponsive behavior regarding the size of the nanogels in solutions and transdermal delivery [35b].

6.1.2.2 Multicompartment Systems Based on Dendritic Structures

Besides the earlier described PG-based nanogels, other methods have also been applied to prepare multicompartment capsules and carrier systems based on dendrimers or hyperbranched polymers.

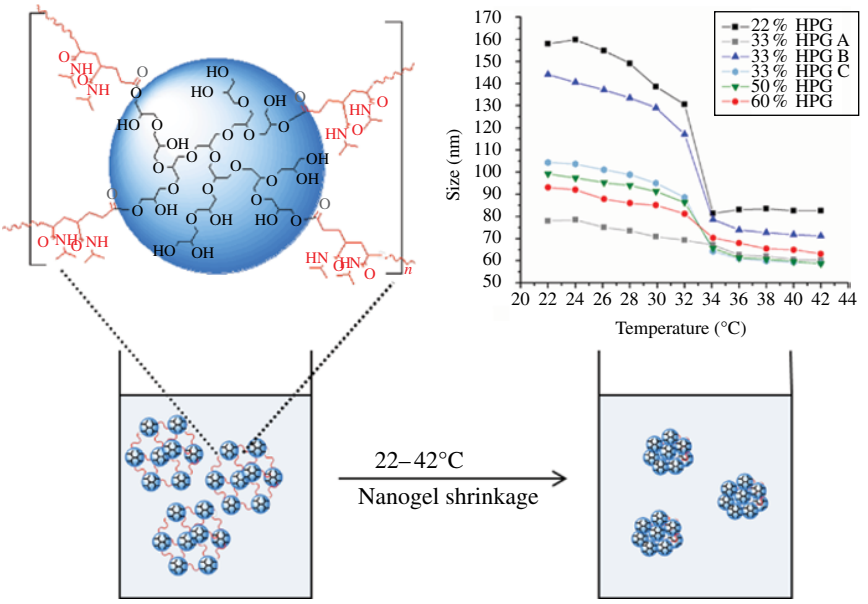

FIGURE 6.14 Thermo-responsive polyglycerol-based nanogels synthesized via precipitation polymerization. The nanogels showed a tendency to shrink with increasing solution temperature as shown by DLS measurements. Source: Cuggino et al. [35a], figure 1, figure 3. Reproduced with permission of Royal Society of Chemistry.

Core–multishell architectures (CMS) have been developed based on hyperbranched polymers, such as poly(ethylene imine) (PEI) and PG with an amphiphilic alkyl-PEG shell. These CMS nanocarriers can encapsulate a wide range of hydrophobic and hydrophilic substances that can be transported in both organic solvents and aqueous systems [36, 37] (Fig. 6.15).

Due to their amphiphilic nature, dendritic nanocarriers can transport various drug and dye molecules very efficiently and form defined aggregates, which have been revealed by DLS as well as cryo-TEM measurements (cf. Fig. 1.2). These nanocarrier aggregates can disassemble upon dilution into individual CMS particles, thereby releasing the active agent. Finally, they are excreted through the kidneys, thus avoiding long-term toxicity due to accumulation in vivo.

These novel CMS architectures mimic the structure of liposomes on a molecular level and form stable supramolecular aggregates. Upon loading with fluorescent dyes, such as Nile red, they show a pronounced transdermal uptake across the stratum corneum (see Fig. 6.16) [38, 39].

Besides the examples given, a variety of other dendritic structures have been used to prepare carrier and drug delivery systems. For example, a

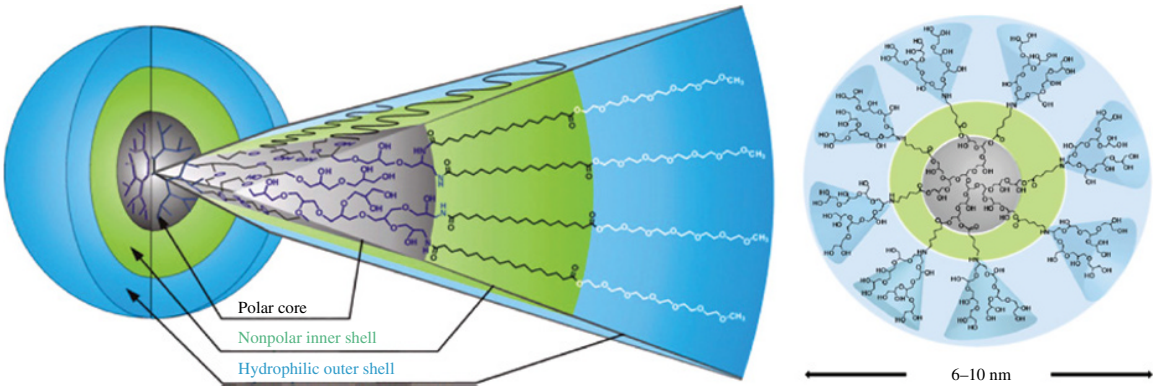

FIGURE 6.15 Dendritic core–multishell nanocarriers as novel amphiphilic architectures for drug delivery having a hydrophobic inner shell and a hydrophilic outer shell: with linear PEG (left; Source: Radowski et al. [36], figure 1. Reproduced with permission of John Wiley & Sons.) or dendritic polyglycerol outer shell (right; Source: Burakowska and Haag [37], figure 1. Reproduced with permission of American Chemical Society.).

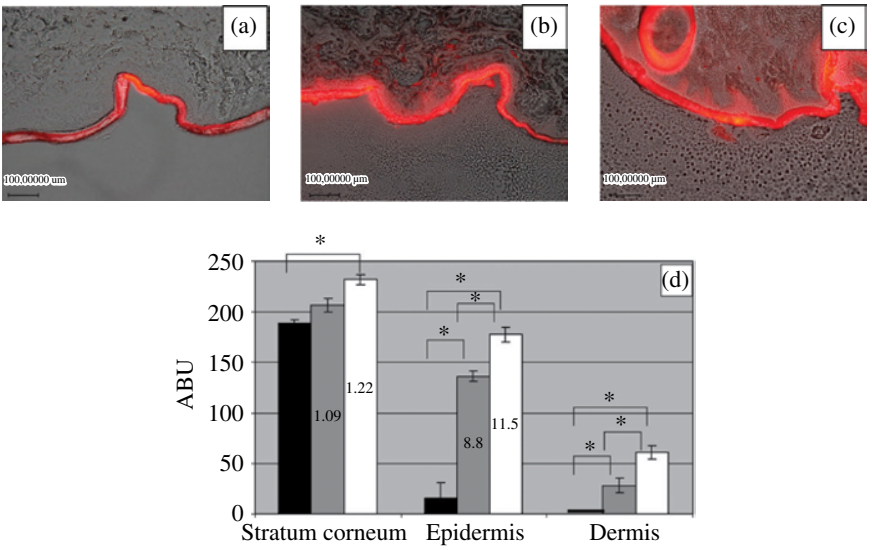

FIGURE 6.16 Rhodamine B penetration into pig skin: staining of pig skin following the application of 0.004% rhodamine B-loaded cream (a), SLN (b), and CMS nanotransporters (c) for 6 h. The representative pictures taken from the identical donor animal are obtained by superposing normal light and fluorescence images of the same area. (d) The arbitrary pixel brightness values (ABU) were obtained by fluorescence picture analysis (cream, black columns; SLN, gray columns; CMS nanotransporters, white columns, $n = 3$). The inserted numbers give the respective enhancement of penetration over cream, *differences ($p \leq 0.05$). Source: Küchler et al. [38], figure 1. Reproduced with permission of Elsevier. (*See insert for color representation of the figure*.)

multicompartment release system was designed by the incorporation of a hyperbranched PEI with a maltose shell into anionic hydrogel particles (PNIPAAM-AA). The selective pH-dependent release of adenosine triphosphate disodium salt hydrate (ATP) as probe molecule or ATP loaded dendritic glycopolymer from the multicompartment system ATP, dendritic glycopolymer, and hydrogel was shown [40].

Percec et al. [41, 42] studied and reviewed various complex self-assembled structures in detail that can be obtained from dendritic molecules. Especially multicompartment capsules obtained by the self-assembly of a library of amphiphilic Janus-type dendrimers are impressive. The chemical linkage of two dissimilar dendritic building blocks results in Janus dendrimers and produces a break in the spherical symmetry characteristic to dendrimers. Consequently, these structures spontaneously promote the self-assembly upon injection of its ethanol solution to form stable unilamellar vesicular nanostructures and other complex architectures (Fig. 6.17). *Dendrimersomes*

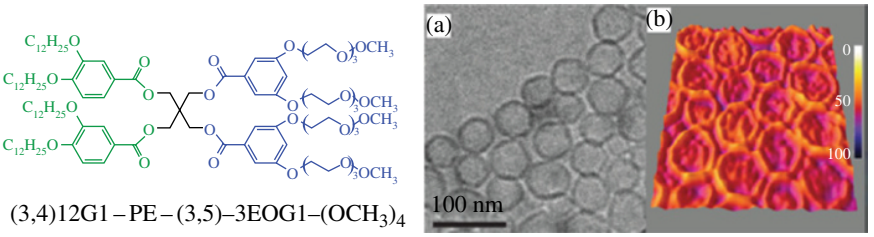

(3,4)12G1 – PE – (3,5)–3EOG1–$(OCH_3)_4$

FIGURE 6.17 TEM (A) and AFM (B) pictures of dendrimersome structures derived from (3,4)-12G1-PE-(3,5)-12EOG1-(OCH3)4 (see chemical structure shown). Source: Percec et al. [43]. Reproduced with permission of American Chemical Society.

provide access to monodisperse vesicles with enhanced stability and mechanical strength as well as ease of formation and chemical functionalization. They have a simple chemical design that allows fast recombination of the hydrophobic and hydrophilic building blocks to produce a large diversity of precise and monodisperse primary structures.

6.1.3 Polyplexes for Gene Delivery

The successful application of gene therapy through DNA or siRNA transfection into the cell is still a great challenge in research. Polymer-based DNA or RNA delivery systems offer a great potential for the facilitation of cellular uptake.

Cationic polymers [44] form polyelectrolyte complexes (polyplexes) with genetic materials. Complexation takes place as a result of electrostatic interactions between the negatively charged phosphate backbone of the nucleic acid and positively charged groups on the carriers. Besides cationic polymers, cationic lipids [45] with a hydrophobic unit and a positively charged group can form self-assembled structures capable of binding to polyanions like DNA or siRNA for gene transfection (Fig. 6.18).

Polycationic dendritic polymers and related structures are a special class of cationic polymers and have gained significant attention in the last two decades, due to their relative ease of preparation, their globular shape, and their multifunctionality. So far, a number of different dendritic polymers have been introduced for gene/siRNA delivery: poly(amido amine) (PAMAM), poly(propylene imine) (PPI), poly(L-lysine) (PLL), (PEI), and poly(glycerol amine) (PGA) [46].

In order to overcome the limitations associated with siRNA delivery *in vivo*, a group of dendritic nanocarriers derived either from PG or PEI were synthesized and their silencing efficiency was evaluated. Among the nanocarriers evaluated in this study, the best siRNA transfection efficiency with regard to toxicity was observed for PG amine. In general, successful systemic delivery

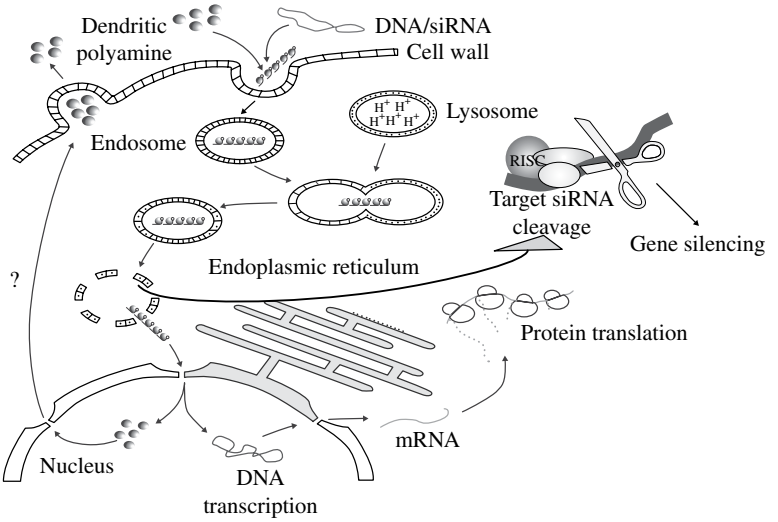

FIGURE 6.18 Proposed mechanism of gene transfection having the following elements: formation of the DNA/siRNA polymer complex (polyplex), endocytosis of the polyplex, fusion of endosome and lysosome, release of the polyplex into the cytosol, incorporation of the polyplex into the nucleus, and transcription of the DNA into mRNA followed by release of the polyamine backbone into the cytosol. Alternatively, direct binding of siRNA to mRNA via RISC complex and knock down is possible. Source: Fischer et al. [46], figure 1. Reproduced with permission of Springer.

of siRNA–PG–amine polyplexes into tumor tissue and inhibition of the target gene was achieved by these polycationic nanocarriers (Fig. 6.19) [47].

6.2 POLYMER THERAPEUTICS AND TARGETING APPROACHES

6.2.1 Current Status of Polymer Therapeutics

Multiple success stories exist already in the emerging field of polymer therapeutics based on innovations related to covalent conjugation of polymers with drugs or proteins (Table 6.1). Although a variety of polymer therapeutics have been conceptualized in the form of drug delivery systems (liposomes, nanoparticles, micelles), polyplexes (e.g., DNA–polycation complexes), polymeric micelles, dendritic core–shell architectures, and nanoparticle depots, the clinical success of nanomedicine is best exemplified by the utilization of polymeric conjugates (Section 5.1.1) to effectively deliver therapeutically relevant drugs, peptides, proteins, or antibodies. Several polymers have been approved for the use as conjugates for delivering bioactive agents in the form of polymer

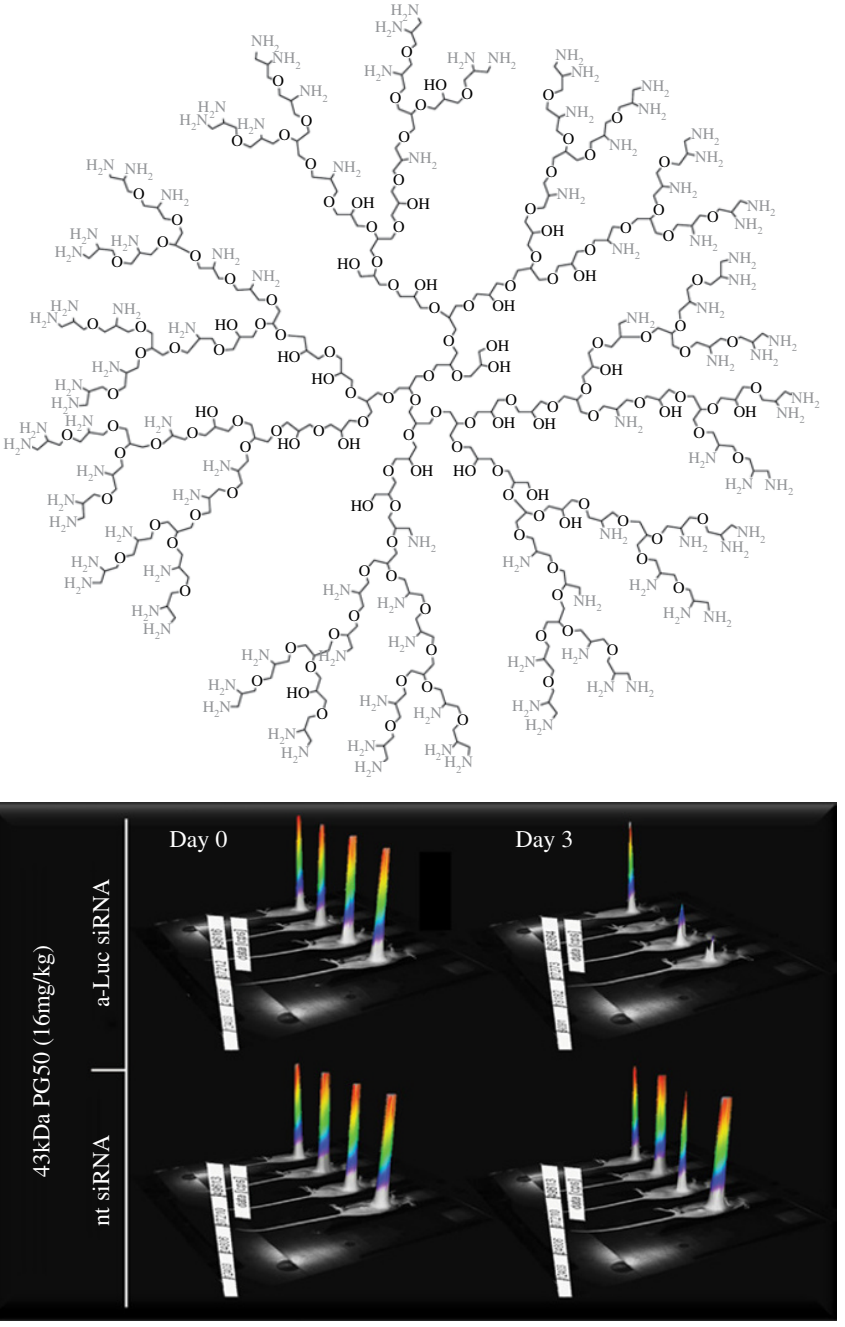

FIGURE 6.19 Idealized fragment of poly(glycerol amine) (PG–NH_2) (top) (reproduced with permission from Mehrabadi et al. [47b]) and *in vivo* silencing of the luciferase gene by siRNA–PG–NH_2 (bottom). 3D bioluminescence image of mice treated with 16 mg kg^{-1} 43 kDa PG50: light emission of tumors before (day 0) and after (day 3) treatment with 16 mg kg^{-1} 43 kDa PG50 complexed with non-targeting (nt) siRNA and luciferase specific (a-Luc) siRNA, respectively on three consecutive days. Source: Staedtler et al. [47c], figure 6. Reproduced with permission of Royal Society of Chemistry. (*See insert for color representation of the figure*.)

TABLE 6.1 Examples of Polymer-Based Nanoconjugates Used Clinically

Drug	Company	Form	Indication	Delivery Route
Xyotax, paclitaxel (37 wt %)	Cell Therapeutics	Poly(L-glutamic acid) (40 kDa)	Non-small cell lung cancer	i.v. or i.m.
VivaGel	Starpharma Holdings	Dendrimer gel	Vaginal microbiocide for prevention of HIV and genital herpes	Vaginal gel
Aurimune (CYT-6091)	CytImmune Sciences	Colloidal gold nanoparticles coupled to TNF and PEG thiol	Solid tumors	i.v.

HIV, human immunodeficiency virus; TNF, tumor necrosis factor.

therapeutics. However, PEG remains the polymer of choice for "clinical" prodrug conjugation. This technology is now commonly referred to as "PEGylation" (see Section 3.4) [48, 49]. Besides PEG-based technologies, several other polymer conjugates are also being evaluated for their potential to ameliorate the treatment of different human diseases. For example, a conjugate of polystyrene-*co*-maleic acid and neocarzinostatin (SMANCS; marketed by Yamanouchi Pharmaceutical Company) is being used to treat hepatocellular carcinoma. The cumulative evidence from these clinical formulations has firmly established that nanoconjugates improve the therapeutic value of bioactives.

6.2.2 Implications and Rationale for Effective Delivery Systems

An advanced area of nanomedicine is based on the potential utility of polymeric systems in the diagnosis and/or treatment of cancer. Indeed, various classes of polymer–drug conjugates, polymer–protein conjugates, nanoparticles, polymeric micelles, and multicomponent polyplexes have been extensively studied, and some are routinely being used in clinical settings [50–52]. Currently, a plethora of highly potent anticancer drugs are available, but the targeting of these drugs selectively to pertinent sites still remains a challenging task. Several important considerations are to be borne in mind when polymer–drug conjugates are being sought to deliver and specifically target anticancer drugs. These include the design of a stable covalent linkage between the drug and polymer, ensuring the uptake of prodrug in tumor cells (e.g., via an endocytotic route) [49], improving the "payload" and retention of drug within cancer cells,

and utilizing ligands (e.g., antibody, peptide, carbohydrate) to increase the targeting ability of the polymer conjugate [53, 54]. Often these various requirements are introduced into linear or dendritic/globular multifunctional polymer drug conjugates as outlined in Section 5.1.1 (Figs. 5.2 and 5.3). The aforementioned parameters are critical for the targeted delivery of not only highly toxic small molecule anticancer drugs but also macromolecular oncologic therapeutics encompassing peptides, oligonucleotides, and antibodies [55, 56].

Although many nanodelivery systems have been adroitly synthesized, each platform technology needs to be critically evaluated for a specific therapeutic application prior to its being labeled as "nanomedicine." Because of the inherent cellular and molecular complexities of myriad human diseases, this remains a challenge. At the same time, this presents several opportunities. In the past, many start-up companies and research laboratories have succeeded in introducing nanoplatforms. As a specific example, Lupron Depot is now routinely used for treating prostate and other hormone-dependent cancers [57]. Another example is Mylotarg, a nanomedicine platform consisting of an antibody–drug conjugate, which is prescribed for acute myeloid leukemia. Several other nanoplatforms including Oncospar, PEGASYS, Neulasta, and Somavert can now be deemed as nanomedicine technology (refer to Table 6.1 for additional nanomedicines in clinic and to Section 3.4 for PEGylated proteins and nanomedicines).

6.2.3 Cellular Uptake and Targeting

In general, only a fraction of macromolecular agents reach their biological targets *in vivo*. Thus, to enhance the therapeutic activity, it is vital to increase the intracellular penetration of drug-bearing nanoconjugates [58]. Typically, the cellular plasma membrane serves as a barrier that occludes the transport of molecules based on the molecular weight, size, polarity, and charge of the macromolecule. Nanocarriers, by virtue of internalization or shielding to anticancer agents, genes, and proteins, can "break" this barrier, cross into the cytoplasmic region, and increase the probability of heightened therapeutic response. Notably, the internalization of the nanocarriers into the cancer cells is achieved most efficiently by simple diffusion- or receptor-mediated endocytosis [59]. Interestingly, several polymeric candidates, designed to augment the therapeutic response of a drug, may not be biocompatible due to their unsuitable polymeric architecture, higher surface charge, and inappropriate molecular weight [51, 60]. Furthermore, the physicochemical characteristics (e.g., immune response, pH dependency profile, pK_a) of the polymeric candidates may also limit their potential use. Accordingly, these factors need to be considered when developing a nanomedicine-based platform. Thus, critical

determinants of nanodelivery systems include the (i) identification of specific molecular target(s), (ii) selection of suitable nanopolymer candidate(s), (iii) design of the nanocomponent delivery system, (iv) characterization of the nanostructure, and (v) *in vitro* and *in vivo* biological activity and pharmacological evaluation. To date, several different approaches (including the use of membrane-permeable peptides such as Tat protein and non-arginines) have been adopted to increase the intracellular uptake of polymer therapeutics [61]. As a specific example, cell-penetrating peptides have been attached onto liposomal carriers and micelles, which results in enhanced uptake of the polymeric carriers [62]. The augmented expression of cell-surface receptors—in particular of the receptors that are molecular mediators of disease—could also be exploited to increase the intracellular uptake of nanodelivery systems. For example, in oncologic indications, the vascular endothelial growth factor (VEGF) receptor, which is prominently present on the surface of several tumor cells, has served as an "internalization facilitator." VEGF plays a major role in tumor-initiated angiogenesis [63]. Furthermore, the largest class of oncologic drugs that block angiogenesis are the multitargeted tyrosine kinase inhibitors (TKIs) targeting the VEGF receptor (VEGFR) [64]. Anti-VEGF therapies and, in particular, bevacizumab as monoclonal antibody against VEGF have demonstrated antitumor efficacy, though the mechanism of action in the latter is not fully understood. In this context, only few vectors and molecular transporters show immense potential for breakthrough therapy as they deliver the drugs at intracellular locations after facilitation of their transport across the biological barriers [56].

Tumor invasion, metastasis, and resistance to chemotherapeutic drugs and radiation are major obstacles for the successful treatment of cancer [65]. Some of these limitations can be overcome by therapeutic strategies that increase specificity and efficacy and at the same time reduce toxicity of the anticancer drugs. One of the approaches includes targeting the polymeric delivery systems specifically to the cancer cells.

The targetability of polymeric forms of nanodelivery systems to cancer cells and tumors can be achieved by adopting either of the following two approaches: (i) passive targeting and (ii) active targeting [66].

6.2.3.1 Passive Targeting

Water-soluble polymers are now routinely used to prolong the drug circulation and residence time within affected cells, to enhance the solubility of drugs, and to reduce the systemic toxicity of drugs [59]. Back in the 1980s, Maeda/Jain observed that covalent conjugates of water-soluble polymers with cytotoxic drugs were more effectively targeted to the tumor tissue than to its free form of cytotoxic drug [67]. Maeda described his finding using the term "enhanced permeability and retention (EPR) effect." The EPR effect, which leads to an

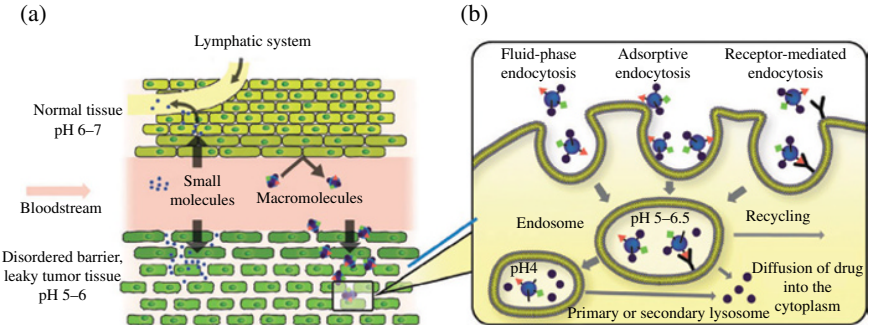

FIGURE 6.20 Schematic representation of (a) the EPR effect and (b) further cellular uptake mechanisms. Source: Khandare et al. [68]. Reproduced with permission of Royal Society of Chemistry. (*See insert for color representation of the figure*.)

increased "passive" accumulation of macromolecules in the tumor tissue, is principally governed by the hyperpermeability of tumor vasculature. This hyperpermeability allows for the selective extravasation of macromolecules into the tumor, and poor lymphatic drainage results in an increased retention of macromolecules within the tumor (Fig. 6.20) as the first example of *passive targeting* [69–71].

Theoretically, any high molecular weight water-soluble drug carrier, including water-soluble polymers, liposomes, and polymeric drugs, should display passive tumor targeting. However, the degree of accumulation of a polymeric nanodelivery system in the tumor will be a function of size, molecular weight, overall charge, and hydrophobic–hydrophilic characteristics of the delivery system [60]. The following examples will illustrate this view point. Abraxane® and Doxil® were two of the first nanocarriers to be approved by the FDA for cancer treatment. Given their relatively large sizes (130 and 150 nm, respectively), it is unlikely that these nanodepots penetrate deeply into a tumor mass [72]. Therefore, the size of these nanocarriers needs to be critically optimized [73]. Indeed, in a recent study, Sisson et al. demonstrated that PG nanogel particles with diameters between 25 and 50 nm are very efficiently and nondisruptively taken up by the cancer cells [27]. These studies highlight the importance of an "optimal" size for at least a partially efficient passive accumulation of polymeric delivery systems in the diseased/distressed tissues [74, 75].

The conjugation of therapeutic agents to the polymeric nanocarriers could potentially afford further beneficial effects. For example, multicomponent macromolecular prodrug delivery systems may influence the drug distribution in the body, with enhanced bioavailability due to a controlled and/or delayed release. Such prodrug systems often demonstrate reduced systemic toxicity in comparison with the free form of the drug. One of the earliest studies involving macromolecular carriers reported the utilization of DNA as a carrier for two oncologic drugs: daunorubicin (DNR) and doxorubicin (DOX) [76]. It has been clearly established

that DNA has a limited carrier ability due to its potential of genomic alterations [65]. In follow-up studies, the authors conjugated DNR to human serum albumin (HAS) via degradable peptide spacers. This conjugate showed a 200% increase in the life-span in mice inoculated with L1210 leukemia cells [77].

In an alternative approach of passive targeting, the molecular conditions in an organ-bearing tumor and/or in tumor environment are exploited to facilitate the drug release from the nanodelivery system [78]. These conditions may include, but are not limited to, a particular pH and the existence of certain enzymes and/or microflora in a specific organ or tumor. For example, drug delivery to the colon might be targeted by formulating tablets with a specific coating that is destroyed in the colon by colon-specific pH and/or colon-specific bacteria [79, 80]. An important limitation of this approach is the targeting of the entire organ and not just the tumor itself. This can potentially cause severe organ cytotoxicity, unless the selective stimuli of the tumor itself (e.g., lower pH) are utilized.

A further passive tumor-targeting approach is based on a direct local delivery of polymeric nanocarrier conjugated anticancer agents directly into the tumor site [78]. This delivery technique has the obvious advantage of excluding drug delivery from the systemic circulation. While topical delivery for some tumors may be achieved by injections or surgical procedures, other tumors, for instance, in lung cancers, are difficult to access for local drug delivery. In order to overcome this problem, several aerosol technologies have been developed to locally deliver anticancer agents into the lung [81].

All of the earlier mentioned "passive" approaches for targeting the polymeric forms of nanodelivery systems can be utilized to enhance a tumor-specific delivery of drugs. However, these approaches are rarely used as the predominant methodologies in current cancer therapies. The preferred and more routinely employed technique involves an "active targeting" of the polymeric forms of nanodelivery systems.

6.2.3.2 Active Targeting

An active tumor targeting of a nanodelivery system is usually achieved by coupling a targeting component onto the polymeric delivery system, which provides preferential accumulation of the entire drug delivery system or only of the drug in an organ bearing a tumor, in the tumor itself, in cancer cells, or in intracellular organelles of specific cancer cells [78]. The active targeting approach is based on the interactions between a ligand and its cognate receptor or between specific biological pairs (e.g., avidin–biotin, antibody–antigen, carbohydrate-lectin) [82]. In most cases, a targeting moiety in a nanodelivery system is focused on the specific receptor or antigen overexpressed in the plasma membrane or intracellular membrane in tumor cells.

This type of targeting is only possible when specific molecular receptors are present in malignant human tumor cells. For example, cancer cells often overexpress specific tumor-associated antigens, carbohydrate epitopes, or growth factor receptors on their cell surfaces [53, 83, 84]. The incorporation of a biorecognizable moiety into the polymer carrier structure affords an actively targeted nanodrug delivery system. So far, the potential targeting moieties that have been explored include monoclonal antibodies, polyclonal antibodies and their fragments, carbohydrates (galactose, mannose), peptides/proteins (melanocyte-stimulating hormone, transferrin, luteinizing hormone-releasing hormone, growth factors), glycolipids, vitamins, and other ligands [27, 83]. Using these targeting moieties, active polymer–drug conjugates can be selectively transported into tumor tissues.

The concept of active tumor targeting has been illustrated by several approaches. Many of these studies have utilized chemoimmunoconjugates wherein either a drug is directly conjugated with a monoclonal antibody or a drug–macromolecule conjugate is formed with a monoclonal antibody using a polymeric carrier. For example, the anticancer agent neocarzinostatin (NCS) has been conjugated with a murine monoclonal IgG1 antibody against a human colon cancer-associated cell-surface antigen. The NCS–monoclonal antibody conjugate showed significant suppression of tumor growth in patients with colon and rectal carcinoma and lower acute toxicity than free NCS [85, 86]. In separate studies, NCS has been covalently conjugated with TES-23, a highly specific antitumor tissue endothelium-specific monoclonal antibody [87, 88]. The TES-23–NCS conjugate induced tumor hemorrhagic necrosis and showed marked antitumor activity against rat/mice KMT-17 fibrosarcoma. Furthermore, mice treated with this immunoconjugate exhibited improved survival with no observable side effects.

These and other observations clearly demonstrate that active targeting enhances the overall accumulation of a polymeric nanodelivery system by the cancer cells, thereby increasing the amount of the applied dose to actually penetrate the cancer cells. This may in turn lead to a substantial increase in the cytotoxicity of the drug and thus to a more effective anticancer activity.

6.3 MULTI- AND POLYVALENT POLYMERIC ARCHITECTURES

After a discussion of the basic concepts for multivalency in Section 2.7 (see also Fig. 6.21) [89–91], functional multivalent and polyvalent systems will be presented in this chapter. For the most part, they are biologically inspired examples with applications in medicine.

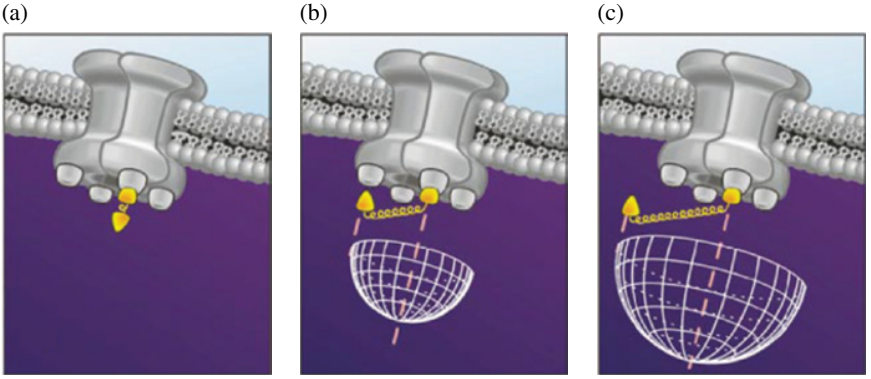

FIGURE 6.21 Bivalent binding of a ligand to the tetravalent cGMP receptor. (a) If the polymeric spacer is too short, only one binding site may be occupied in the multivalent protein receptor. (b) The highest bond strength is achieved with an adequate spacer length and optimal operating range for the second bond. (c) Too long a spacer increases the number of unproductive degrees of freedom and reduces the binding strength again. Source: Fasting et al. [89]. Reproduced with permission of John Wiley & Sons.

In multivalency the multifunctional polymeric spacer between the ligands plays a crucial role and significantly affects the binding event. First of all, the spacer could interact positively or negatively with the receptor because of its chemical nature and thus change the multivalent binding enthalpy. Secondly, an inexact geometric preorganization of the ligands can cause an enthalpic weakening of the multivalent binding. Finally, a spacer may directly affect the electrostatic characteristics of the ligands and lead to a change in the bond strength. These effects can be easily studied by theoretical methods like molecule dynamics and are very helpful because a systematic exchange of spacer groups is usually expensive to synthesize. However, it is possible to combine entropic and enthalpic effects, if the spacers' flexibility allows the ligands to be optimally geometrically oriented despite imperfect preorganization (Fig. 6.21) [92, 93].

6.3.1 Polyvalent Interactions on Biological Interfaces

Multi- and polyvalent interactions between lectins and glycans are of fundamental importance for the interaction of biological surfaces. Lectins are proteins with defined glycan-recognition domains on the surface of viruses and bacteria as well as of plant and animal cells. Affine inhibitors of lectins are, therefore, suitable for clarifying the function of defined carbohydrate structures, when they are used as a competitive binding partner. They also provide an opportunity for pharmacological intervention. The phenomenon of

multivalent lectin–glycan interaction, which has been commonly referred to and described in the glycosciences as a glucoside cluster effect, emphasizes the special biological relevance of this system [94, 95].

The binding of an individual lectin to a glycan (monovalent bond) is relatively weak, with dissociation constants (K_D) typically in the millimolar range. Stronger interactions occur if both binding partners develop clusters, whereby either several complementary, monovalent functionalities are presented on the interacting cellular surfaces (polyvalent surfaces) or a multivalent interaction between two molecules occurs because of multiple presentations of functionality within the molecule (multivalent molecule) [96–98].

Well-studied examples of strong lectin–glycan interactions between polyvalent surfaces are selectins and their glycan ligands. In these cell–cell interactions, selectins and ligands, which are presented on both surfaces, initiate the adhesion of leukocytes from the blood to the vascular endothelium. This leads to the extravasation of leukocytes into the inflamed tissue (Fig. 6.22). In pathophysiological situations, this extravasation is deregulated

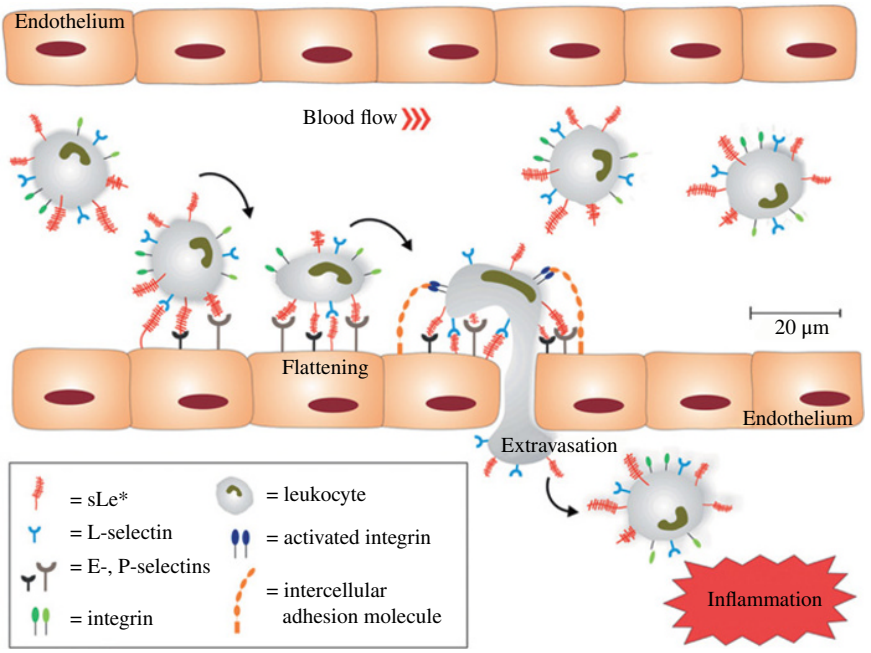

FIGURE 6.22 The selectin–ligand interaction recruits leukocytes to the vascular endothelium, which allows them to adhere. Following the inflammatory mediators, leukocytes migrate from the blood vessels toward the focus of inflammation. Source: Fasting et al. [89], figure 21. Reproduced with permission of John Wiley & Sons.

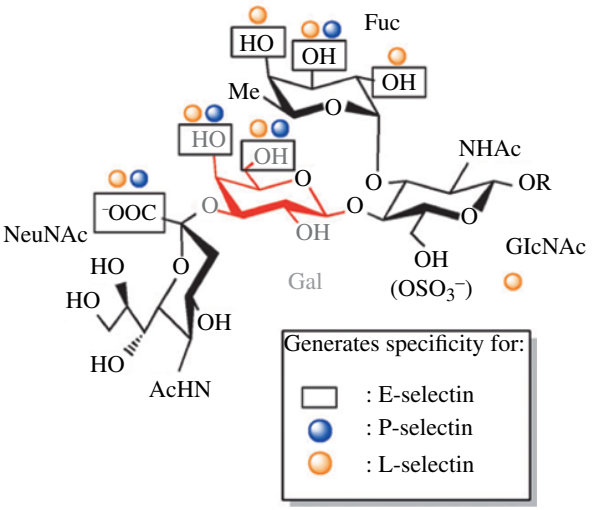

FIGURE 6.23 Structure of a sialyl Lewis^X ligand (sLe^X) und its selectin specific interaction. Source: Fasting et al. [89], figure 22. Reproduced with permission of John Wiley & Sons.

and the massive infiltration of leukocytes amplifies the inflammatory response with increased tissue damage.

Selectins are C-type lectins that form calcium-dependent bonds with their physiological ligands. The leukocyte L-selectin and the E- and P-selectins presented on the endothelium recognize all the sialyl Lewis^X tetrasaccharide ligands (sLe^X; Fig. 6.23) that are presented by membrane-bound proteins or lipids on both interacting cellular surfaces (Fig. 6.22).

Additional sulfation of the ligand is a modification that further enhances the binding of L- and P-selectin. The monovalent selectin–sLe^X interaction is weak and has a K_D value in the mm range. In a reductionist approach, the leading structure sLe^X could be successively simplified, and sLe^X mimetics could even be generated by using partial structures with only one glycan (fucose, galactose, sialic acid, and others). Although these monovalent building blocks show poorer affinities to the selectins, their activity could also dramatically increase by n-valent presentation; however, relatively low-valent systems ($n < 10$) have been examined in most cases [99, 100]. Investigations of polyvalent systems that help strengthen this interaction with their 2D interfacial character (similar to the velcro) have been very important. Such polyvalent selectin inhibitors could hinder the building of conformed cell junctions far more efficiently and should, therefore, be suitable for reducing the inflammation [101, 102].

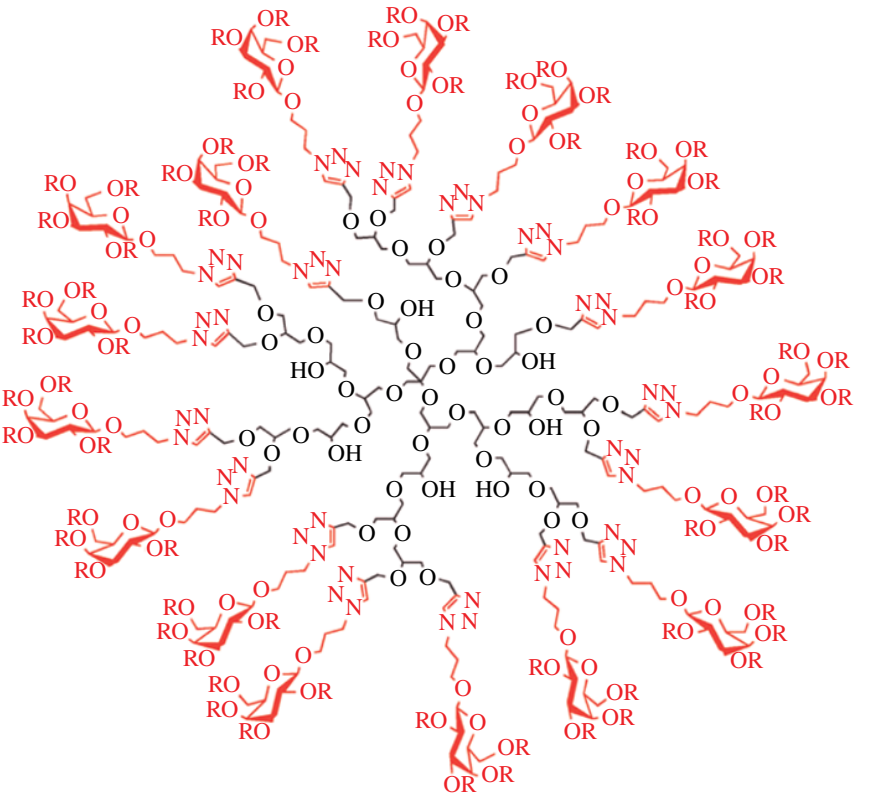

FIGURE 6.24 Schematic structure of a dendritic galactose conjugate with high L-selectin binding; IC_{50} = 2.45 mm (R═H) and 35 nm (R═SO_3Na). Source: Fasting et al. [89], figure 23. Reproduced with permission of John Wiley & Sons.

Thoma et al. were able to show that linear polylysine conjugated to a sLe^X analog could dramatically reduce the E-selectin-mediated cell–cell interaction under physiological flow conditions [103]. While the monovalent ligand had an IC_{50} value of 30–40 µm, a functionalized polymer decorated with 420 ligands gave an IC_{50} value of 50 nm, based on the ligand concentration of the polymer. The multivalent presentation of just the E-selectin ligand alone increased the inhibitory effect of a single ligand by a factor of 700. The authors could further show that the size and the degree of the polymer's functionalization are crucial for the inhibitory effect and lead to a high loading density, which sterically hinders the interaction.

In studies on selectin inhibition with functionalized dendritic glycopolymers (Fig. 6.24), Papp et al. were able to demonstrate with a competitive SPR-based measurement system that galactose acts as a minimal selectin ligand, if available in sufficient concentration [104]. Compared to a tetravalent architecture

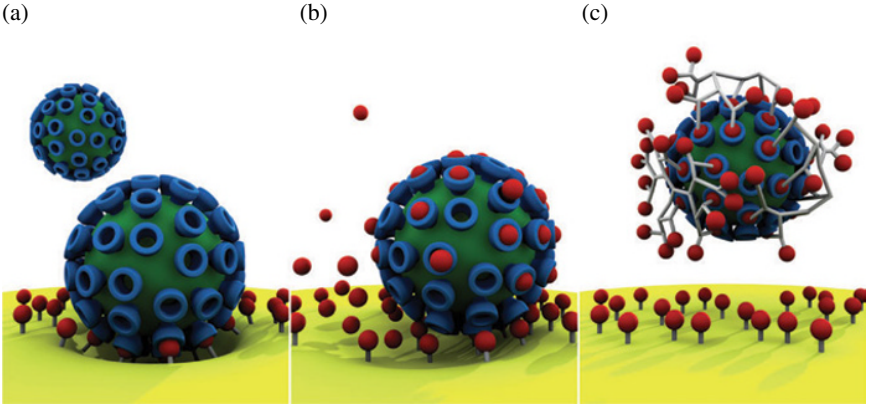

FIGURE 6.25 (a) A multivalent binding of a virus to a cell surface is compared to (b) a noncompetitive binding with monovalent ligands. (c) Multi- and polyvalent ligands are considerably more effective in binding and shielding a virus surface than monovalent ligands, thus preventing viral adhesion. Source: Fasting et al. [89], figure 2. Reproduced with permission of John Wiley & Sons. (*See insert for color representation of the figure*.)

(IC_{50} = 240 μM), a dendritic PG–glycan conjugate with 35 galactose units effected a 100-fold strengthening of the L-selectin ligand inhibition, based on a single galactose unit (IC_{50} = 2.45 μM). The additional introduction of sulfate groups into the galactose conjugate enhanced the inhibition by a factor of 70, and an IC_{50} value of 35 nM was reached. This clear evidence of a polyvalent effect can still be significantly improved upon using a more rigid scaffold architecture.

Analogous to the sulfated multivalent glycoconjugates, the dendritic polyglycerol sulfate (dPGS), which binds in the nanomolar range to L- and P-selectins, as well as to other inflammatory mediators, was identified to be a highly active anti-inflammatory compound [105, 106].

Even if the presentation of the ligands on a spherical or planar polymer surface cannot be rationally coordinated to the complementary receptor positioning but is statistically distributed instead the result is a significantly higher inhibition that can now be reconciled with theoretical methods in terms of binding kinetics (e.g., possibly increased rebinding of the ligands) and better thermodynamics.

Another well-studied example is the distribution of the hemagglutinin receptors on the virus surface, which does not allow low-valent systems to efficiently interact with the individual receptors. Therefore, large polyvalent polymeric scaffolds would be ideal candidates to inhibit these biological nano-objects (Fig. 6.25).

Statistical random polymers, such as linear polyacrylamide sialic acid conjugates with high molecular weight (10^6 Da), show a 10^8-fold increase in binding affinity and block cell adhesion through large interfacial, polyvalent interactions. The high molecular weight of the polymer and thus the related long residence time in the body, however, make *in vivo* applications unrealistic. Nevertheless, the high effectiveness of these linear polymers *in vitro* has been proven [107, 108]. In addition to their extreme binding affinity, they can sterically shield the virus particles when used in combination with other monovalent ligands [109].

An alternative approach to high molecular weight linear polymers is dendritic nanogels (see Fig. 6.10) that have the same dimensions as influenza viruses and can partake in competitive surface interactions (Fig. 6.26). Novel biocompatible and biodegradable nanogels based on PG (20–100 nm) that can be decorated with the appropriate sialic acid ligand by a simple modular functionalization at their surfaces have been developed in some fundamental studies [27, 31]. For the first time, strong interactions could be achieved between the sialic acid-functionalized nanogels and the hemagglutinin of influenza virus receptors, and cellular infection could be inhibited up to 80% [110]. It is interesting that nanogels with low functionalization performed better than highly functionalized ones, which may have been due to steric overloading of the latter. These polyvalent nanogels are promising candidates for more effective antiviral therapies.

6.3.2 Prospects for Multivalent Drugs

Despite long-standing, fundamental research on multivalent drugs, no major pharmaceutical company has seriously engaged itself with the great potential of multivalent interactions. The reason probably lies in the extreme focus that was first on "small molecules" and nowadays on "biologicals." The emerging field of polymer therapeutics has, therefore, been taken up more by innovative small- and medium-sized enterprises. Two examples of multivalent drugs will be given.

In analogy to sulfated multivalent glycoconjugates (Fig. 6.26), it was possible to synthesize a simple polysulfated heparin analogous structure [97]. Recently, a highly active anti-inflammatory interaction with dPGS (Fig. 6.27) was discovered that bound other inflammatory mediators in the nanomolar range of L- and P-selectins as well as in an *in vivo* mouse model with contact dermatitis that was as effective as the commercial glucocorticoid prednisolone [105].

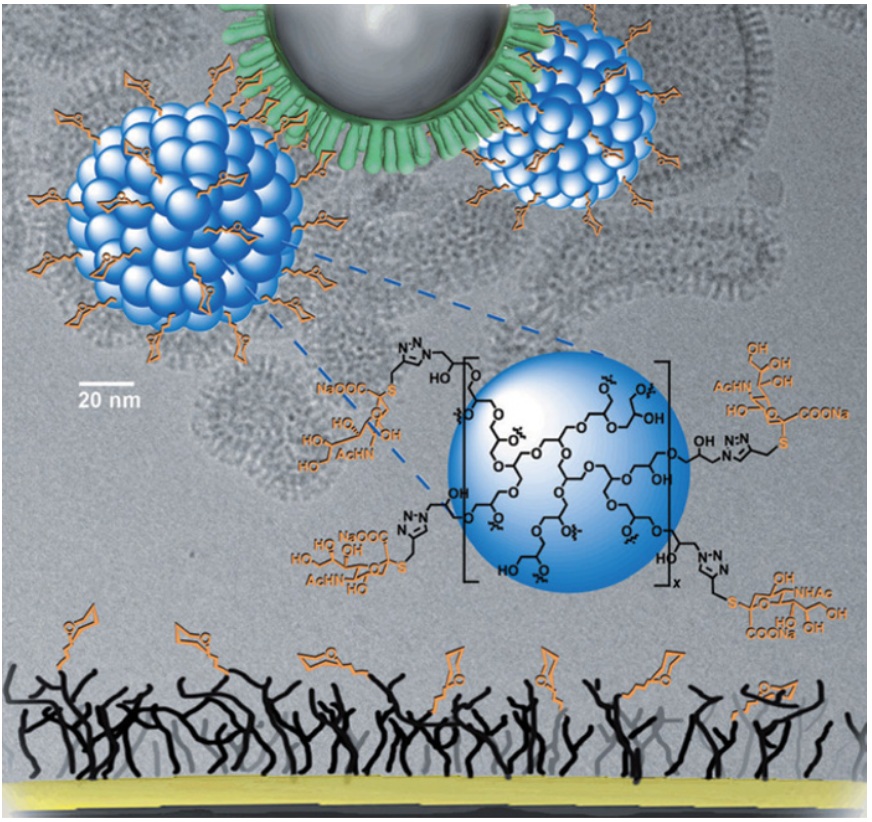

FIGURE 6.26 A polyvalent interaction of sialic acid-functionalized polyglycerol nanogels with hemagglutinin receptors on the virus surface. The viral binding and thus the cellular infection of the influenza virus can be reduced by up to 80% through efficient competition between the nanogel and glycan structures, such as sLe^X, presented on the cell surface. Source: Fasting et al. [89], figure 26. Reproduced with permission of John Wiley & Sons.

The great advantages of dPGS are that it is easily available on a large scale and it is possible to conjugate effector molecules, for example, dyes and drugs [111].

There has also been a first clinical development of multivalent drugs in the antiviral area. VivaGel was developed as a topical vaginal gel that can prevent or reduce the transmission of HIV (Table 6.1). The sulfonated dendritic scaffold is currently being tested in a clinical phase II study [112]. The limited size of the low-generation dendrimers used compared to the distribution of hemagglutinin receptor sites on the virus surface is a limitation for efficient multivalent interactions. However, the elimination of such polymeric drugs through the kidneys is a general consideration that has to be kept in mind

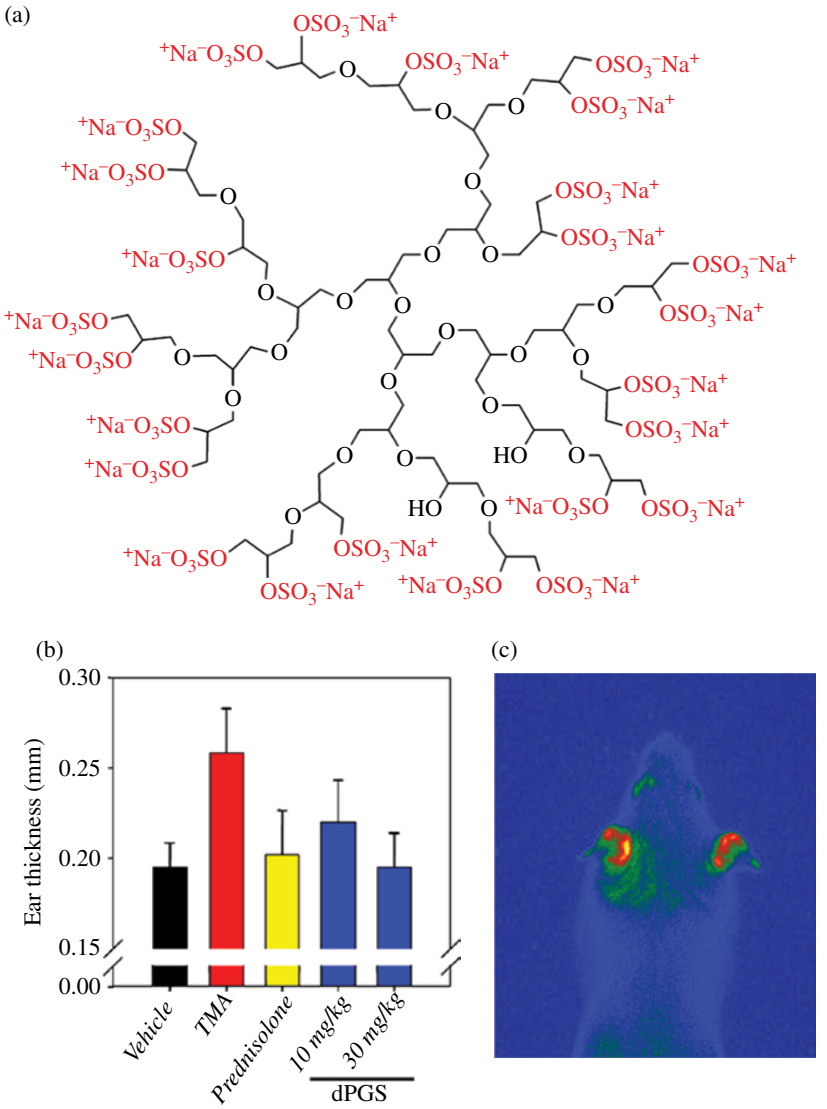

FIGURE 6.27 (a) Structure of dPGS, (b) therapeutic study of contact dermatitis in a mouse model involving ear swelling after stimulation by trimellic acid anhydride (TMA) and dPGS (blue bar) compared to commercial prednisolone (dose: 30 $mgkg^{-1}$, yellow bar), and (c) an inflammation selective fluorescence diagnosis with a dPGS–dye conjugate. Source: Fasting et al. [89], figure 27. Reproduced with permission of John Wiley & Sons. (*See insert for color representation of the figure.*)

(limit is ~40 kDa). For future investigations, biodegradable, polyvalent polymeric systems with large interfacial contact sides need to be designed.

6.4. BIORESPONSIVE NETWORKS

6.4.1 Active Principle

Bioresponsive networks, and in particular bioresponsive hydrogels, are an emerging class of materials with numerous applications in fields like mediated drug delivery, biosensing, or tissue engineering. In order to narrow down the term bioresponsive hydrogel, systems with a simple material-to-biology communication should be distinguished from systems with a biology-to-material communication that are discussed here [113]. In the first case, ligands incorporated into the hydrogel structure provide control over the biological interactions of the material. The most common example for this strategy is the presentation of the immobilized tripeptide Arg-Gly-Asp (RGD) that facilitates an improved adhesion of many cell types to surfaces via integrin interactions. For biology-to-material communication, the underlying mechanism is more complex: An appropriate biological impact triggers the macroscopic response of a stimuli-responsive hydrogel by an incorporated recognition species. In this versatile concept, the highly specific recognition capacity of bioreceptors is paired with the tailored response of a macromolecular structure. The range of recognition units (either native or synthetic) comprises peptides, enzymes, or antibodies that are attached to or incorporated into the hydrogel structure (covalently or noncovalently bound to the polymer chain or polymerized into the backbone). Upon the initial recognition event (e.g., binding or catalysis), a transduction mechanism enables the response of the system that finally restores the equilibrium [114]. According to Figure 6.28, the majority of bioresponsive hydrogels can be assigned to three classes. The response (swelling/collapsing or degradation of the hydrogel) occurs upon receptor–ligand interactions (I), enzymatic cleavage of incorporated enzyme-sensitive peptide structures (II), or enzymatic conversion of small biomolecules with the subsequent release of products with different physical properties (e.g., acidic or basic) (III).

All active principles introduced earlier are per se unidirectional. However, the implementation of feedback loops allows for bioresponsive hydrogels that exhibit a true self-regulation capacity. These next-generation systems can adopt magnitude and direction of the response to the respective stimulus like the concentration of a particular biomolecule in the local environment. This

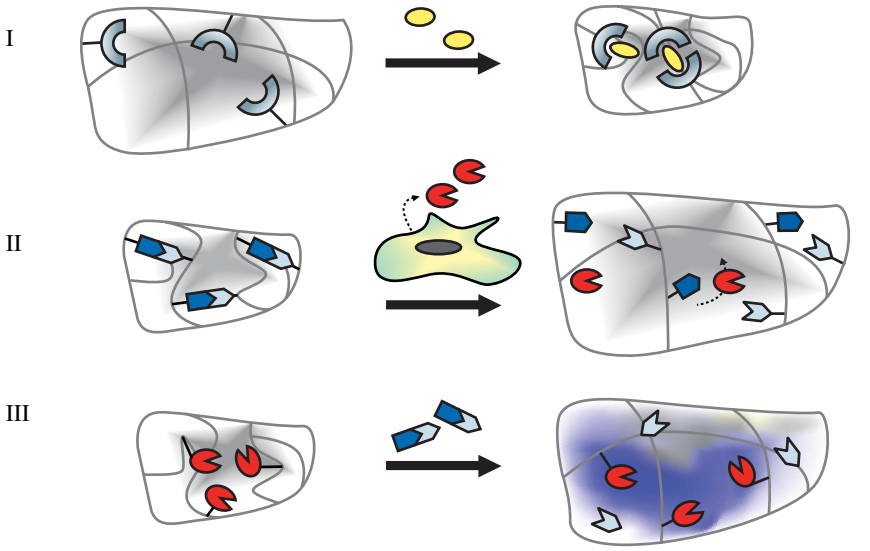

FIGURE 6.28 Different types of bioresponsive hydrogels that change properties in response to (I) small molecules via receptor/ligand interactions; (II) (cell-secreted) enzymes via cleavable linkers; and (III) small molecules that are converted by immobilized enzymes. The macroscopic response (swelling/collapse of the hydrogel) is shown. Source: Ulijn et al. [113]. Reproduced with permission of Elsevier.

paves the way for a range of challenging applications, for example, in drug delivery where a spatiotemporal control over the release behavior in the human organism is desired. In order to illustrate the potential of bioresponsive hydrogels, some examples will be introduced in more detail in the following chapters. It will be shown how basic physicochemical and biochemical mechanisms can be combined within this concept toward responsive, self-regulating, or self-amplifying systems that provide answers to prevalent biomedical problems.

6.4.2 Homeostatic Regulation of Blood Coagulation

Maitz et al. [115] report on a blood coagulation-responsive hydrogel that provides a release of the anticoagulant heparin triggered by the environmental concentration of the coagulation factor thrombin. Since the response (heparin) downregulates the trigger (thrombin), the system features an integrated feedback loop. The detailed working principle is illustrated in Figure 6.29. In the coagulation cascade, thrombin is generated from prothrombin when blood is exposed to foreign materials (a). As a protease, thrombin selectively

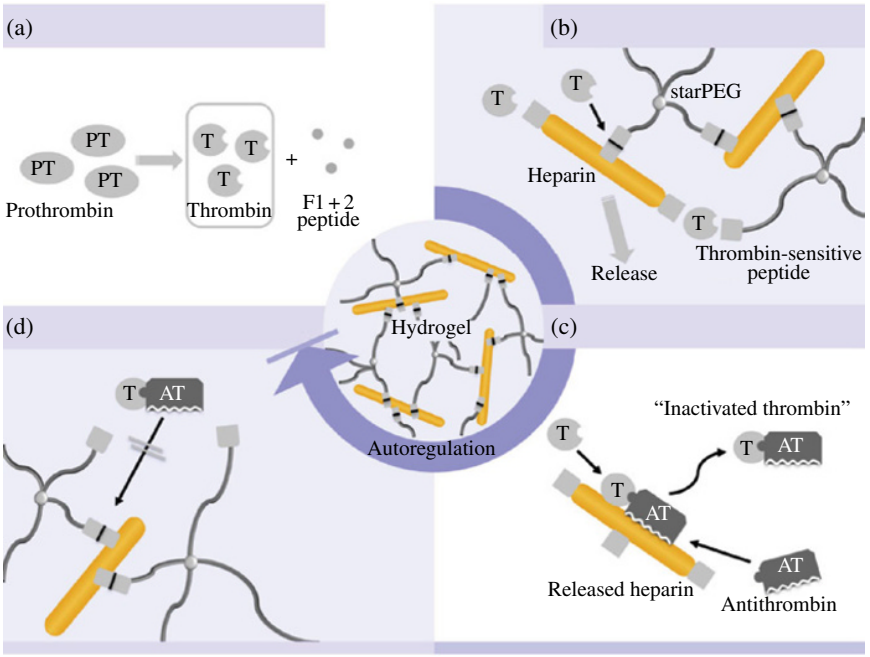

FIGURE 6.29 Autoregulation of heparin release from a thrombin-sensitive bioresponsive hydrogel. (a) Thrombin formation. (b) Responsive heparin release. (c) Heparin-catalyzed thrombin inhibition. (d) No further heparin release. Source: Maitz et al. [115]. Reproduced with permission of Nature Publishing Group.

attacks a cleavable peptide sequence in the linker unit of the biohybrid starPEG–heparin hydrogel (b). The rate of subsequent heparin release can be preselected by the initial cross-linking degree of the hydrogel. In the next step, heparin catalyzes the inhibition of thrombin by its physiological inhibitor antithrombin (c). This inactivation process lowers the active thrombin concentration in the medium and gradually stops hydrogel degradation and heparin release (feedback loop). The ability of the gel to provide a sustainable, autoregulated anticoagulation was tested successfully in comparison with clinically applied heparin-functionalized vascular grafts made of expanded poly(tetrafluoroethylene).

6.4.3 Insulin Release in Response to Glucose Concentration

Bioresponsive hydrogels can be employed to implement a self-regulating system for controlled release of insulin in response to an environmental glucose concentration. Toward this goal, Podual et al. [116] prepared a series

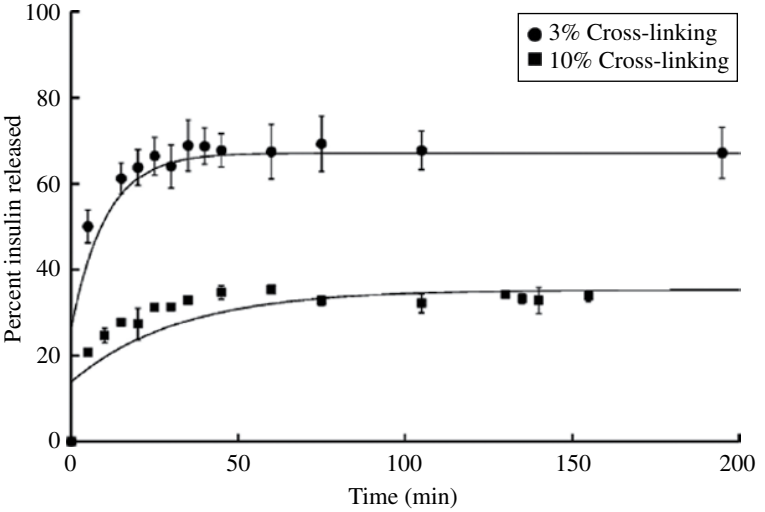

FIGURE 6.30 Release profile of insulin-loaded microparticles in response to a glucose stimulus. Source: Marek and Peppas [118], figure 7. Reproduced with permission of John Wiley & Sons.

of pH-sensitive cationic hydrogels with immobilized glucose oxidase. When exposed to a glucose containing medium, glucose oxidase reacts with glucose and forms gluconic acid. This decreases the pH in the microenvironment and triggers a swelling of the hydrogel. The corresponding increase in the mesh size allows in principle for the release of embedded molecules. The glucose-dependent swelling of microparticles was shown to be reversible. In response to repeated variations of glucose concentration, it leads to a pulsatile behavior [117]. Finally, the glucose-stimulated release of physiologically relevant amounts of entrapped insulin from the microparticle system was demonstrated [118]. The cross-linking of the hydrogel was identified as an effective parameter to optimize the release profile for an insulin delivery device (Fig. 6.30).

6.4.4 Urate-Responsive Release of Urate Oxidase

A biohybrid hydrogel with a uric acid-triggered degradation was proposed by Geraths et al. [119]. The gel system is based on polyacrylamide and cross-linked by the uric acid-sensitive interaction between the uric acid-responsive transcription factor and its cognate DNA binding sequence. Urate oxidase stabilized by PEGylation was incorporated into the stimuli-responsive hydrogel matrix. It was released as an active agent upon elevated uric acid concentrations in the ambient medium and subsequent hydrogel degradation. The

release decreases the uric acid level, which, in turn, decelerates and finally stops gel degradation (feedback loop). The release system is intended to counteract pathological concentrations of uric acid due to gouty arthritis attacks. As a proof of principle experiment, the autonomous compensation of externally induced uric acid pulses in mice by an implanted stimuli-responsive urate oxidase reservoir was shown [119]. Beyond this, the general concept of transcription factor–DNA pairs as recognition units for disease-relevant metabolites that induce the degradation of a hydrogel matrix with subsequent release of an embedded effector molecule is applicable to many other cases after simple exchange of the cleavable structure.

6.4.5 Cell-Responsive Degradation of Hydrogel Networks

Hydrogels can mimic native extracellular matrices when used as scaffolds in tissue engineering applications. In addition to the mechanical support, bioresponsive hydrogel systems can provide a distinct cell-responsive degradation behavior. This is commonly achieved by the incorporation of cross-linkers with peptide sequences that are cleavable by cell-released enzymes like matrix metalloproteinases (MMPs). The mechanism allows for cell invasion into the 3D structure of the artificial matrix, while the rate of matrix degradation is controlled by the actual migration activity of the cells. This basic concept of MMP-mediated matrix remodeling can be refined following different routes. In particular, the effect can be further amplified by an additional cell stimulus that is coupled to the progressive matrix degradation (i.e., a positive feedback contrary to the self-limiting systems described earlier). This has been demonstrated by Tsurkan et al. [120] for an MMP-cleavable starPEG–heparin hydrogel. Primary human umbilical vein endothelial cells (HUVECs) possess an improved 3D migration behavior in an MMP-cleavable hydrogel matrix compared with a noncleavable control. Moreover, the effect is strongly amplified when loading the cleavable matrix with VEGF that is released upon gel degradation (Fig. 6.31).

6.5 BIOFUNCTIONAL SURFACES

6.5.1 Concepts and Aims of Biofunctional Material Surfaces

When man-made solid materials come into contact with biofluids, *in vitro* or *in vivo* several unspecific and highly specific reactions/processes might occur, for instance, blood coagulation, denaturation of proteins, cell adhesion, or

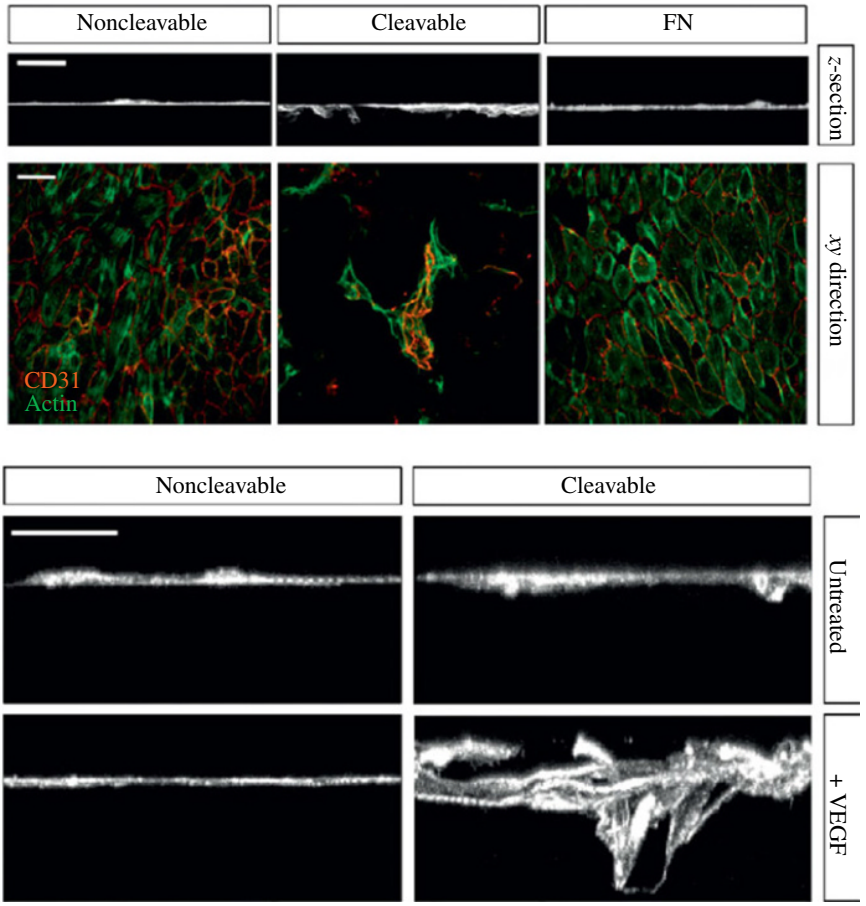

FIGURE 6.31 Top: Representative surface and cross-sectional images indicating three-dimensional growth of HUVECs within MMP-cleavable gels after 7 days. Bottom: Representative cross-sectional images illustrating enhanced three-dimensional cell migration in VEGF-loaded MMP-cleavable hydrogels after 1 day of culture, scale bars = 50 µm. Source: Tsurkan et al. [120], figure 3. Reproduced with permission of John Wiley & Sons. (*See insert for color representation of the figure*.)

biofilm formation. The biological response is strongly influenced by the material surface properties.

Surface engineering aims for a defined physical, chemical, or biomolecular modification of material surfaces in order to create biofunctional surfaces that ensure biocompatibility (noninteractive materials) and in many cases additionally bioactivity of the material (interactive biomaterials) for a certain application. The design of appropriate biofunctional surfaces is important for the proper function of biosensors, membranes or implants, for the use as

TABLE 6.2 Bioactive Molecules

Synthetic Bioactive Units	Biopolymers: Proteins, Polysaccharides	Matrix Assemblies and Supramolecular Structures
Benzamidine-type coagulation inhibitors	Thrombomodulin, heparin	Collagen I/ glycosaminoglycan fibrils
(Per)sulfated mono- and disaccharides	Growth factors, cytokines, chemokines (BMPs, LIF, SCF, SDF1-α), enzymes (proteases, glycosidases, etc.)	Collagen IV/laminin meshworks
Peptides	Matrix polymers (fibronectin, heparin sulfate, hyaluronic acid)	Lipid bilayer membranes

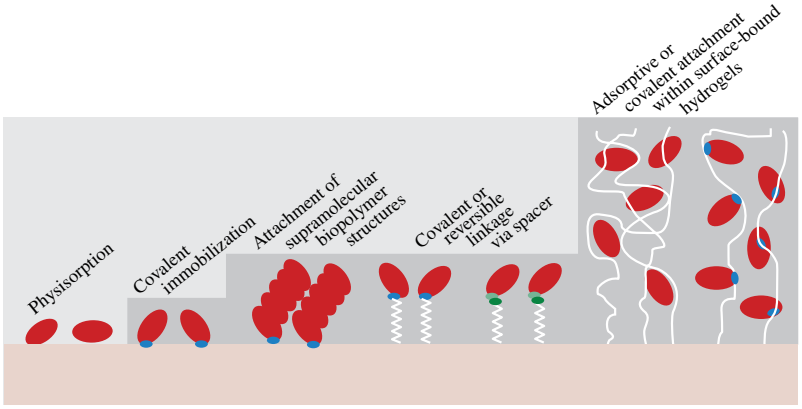

FIGURE 6.32 Binding modes for biofunctionalization.

model surfaces for cell-biological studies, and for controlled drug release in medical applications. An excellent overview on concepts and technologies in that area can be found in reference [121].

For implementing dedicated functions of living matter into man-made materials, the binding of bioactive molecules, that is, synthetic bioactive units, biopolymers or matrix assemblies, and supramolecular structures (for details, see Table 6.2), at the material surface is of raising interest. In general these bioactive molecules can be immobilized by different binding modes as schematically shown in Figure 6.32.

Surface density, orientation and/or molecular conformation of the immobilized bioactive components, and/or nonspecific adsorption of biopolymers will control the performance of biofunctional surfaces. Options to address

these aspects concern the choice of the bioactive molecule, the mode of immobilization/assembly, and the physicochemical characteristics of the material surface. The latter can be modified by chemical or physical processes. For instance, microstructuring was shown to influence wetting behavior of a surface and thus, for instance, the extent of bioadhesion. For an oriented and switchable immobilization of bioactive molecules, biomimetic principles like antibody–antigen or receptor–ligand interaction can be utilized. Common examples for site-specific immobilization include linking of histidine (His)-tagged biomolecules (proteins) to surface-bound NTA (nitrilotriacetic acid)-Ni^{2+} or linking of streptavidin to biotin. Furthermore, bioresponsive coatings that release bioactive molecules only on demand offer new possibilities.

In order to organize biomolecules and/or cells at material surfaces in a highly controlled manner, physical and chemical patterning of surfaces (cf. Section 3.10) into binding and nonbinding areas in the micro- to nanometer range has become an important tool. Patterns of bioactive molecules can moreover be utilized for combinatorial approaches in order to screen newly designed biofunctional surfaces. Preparation of multiarrays—that is, a multitude of spots presenting bioactive molecules in different concentrations and compositions and deposited by localized immobilization on a given material surface—allows for multiparameter studies on the role of bioactive molecules for a certain application. For instance, the interaction of cells with different ECM proteins (and combinations thereof) can be screened in order to develop cell-adhesive coatings for implants and cell culture systems.

Although a very large number of promising surface engineering strategies have been developed, the availability of biofunctional surfaces that resist nonspecific bioadsorption and retain bioactivity is often still a challenge.

Due to the multitude of different biofunctional surfaces for various applications, we will concentrate on selected examples highlighting some principles to control the interaction of a biomaterial (i.e., adsorption, adhesion, and activation) with the bioenvironment, including proteins, cells, and organisms.

6.5.2 Biofunctional Surfaces for the Prevention of Biofouling

Biofouling is the undesired deposition of organic material and organisms, from unicellular to invertebrate species, on man-made surfaces. This phenomenon can occur in an extremely wide range of situations, from the colonization of medical devices to the production of ultrapure, drinking, and process water and the fouling of ship hulls, pipelines, and reservoirs limiting their performance and generating high economical costs. It is a dynamic process, which spans numerous length scales and involves a complex variety of molecules and organisms.

Nature provides various examples of antifouling surfaces. The prominent ability of fish skin to prevent biofouling is due to a smooth and soft mucus layer on its surface. Also other marine organisms such as sharks, mussels, and crabs have natural antifouling techniques. Another example is the skin of springtails (Collembola) that features mechanically stable, hierarchical, micro- to nanoscale structural elements that equips the animal with omniphobic, antiadhesive properties. Natural antifouling is often a combination of chemical and physical factors, including micro- and nanotopography [122].

Inspired by nature, common antifouling strategies are based on both chemical and physical concepts. Surface modification with smooth hydrophilic polymers layers, such as PEG, polyglycerol, poly(hydroxyethyl methacrylate) (PHEMA), and poly(oligo(ethylene glycol) methacrylate) (POEGMA), have been shown to be efficient approaches for changing the unspecific adsorption of proteins. Recently, zwitterionic polymers have received significant attention as antifouling coatings due to the prevention of cellular attachment and protein adsorption [123]. Alternatively, natural or synthetic bioactive molecules can be immobilized onto the surface or surface microstructuring can be utilized [122, 124]. However, no single technology has been demonstrated universally applicable and effective for different antifouling requirements.

The following two antifouling strategies using biofunctional surfaces will be exemplarily described in more detail:

1. Active enzyme coatings by immobilization of proteolytic enzymes onto reactive polymer layers
2. Biologically inspired omniphobic surfaces by reverse imprint lithography

6.5.2.1 Active Enzyme Coatings by Immobilization of Proteolytic Enzymes onto Reactive Polymer Layers

As many fouling organisms use proteins and glycoprotein polymers to attach to surfaces, enzymes able to hydrolyze these adhesive proteins were considered to prevent biofouling [124, 125]. Especially, the incorporation of proteolytic enzymes into surface coatings was demonstrated to be an appropriate technology.

Recently, a well-defined model system was used to investigate the influence of immobilized subtilisin A, a serine protease, on the adhesion of major marine foulers [125–127]. The model system was based on reactive maleic anhydride copolymers covalently attached as nanometer-thick films to amino-functionalized surfaces (Fig. 6.33) [129]. These copolymer films are a versatile platform for biosurface engineering as the physicochemical profile of the films can be tuned by the choice of the comonomer, molecular weight, and preparation

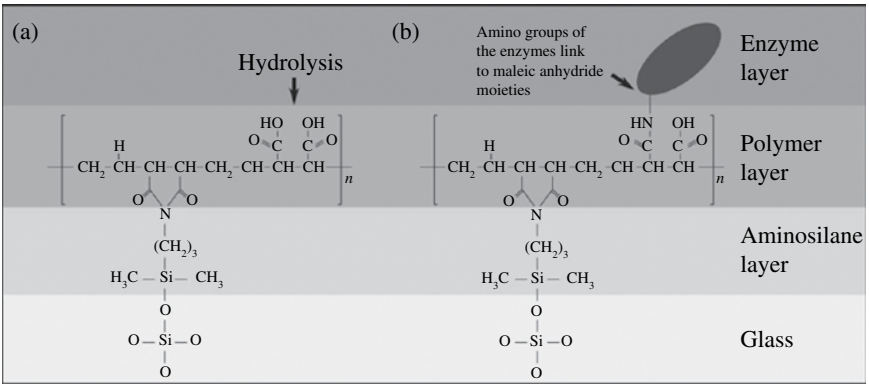

FIGURE 6.33 Schematic illustration of the maleic anhydride copolymer thin film system used to covalently immobilize biofilm-degrading enzymes. (a) Initial state–PEMA film covalently attached to amine-functionalized glass. (b) Immobilization of biofilm-degrading enzymes through reaction of the primary amino groups of lysine side chains to the anhydride groups of the polymer. Source: Friedrichs et al. [128], figure 2. Reproduced with permission of John Wiley & Sons.

conditions. The reactivity of the anhydride moieties allows for the introduction of further functionalities and the immobilization of bioactive molecules using different binding strategies [129]. Covalent binding of subtilisin A via its amino (lysine) groups provided active enzyme-containing coatings of distinct physicochemical and biocatalytic characteristics (Fig. 6.33).

The characteristics of the polymer substrates determined the availability and activity of the immobilized enzyme. The immobilization of subtilisin A onto highly swelling poly(ethylene-alt-maleic anhydride) (PEMA) copolymer films was found advantageous since it permitted higher enzyme loadings and total activities as compared with enzyme immobilization onto the compact hydrophobic poly(octadecene-alt-maleic anhydride) (POMA) copolymer films [125].

The bioactive coatings were tested for their effect on the settlement and adhesion strength of two major fouling species: the green alga *Ulva linza* and the diatom *Navicula perminuta*. The results showed that the immobilized enzyme effectively reduced the settlement and adhesion strength of zoospores of *Ulva* and the adhesion strength of *Navicula* cells. The antifouling efficacy of the bioactive coatings increased with increasing enzyme surface concentration and activity and was found to be superior to the equivalent amount of enzyme in solution [126], indicating improved enzyme stability, activity, and/or selectivity due to immobilization. Furthermore, covalent immobilization of the bioactive enzyme to the solid surface is expected to

minimize possible negative effects on nontarget species due to nonrelease of the enzyme into the environment.

Besides the degradation of secreted adhesives by enzymes, the production of antifouling compounds is a main strategy to control marine biofouling, while the main concepts to control pathogenic biofilms rely on cell lysis and on the degradation of ECM polymers [124].

Although the use of enzymes emerges among the investigated approaches as one of the favorite candidate antifouling technologies, the successful incorporation of enzymes into coatings yielding surfaces with broad antifouling spectrum and long-term efficacy still remains a challenge.

6.5.2.2 Biologically Inspired Omniphobic Surfaces by Reverse Imprint Lithography

Surface roughness can determine the macroscopic wetting characteristics of solid surfaces and consequently their susceptibility to biofouling. Artificial surfaces that mimic the needle or pillar structures of superhydrophobic leaves, for example, lotus leaves, have attracted attention due to their excellent repellence of water droplets and resulting self-cleaning capability (lotus effect). Upon immersion into aqueous media, superhydrophobic surfaces effectively retain air. Due to a minimized contact area between the applied medium and the solid surface, such superhydrophobic surfaces can prevent biofouling. However, lotus-leaf-inspired superhydrophobic surfaces cannot inhibit wetting by low-surface-tension liquids such as oils or water contaminated by soluble substances that decrease the surface tension. Moreover, they are not suitable for large immersion depths and their mechanical stability is insufficient, which limits the long-term durability of these surfaces [130].

A novel and promising strategy for the fabrication of omniphobic polymer coatings that exhibit resistance even against wetting with low-surface tension liquids was recently introduced by Hensel et al. [130] inspired by the effectively liquid-repellent and mechanically stable morphology of the springtail skin [131–134]. The skin of springtails (*Collembola*) provides an impressive example of such omniphobic surfaces that occurs in nature and protects these skin-breathing species against suffocation by complete wetting. The entire body of springtails is covered with nanoscopic granules and interconnecting ridges, which together form a comblike pattern [132], as exemplarily shown for the skin morphology of *Folsomia candida* in Figure 6.34a [130]. Recent analyses demonstrated the decisive role of these structural features—specifically the overhangs of the nanoscopic granules—for the prevention of wetting, independent of the surface chemistry [133, 134] and even upon immersion into many polar and nonpolar solvents [131]. Furthermore, due to the comblike

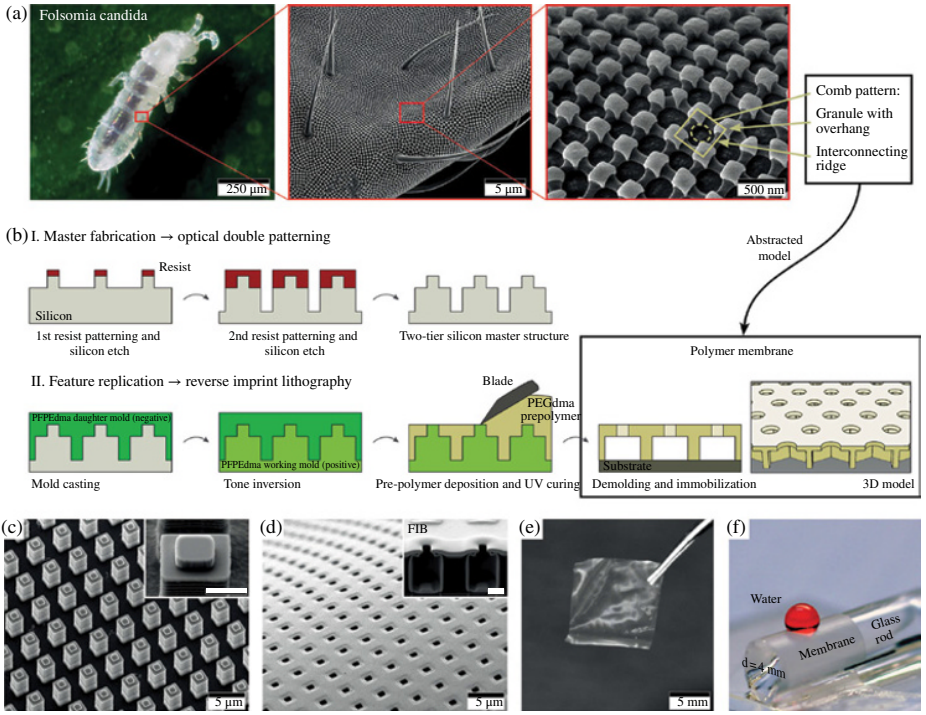

FIGURE 6.34 Springtail skin morphology and process scheme for manufacturing polymer membranes with similar structural features. (a) Habitus image of *Folsomia candida*. Insets show scanning electron micrographs (SEMs) of the characteristically contained bristles, granules, and ridges. The nanoscopic granules and interconnecting ridges form cavities, are arranged in a comb-like pattern, and provide a template for the developed polymer membranes. (b) Process scheme for membrane fabrication: Firstly, a two-tier silicon master structure is fabricated by optical lithography. Secondly, the master structure serves as template for reverse imprint lithography. (c) SEM image of the two-tier silicon master structure (inset: detailed view of a small pillar centered on a larger pillar, scale bar: 1 µm). (d) SEM image (inset: cross-section after focused ion beam preparation, scale bar: 1 µm) and (e) photograph of the springtail-skin-inspired polymer membrane. (f) Water droplet (colored with red dye) deposited on the membrane, which was transferred to a 4 mm diameter glass rod. Source: Hensel et al. [130], figure 1. Reproduced with permission of John Wiley & Sons.

arrangement of the granules, springtail skin is stable against wear and friction as confirmed in sand abrasion experiments [131].

Utilizing a reverse imprint lithographic technique (Fig. 6.34b), the advantageous properties of the springtail skin were effectively translated into polymer membranes that mimic the contained comblike patterned cavities with overhangs. The process scheme for membrane fabrication is shown in Figure 6.34b. Firstly, a two-tier silicon master structure that consisted of small pillars centered on larger pillars (Fig. 6.34c) was fabricated by optical lithography. This master served as a template for feature replication based on a reverse imprint lithography approach. The cavities of perfluoropolyether dimethacrylate (PFPEdma) templates cast from the silicon master were filled with a poly(ethylene glycol) dimethacrylate (PEGdma) prepolymer solution by doctor-blade technique without a residual layer on the small pillar structures. After subsequent cross-linking, a perforated membrane was obtained. Each cavity of the membrane had a narrow opening at the top, which provided an overhang inside the cavity (Fig. 6.34d). After demolding, the flexible free-standing membrane (Fig. 6.34e) could be transferred to various even non-flat bulk materials, for example, a glass rod (Fig. 6.34f).

6.5.3 Anticoagulant Coatings for Blood-Contacting Devices

As already discussed in Section 4.5, activation of blood coagulation pathways and thrombus formation on synthetic surfaces remain the major complications during the clinical use of blood contacting artificial devices such as catheters or cardiovascular implants. Numerous studies have shown that the hemocompatibility of such materials could be enhanced by regulating the activity of the serine protease thrombin, the key enzyme of the coagulation process, through thin film coatings at the biomaterials surface. Usually, such coatings are based on natural biologically active substances (e.g., heparin, hirudin, or thrombomodulin [135]) or synthetic drugs, which are physiologically active in preventing blood clotting [136, 137]. Other strategies rely on the passivation of the blood-contacting material surface. Materials passivated with polyethylene glycol (PEG) molecules were reported as blood-compatible cushions by minimizing and retarding the adsorption of plasma proteins as well as limiting the platelet adhesion. Other protein-resistant surfaces were obtained by decorating the surface with phosphorylcholines or polyglycerol [123].

Here, we will shortly highlight a commercially available heparin-based biofunctional surface coating that is used to enhance blood compatibility of medical devices. The second example will illustrate that biomolecular function can be translated into fully synthetic systems and altered beyond the naturally

occurring variations. It introduces a surface engineering strategy utilizing synthetic thrombin inhibitors based on benzamidine (hirudin analogs) to reduce coagulation activation.

6.5.3.1 Commercially Available Heparin-Based Hemocompatible Surface Coating

For the prevention of blood coagulation, blood-contacting surfaces are often modified with polysaccharides (dextran, heparin). Carmeda™ BioActive Surface (CBAS™) is the most clinically proven hemocompatible surface coating available on the market. It is certified by EN ISO 9001/EN 46001 and used for cardiopulmonary bypass devices. The general principle of the CBAS coating technology is to attach functionally active heparin to the surfaces of medical devices. Heparin is an extended polymer of repeating sugar units that requires an intact 3D structure to express its biological activity.

Therefore, it is bound to the blood-contacting material surface by attachment at one terminus of the heparin molecule. Antithrombin—the most important inhibitor of enzymes controlling the clotting of blood—binds to the highly specific "active sequence" of five sugar residues in the immobilized heparin molecule. That accelerates the inactivation of thrombin and other coagulation factors. Finally, the complex formed between the antithrombin and thrombin is released, reexposing the surface-bound heparin molecule and sustaining the anticoagulant activity.

6.5.3.2 Immobilized Synthetic Thrombin Inhibitors Based on Benzamidine to Reduce Coagulation Activation

Whereas heparin acts indirectly via activation of antithrombin, hirudin—a peptide naturally occurring in the saliva of medicinal leeches (e.g., *Hirudo medicinalis*)—directly inhibits thrombin. However, hirudin has a limited stability and therefore restricted applicability.

Synthetic thrombin inhibitors can mimic this function. Especially, non-peptide low molecular weight direct thrombin inhibitors can be produced at lower expenses than the complex protein inhibitors. Low molecular weight molecules are also more stable at handling and sterilization and are not subject to physiological regulation mechanisms. Moreover, oriented immobilization at material surfaces is easier due to the lower number of reactive groups.

In the following, we will focus on low thrombogenic material surfaces prepared by covalent attachment of synthetic thrombin inhibitors based on benzamidine (benzenecarboximidamide) [136–138] on the top of macroscopic flat surfaces precoated with reactive maleic anhydride copolymer thin

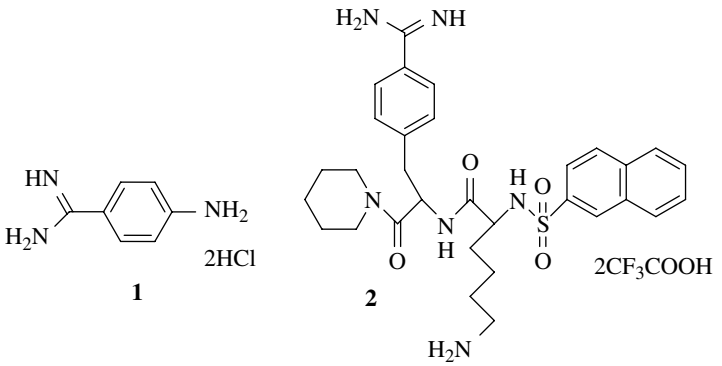

FIGURE 6.35 Structure of selected benzamidine-type inhibitors [137]. Source: Gouzy et al. [137]. Reproduced with permission of AIP Publishing LLC.

films with or without a linking spacer molecule. Maleic anhydride copolymer thin films have already been introduced as a versatile platform for molecular biosurface engineering in Section 6.5.2. From the chemical point of view, inherent advantages of these copolymers are a regular alternating and reproducible structure and the reactivity of anhydride moieties, which permits an effective grafting of nucleophilic agents (such as amine).

The structures of two benzamidine-type thrombin inhibitors (hirudin analogs), a small benzamidine derivative (**1**) and a NAPAP (*N*α-(2-naphthylsulphonyl-glycyl)-DL-*p*-amidinophenylalanyl-piperidine) analog (**2**), are displayed in Figure 6.35. The presence of the primary amino group allows for an effective attachment of the active compounds onto the reactive polymeric carrier (Fig. 6.36).

The *in vitro* hemocompatibility tests using freshly drawn human whole blood (cf. Section 4.5) indicated, in agreement with the SEM images, that the immobilization of the benzamidine-type thrombin inhibitors can significantly enhance the short-term blood compatibility of the coated materials. The surface modification was associated with lower cell adhesion, lower coagulation activation, and lower inflammatory response. The introduction of a PEG spacer further reduced thrombogenicity, possibly due to a greater physical separation of the synthetic thrombin inhibitors from the surface (increase of the spacer length) in synergy with intrinsic PEG properties (reduction of protein adsorption).

Consequently, benzamidine-modified material surfaces show a promising potential for the development of thrombin-inhibiting biomaterials to be applied in blood-contacting devices. However, due to their permanent character, immobilized inhibitors are difficult to dose.

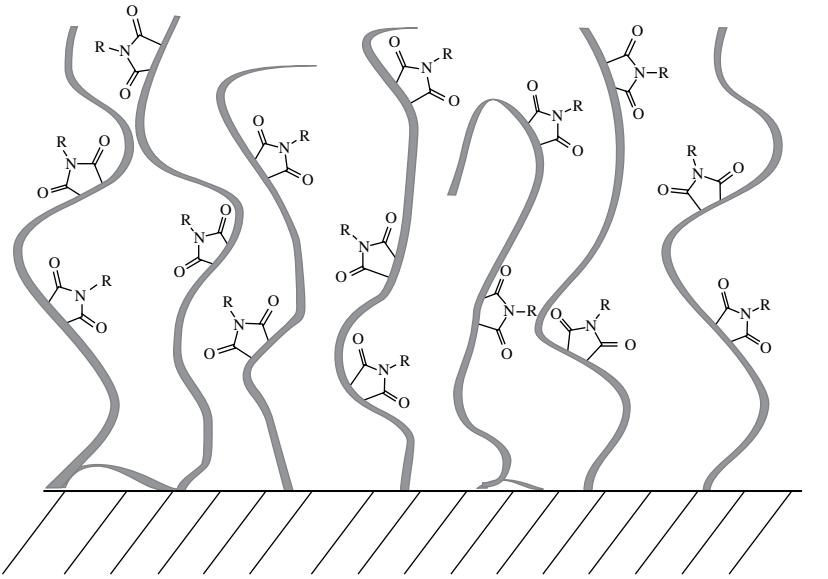

FIGURE 6.36 Scheme of the inhibitor modified polymer film where R represents one of the benzamidine-based inhibitors (Fig. 6.35) [137]. Source: Gouzy et al. [137], figure 4. Reproduced with permission of AIP Publishing LLC.

Activation-triggered delivery of thrombin inhibitors may offer a solution. As an example a recently developed thrombin-responsive starPEG–heparin hydrogel, already introduced in Section 6.4.2, is a promising biofunctional coating for feedback controlled release of heparin at blood-contacting material surfaces.

REFERENCES

[1] Kataoka, K.; Harada, A.; Nagaski, Y. *Advanced Drug Delivery Reviews* 2001, *47*, 113–131.

[2] Kakizawa, Y.; Kataoka, K. *Advanced Drug Delivery Reviews* 2002, *54*, 203–222.

[3] Kataoka, K.; Kwon, G. S.; Yokoyama, M.; Okano, T.; Sakurai, Y. *Journal of Controlled Release* 1993, *24*, 119–132.

[4] Discher, D. E.; Discher, B. M.; Won, Y. Y.; Ege, D. S.; Lee, J. C. M.; Bates, F. S.; Hammer, D. A. *Science* 1999, *284*, 1143–1146.

[5] Huang, X.; Voit, B. *Polymer Chemistry* 2013, *4*, 435–443.

[6] Brinkhuis, R. P.; Rutjes, F. P. J. T.; van Hest, J. C. M. *Polymer Chemistry* 2011, *2*, 1449–1462.

[7] van Dongen, S. F. M.; de Hoog, H. P. M.; Peters, R. J. R. W.; Nallani, M.; Nolte R. J. M.; van Hest, J. C. M. *Chemical Reviews* 2009, *109*, 6212–6274.

[8] Renggli, K.; Baumann, P.; Langowska, K.; Onaca, O.; Bruns, N.; Meier, W. *Advanced Functional Materials* 2011, *21*, 1241–1259.

[9] Gaitzsch, J.; Appelhans, D.; Wang, L. G.; Battaglia, G.; Voit, B.; *Angewandte Chemie International Edition* 2012, *51*, 4448–4451.

[10] Canton, I.; Battaglia, G. *Chemical Society Reviews* 2012, *41*, 2718–2739.

[11] Martin, A. L.; Li, B.; Gilles, E. R. *Journal of the American Chemical Society* 2009, *131*, 734–741.

[12] Yu, S.; Azzam, T.; Rouiller I.; Eisenberg, A. *Journal of the American Chemical Society* 2009, *131*, 10557–10566.

[13] Marguet, M.; Edembe L.; Lecommandoux, S. *Angewandte Chemie International Edition* 2012, *51*, 1173–1176.

[14] Blomberg, S.; Ostberg, S.; Harth, E.; Bosman, A. W.; Van Horn B.; Hawker, C. J. *Journal of Polymer Science Part A: Polymer Chemistry* 2002, *40*, 1309–1320.

[15] Huang, X.; Appelhans, D.; Formanek, P.; Simon F.; Voit B. *Macromolecules* 2011, *44*, 8351–8360.

[16] Ali, S. I.; Heuts J. P. A.; Van Herk, A. M. *Langmuir* 2010, *26*, 7848–7858.

[17] Li, G.; Lei, C.; Wang, C.; Neoh, K.; Kang E.; Yang, X. *Macromolecules* 2008, *41*, 9487–9490.

[18] Caruso, F.; Caruso R. A.; Möhwald, H. *Science* 1998, *282*, 1111–1114.

[19] Städler, B.; Chandrawati, R.; Goldie K.; Caruso, F. *Langmuir* 2009, *25*, 6725–6732.

[20] Landfester, K.; Musyanovych A.; Mailänder, V.; *Journal of Polymer Science Part A: Polymer Chemistry* 2010, *48*, 493–515.

[21] Oudshoorn, M. H.; Rissmann, R.; Bouwstra, J. A.; Hennink, W. E. *Biomaterials* 2006, *27*, 5471–5479.

[22] Oudshoorn, M. H.; Penterman, R.; Rissmann, R.; Bouwstra, J. A.; Broer, D. J.; Hennink, W. E. *Langmuir* 2007, *23*, 11819–11825.

[23] (a)Seiffert, S. *Angewandte Chemie International Edition* 2013, *53*, 11462–11468; (b)Landfester, K.; Musyanovych, A. *Advances in Polymer Science* 2010, *234*, 39–63.

[24] Xu, J.; Wong, D. H. C.; Byrrne, J. D.; Chen, K.; Bowerman, C.; DeSimone, J. M. *Angewandte Chemie International Edition* 2013, *52*, 6580–6589.

[25] Chacko, R. T.; Ventura, J.; Zhuang, J.; Thayumanavan, S. *Advanced Drug Delivery Reviews* 2012, *64*, 836–851.

[26] Sisson, A. L.; Papp, I.; Landfester, K.; Haag, R. *Macromolecules* 2009, *42*, 556.

[27] Sisson, A. L.; Steinhilber, D.; Rossow, T.; Welker, P.; Licha, K.; Haag, R. *Angewandte Chemie International Edition* 2009, *48*, 7540–7545.

[28] Zhou, H.; Steinhilber, D.; Schlaad, H.; Sisson, A. L.; Haag, R. *Reactive and Functional Polymers* 2011, *71*, 356–361.

[29] (a) Steinhilber, D.; Seiffert, S.; Heyman, J. A.; Paulus, F.; Weitz, D. A.; Haag, R. *Biomaterials* 2011, *32*, 1311–1316; (b) Rossow R.; Heyman J. A.; Ehrlicher, J. A.; Langhoff, A.; Weitz, D. A.; Haag, R; Seiffert, S. *Journal of the American Chemical Society* 2012, *134*, 4983–4989; (c) Steinhilber,D.; Rossow, T.; Wedepohl, S.; Paulus, F.; Seiffert, S.; Haag R. *Angewandte Chemie International Edition* 2013, *52*, 13538–13543.

[30] Sisson, A. L.; Haag, R. *Soft Matter* 2010, *6*, 4968–4975.

[31] Steinhilber, D.; Sisson, A. L.; Mangoldt, D.; Welker, P.; Licha, K.; Haag, R. *Advanced Functional Materials* 2010, *20*, 4133–4138.

[32] Steinhilber, D.; Haag, R.; Sisson, A. L. *The International Journal of Artificial Organs* 2011, *34*, 118–122.

[33] (a) Groll, J.; Singh, S.; Albrecht, K.; Moeller, M. *Journal of Polymer Science Part A: Polymer Chemistry* 2009, *47*, 5543; (b) Wu, C.; Böttcher, C.; Haag, R.; *Soft Matter* 2015, *11*, 972–980.

[34] Singh, S.; Topuz, F.; Hahn, K.; Albrecht, K.; Groll, J. *Angewandte Chemie International Edition* 2013, *52*, 3000–3003.

[35] (a) Cuggino, J.; Alvarez I. C. I.; Strumia, M.; Welker, P.; Licha, K.; Steinhilber, D.; Mutilac, R.-C.; Calderòn, M. *Soft Matter*, 2011, *7*, 11259–11266; (b) Adeli, M.; Namazi, H.; Du, F.; Hönzke, S.; Hedtrich, S.; Keilitz, J.; Haag, R. *RSC Advances* 2015, *5*, 14958–14966.

[36] Radowski, M. R.; Shukla, A.; von Berlepsch, H.; Böttcher, C.; Pickaert, G.; Rehage, H.; Haag, R. *Angewandte Chemie International Edition* 2007, *46*, 1265–1269.

[37] Burakowska, E.; Haag, R. *Macromolecules* 2009, *42*, 5545–5550.

[38] Küchler, S.; Adbel-Mottaleb, M.; Lamprecht, A.; Radowski, M.; Haag, R.; Schäfer-Korting, M. *International Journal of Pharmaceutics* 2009, *377*, 169–172.

[39] Küchler, S.; Radowski, M. R.; Blaschke, T.; Dathe, M.; Plendl, J.; Haag, R.; Schäfer-Korting, M.; Kramer K. D. *European Journal of Pharmaceutics and Biopharmaceutics* 2009, *71*, 243–250.

[40] Polikarpov, N.; Appelhans, D.; Welzel, P.; Kaufmann, A.; Dhanapal, P.; Bellmann C.; Voit, B. *New Journal of Chemistry* 2012, *36*, 438–451.

[41] Rosen, B. M.; Wilson, C. J.; Wilson, D. A.; Peterca, M.; Imam, M. R.; Percec, V. *Chemical Reviews* 2009, *109*, 6275–6540.

[42] Percec, V.; Wilson, D. A.; Leowanawat, P.; Wilson, C. J.; Hughes, A. D.; Kaucher, M. S.; Hammer, D. A.; Levine, D. H.; Kim A. J.; Bates, F. S. *Science*, 2010, *328*, 1009–1014.

[43] Percec, V.; Leowanawat, P.; Sun, H.-J. Kulikov, O.; Nusbaum, C. D.; Tran, T. M.; Bertin, A.; Wilson, D. A.; Peterca, M.; Zhang, S.; Kamat, N. P.; Vargo, K.; Moock, D.; Johnston, E. D.; Hammer, D. A.; Pochan, D. J.; Chen, Y.; Chabre, Y. M.; Shiao, T. C.; Bergeron-Brlek, M.; André, S.; Roy, R.; Gabius, H.-J.; Heiney, P. A. *Journal of the American Chemical Society* 2013, *135*, 9055−9077.

[44] Wong, S. Y.; Pelet, J. M.; Putnam, D. *Progress in Polymer Science* 2007, *32*, 799–837.

[45] Karmali, P. P.; Chaudhuri, A. *Medicinal Research Reviews* 2007, *27*, 696–722.

[46] Fischer, W.; Calderón, M.; Haag, R. "Nucleic Acid Transfection in Topics in Current Chemistry" in *Nucleic Acid Transfection* (eds. Bielke, W.; Erbacher, C.); Springer, Berlin, Heidelberg: 2010, 95–129.

[47] (a) Ofek, P.; Fischer, W.; Calderon, M.; Haag, R.; Satchi-Fainaro, R. *The FASEB Journal* 2010, *24*, 3122–3134; (b) Mehrabadi, F.S.; Fischer, W.; Haag, R. *Current Opinion in Solid State and Materials Science* 2013, *16*, 310–322; (c) Staedtler, A. M.; Hellmund, M.; Sheikhi Mehrabadi, F.; Thota, B. N. S.; Zollner, T. M.; Koch, M.; Haag, R.; Schmidt, N. *Journal of Materials Chemistry B* 2015, *3*, 8993–9000.

[48] (a)Duncan, R. *Current Opinion in Biotechnology* 2011, *22*, 492–501; (b)Ringsdorf, H. *Journal of Polymer Science, Part C: Polymer Symposia* 1975, *256*, 495–497.

[49] Duncan, R. *Nature Reviews Drug Discovery* 2003, *2*, 347–360.

[50] Harris, J. M.; Chess, R. B. *Nature Reviews Drug Discovery* 2003, *2*, 214–221.

[51] Kano, M. R.; Bae, Y.; Iwata, C.; Morishita, Y.; Yashiro, M.; Oka, M.; Fujii, T.; Komuro, A.; Kiyono, K.; Kaminishi, M.; Hirakawa, K.; Ouchi, Y.; Nishiyama, N.; Kataoka, K.; Miyazono, K. *Proceedings of the National Academy of Sciences of the United States of America* 2007, *104*, 3460–3465.

[52] Khandare, J.; Minko, T. *Progress in Polymer Science* 2006, *31*, 359–397.

[53] Dharap, S. S.; Wang, Y.; Chandna, P.; Khandare, J. J.; Qiu, B.; Gunaseelan, S.; Stein, S.; Farmanfarmaian, A.; Minko, T. *Proceedings of the National Academy of Sciences of the United States of America* 2005, *102*, 12962–12967.

[54] Wang, Y.; Saad, M.; Pakunlu, R. I.; Khandare, J. J.; Garbuzenko, O. B.; Vetcher, A. A.; Soldatenkov, V. A.; Pozharov, V. P.; Minko, T. *Clinical Cancer Research* 2008, *14*, 3607–3616.

[55] Ferrari, M. *Nature Reviews Cancer* 2005, *5*, 161–171.

[56] Hamilton, S. K.; Harth, E. A. *ACS Nano* 2009, *3*, 402–410.

[57] Bolla, M.; Collette, L.; Blank, L.; Warde, P.; Dubois, J. B.; Mirimanoff, R. O.; Storme, G.; Bernier, J.; Kuten, A.; Sternberg, C.; Mattelaer, J.; Lopez Torrecilla, J.; Pfeffer, J. R.; Cutajar, C. L.; Zurlo, A.; Pierart, M. *The Lancet* 2002, *360*, 103–106.

[58] Belting, M.; Sandgren, S.; Wittrup, A. *Advanced Drug Delivery Reviews* 2005, *57*, 505–527.

[59] Greish, K.; Fang, J.; Inutsuka, T.; Nagamitsu, A.; Maeda, H. *Clinical Pharmacokinetics* 2003, *42*, 1089–1105.

[60] Khandare, J.; Mohr, A.; Calderón, M.; Welker, P.; Licha, K.; Haag, R. *Biomaterials* 2010, *31*, 4268–4277.

[61] Goun, E. A.; Pillow, T. H.; Jones, L. R.; Rothbard, J. B.; Wender, P. A. *Chembiochem: A European journal of chemical biology* 2006, *7*, 1497–1515.

[62] Zhang, K.; Fang, H.; Chen, Z.; Taylor, J. S. A.; Wooley, K. L. *Bioconjugate Chemistry* 2008, *19*, 1880–1887.

[63] Grothey, A.; Ellis, L. M. *Cancer Journal* 2008, *14*, 170–177.

[64] Cabebe, E.; Wakelee, H. *Oncology* 2007, *8*, 15–27.

[65] Luo, Y.; Prestwich, G. D. *Current Cancer Drug Targets* 2002, *2*, 209–226.

[66] Minko, T.; Dharap, S. S.; Pakunlu, R. I.; Wang, Y. *Current Drug Targets* 2004, *5*, 389–406.

[67] Matsumura, Y.; Maeda, H. *Cancer Research* 1986, *46*, 6387–6392.

[68] Khandare, J.; Calderón, M.; Dagia, N.M.; Haag, R. *Chemical Society Reviews* 2012, *41*, 2824–2848.

[69] Greco, F.; Vicent, M. J. *Frontiers in Bioscience* 2008, *13*, 2744–2756.

[70] Maruyama, K. *Advanced Drug Delivery Reviews* 2011, *63*, 161–169.

[71] Torchilin, V. *Advanced Drug Delivery Reviews* 2011, *63*, 131–135.

[72] Oku, N. *Advanced Drug Delivery Reviews* 1999, *40*, 63–73.

[73] Cho, K.; Wang, X.; Nie, S.; Chen, Z. G.; Shin, D. M. *Clinical Cancer Research* 2008, *14*, 1310–1316.

[74] Haag, R.; Kratz, F. *Angewandte Chemie International Edition* 2006, *45*, 1198–1215.

[75] Maeda, H.; Greish, K.; Fang, J. *Advances in Polymer Science* 2006, *193*, 103–121.

[76] Trouet, D.-D.; Campeneere, D. D.; Duve, C. *Nature: New Biology* 1972, *239*, 110–112.

[77] Trouet, A.; Masquelier, M.; Baurain, R.; Campeneere, D. D. *Proceedings of the National Academy of Sciences of the United States of America* 1982, *79*, 626–629.

[78] Minko, T.; Khandare, J.; Jayant, S. "Drug Delivery in Oncology: From Basic Research to Cancer Therapy" in *Macromolecular Engineering: Precise Synthesis, Materials Properties, Applications* (eds. Matyjaszewski, K.; Gnanou, Y.; Leibler, L.); Wiley-VCH Verlag, Weinheim: Vol. *4*, 2007, 2541–2595.

[79] Khan, M. Z.; Stedul, H. P.; Kurjakovic, N. *Drug Development and Industrial Pharmacy* 2000, *26*, 549–554.

[80] Nykanen, P.; Lempaa, S.; Aaltonen, M. L.; Jurjenson, H.; Veski, P.; Marvola, M. *International Journal of Pharmaceutics* 2001, *229*, 155–162.

[81] Gautam, A.; Koshkina, N. *Current Cancer Drug Targets* 2003, *3*, 287–296.

[82] Jayant, S.; Khandare, J. J.; Wang, Y.; Singh, A. P.; Vorsa, N.; Minko, T. *Pharmaceutical Research* 2007, *24*, 2120–2130.

[83] Minko, T. *Advanced Drug Delivery Reviews* 2004, *56*, 491–509.

[84] Zhang, Y.; Thomas, T. P.; Desai, A.; Zong, H.; Leroueil, P. R.; Majoros, I. J.; Baker Jr., J. R. *Bioconjugate Chemistry* 2010, *21*, 489–495.

[85] Trail, P. A.; Willner, D.; Lasch, S.; Henderson, A.; Hofstead, S.; Casazza, A.; Firestone, R.; Hellstrom, I.; Hellstrom, K. E. *Science* 1993, *261*, 212–215.

[86] Okamoto, K.; Yamaguchi, T.; Otsuji, E.; Yamaoka, N.; Yata, Y.; Tsuruta, H.; Kitamura, K.; Takahashi, T. *Cancer Letters* 1998, *122*, 231–236.

[87] Remsen, L. G.; Trail, P. A.; Hellstrom, I.; Hellstrom, K. E.; Neuwelt, E. A. *Neurosurgery* 2000, *46*, 704–709.

[88] Wakai, Y.; Matsui, J.; Koizumi, K.; Tsunoda, S. I.; Makimoto, H.; Ohizumi, I.; Taniguchi, K.; Kaiho, S.-I.; Saito, H.; Utoguchi, N.; Tsutsumi, Y.; Nakagawa, S.; Ohsugi, Y.; Mayumi, T. *Japanese Journal of Cancer Research* 2000, *91*, 1319–1325.

[89] Fasting, C.; Schalley, C. A.; Weber, M.; Seitz, O.; Hecht, S.; Koksch, B.; Dernedde, J.; Graf, C.; Knapp, E. W.; Haag, R. *Angewandte Chemie International Edition* 2012, *51*, 10472–10498.

[90] Mammen, M.; Choi, S.-K.; Whitesides, G. M. *Angewandte Chemie International Edition* 1998, *37*, 2754–2794.

[91] Choi, S.-K. *Synthetic Multivalent Molecules*; John Wiley & Sons, Inc., New York: 1975.

[92] Kramer, R. H.; Karpen, J. W. *Nature* 1998, *395*, 710–713.

[93] Diestler, D. J.; Knapp, E. W. *Physical Review Letters* 2008, *100*, 178101–178104.

[94] Lee, Y. C.; Lee, R. T. *Accounts of Chemical Research* 1995, *28*, 321–327.

[95] Lundquist, J. J.; Toone, E. J. *Chemical Reviews* 2002, *102*, 555–578.

[96] Ting, S. R. S.; Chen, G.; Stenzel, M. H. *Polymer Chemistry* 2010, *1*, 1392–1412.

[97] Dam, T. K.; Brewer, C. F. "Multivalent Lectin—Carbohydrate Interactions: Energetics and Mechanisms of Binding" in *Advances in Carbohydrate Chemistry and Biochemistry* (ed. Horton, D.); Academic Press, New York: Vol. *63*, 2010, 139–164.

[98] Y. M. Chabre, R. Roy "Design and Creativity in Synthesis of Multivalent Neoglycoconjugates" in *Advances in Carbohydrate Chemistry and Biochemistry* (ed. Horton, D.); Academic Press, New York: Vol. *63*, 2010, 165–393.

[99] Lindhorst, T. *Topics in Current Chemistry* (ed. Penadés, S.); Springer, Berlin: Vol. *218*, 2002, 201–235.

[100] Elsner, K.; Boysen, M. M. K.; Lindhorst, T. K. *Carbohydrate Research* 2007, *342*, 1715–1725.

[101] Simanek, E. E.; McGarvey, G. J.; Jablonowski, J. A.; Wong, C. H. *Chemical Reviews* 1998, *98*, 833–862.

[102] Chabre, Y. M.; Roy, R. *Current Topics in Medicinal Chemistry* 2008, *8*, 1237–1285.

[103] Thoma, G.; Duthaler, R. O.; Magnani, J. L.; Patton, J. T. *Journal of the American Chemical Society* 2001, *123*, 10113–10114.

[104] Papp, I.; Dernedde, J.; Enders, S.; Haag, R. *Chemical Communications* 2008, 5851–5853.

[105] Dernedde, J.; Rausch, A.; Weinhart, M.; Enders, S.; Tauber, R.; Licha, K.; Schirner, M.; Zügel, U.; von Bonin, A.; Haag, R. *Proceedings of the National Academy of Sciences of the United States of America* 2010, *107*, 19679–19684.

[106] Weinhart, M.; Gröger, D.; Enders, S.; Riese, S. B.; Dernedde, J.; Kainthan, R. K.; Brooks, D. E.; Haag, R. *Macromolecular Bioscience* 2011, *11*, 1088–1098.

[107] Choi, S. K.; Mammen, M.; Whitesides, G. M. *Journal of the American Chemical Society* 1997, *119*, 4103–4111.

[108] Mammen, M.; Dahmann, G.; Whitesides, G. M. *Journal of Medicinal Chemistry* 1995, *38*, 4179–4190.

[109] Choi, S. K.; Mammen, M.; Whitesides, G. M. *Chemistry & Biology* 1996, *3*, 97–104.

[110] Papp, I.; Sieben, C.; Sisson, A. L.; Kostka, J.; Bottcher, C.; Ludwig, K.; Herrmann, A.; Haag, R. *A European Journal of Chemical Biology—ChemBioChem* 2011, *12*, 887–895.

[111] (a) Licha, K.; Welker, P.; Weinhart, M.; Wegner, N.; Kern, S.; Reichert, S.; Gemeinhardt, I.; Weissbach, C.; Ebert, B.; Haag, R.; Schirner, M. *Bioconjugate Chemistry* 2012, *22*, 2453–2460; (b) Paulus, F.; Schulze, R.; Steinhilber, D.; Steinke, I.; Welker, P.; Licha, K.; Wedepohl, S.; Dernedde, J.; Haag, R. *Macromolecular Bioscience* 2014, *14*, 643–654.

[112] http://www.starpharma.com/vivagel (accessed on November 19, 2015).

[113] Ulijn, R. V.; Bibi, N.; Jayawarna, V.; Thornton, P. D.; Todd, S. J.; Mart, R. J.; Smith, A. M.; Gough, J. E. *Materials Today* 2007; *10*, 40–48.

[114] Wilson A. N.; Guiseppi-Elie, A. *Advanced Healthcare Materials* 2013, *2*, 520–532.

[115] Maitz, M. F.; Freudenberg, U.; Tsurkan M. V.; Fischer, M.; Beyrich, T.; Werner, C. *Nature Communications* 2013, *4*, article no. 2168.

[116] Podual K.; Doyle, F. J.; Peppas, N. A. *Polymer* 2000, *41*, 3975–3983.

[117] Podual K.; Doyle, F. J.; Peppas, N. A. *Journal of Controlled Release* 2000, *67*, 9–17.

[118] Marek S. R.; Peppas, N. A. *American Institute of Chemical Engineers Journal* 2013, *59*, 3578–3785.

[119] Geraths, C.; Dauad-El Baba, M.; Charpin-El Hambri, G.; Weber, W. *Journal of Controlled Release* 2013,*171*, 57–62.

[120] Tsurkan M. V.; Chwalek, K.; Levental, C. R.; Freudenberg, U.; Werner, C. *Macromolecular Rapid Communications* 2010, *31*, 1529–1533.

[121] Grandin H. M., Textor, M., eds., *Intelligent Surfaces in Biotechnology: Scientific and Engineering Concepts, Enabling Technologies, and Translation to Bio-Oriented Applications*; John Wiley & Sons, Inc., Hoboken: 2012.

[122] Magin, C. M.; Cooper, S. P.; Brennan, A. B. *Materials Today* 2010, *13*, 36–44.

[123] (a) Chen, S.; Lu, X.; Hu, Y.; Lu, Q. *Biomaterials Science*, 2015, *3*, 85–93; (b) Wei, Q.; Becherer, T.; Angioletti-Uberti, S.; Dzubiella, J.; Wischke, C.; Neffe, A. T.; Lendlein, A.; Ballauff, M.; Haag, R.; *Angewandte Chemie International Edition* 2014, *53*, 8004–8031.

[124] Cordeiro, A. L.; Werner, C. *Journal of Adhesion Science and Technology* 2011, *25*, 2317–2344.

[125] Tasso, M.; Cordeiro, A. L.; Salchert, K.; Werner, C. *Macromolecular Bioscience* 2009, *9*, 922–929.

[126] Tasso, M.; Pettitt, M. E.; Cordeiro, A. L.; Callow, M. E.; Callow, J. A.; Werner, C. *Biofouling* 2009, *25*, 505–516.

[127] Cordeiro, A. L.; Pompe, T.; Salchert, K.; Werner, C. "Enzyme Immobilization on Reactive Polymer Films" in *Bioconjugation Protocols: Strategies and Methods, Methods in Molecular Biology* (ed. Mark, S. S.); Springer Science + Business Media, LLC, New York: Vol. *751*, 2011, 465–474.

[128] Friedrichs, J.; Zieris, A.; Prokoph, S.; Werner, C. *Macromolecular Rapid Communications* 2012, *33*, 1453–1458.

[129] Pompe, T.; Zschoche, S.; Herold, N.; Salchert, K.; Gouzy, M. F.; Sperling, C.; Werner, C. *Biomacromolecules* 2003, *4*, 1072–1079.

[130] Hensel, R.; Finn, A.; Helbig, R.; Braun, H.-G.; Neinhuis, C.; Fischer, W. J.; Werner, C. *Advanced Materials* 2014, *26*, 2029–2033.

[131] Helbig, R.; Nickerl, J.; Neinhuis, C.; Werner, C. *PloS One* 2011, *6*, e25105.

[132] Nickerl, J.; Helbig, R.; Schulz, H.-J.; Werner, C.; Neinhuis, C. *Zoomorphology* 2013, *132*, 183–195.

[133] Hensel, R.; Helbig, R.; Aland, S.; Voigt, A.; Neinhuis, C.; Werner, C. *NPG Asia Materials* 2013, *5*, e37.

[134] Hensel, R.; Helbig, R.; Aland, S.; Braun, H.-G.; Voigt, A.; Neinhuis, C.; Werner, C. *Langmuir* 2013, *29*, 1100–1112.

[135] Sperling, C.; Salchert, K.; Streller, U.; Werner, C. *Biomaterials* 2004, *25*, 5101–5113.

[136] Gouzy, M.F.; Sperling, C.; Salchert, K.; Pompe, T.; Streller, U.; Uhlmann, P.; Rauwolf, C.; Simon, F.; Böhme, F.; Voit, B.; Werner, C. *Biomaterials* 2004, *25*, 3493–3501.

[137] Gouzy, M. F.; Sperling, C.; Salchert, K.; Pompe, T.; Rauwolf, C.; Werner, C. *Biointerphases* 2006, *1*, 146–155.

[138] Salchert, K.; Gouzy, M. F.; Glorius, M.; Kühn, A.; Nitschke, M.; Werner, C. *Acta Biomaterialia* 2005, *1*, 441–449.

ABBREVIATIONS

AAMA	acetylacetonato methacrylate
ABU	arbitrary pixel brightness value
AF4	asymmetrical flow field-flow fractionation
AFM	atomic force microscopy
AIBN	azobisisobutyronitrile
ANS	1-anilinonaphthalene-8-sulfonic acid
ATP	adenosine triphosphate
ATR	attenuated total reflection
ATR-FTIR	attenuated total reflection - Fourier transform infrared
ATRP	atom transfer radical polymerization
BOC	boc-packed spheres / body-centered cubic
BCN	bicyclononyne
BPMA	benzophenone methacrylate
CAD	computer-aided design
CBAS™	Carmeda™ bio active surface
CD	circular dichroism
CE	capillary electrophoresis
CLSM	confocal laser scanning microscopy
CMC	critical micelle concentration
CMS	core-multishell architectures
COD	cyclooctadiene
ConA	concanavalin A
COT	cyclooctatetraene
CROB	cationic ring-opening polymerization
CRP	controlled radical polymerization
cryo-TEM	cryogenic transmission electron microscopy
CT	computerized tomography
CWP	chain-walking polymerization
3D	three dimensional

Bio- and Multifunctional Polymer Architectures: Preparation, Analytical Methods, and Applications, First Edition. Brigitte Voit, Rainer Haag, Dietmar Appelhans, and Petra B. Welzel.

D	dendritic
DB	degree of branching
DBCO	dibenzylcyclooctyne
DCC	dicyclohexane carbodiimide
DDS	drug delivery system
DIC	differential interference contrast
DIFO	difluorinated cylcooctyne
DLS	dynamic light scattering
DMA	dynamic mechanical analysis
DNA	deoxyribonucleic acid
DNR	daunorubicin
DOPC	1,2-dioleoyl-*sn*-glycero-3-phosphocholine
DOX	doxorubicin
DP	degree of polymerization
dPGS	dendritic polyglycerol sulfate
DSC	differential scanning calorimetry
DTT	dithiothreitol
EAM	enzyme-activated monomer
ECM	extracellular matrix
EDA	ethylenediamine
EDC/sulfo-NHS	1-ethyl-3-(3-dimethylaminopropyl)carbodiimide/*N*-hydroxysulfosuccinimide
EI	electron ionization
ELISA	enzyme-linked immunosorbent assay
ELPs	elastin-like polypeptides
EPR	enhanced permeability and retention
ESEM	environmental scanning electron microscopy
ESI	electrospray ionization
EU	endotoxin unit
FAB	fast atom bombardment
FCC	fluid catalytic cracking
FDA	US Food and Drug Administration
FFF	field-flow fractionation
FGF-2	basic fibroblast growth factor
FGN	adsorption of the plasma protein fibrinogen
Fmoc	9-fluoroenylmethyloxycarbonyl
FRET	fluorescence resonance energy transfer
GAG	glycosaminoglycan
GalT	galactosyl transferase
GC	gas chromatography
GPC	gel permeation chromatography
HA	hyaluronic acid
HABA	2-(4-hydroxy-phenylazo)benzoic acid
HAS	human serum albumin
HEX	hexagonally packed cylinders
His	histidine
HOBT	1-hydroxybenzotriazole
HPC	hematopoietic progenitor cells

hPEI	hyperbranched poly(ethylene imine)
hPG	hyperbranched polyglycerol
HPLC	high performance liquid chromatography
hSAF	hydrogelating self-assembling fiber
HUVECs	human umbilical vein endothelial cells
IC	internal conversion
IPN	interpenetrating polymer network
IR	infrared
ISC	intersystem crossing
ISO	International Organization for Standardization
ITC	isothermal titration calorimetry
L	linear
LAL	limulus amoebocyte lysate
LAM	simple lamellae
LB	Langmuir-Blodgett
LBL	layer-by-layer
LCST	lower critical solution temperature
LILBID-MS	laser-induced liquid bead ion desorption mass spectrometry
LPS	lipopolysaccharide
LYZ	lysozyme
$\mathbf{M_n}$	number averaged molecular weight
$\mathbf{M_w}$	weight averaged molecular weight
MAA	methacrylic acid
MADIX	macromolecular design via interchange of xanthates
MALDI	matrix-assisted laser desorption/ionization
MAT	monocyte activation test
MEM	minimum essential medium
MLAM	modulated lamellae
MMA	methyl methacrylate
MMP	matrix-metalloproteases
MRE	magnetic resonance elastography
MRI	magnetic resonance imaging
NAPAP	(*Na*-(2-naphthyl-sulphonyl-glycyl)-DL-*p*-amidinophenylalanyl-piperidine)
NCA	*N*-carboxyanhydride
NCS	neocarzinostatin
NHS	*n*-hydroxysuccinimide
NIPAM	*N*-isopropylacrylamide
NMR	nuclear magnetic resonance
NMRP/NMP	nitroxide-mediated radical polymerization
NOE	nuclear Overhauser effect
NTA	nitrilotriacetic acid
P(PF-co-EG)	poly(propylene furmarate-co-ethylene glycol)
PA	peptide amphiphiles
PAA	poly(acrylic acid)
PAAm	poly(acrylamide)
PAH	poly(allylamine hydrochloride)
PAMAM	poly(amidoamine)

PAsp	poly(aspartate)
PB-*b*-P*t*BMA-*b*-PDMAEMA	polybutadiene-*block*-poly(*tert*-butyl methacrylate)-block-poly(2-(dimethylamino)ethyl methacrylate)
PCL	poly(ε-caprolactone)
PCR	polymerase chain reaction
PCS	photon correlation spectroscopy
PDEAEM	poly(diethylaminoethyl methacrylate)
PDMS	poly(dimethylsiloxane)
PEG	poly(ethylene glycol)
PEGdma	poly(ethylene glycol) dimethacrylate
PEI	poly(ethylene imine)
PEMA	poly(ethylene-alt-maleic anhydride)
PEO	poly(ethylene oxide)
PET	poly(ethylene terephthalate)
PFG	pulsed field gradient
PFG-NMR	pulsed field gradient nuclear magnetic resonance
PFPEdma	perfluoropolyether dimethacrylate
PG	polyglycerol
PGA	poly(glycerol amine)
PHEMA	poly(hydroxyethyl methacrylate)
PLA	poly(lactic acid)
PLAM	perforated lamellae
PLL	poly(L-lysine)
PMAA	poly(methacrylic acid)
PMMA	poly(methyl methacrylate)
PNIPAM	poly(*N*-isopropyl-acrylamide)
POEGMA	poly(oligo(ethylene glycol) methacrylate)
POMA	poly(octadecene-*alt*-maleic anhydride)
PPI	poly(propylene imine)
ppm	parts per million
PPS	poly(propylene sulfide)
PRINT	particle replication in non-wetting templates
PS	polystryrene
PSS	poly(styrene sulfonate)
PVA	poly(vinyl alcohol)
PVP	poly(vinyl pyrrolidone)
QCM	quartz crystal microbalance
QCM-D	quartz crystal microbalance with dissipation monitoring
RAFT	reversible addition-fragmentation chain transfer
RES	reticuloendothelial system
RET	rubber elasticity theory
RGD	Arg-Gly-Asp
RI	refractive index
RICM	reflection interference contrast microscopy
RNA	ribonucleic acid
ROMP	ring-opening metathesis polymerization
ROP	ring-opening polymerization
RP	rapid prototyping

SAF	self-assembling fiber
SAM	self-assembled monolayer
SANS	small-angle neutron scattering
SAXS	small-angle X-ray scattering
SBM	poly(styrene-block-2-butadiene-*block*-methylmethacrylate)
SCID	severe combined immunodeficiency disease
SCSF	single-cell force spectroscopy
SEC	size exclusion chromatography
SEM	scanning electron microscopy
SFF	solid free-form fabrication
sfMA	semi-fluorinated methacrylate
SFRP	stable free radical polymerization
SIP	surface initiated polymerization
SLS	static light scattering
SMANCS	styrene maleic acid neocarzinostatin
SPPS	solid phase peptide synthesis
SPR	surface plasmon resonance
ssDNA	single-stranded deoxyribonucleic acid
T	terminal
***t*-Boc**	*t*-butoxycarbonyl
TBS	*t*-butyldimethylsilyl ether
TBTU	*O*-(benzotriazol-1-yl)-*N,N,N′,N′*-tetramethyluronium tetrafluoroborate
TcTs	trypanosoma cruzi trans-sialidase
TEM	transmission electron microscopy
TFA	trifluoroacetic acid
TIPS	triisopropylsilane
TKI	tyrosine kinase inhibitor
TMA	trimellic acid anhydride
TMS	trimethylsilane
TOF	time-of-flight
UV	ultraviolet
UV / Vis	ultraviolet and visible light
VEGF	vascular endothelial growth factor
VEGFR	vascular endothelial growth factor receptor
VPGXG	amino acid sequence of the tropoelastin molecule
XPS	x-ray photoelectron spectroscopy

INDEX

Bio- and Multifunctional Polymer Architectures: Preparation, Analytical Methods, and Applications, First Edition. Brigitte Voit, Rainer Haag, Dietmar Appelhans, and Petra B. Welzel.

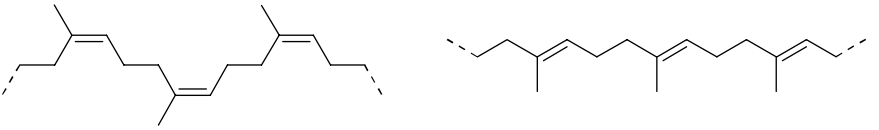

Poly(*cis*-1,4-isoprene)
natural rubber

Poly(*trans*-1,4-isoprene)
gutta-percha, balata

Stereo-arrangement in polymers

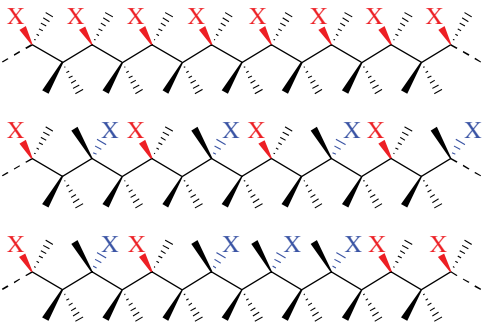

FIGURE 2.2 Monomer arrangements in linear homopolymer chains.

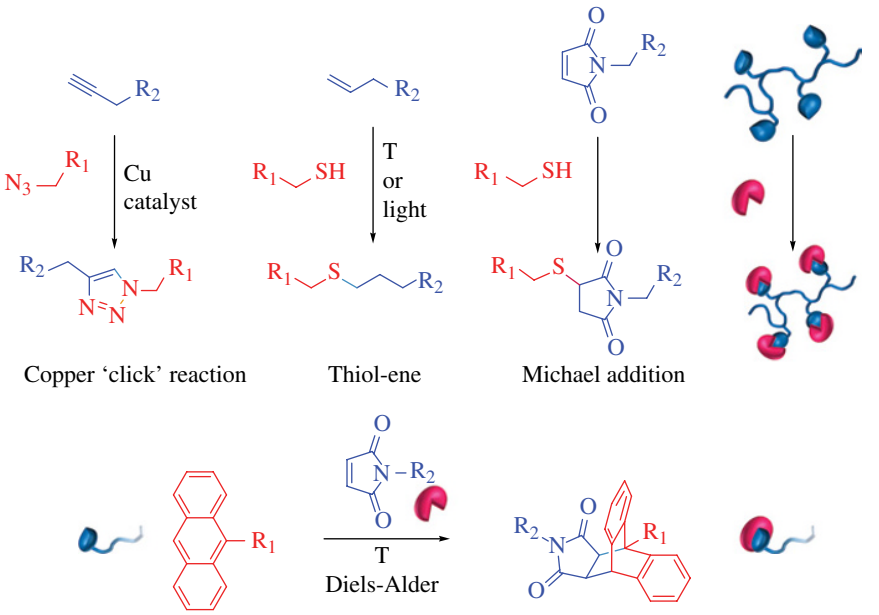

FIGURE 3.28 Some examples of efficient reactions used for polymer modification that allow also orthogonal coupling (REO chemistry).

Bio- and Multifunctional Polymer Architectures: Preparation, Analytical Methods, and Applications, First Edition. Brigitte Voit, Rainer Haag, Dietmar Appelhans, and Petra B. Welzel.

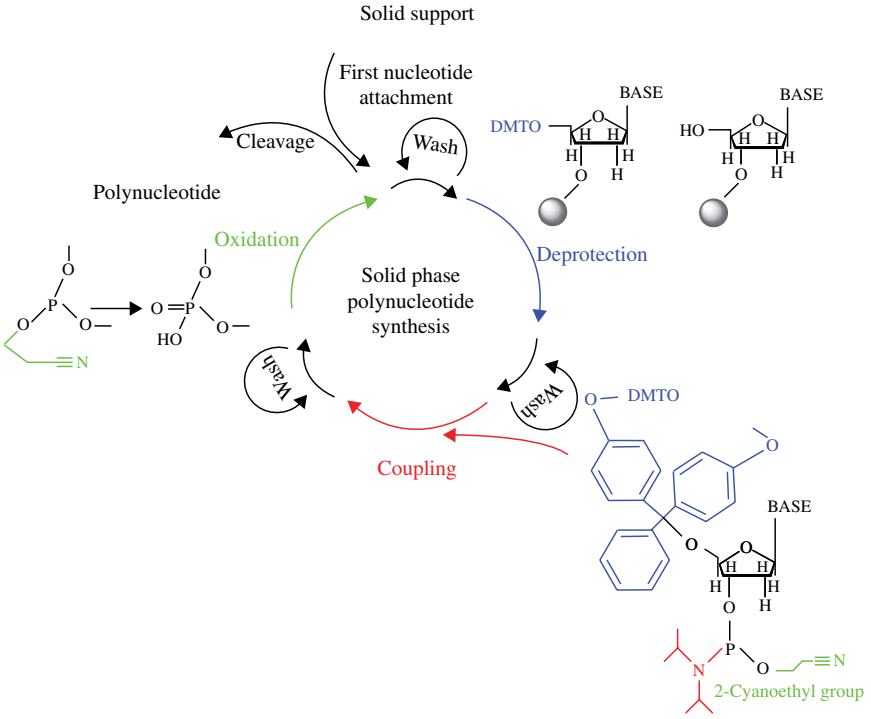

FIGURE 3.47 Left: schematic view of the solid phase polynucleotide synthesis. Right: the structure of DNA building block with the protection (red) and activation groups (blue).

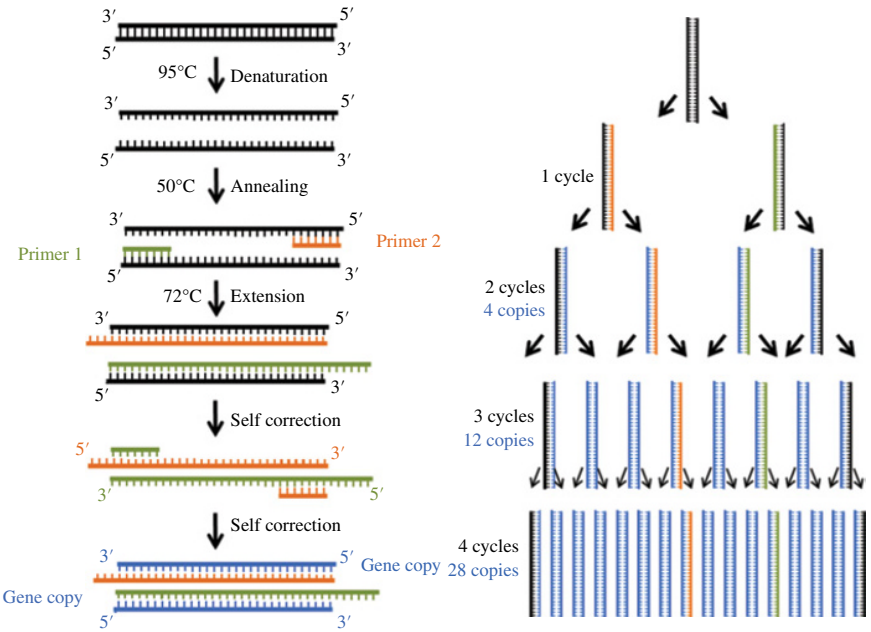

FIGURE 3.50 Schematic view of PCR cycle (left) and propagation (right).

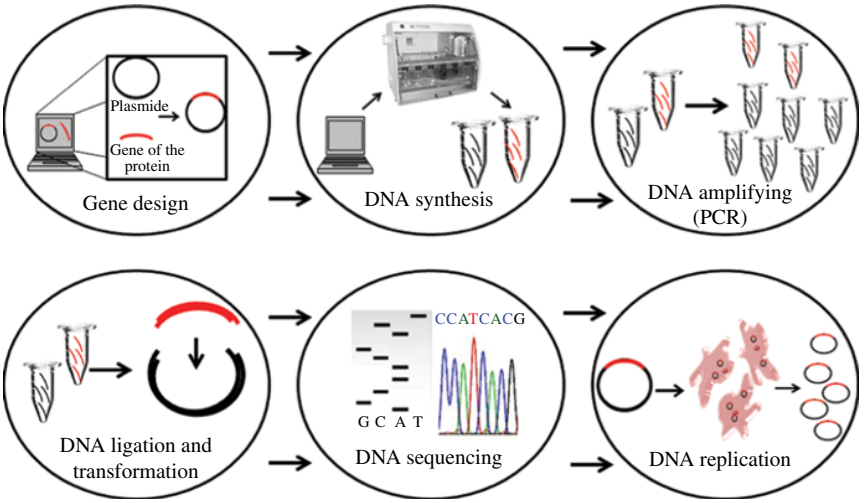

FIGURE 3.51 Schematic view of DNA replication.

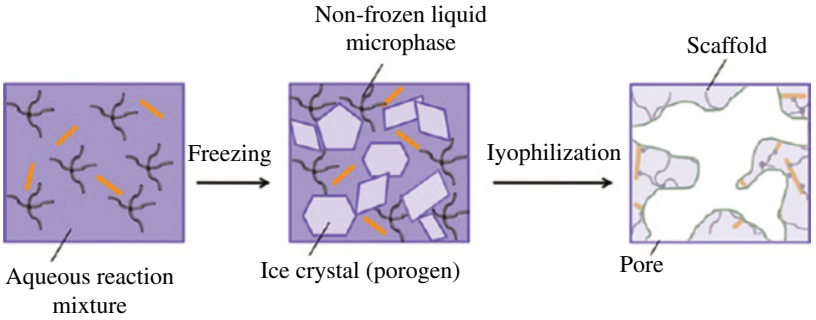

FIGURE 3.55 Formation of macroporous starPEG–heparin cryogels by combined cryotreatment of the aqueous gel-forming reaction mixture and lyophilization of the incompletely frozen gel. Yellow rods, heparin; grey crosses, starPEG. Source: Welzel et al. [78]. Reproduced with permission from American Chemical Society.

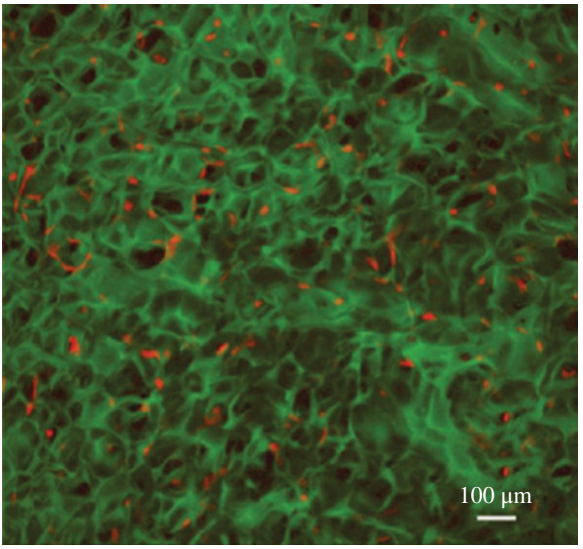

FIGURE 3.56 Representative confocal microscopy image of human umbilical vein endothelial cell colonization on RGD-modified cryogels after seven days in culture in *xy* direction (3D projection) indicating three-dimensional cell growth. Green: cryogel dyed by Alexafluor488. Red: actin of endothelial cells dyed by Alexafluor633-labeled phalloidin.

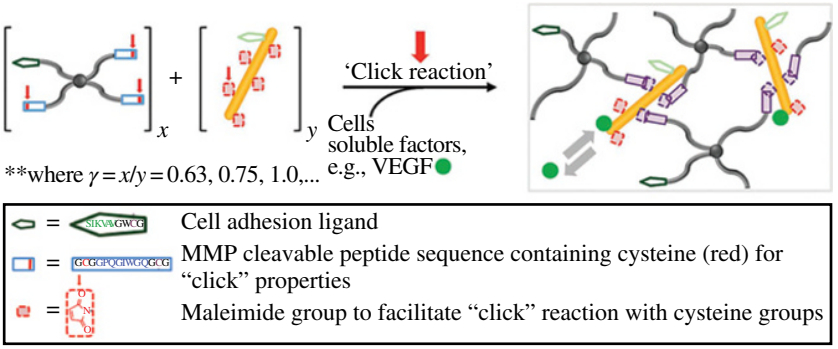

FIGURE 3.58 Schematic representation of the *in situ* gelling of poly(ethylene glycol)–peptide and glycosaminoglycan–peptide conjugates by Michael-type addition. Source: Tsurkan et al. [86]. Reproduced with permission from John Wiley & Sons.

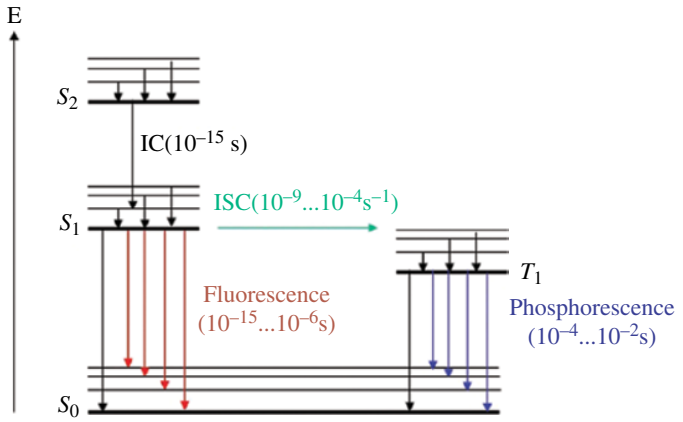

FIGURE 4.5 Jablonski diagram.

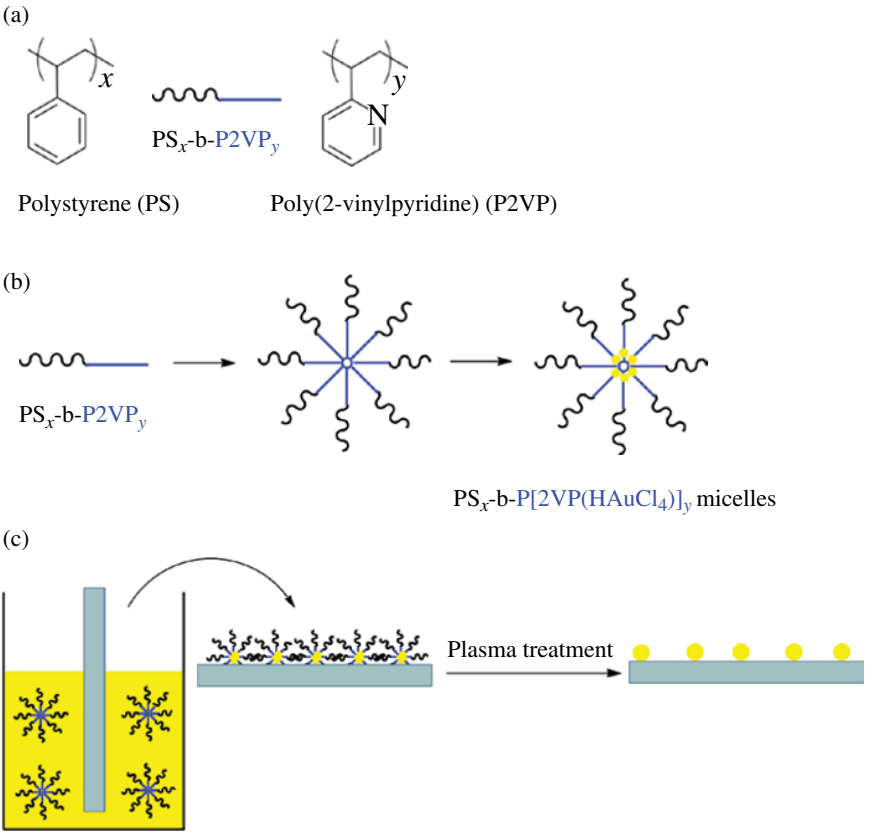

FIGURE 5.7 Principle of block copolymer lithography for spatially defined placing of gold nanoparticles on surfaces [16]. (a) Block copolymer structure, (b) formation of micelles with a metal ion core, and (c) formation of thin films by dip coating and plasma treatment to remove organic layer.

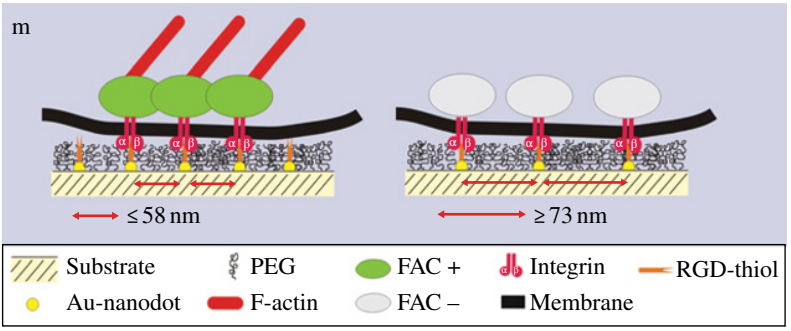

FIGURE 5.8 Scheme for the control of cell's integrin clustering at nanostructured and biofunctionalized substrates (based on spatially defined deposition of gold nanodots through block copolymer lithography). Source: Adapted from Arnold et al. [17], figure 2. Reproduced with permission from John Wiley & Sons.

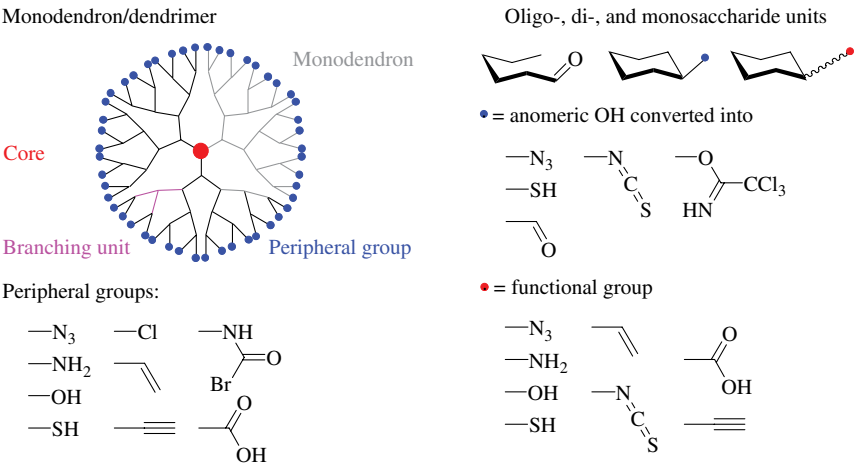

FIGURE 5.22 Main functional groups for the introduction of oligo-, di-, and monosaccharide units on monodendron and dendrimer surfaces.

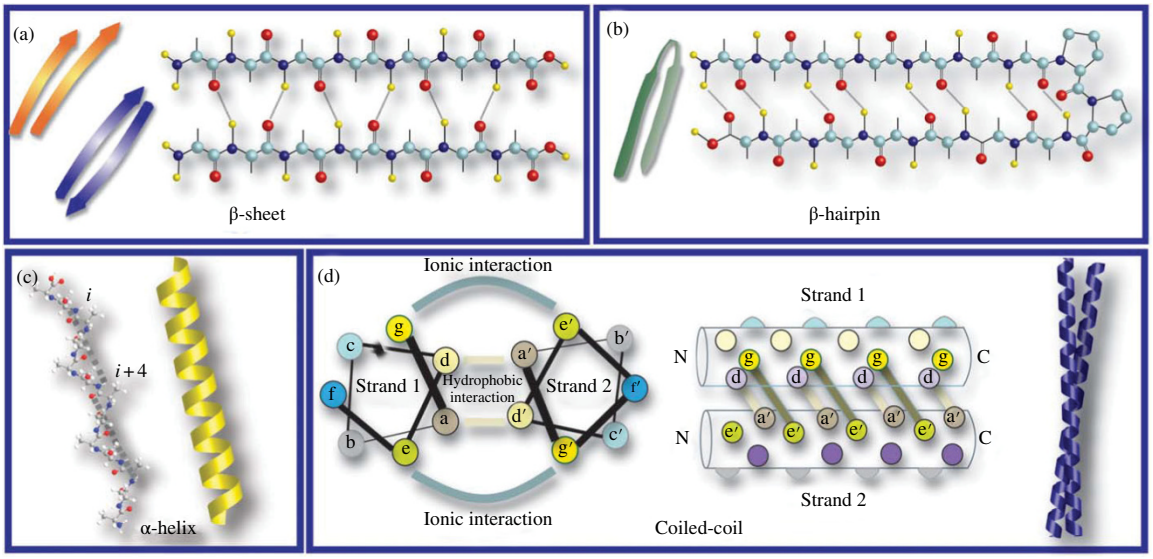

FIGURE 5.26 Schematic illustration of different secondary structures formed by polypeptides: (a) β-sheet, (b) β-hairpin, (c) α-helix, and (d) the supercoiled multistranded protein motif coiled coil. Source: Dasgupta et al. [55]. Reproduced with permission from the Royal Society of Chemistry.

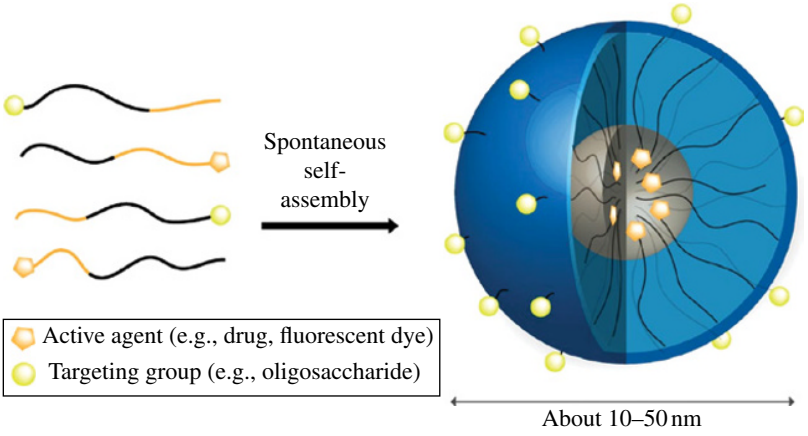

FIGURE 6.1 Formation and architecture of block copolymer micelles, which spontaneously form by self-assembly in water. The characteristic features are a pronounced core–shell architecture, which can be controlled by the individual polymer blocks. Typical examples for block copolymers are PEO-*b*-PPO, PEO-*b*-PCL, and PEO-*b*-PAsp. Source: Kataoka et al. [1], figure 1. Reproduced with permission of Elsevier.

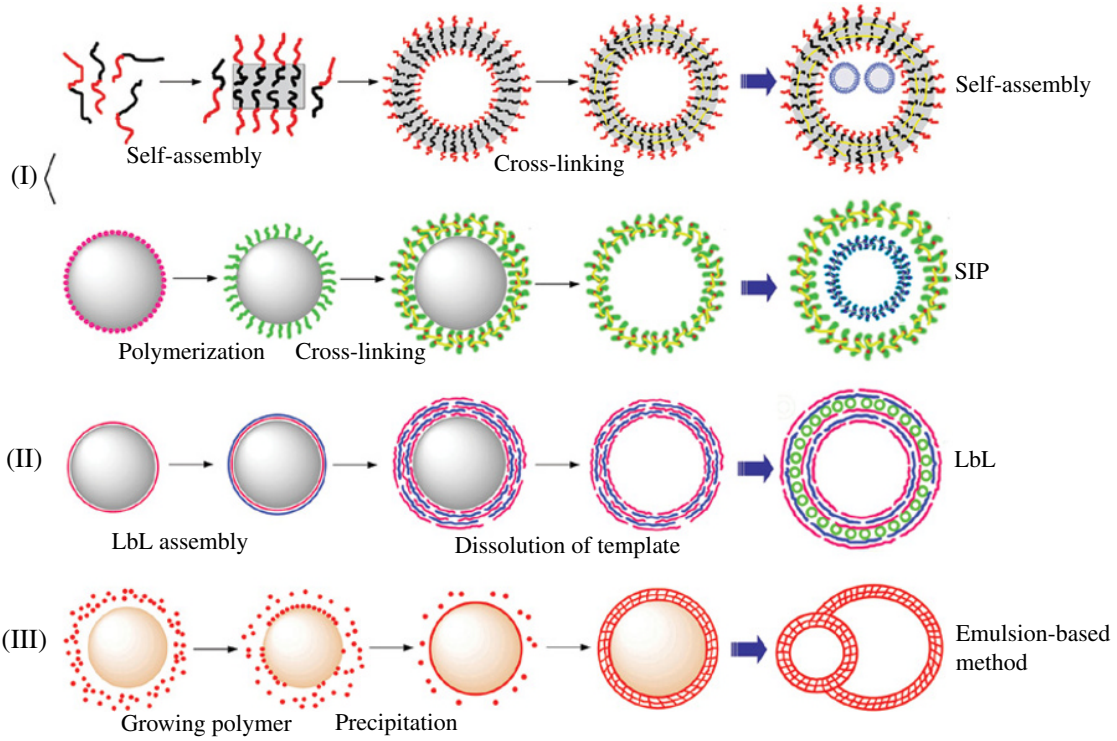

FIGURE 6.2 Preparation methods for polymeric capsules that can be used for multicompartmentalization: in type I, the polymer in the shell is arranged vertically along the core surface. These systems can be obtained by self-assembly of amphiphilic copolymers into polymersomes and subsequent cross-linking or by surface-initiated polymerization (SIP) from the surface of nanoparticle templates; in type II, the polymer in the shell arranges horizontally along the core surface, mainly synthesized by layer-by-layer (LbL) assembly of polyelectrolytes onto a particle; in type III, the polymer in the shell arranges disorderly along the droplet surface, commonly synthesized by an emulsion-based method where a polymer is deposited at an aqueous/organic interface, yielding a polymer wall around a stabilized droplet. Source: Reproduced with permission from Ref. 5.

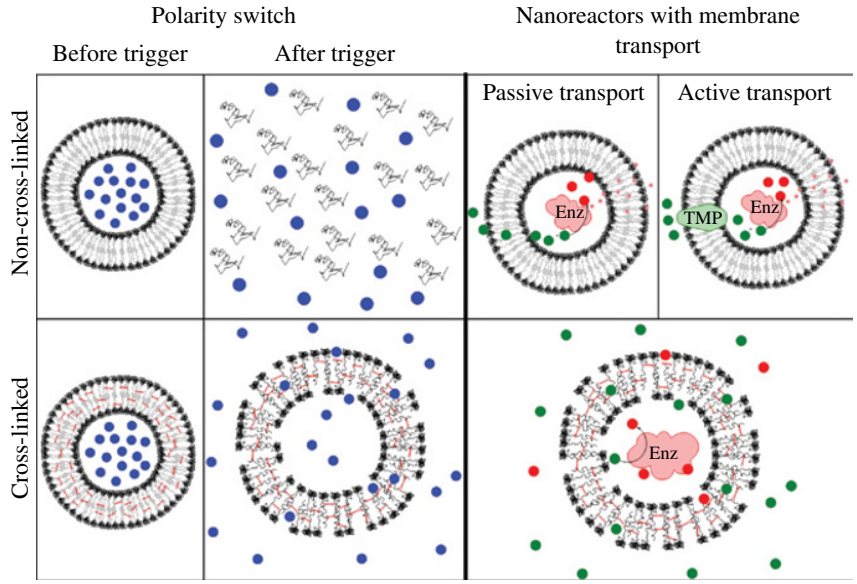

FIGURE 6.5 Schematic representation of polymersomes, with non-cross-linked and cross-linked membranes. Only in cross-linked polymersome membranes, transport can be reversibly activated upon polarity switch.

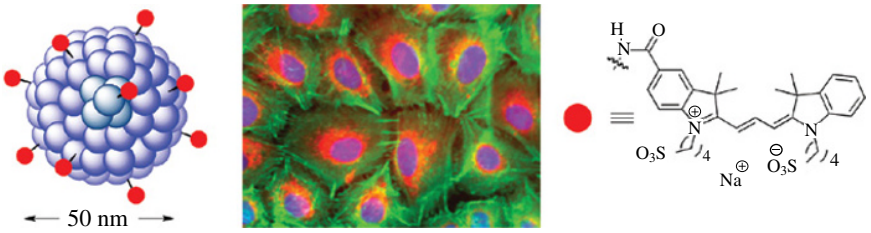

FIGURE 6.12 Fluorescence microscopy shows clear evidence for cellular uptake of fluorescently labeled PG nanogels via an endocytotic pathway. Source: Sisson et al. [27], scheme 1, figure 3. Reproduced with permission of John Wiley & Sons.

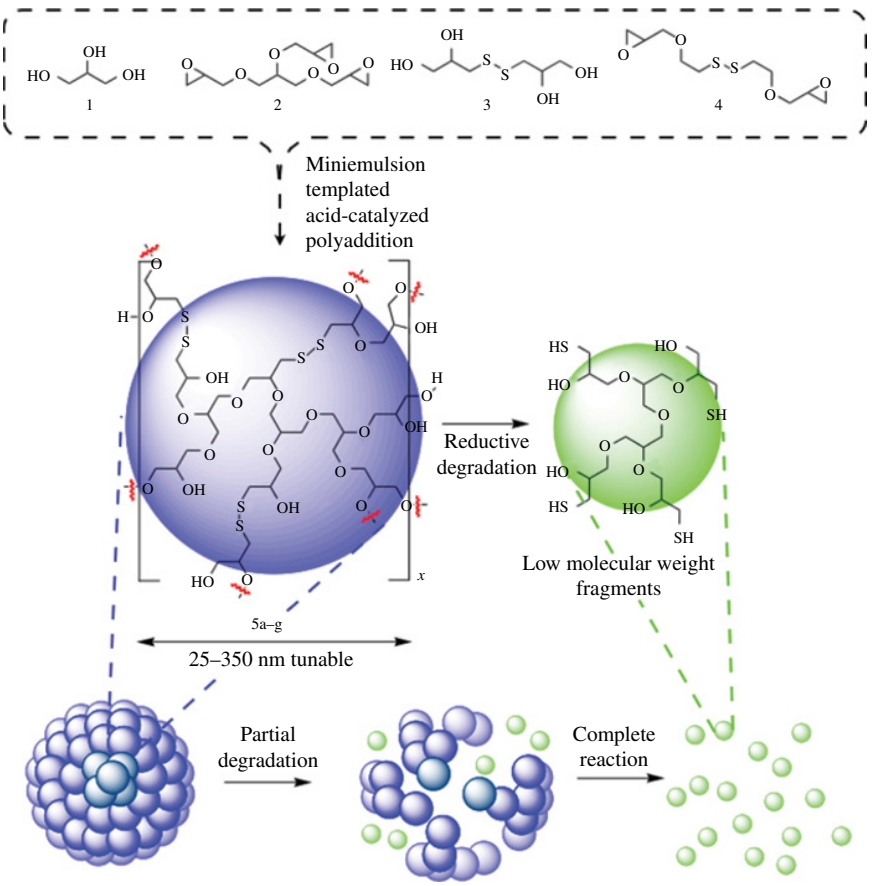

FIGURE 6.13 Synthetic route to biodegradable polyglycerol nanogels, showing a generalized depiction of a nanogel and degradation fragments [31, 32]. Source: Steinhilber et al. [31], scheme 1. Reproduced with permission of John Wiley & Sons.

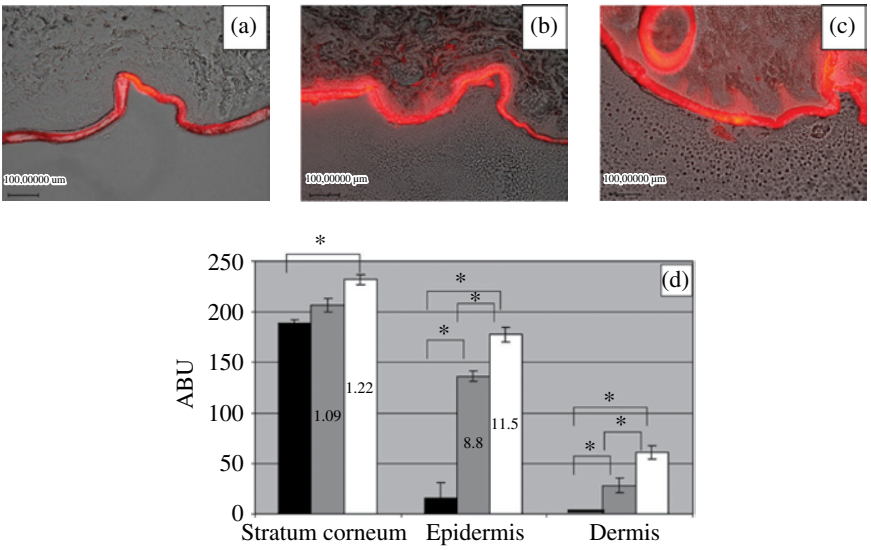

FIGURE 6.16 Rhodamine B penetration into pig skin: staining of pig skin following the application of 0.004% rhodamine B-loaded cream (a), SLN (b), and CMS nanotransporters (c) for 6 h. The representative pictures taken from the identical donor animal are obtained by superposing normal light and fluorescence images of the same area. (d) The arbitrary pixel brightness values (ABU) were obtained by fluorescence picture analysis (cream, black columns; SLN, gray columns; CMS nanotransporters, white columns, $n=3$). The inserted numbers give the respective enhancement of penetration over cream, *differences ($p \leq 0.05$). Source: Küchler et al. [38], figure 1. Reproduced with permission of Elsevier.

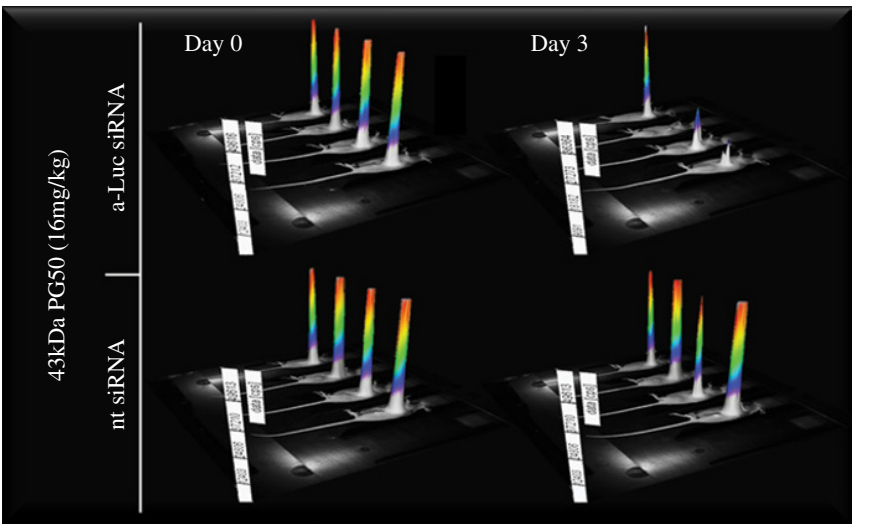

FIGURE 6.19 Idealized fragment of poly(glycerol amine) (PG–NH_2) (top) (reproduced with permission from Mehrabadi et al. [47b]) and *in vivo* silencing of the luciferase gene by siRNA–PG–NH_2 (bottom). 3D bioluminescence image of mice treated with 16 mg kg^{-1} 43 kDa PG50: light emission of tumors before (day 0) and after (day 3) treatment with 16 mg kg^{-1} 43 kDa PG50 complexed with non-targeting (nt) siRNA and luciferase specific (a-Luc) siRNA, respectively on three consecutive days. Source: Staedtler et al. [47c], figure 6. Reproduced with permission of Royal Society of Chemistry.

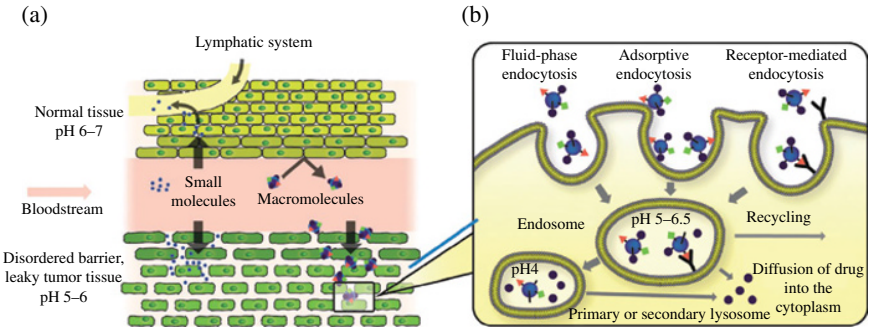

FIGURE 6.20 Schematic representation of (a) the EPR effect and (b) further cellular uptake mechanisms. Source: Khandare et al. [68]. Reproduced with permission of Royal Society of Chemistry.

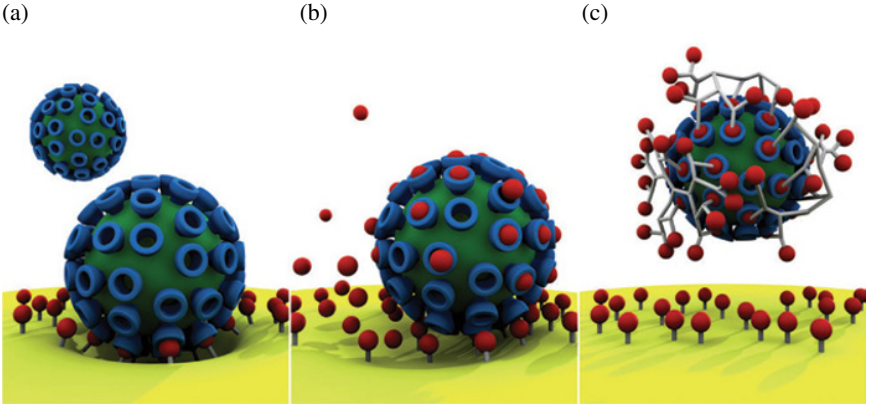

FIGURE 6.25 (a) A multivalent binding of a virus to a cell surface is compared to (b) a noncompetitive binding with monovalent ligands. (c) Multi- and polyvalent ligands are considerably more effective in binding and shielding a virus surface than monovalent ligands, thus preventing viral adhesion. Source: Fasting et al. [89], figure 2. Reproduced with permission of John Wiley & Sons.

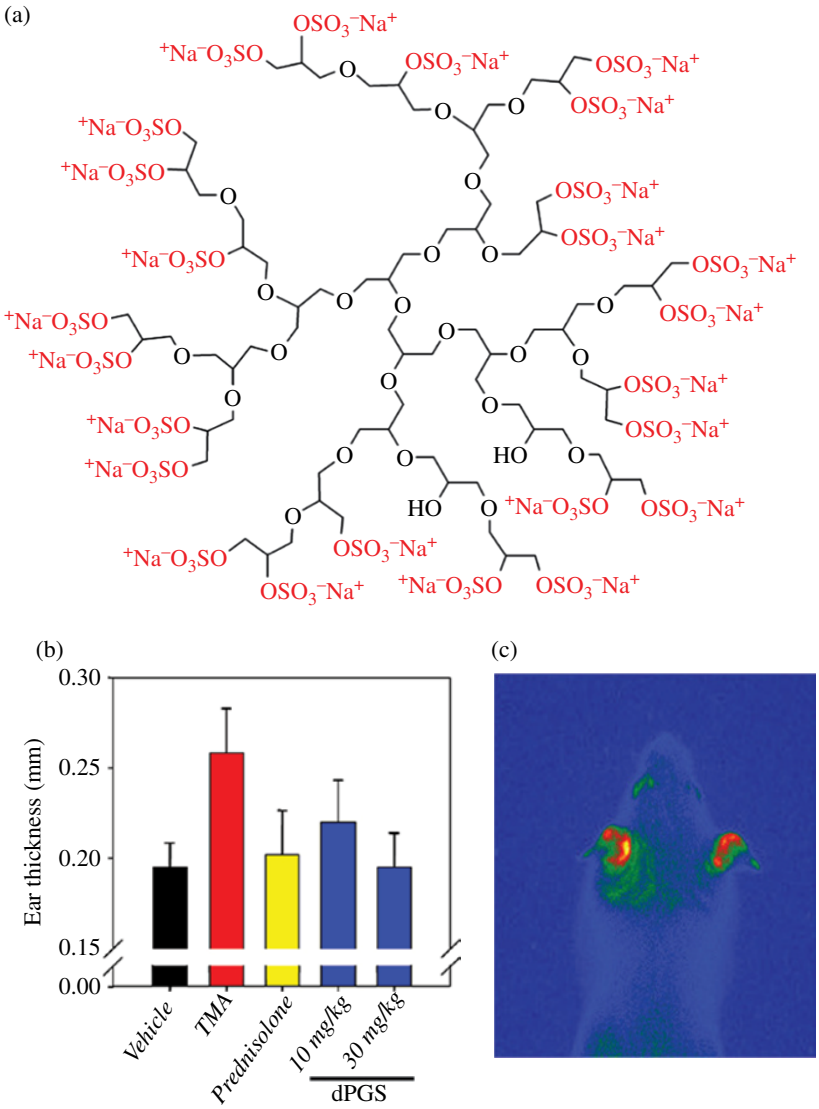

FIGURE 6.27 (a) Structure of dPGS, (b) therapeutic study of contact dermatitis in a mouse model involving ear swelling after stimulation by trimellic acid anhydride (TMA) and dPGS (blue bar) compared to commercial prednisolone (dose: 30 $mgkg^{-1}$, yellow bar), and (c) an inflammation selective fluorescence diagnosis with a dPGS–dye conjugate. Source: Fasting et al. [89], figure 27. Reproduced with permission of John Wiley & Sons.

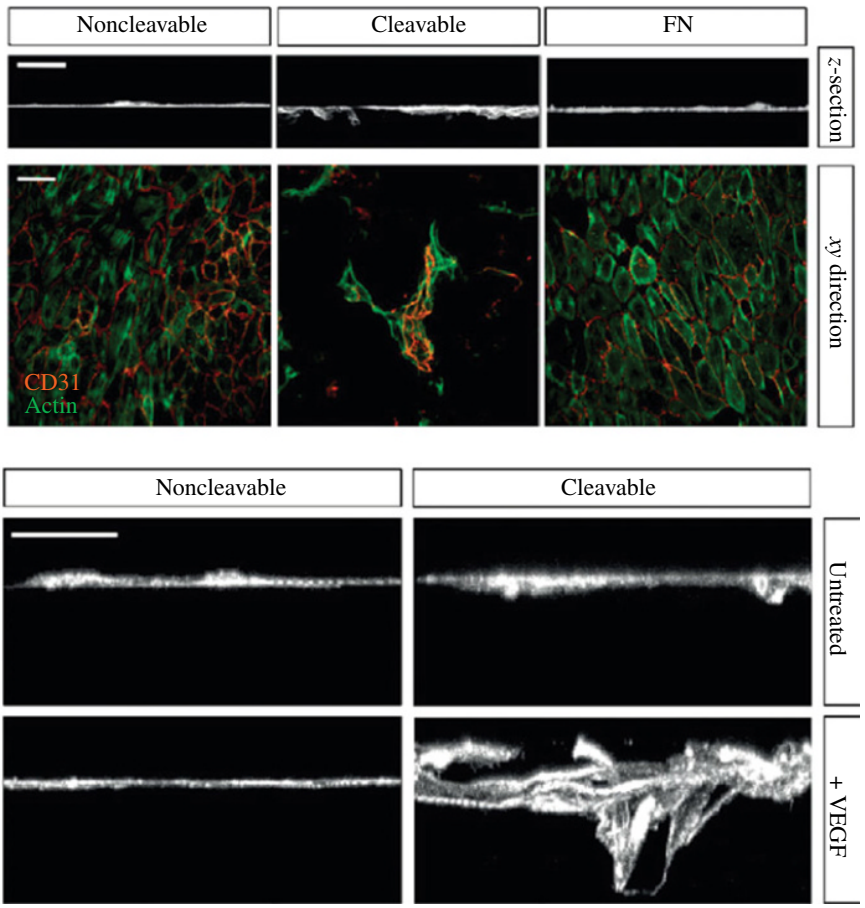

FIGURE 6.31 Top: Representative surface and cross-sectional images indicating three-dimensional growth of HUVECs within MMP-cleavable gels after 7 days. Bottom: Representative cross-sectional images illustrating enhanced three-dimensional cell migration in VEGF-loaded MMP-cleavable hydrogels after 1 day of culture, scale bars = 50 μm. Source: Tsurkan et al. [120], figure 3. Reproduced with permission of John Wiley & Sons.

WILEY END USER LICENSE AGREEMENT

Go to www.wiley.com/go/eula to access Wiley's ebook EULA.